COPY NO. _____

NASA Contractor Report 181888

FINAL REPORT

Structural Development of Laminar Flow Control Aircraft Chordwise Wing Joint Designs

J. E. Fischler, N. M. Jerstad, F. H. Gallimore, Jr., and T. J. Pollard

DOUGLAS AIRCRAFT COMPANY
MCDONNELL DOUGLAS CORPORATION
LONG BEACH, CALIFORNIA

CONTRACT NAS1-18037
APRIL 1989

National Aeronautics and
Space Administration

Langley Research Center
Hampton, Virginia 23665

FOREWORD

This document covers the contract work performed by Douglas Aircraft Company, of McDonnell Douglas Corporation, on the Development of Laminar Flow Enabling Technology, Task 1 — Structural Design and Test of Advanced Materials for Laminar Flow Wings, under NASA Contract NAS1-18037.

Acknowledgment of their support and guidance is given to the NASA Laminar Flow Control (LFC) Project Manager, Mr. R. D. Wagner, and the Project Technical Monitor, Mr. D. V. Maddalon.

The Douglas personnel primarily responsible for this work were:

Max Klotzsche	Program Manager, CRAD and Cooperative Technology Development
W. E. Pearce	LFC Project Manager
J. E. Fischler	WSSD Project Manager and Structural Analysis
N. M. Jerstad	Structural Design
F. H. Gallimore, Jr.	Materials and Processing
T. J. Pollard	Mechanical Test Engineer

SYMBOLS AND ABBREVIATIONS

LFC	laminar flow control
μe	microstrain (in./in $\times 10^{-6}$)
ϵ	strain (in./in.)
psi	pounds per square inch
g	load factor, acceleration (lg = 32 fps^2)
sliding joint	a chordwise joint that allows sliding when tension loads are applied spanwise
three-rib joint	a joint that uses a center rib and two end ribs to sustain the eccentric loading
SPF/DB	superplastic forming and co-diffusion bonding
h	wave height (in inches)
λ	wavelength (in inches)
n	load factor

CONTENTS

ILLUSTRATIONS

ILLUSTRATIONS
(Continued)

ILLUSTRATIONS
(Continued)

ILLUSTRATIONS
(Continued)

ILLUSTRATIONS
(Continued)

ILLUSTRATIONS
(Continued)

ILLUSTRATIONS
(Continued)

TABLES

TABLES
(Continued)

SECTION 1
SUMMARY

For laminar flow to be achieved, any protuberances on the surface must be small enough to avoid transition to turbulent flow. However, the surface must have joints between the structural components to allow assembly or replacement of damaged parts, although large continuous surfaces can be utilized to minimize the number of joints. Aircraft structural joints usually have many countersunk bolts or rivets on the outer surfaces. To maintain no mismatch on outer surfaces, it is desirable to attach the components from the inner surface. It is also desirable for the panels to be interchangeable, without the need for shims at the joint, to avoid surface discontinuities that could cause turbulence. Fabricating components while pressing their outer surfaces against an accurate mold helps to ensure surface smoothness and continuity at joints. These items were considered in evaluating the advantages and disadvantages of the joint design concepts discussed in Section 3.

After evaluating the six design concepts, two of the leading candidates were fabricated and tested using many small test panels. One joint concept was also built and tested using large panels. The small and large test panel deflections for the leading candidate designs at load factors up to + 1.5 g's were well within the step and waviness requirements for avoiding transition.

Figure 1 shows the acceptable wave height, h, for preventing turbulence versus the wavelength, λ. A maximum step of 0.004 inch is considered acceptable for avoiding turbulence. (This was the criterion used previously when fabricating the successful laminar flow control flight test component for the NASA JetStar.) The modified panel developed during this subsequent work had a maximum step of only 0.0012 inch (see Figure 2). This was at a load factor of 1.5 g's, equivalent to a compression load of 8,000 pounds.

The small panels were designed and tested for compression and tension at -65°F, at ambient conditions, and at 160°F. The small panel test results for the three-rib and the sliding-joint concepts indicated that both would be acceptable.

Figures 3 through 9 show photographs of the panels and joints fabricated and tested. The panels that were fabricated and tested are listed and their respective sizes shown in Table 1.

The six candidate concepts are shown in Table 2. Ranked in order of preference, they are:

1. Sliding Concept
2. Three-Rib Concept
3. Two-Rib Concept

4. Expansion Concept
5. Blade Concept
6. Beam Concept

The advantages of each concept were considered and the best three selected.

The seal between the panels was a problem area. Since the leading edge suction panels were expected to be 100 to 130 inches long, sufficient gap was required between the ends of the panels to allow installation, considering tolerances and wing strain conditions. This gap had to be filled with sealing material capable of sustaining the high ultimate compression and fatigue loads without failing. After extensive flying, it must not crack, bulge, or contract enough to create a discontinuity that would cause turbulence. The initial seal material had bulged significantly during the compression test of two small panels at 160°F, so development of a seal material that would meet the strength and rigidity requirements over the required temperature range was undertaken. Titanium strips were inserted between ends of the panels to reduce the width of the required seal material. Then, by reinforcing the sealant with steel wool, the effective modulus of elasticity of the filled gap was increased sufficiently to allow the compression load to be transferred directly between the ends of the panels. The resulting compression load path was then closer to the neutral axis of the panel. This reduced the load path eccentricity and the corresponding bowing or waviness of the panel, which could have caused the airflow to make the transition to turbulence. Hot and cold testing showed that the final seal material could withstand the ultimate compression load, while its shape remained stable.

After testing the small panels, two large panels that utilized the sliding-joint concept were fabricated and tested to the design loads. The strain gage readings indicated that, in spite of the load eccentricities, the stresses recorded were well within the ability of the panel to withstand them. The only concern was a slight step that occurred at the sliding joint. The step was due to the oversized bolt holes needed to allow the sliding joint to move freely. With the sliding concept, it was difficult to machine the fitting and to maintain the close-tolerance holes for the long bolts needed to prevent steps from occurring at the surface. The three-rib concept, with tapered splice plates, was considered to be the most practical. It also cost less to fabricate and was lighter.

A modified three-rib joint that combined the best attributes of both previous candidates was designed, developed, and tested. This improved joint met all of the structural strength and surface smoothness and waviness criteria for laminar flow control (LFC). The design eliminated all disadvantages of the initial three-rib concept except for unavoidable eccentricity, which was reduced and reacted satisfactorily by the rib supports. It should also result in a relatively simple low-cost installation, and make it easy to replace any panels damaged in the field. This panel, which gave the best test results, is recommended for future large-scale development.

Figures 10 through 12 show representative deflections with different loading parameters. The joint steps for loaded and unloaded panels are shown in Figures 13 through 20 and in Table 3. The panel strains for the various concepts are listed in Tables 4 through 15 and in Figures 21 through 47.

The work done in this contract has brought the technology for chordwise joints between LFC panels far along the path of proving that practical joints are possible. The guiding principles and approaches to design, fabrication, and installation that were developed during this program would be equally applicable to alternative panel designs. They should result in acceptable LFC panel joints and allow installation and replacement of LFC panels without difficulty.

Recommendations are made for an additional development program to accomplish the following: (1) test the fatigue characteristics of the chordwise joints, (2) build a large test panel representative of an LFC curved leading edge, and (3) test two panels with chordwise and spanwise joints under combined axial compression and lateral airloads.

This page intentionally left blank

SECTION 2
INTRODUCTION

Providing satisfactory joint conditions for LFC panels on the suction surface is one of the most formidable problems that must be faced in design of a practical LFC system for production aircraft. Existing techniques are inadequate for structural joints, and innovative design is necessary to control joint smoothness and achieve continuity of LFC suction necessary to maintain laminar flow past panel joints. Chordwise joints are necessary to limit the span of the leading edge panels for ease of fabrication, installation, and replacement in the event of damage in service. Excessive hand-adjustment or the use of shims, which would be acceptable for flight experiments, are unacceptable for service aircraft. The external smoothness and waviness of the joint, its weight and relative stiffness, eccentricity of the compression and tension load paths, the relative cost of fabrication, and ease of changing damaged panels were major considerations in this investigation.

A gap is needed between the ends of the panels that is large enough to provide clearance for panel installation, taking into account the fabrication tolerances and the static wing strain conditions. This gap must be made smooth enough to avoid boundary layer transition to turbulence when filled with material that also acts as a seal. This seal must hold its shape and not bulge when subjected to high temperature or compression loads, and not become concave at cold temperatures. It must also remain ductile throughout the life of the vehicle, and not let moisture seep in. An objective was that the effective modulus of the seal be at least equal to that of the panel, so that the seal would transfer most of the compression load close to the neutral axis of the panel and thus minimize eccentricity. This would also result in little surface waviness.

Another major consideration in selecting the joint design was to minimize the width of the nonporous surface strip along the joint. To achieve this, the porous suction holes in the active flutes were brought as close to the edge of the panel as possible. This was accomplished by using only the inactive flutes to provide the bolted joint load carry-through.

Two basic concepts were considered. In one, fixed structure was used to react the loads caused by eccentricities in the load path at the joint. Alternative structural arrangements of this type were investigated. The other concept relied on direct load transfer between the ends of the panels under compression during steady flight with LFC in operation. Small gaps could occur between the panel ends under negative g-loading or on the ground, but LFC would not be operating under these conditions.

Both concepts were first fabricated with small panels and tested. Two large panels of the sliding concept were then fabricated and tested. The test results showed that the designs would withstand the limit loads and meet the LFC waviness criteria with load factors up to 1.5 g's. However, a slight step occurred with the sliding-joint concept because of bolt clearances needed to allow easy sliding.

As a result of these tests, an additional type of joint was designed, fabricated, and tested. This joint incorporated the best features of the previous joint designs but most closely resembled an improved three-rib concept. It met all of the requirements for a chordwise joint in an LFC leading edge panel, as defined in Section 3.1. The final three-rib joint design is therefore recommended as the best type of joint for this application.

The small and large panel deflections and steps through the range of – 65°F to + 160°F and from 0 to 1.5 g's were measured and compared to the specified requirements. In all cases, these requirements were met.

The final three-rib splice is recommended in Section 4 as the most successful in meeting the design objectives for chordwise joints between removable LFC panels.

Test results showed slippage from the bolts connecting the LFC panels. It is therefore recommended that metal bushings be used for the close-tolerance holes in the composite material. This would also minimize hole deflection under bearing loads and reduce the possibility of bolt bending.

SECTION 3
LFC PANEL JOINT DEVELOPMENT

3.1 PRELIMINARY CONCEPTS

The following objectives were considered in reviewing the preliminary joint concepts:

- The joints must not disturb laminar flow.
- Contour control is to be accomplished by holding the parts against a lofted surface (mold) during assembly so that when the parts are joined, the panel edges match the lofted surface within 0.001 to 0.002 inch.
- The panels must be interchangeable. This is to be accomplished by building like panels against the same mold, so that if spare panels are ordered by a maintenance base, they will be interchangeable without a need for shims.
- The nonporous strip along the joint where the panel ends are plugged must not be wide enough to cause transition.
- The joints must sustain the ultimate spanwise loads for the leading edge panel without failure; this is equivalent to – 4,500 μin./in. (μe) strain in compression. The joints must also sustain the maximum tension load or sustain the equivalent ultimate tensile strain for a load factor of –1.5 g's.
- The LFC surface waviness tolerance, as shown in Figure 1, should not be exceeded at + 1.5-g limit load in compression.
- Although fatigue testing was not included in this study, the joints should sustain the fatigue spectra for two lifetimes without cracking.
- After sustaining the loads defined above, the seal must remain sufficiently smooth (without bulges, concavities, or rough surface cracks) to avoid transition to turbulence starting from the joint.

Six preliminary concepts were considered, as discussed in the following text. These were ranked in the following order of preference: (1) sliding concept, (2) three-rib concept, (3) two-rib concept, (4) expansion concept, (5) blade concept, and (6) beam concept.

1. Sliding Concept: This concept, shown in Figure 48, avoids having the leading edge panels sustain spanwise tensile loads by allowing the panels to slide along the bolts shown in section B-B. It also reduces shear transfer to the leading edge from the main wing box. The airloads are transferred from the leading edge box to the front spar by local ribs. The bolt holes through the attach fittings and rib fittings are jig-drilled in line while the connecting panels are held against a mold tool matching the

external panel contours at the joint. The panels are allowed to "breathe" with expanding wing deflections during flight. Tests of dry bolts showed very little bending in the bolts; lubrication would have reduced the strain in the bolts to still lower values.

Because the leading edge panels can slide on the bolts, they are not forced to accept a share of the tensile bending loads; the panels would therefore have increased fatigue life. In flight, the LFC panels are normally in compression, and loads are transmitted directly between the ends of the panels through the stiff sealing material. Since the main wing box, as presently constructed, can carry all the wing bending loads, soft seals would cause the seal to bulge. To avoid this, the seals were designed to be as stiff as or stiffer than the spanwise panels. The seals were finally made in two parts, a hard part to bridge the spanwise compression load between the panels and a soft part to prevent water from entering the panel.

Section B-B of Figure 48 shows the double-bladed tees bonded to the ends of the panels. A fitting attached to two ribs has two blades between the double blades of the panel tees and a wider blade between the two panel assemblies. Holes are jig-drilled into the three blades of the fitting to match the tees, and the joint is completed by installing the bolts. This system restricts the ends of the panels from bending because of load eccentricity and controls local surface waviness.

2. Three-Rib Concept: Three ribs are used to react eccentric loading at the joint in order to avoid surface waviness. The joint has plates bonded onto the panels so that the inner surface of each plate is held in a jig at a specified dimension from the outer surface of the panel. The varying gap is filled with liquid shim as shown in Figure 49. The panels are joined by installing fasteners through the splice plate, the bonded plate, and the inner face of the panel. The fasteners are retained by nut channels in the nonactive flutes. The outer ribs are attached near each end of the joint and a third rib is attached at the center. The three ribs react the bending moments caused by the joint eccentricity by creating equal and opposite force couples. The axial loads are taken out in shear through the bolts. Figure 49 shows a preliminary version of this concept.

Figures 50 through 55 show the further development of this concept. Figure 51 shows the bonded plate that has a liquid shim to provide the specified dimension from the outer surface of the panel located by a jig. (See Figure 49.) Figure 53 shows the four sheets of titanium that are bonded to form the tapered splice plate. The holes shown are for installing fasteners through the splice plate. Figure 54 shows how these fasteners go through the inactive flute to the nut channel assembly.

3. Two-Rib Concept: This concept (Figure 56) uses a splice beam with a high moment of inertia to handle the bending moment caused by joint eccentricity. This eliminates the need for the center rib. In order to sustain the eccentric loads, the splice plates must be deep enough to take the bending stresses and provide sufficient stiffness to control waviness within acceptable limits.

4. Expansion Concept: This concept (Figure 57) allows the panel ends to slide apart from each other. Plates bonded to the end of the panel slide along a plate fastened between two ribs. Fiberglass tees bonded to the ends of the panels are joined to the ribs by fasteners. The blades of the fiberglass tees are flexible enough to allow the panel ends to slide apart, but they can resist any upward load on the panel. The plate fastened between the ribs resists any downward load on the panel. Compression loading between the panels is reacted through the plug. The metal plate is in two pieces, each bonded to the fiberglass attach tee, which is then bonded to each panel end. When the wing bends down (negative load factor and/or dead weight of the wing under 1 g loading during takeoff and landing), then the panel end pulls on the attach tee, causing side bending. The metal plate rubs on the contact plate which is attached to the angles that are also attached to the ribs. The plug seals prevent internal fluid leakage for these tension conditions. The attach tee is designed to sustain the side bending for these conditions. During the normal flight conditions that cause upper surface compression loads, the panel ends compress the plug which is attached to the contact plate. Thus, compression loads are transmitted by direct pressure and tension loads — that would otherwise bend the lugs and cause eccentric loading — are avoided by movement along the sliding joint.

5. Blade Concept: This concept (Figure 58) reacts eccentric loading with a splice beam fastened to two ribs like the two-rib concept except that the fasteners are installed through the blades of the two extrusions that are bonded to the inner surface of the panels and the splice beam, instead of going through the inner face of the panel. Since the space between the tees is limited, an extension plate is fastened to the blade of the tee to provide room to precision-drill and ream the fastener holes through the extension plate and the splice beam and accurately match the surfaces of the two panels.

6. Beam Concept: In this simpler concept (Figure 59), the splice beam has sufficient moment of inertia to handle the bending moment. A thick plate is used with channels machined into it. The fasteners are placed in the channel portions of the splice beam. The ribs are located outside the splice area. The lack of a center rib could result in the plate being very thick to control panel deflection.

The advantages and disadvantages of each of the concepts, as listed in Table 2, were considered in the selection of the top three candidates. The top three were the sliding concept, the three-rib concept, and the two-rib concept.

3.2 SUMMARY OF JOINTS BUILT AND TESTED

Figures 3 and 4 show the small three-rib design that was fabricated and tested. The test dimensions are 4.4 inches wide, 18.5 inches long, and 1.125 inches thick. Figure 5 shows the small sliding-joint design assembled for testing. The panel dimensions are 4.5 inches wide, 14 inches long, and 0.8 inch thick.

Figures 6 to 8 show the large sliding-joint design. Both sides are shown, along with the test jig setup for tension. The dimensions are 23 inches wide, 30 inches long, and 0.875 inch thick.

Figure 9 shows the initial composite tapered "back-to-back" bolted angles used to test the final improved three-rib design. The dimensions are 4.5 inches wide, and 10.5 inches long, and the composite is tapered from 0.6 to 0.3 inch.

Figures 60 and 61 show the final improved three-rib design which is a small panel with a width of 4.5 inches, a length of 22 inches, and a thickness of 1.1 inches at the joint, tapering to 0.9 inch at the rib. Table 2 summarizes the various panels and joints that were fabricated and tested.

3.3 CONCEPTS FOR TESTING

Layouts were prepared of the three selected joint concepts. Figure 62 shows plan views of the wing at the splice area taken from these layouts. Cross sections of these views at the center of the joints are shown in Figure 63. Detail layouts were made to develop the test specimen as described in the following sections.

3.3.1 Rib Concepts

In the three-rib and two-rib concepts, the panels are bolted to a splice plate or beam which is attached to the ribs as shown in the detail views of Figures 64 and 65. These views indicate that installing the bolts would be a problem if rib flanges were needed to carry the rib bending loads because the splice plates are not continuous chordwise. This problem was avoided by lengthening the two rib joints as shown in Figures 65 and 66 so that the affected bolts are moved far enough away from the flanges. Also, in the three-rib concept, the rib flanges were moved to the outside ribs.

Preliminary drawings of the tension and compression short-chordwise joint test specimens for the three-rib and two-rib joints are shown in Figures 67 and 68, respectively. Two versions of the complete three-rib joint were evaluated for strength and cost. One had a single flat splice plate and the other several thinner splice plates bonded together to create a step-tapered effect. Figures 69 and 70 show the two concepts. In both versions, each rib was attached by a pair of angles to avoid any eccentricity induced by a single-shear attachment. The step-tapered splice plates were designed to give a more even load distribution and less load eccentricity. The bonded laminations were easier and cheaper to manufacture than machining steps in a single titanium plate. In both versions, the lower faces of the panels were reinforced by a 16-ply layup of carbon and fiberglass cloth because the load is transferred through the lower face of the panel at the joint.

Analysis determined the tension and compression loads for the joints, the required sizes and number of bolt attachments, and the thicknesses of the parts needed to provide adequate strength and bearing

area to sustain the direct loads and bending caused by the eccentricity. The test specimen for the three-rib joint with a step-tapered splice plate was then designed and fabricated as illustrated in Figure 52.

Four 0.071-inch-thick titanium sheets were bonded together as shown in Figure 53 to produce the 3.34- by 10.94-inch splice plate. Bonding the sheets assured a flat splice, free from warpage which could have occurred if only a single splice plate had been machined. Although care must be taken in preparing surfaces for bonding, this procedure is less expensive than machining the splice plate.

The inner face of the -13 panel was reinforced with 10 plies of carbon-epoxy and fiberglass-epoxy cloth and the titanium -25 plate was bonded to it so that the combined thickness was 1.12 inches, as shown in Figure 54. Close tolerance holes (0.003-inch clearance) were provided to transfer the load in shear, but the -9 and -11 angles (Figure 52) could have loose tolerance holes for ease of installation and were predrilled. Three -15 nut channel assemblies, shown in Figure 55, were located in the inactive flutes, and foam spacers (-23) were used to prevent the nut channel from bending excessively when the fasteners were installed. The flute ends were filled with sealing compound and topped with filler, and a titanium -27 plate was bonded and fastened to the ends of the panels. The foam spacers (-23) were provided to hold the nut channel plate down when the blind rivet fasteners attached the nut channel plate to the panel.

Since the specimen was to be tested in tension as well as compression, the ends of the specimen were designed to fit the tensile test machine. The standard clevis 1-inch hole normally provided to load the specimen would have cut through a completed flute; therefore, three 1/4-inch holes were drilled into the specimen and steel plates were used to connect the specimen to the clevis. Steel -31 bearing plates (Figure 54) were bonded to the panels to match the thicknesses of the two clevis halves. In addition, a titanium -29 plate was bonded to the upper surface at the panel ends to reinforce the 0.25-inch-thick titanium skin and the upper bearing plate was bonded to this plate. A bulb seal was placed between the -3 panel assemblies near the lower face to support the filler between the panels (Figure 52) with an aluminum channel supporting the bulb seal. The aluminum channel was provided to hold the seal in place. A filler with sufficient modulus of elasticity to allow load to be transferred through it was used to fill the remaining gap. It was an epoxy resin reinforced with milled fiberglass and glass bubbles.

3.3.2 Sliding Concept

The overall arrangement of the sliding-joint concept, which allows the ends of the panels to slide along bolts in the spanwise direction, is detailed in Figure 71. In this concept, when the upper wing is in compression, the panel ends make contact and transfer load. This is the normal flight condition when an LFC system is provided. The inactive flutes are filled at their ends to help transfer the load into the next panel and the whole end is capped with a titanium strip. The filler used normally has a relatively high coefficient of expansion because it contains aluminum mixed with epoxy resin. This caused

two panels that were cycled 15 times from 0°F to 160°F to separate from the flute walls. A more suitable filler with a lower coefficient of expansion was developed to avoid this possibility. No damage was done from fluctuating wing loads. The panel ends were designed to transmit compression without buckling. When the upper wing surface is in tension, no tension existed across the joint, which slides apart yet remains sealed. Laminar flow is not expected under this negative g-condition because of the adverse pressure distribution existing temporarily over the wing surface. The simple sliding-joint specimen shown in Figure 72 was tested first without the complication of the spanwise joint to determine if the panel ends could handle the compression load and slide as intended. Deflections were measured, and strain gages on the bolts indicated whether any bolts bent because of load eccentricity and bolt tolerances.

The test configuration shown in Figure 73 allows the two -3 panels to slide along the -7 pins inserted through the -9 panel fittings and the -5 rib fitting. Elastic grommets were provided between the nut and the fitting attached to the -3 panel to prevent uncontrolled sliding of the pin. When the panels were loaded in tension, the grommets compressed to allow the joint to open. Standard aluminum extrusions were used for the panel fittings. The design of the rubber seals (Figure 72) and the design of the grommets prevented uncontrolled sliding of the pin. The final improved three-rib concept does not have grommets, and there is very little pin wear, thus assuring long life.

The -3 panel assembly shown in Figures 74 and 75 combines the -9 reinforced LFC panel with the -11 fitting. Holes in the sliding fitting were drilled to a jig-controlled dimension below the outer surface, and aluminum bronze bushings were inserted to protect the holes from wear. At the end of the panel, the -13 plate was bonded to spread the load as in the three-rib concept. The other end of the panel was designed similar to the three-rib panel to accept tension and compression loading from the test machine. The active flute ends were plugged and the inside end of the plug was sloped 30 degrees to reduce the distance across the joint without suction occurring.

The -11 fitting was attached to the -9 panel with flush head bolts secured by nut channel plates inside the inactive flutes in addition to an adhesive bond. Unlike the three-rib joint, the bolts were installed permanently before the flute ends were filled. The limited amount of space in the flutes prevented blind fasteners from being used.

The sliding bolt holes in the -5 rib fitting were jig-drilled in line and aluminum bronze bushings inserted as shown in Figure 76. These bushings provide a closer tolerance fit of the bolts. This reduces the step of the joint and it also reduces wear in the aluminum, providing a longer life. The bushings are expected to wear so well that they need not be changed over the life of the aircraft.

3.4 SMALL PANEL TESTING

The primary structural strength requirement is that the panel must withstand 4,500 μin./in. ultimate compressive strain in the swept spanwise direction. This strain level is typical for the wing box of a

commercial transport to which the leading edge LFC panel is attached. For the test specimen, this strain level corresponds to an end load of 20,000 pounds in compression. The strain levels measured on the test specimen will be less than 4,500 μin./in. at a 20,000-pound load, due to local reinforcing.

3.4.1 Three-Rib Concept — Test Setup

Figures 77 and 78 are photographs of the test article for the three-rib concept (Figure 52). A subassembly stage is shown in Figure 79. The nut channel plates inserted into the inactive flutes to provide for attachments between the panels and the splice plate are shown in Figure 80.

Strain gages were added as shown in Figures 81 through 84 to indicate the stress distribution under load. A steel rod was used to anchor the simulated rib supports and restrict differential movement.

3.4.2 Three-Rib Concept — Test Results

The splice behaved well under compression loading up to 20,000 pounds at room temperature. The maximum strain on the outer perforated titanium side was + 2,218 μin./in. at strain gage 13, as shown in Table 4. On the inner splice plate side, hardly any strain was recorded: the highest strain was 970 μin./in. at location 2. These strains, when multiplied by the modulus for titanium of 16.1×10^6 at room temperature, result in 35,709 psi for the outer perforated titanium and only 15,617 psi on the inner splice plate. These low strains helped to prevent excessive waviness from the eccentricity of the load path through the joint.

Dial indicators were provided to measure lateral movement and detect any bowing. Table 16 shows that a compression load caused the perforated titanium surface to bow outward. The dial readings at the top, middle, and bottom of the 18.5-inch-long test panel with the single wavelength, λ, were well below the value that would cause turbulence, which is 15.7×10^{-4} streamwise at the root and 24.2×10^{-4} at the streamwise tip (see Figure 1). The calculated waviness is perpendicular to the joint, and would be even less in the streamwise direction. It should be noted in Figure 10 that the dial readings were almost all in the negative direction, indicating a single wave to the left. Table 5 shows the strains in compression for the three-rib concept at –65°F and + 160°F. The strains were slightly higher than at room temperature for the outer perforated titanium, reaching + 2,679 μin./in. at gage 19 at –65°F, and –2,474 μin./in. at gage 11 for + 160°F. On the inner splice plate, gage 2 was the highest with a –1,543 μin./in. strain at –65°F, and gage 14 showed a –1,116 μin./in. strain at + 160°F. The thermal expansion or contraction with a combination of dissimilar materials probably caused these slight increases from the room temperature values. Compression testing was repeated with the seals removed to determine how this would affect the performance of the joint. As shown in Table 6, the strains increased to –3,176 μin. at strain gage 19, at 160°F. However, the modulus decreased to

15.6×10^6 at 160°F, making the stress level 49,000 psi, which is 39 percent more than the maximum stress at room temperature for gage 13.

Without the seal, there was no direct load path between the ends of the panel. The load was consequently transferred only by the splice plate at the inner surface and the resulting eccentricity bent the joint. This is apparent in Figures 85 and 86. The angular movement of the upper panel caused the upper simulated rib support to bend, as shown in Figures 87 and 88. The figures also disclose partial closure of the gap on the outer titanium side.

A stiffer rod supporting the simulated ribs would have prevented bending at the joint. When applied to a complete leading edge structure, the ribs will be more effectively supported to minimize relative deflections. Also, with a stiff seal transmitting some axial load, no permanent set would be expected.

Close inspection indicated that the high stresses had caused the composite material at the joint to be partly crushed. Titanium strips were therefore bonded to the ends of the next panels to be tested.

The three-rib concept was also tested in tension. The dial indicator readings for tension are shown in Table 17 and are plotted in Figure 89. These deflections do not apply to laminar flow conditions with a design operating range of 1 g ± 0.5 g. As a result, the upper wing surface is always in compression when the LFC system is operating.

The strain values are shown in Tables 7 through 9 for tension loads up to 8,000 pounds (–1.5 g ultimate). The corresponding stress levels are very low. On the titanium side (gages 1, 5, 7, 9, 11, 17, and 18 and Figure 81), the maximum strain was only – 372 μin./in. in the hot condition (+ 160°F) (Table 8), which corresponds to 5,989 psi. The low stress levels in tension resulted from the higher design loads in compression and the doubler reinforcement used to increase stiffness to avoid the waviness that could cause transition from laminar to turbulent airflow in flight with the splice loaded in compression.

Figures 3 and 4 show the dimensions of the test article and a close-up of the composite side.

3.4.3 Sliding-Joint Concept — Test Setup

Figure 90 shows the sliding joint with titanium edge sheets added to the ends of the panels. This was done to avoid local crushing of the composite material and to increase the modulus of elasticity of the gap filler so that the compression loads would go through the panel ends and minimize load eccentricity. If the modulus of elasticity of the filler in the gap were too low and the fittings did not slide on the bolts, the panel would bow, causing eccentricity and increasing bolt bending loads.

Figure 91 shows the sliding joint small test panel. The panels were free to move apart sufficiently to avoid tension loads being transmitted across the joint during flight or on the ground. Aerodynamic

loading and any end moments were reacted by the bolts and the rib attachment fittings. When the panel was in compression, the gap filler transmitted loads between the ends of the panels; the panel slid on the bolts and any eccentricity was sustained by the bolts and rib fitting. When installed, the panels will also be attached to the front spar. (Figures 48, 62, and 63 show the panel attachment to the spar cap.) The panels must therefore match the tensile strain of the spar cap and will accumulate tension loads between panel joints but not across the joints. The panels will be in compression during cruise flight so that there will be no gaps at the joints. Figure 92 shows a close-up of the composite side with the rib attachment in the background and Figure 93 shows the titanium side. Strain gages were installed on the test component as indicated in Figures 94 through 96. A flat surface was machined on the center bolt so that its four gages could be installed.

3.4.4 Sliding Concept — Test Results

The compression results for the small sliding joint tests at room temperature, - 65°F, and + 160°F are shown in Tables 10 through 12. Taking 16.1 million for the modulus of elasticity of titanium, at ultimate load at room temperature, gage 3 registered a strain of - 3,014 μin./in. The equivalent maximum stress was 48,525 psi, which is low for titanium. Strain gage 12 read - 3,675 μin./in. for the maximum composite strain at room temperature, which is equivalent to 29,768 psi at a composite modulus of 8.1 million. This is also a low stress at ultimate load. The 6Al-4V titanium bolts, heat-treated to 160,000 to 180,000 psi, had a maximum strain of - 849 μin./in. at room temperature, corresponding to a stress level of 13,669 psi.

At - 65°F, gage 5 indicated a maximum strain of - 3,092 μin./in. The modulus of elasticity of titanium rises slightly to 16.4 million at - 65°F, resulting in a higher stress of 50,777 psi. The composite stress and bolt stresses were slightly lower than the room temperature values.

At elevated temperature, 160°F, gage 3 indicated a strain of - 3,129 μin./in. This was equivalent to a stress level of 48,866 psi for the titanium using a modulus of 15.6 million. The composite strain gage 12 read 5,206 μin./in., which raised the composite stress to 42,169 psi without correcting the composite modulus. The bolt stress rose to 15,115 psi at strain gage 16, after correcting the titanium modulus for temperature. All these stresses were well within the allowables.

The dial indicator readings for the compression of the sliding joint at room temperature are listed in Table 18 and plotted in Figure 97. Using the dial indicator readings for the 1.5-g loading of 8,000 pounds results in a midpanel deflection, h, of 0.005 inch. With the dial spacing length, λ, of 8.0 inch, the $h/\lambda = 6.25 \times 10^{-4}$. This value is much better than the three-rib concept value of 12.5×10^{-4}, and is well under the value of 15.7×10^{-4} that could cause turbulence.

Tension tests were performed at room temperature, –65°F, and 160°F. Table 13 shows the strain gage readings up to a tension load of 8,000 pounds at room temperature. This load is for ultimate tension strength at a maximum load factor of –1.5 g. The joint was designed to slide under tensile strain so that no tensile load could exist other than that due to slide friction. However, to ensure complete safety, the joint was tested under tensile loading that could occur only if the sliding joint were jammed. The strain gage locations are shown in Figures 94 through 96. At 8,000 pounds of tension, a strain of –4,940 μin./in. was recorded at gage 16 on the center titanium bolt. Using 16×10^6 as the modulus of elasticity for titanium, the equivalent bolt stress was 79,040 psi in tension. Thus, even with a jammed or dry bolt, there would still be a large safety margin.

Lateral deflections and the seal gap were measured during tension testing, and the results are presented in Table 19. The amount of bowing over the 8-inch distance between the outer dial gages is plotted in Figure 98. The continuous straight-line relationship between the applied load and the extent of bowing show that the structure remained elastic without permanent deformation. The bowing is not significant.

The seal gap measurements are not representative of flight conditions with the panels installed because the seal gap could not exceed the amount allowed by tensile strain in the main wing box. For a 10-foot-long leading edge panel, the strain of the upper surface of the wing box would be 0.114 inch at the limit load in tension. In practice, the seal gap would be much less than this because of restraints at the front spar and leading edge that would eliminate the gap at these locations. Tension tests were repeated at –65°F and 160°F with the specimen housed in an environmental chamber, as shown in Figure 99. The test results, given in Tables 14 and 15, show no abnormalities and the test component remained undamaged.

3.5 SEAL DEVELOPMENT

The first seal material tested was too soft to transfer compression load directly between the ends of the panels at the joint. It also tended to bulge above the surface. An effort was therefore undertaken to develop a satisfactory gap filler and seal which would meet the following objectives:

- Maintain a smooth exterior in compression without bulging, especially at higher temperatures.
- Maintain a smooth exterior for cold conditions without contracting and forming a concave (dish) shape in the gap.
- Have very little permanent set that might result in a significant crack or gap between the seal and the panel edges during flight with LFC.
- Sustain repeated compression, fatigue, and tension joint loads throughout the hot and cold flight environment without cracking, becoming brittle, or allowing water to seep through the gap.

Be hard enough and strong enough to transmit the panel compression loads across the seal with very little compression strain. This requires a modulus of elasticity equal to or greater than the panel's modulus.

Blocks of alternative seal compounds measuring 1.5-inch square by 1.0-inch deep, with strain gages attached to the 1.0-inch sides in the load direction, were provided for compression testing. Equal percentages of EPON 28 resin and hardener were used with various fillers. The fillers included milled fibers of glass, carbon and kevlar, glass shot, ground walnut shells, steel wool, steel granules, and aluminum oxide powder.

It is possible to keep the bulging within the limit for LFC, but none of the fillers increased the modulus of elasticity enough to reduce the bulge. In order to transfer load directly between the panel ends, it was necessary to introduce a strip of titanium into the gap, leaving a minimum thickness of filler. (See Section 4.2.)

3.6 LARGE PANEL TEST — SLIDING JOINT

A sliding-joint test specimen approximately 24 inches wide by 30 inches long was fabricated. Figure 100 shows the base composite panel before the inner skin doublers and outer titanium porous skin were added. Steel rods were inserted in holes in the rubber mandrels to limit thermal expansion during the cure cycle and to ease removal of the mandrels after withdrawing the rods. After bending the outer titanium skin, the panel periphery was machined to size.

Figures 101 and 102 show the details for the axial loaded side of the panels where an end titanium strip was added and tied with countersunk screws into the composite fillers in the inactive flutes. The end titanium strips bore the axial loading across the seal without crushing the flutes.

Figure 103 shows a view of the large sliding-joint panel before the holes were jig-drilled through both fittings at the precise distance parallel to the outer surface. Figure 95 shows the three bolts through both fittings and Figure 104 shows a subassembly of the sliding joint and the panels. Three of the six long bolts on which the panel slides are shown. Figure 104 also shows the relative size of the small sliding-joint test panel resting on top of the large panels. The large panels were attached to a continuous angle along one edge to simulate the attachment to the front spar cap, after which the strain gages were installed.

Figure 105 shows the sliding-joint large test specimen with edge attachments added just before installation in the compression jig fixture. Figures 106 through 108 show the panels modified for tension testing, with holes drilled at the edges for applying tension loads.

3.6.1 Compression Test Arrangement — Large Sliding Joint

Figure 109 shows the 24- by 30-inch panel in its test frame. Details of the setup for compression testing are given in Figures 110 and 111, which show how the test panel was supported to provide precise pin-jointed conditions at all edges. Angle sections were attached to one edge of the panel to simulate continuous attachment of the panel along the front spar. Holes and local doublers were added after compression testing in order to test the joint in tension. These changes are shown in Figure 112.

An MTS machine with a capacity of 250,000 pounds was used for compression testing. The MTS machine and the test equipment automatically plotted the data. A new environmental box was designed around the panels for the hot and cold conditions. Figures 113 through 123 show the final test setup, the instrumentation, and insulation box made for this test.

Figure 113 shows the panels in the MTS machine ready for the room temperature tests. The composite side of the panels in the background is shown in Figure 114. Figure 115 is a side view of the test setup. Figure 116 is a close-up of the composite side. The rib supports are simulated by plates with four bolts through each plate. Figure 117 shows the test setup on the titanium side of the panels with dial indicators to measure any deflections perpendicular to the titanium face. Figure 118 is a close-up of the upper and lower panels. Figure 119 shows three dial gages, used before one was added to measure the step between the panels during the test, as shown in Figure 120. The white box in the foreground is the environmental box containing the hot and cold test specimens. Figure 121 is a view of the white environmental box and the pipe (with insulation covering it) leading to the heating and cooling unit on the right. Figure 122 shows the computer facility for monitoring the temperature and strain gage readings and the input computer facility.

3.6.2 Compression Test Results

The large sliding-joint panels sustained a limit load of 2.5 g (72,120 pounds) at room temperature, -65°F, and 160°F without permanent set and with deflections that were within the LFC waviness tolerance of Figure 1. There was an initial misalignment of the panel surfaces of 0.004 inch, which did not increase by more than 0.0006 inch during loading to the equivalent of 1.67 g (48,000 pounds) under all temperature conditions. No misalignment would occur with the jig control for production panels.

Dial Indicator Analyses — Initially, the room temperature compression test was run to loads that represented a 1.67 load factor and the dial gage readings of Figure 123 were obtained. The maximum value of the wave height was -0.0048 inch. Referring to Figure 1, the maximum allowable height for a wavelength of 6 inches is 0.017 inch at the wing root and 0.027 inch at the wing tip. Although the wave height was well within acceptable limits, a slight step was noticed in the outer surface at the joint. A "feeler" gage was inserted at the joint and a mismatch (step) of 0.004 inch was estimated. Half of this mismatch

was eliminated when the bolts were loosened. A dial indicator was added to monitor the step during loading (see Figure 124).

The loading was then increased to the limit load factor of 2.5 g. At a load factor of 1.67 g (48,000 pounds), the dial readings were +0.001 (upper), 0.000 (center upper), -0.003 (center lower), and +0.0025 (lower) (see Table 3). Two dial gages that were sensitive to 0.0001 inch were then substituted for the center gages and readings were measured up to a limit load factor of 2.5 g, back to 1 g, and finally to zero: Table 20 shows these readings. The more sensitive gages showed a step of only 0.0047 minus 0.0043 or 0.0004 inch at the center, at a load factor of 1.67 (48,000 pounds). The maximum step increase at the 2.5-g limit load of 72,000 pounds was still only 0.0007 inch and the increase remaining at zero load was 0.0002 inch. These were well below the steps that would cause transition if the panels were originally accurately located in line in a jig.

Since the cold and hot conditions were tested in an enclosed thermal box with only the dial indicators exposed, the dial gage stems were adhesively bonded to the titanium with Eastman 910 adhesive to ensure that they would follow the panel deflections. Figure 125 shows these results for the cold condition (-65° F). The single wave deflection at 1.67-g loading was only 0.0032 inch over 6.0 inches and the step was eliminated.

For the hot condition, Figure 126 shows a maximum wave height of only 0.0037 inch.

Strain Gage Analyses — Strain gage values were automatically printed out by the test equipment, and those requested were automatically plotted. Figure 127 shows the strain gage locations. Generally, the odd numbers are on the titanium side of the panel and the even numbers are on the composite side. The automatically plotted and computed results of the strain versus voltage are presented in Figures 21 through 29, where 1 volt is equivalent to 11,000 pounds. At room temperature, gage 13, closest to the joint, had the highest titanium strain of -1,624 μe at a voltage of - 6.5557 (72,120 pounds), which in the titanium is only 25,984 psi. The composite results shown in Figure 22 indicate that gage 10 showed the maximum strain of -3,554 μe at -6.5557 volts (72,120 pounds), which is about 28,320 psi, using a modulus of 8×10^{-6} for the composites. Figure 23 shows a maximum strain on the bolt of 346 μe at gage 19. This gives a maximum stress of only 5,536 psi in the bolt.

At - 65° F, the maximum strain in the titanium is again at the channel 13 strain gage, as shown in Figure 24. At - 6.5826 volts (72,400 pounds), the digital computer showed a strain of -1,790 μe. This is a stress of approximately 28,640 psi, 10 percent more than at room temperature. It should be noted that channel 1 (Figure 24), channel 8 (Figure 25), and channels 18 and 19 (Figure 26) are acting in an irregular manner. This may be due to repeated holding and sliding of the fittings on the bolts. Figure 23 shows that the maximum strain for the composites was again at channel 10. The strain of

$-3{,}303\ \mu e$ is equivalent to 26,424 psi using a modulus of 8×10^{-6}. Figure 26 shows the titanium bolt strain levels. The maximum strain was slightly higher than at room temperature. The erratic readings were most noticeable at - 65°F; this may have been due to shrinkage of the aluminum fitting and bronze bushes, causing them to grip the bolts more tightly at low temperature. Figures 27 through 29 show the strain gage results at 160°F. The maximum strain on the titanium side corresponded to a stress level of 28,352 psi, slightly less than at room temperature. The maximum stress on the composite side was only 11,520 psi. There was a sudden increase in the strain level of the titanium bolt (gage 19, Figure 29), resulting in a higher strain level than at room temperature or - 65°F. However, the maximum strain level of $850\ \mu e$ still resulted in a low stress level of only 13,600 psi.

3.6.3 Tension Test Setup

The ends of the panels used previously in gage compression testing were modified to enable tensile loads to be applied. Holes were drilled in the ends of the large sliding-joint panels as shown in Figures 128 through 130. Figure 128 shows an aluminum block on the right that simulates the front spar, and on the left, titanium strips that are bolted through the panel to bridge the gap. These strips simulated the reinforcement that would occur near the leading edge of actual panels. These strips minimized the gap separation and sustained some of the axial tension loads. Figure 129 shows a side view of the panel with the tension straps. Figure 130 is a close-up of the end of the panels showing two typical bolts attaching the test plates to the sliding-joint panel. The one large bolt (partially in the hole) connects the plates to the head of the test machine.

The tension test setup for the large sliding-joint panels is shown in Figures 131 through 140 and in Table 21. Figures 131 through 133 and especially, Figures 135 and 136 show the simulated rib plates. Figure 135 shows the four rib plates that extend from the fitting flanges. In the foreground, a common long bolt extends through two plates. Inbetween these plates, a heavier plate with the common bolt through it simulates the support structure. Two heavy plates are attached to one flange of a heavy aluminum channel. A collar, with bolts through it and the channel, is attached to the vertical support post of the MTS test machine. After some initial testing, it was determined that the eccentric loading from the heavy plate to the channel, which was then transmitted to the vertical post through the collar, caused excessive deflections. To reduce these deflections, the channel was supported by an additional collar (see Figure 137). This significantly reduced the bowing deflection of the panel when the tension loads were applied.

3.6.4 Tension Test Results

Tensile loading of the LFC panel joint cannot affect the performance of the LFC system, which is designed to operate within 1.0 ± 0.5 g. The joint would still be in compression even at the lowest operating load factor of + 0.5 g. Any waviness, steps, or gaps that occur under tension loading are therefore not relevant to LFC. However, the panel joint must be able to withstand tensile strains that can occur

when the aircraft is landing or experiencing negative g conditions. The effects of tensile loading on surface anomalies are presented for the record in Figures 12, 13 through 17, and 141, but warrant no comment for the reasons stated above.

Figure 142 shows the strain gage placement for the tension tests. Tables 22 through 30 show the strain values up to the limit tension load of -1.0 g. The maximum strain on the titanium side was 473 μe, which gave a maximum stress of only 7,568 psi using an elastic modulus of 16×10^{-6}. All of these stress and strain levels were very low compared with the material strengths.

This page intentionally left blank

SECTION 4
FINAL PANEL JOINT CONFIGURATION

Although both of the tested configurations met the requirements for strength and contour control for LFC, a number of shortcomings had been discovered. With the three-rib concept, it would be difficult to align the attachment holes in the panel and substructure when replacing the panel without using jacks to bring the wing into an unstrained condition. In addition, the panel fasteners were bolted into anchor nuts within the panel. If damage occurred, possibly through misalignment, the anchor nuts would be difficult to replace. With the sliding joint, there was concern that the fittings might not always slide. Any misalignment would increase friction, and increasing clearance on the bolt diameter to reduce friction would allow a corresponding mismatch at the surface. Another consideration was the heaviness of the sliding fittings. Further development of the panel joint was needed.

4.1 IMPROVED PANEL DESCRIPTION

The final panel joining design utilized the best features of the previous concepts and avoided the concerns. The improved design is shown in Figures 143 and 144. This modified three-rib concept offers the following advantages:

1. The fittings are permanently attached to the panels, making it unnecessary to disturb and possibly damage the trapped anchor nuts when changing panels.
2. There is no longer a need for liquid shim to control the distance from the surface to the face of the splice plate.
3. The holes in the end flanges of the panel can be drilled in a master jig to ensure their exact matching distance to the outer surface contours at the joint. The panels can then be changed easily in service with no need for shims or skills in fitting. This was an advantage of the sliding joint, but the new joint avoids the need for in-line reamed holes for the long bolts and a sliding fit.
4. It is no longer necessary to jack the wing to achieve a stress-free condition in order to insert the attachments. When panels are replaced, the airplane will normally be supported by the gear. The resulting wing bending stretches the upper wing surface, thereby increasing the gap in which the panel is installed. Then, when the bolts connecting the end flanges of the panels are tightened, the panels will be stretched until their strain matches that of the wing surface. The panel attachment holes along the front spar and those on the panel will then automatically come into alignment, enabling the remaining fasteners to be installed easily.

4.2 FINAL PANEL TEST SPECIMEN

4.2.1 Improved Panel Joint

The complete test specimen is shown in Figures 143 through 145. Detail components are displayed in Figure 146. The channel sections and a steel bar were bolted to the simulated rib webs to provide a resistance to differential rib movement that would be present with a complete leading edge box assembly. The test specimen is shown alongside the previous joint test specimens in Figure 147.

The flanged fitting, shown attached to a panel in Figure 148, is of composite material. The composite was a fiberglass cloth with a balanced weave and an epoxy-resin system. The resin content was 36 percent. Thirty plies were built-up at the flange. After a 90-degree turn, the 30 plies were held for approximately 1 inch and then tapered down to 14 plies at the ends. It was laid up on the panel to ensure that it exactly matched the panel surface. A titanium plate was provided to spread the bolt loads and to reduce bending stresses in the flange.

A titanium strip and a stiff sealant were inserted between the ends of the panels, as shown in Figure 149. This was to provide a direct load path between the ends of the panels when under compression.

4.2.2 Composite Flange Test Specimen

An additional specimen was fabricated to test the strength and stiffness of the composite flange before proceeding with the main test. Figure 150 shows the completed test specimen with two flanged test components assembled back-to-back.

4.2.3 Composite Flanged Component Test

Strain gages and a dial gage were located on the test specimen as shown in Figure 151. The strain gage readings from tensile testing at room temperature, –65°F, and 160°F are shown in Tables 31 through 36 and the values are plotted in Figures 152 through 160. As expected, channels 5 and 6, located at the beginning of the thinner section, showed the highest stresses. Testing in the hot condition was continued until failure occurred at a load of 14,160 pounds. Cracks occurred at the flange root at approximately 45 degrees to the load direction, as shown in Figures 151 and 161, due to a combination of bending tension and shear stresses.

Progressive dial gage readings showed nothing unusual. The lateral displacement was 0.020 inch at the 8,000-pound ultimate tension load for the 4.5-inch-wide specimen and occurred at room temperature. The test indicated that a flanged composite member of this type should meet the requirements for load transfer in tension.

4.2.4 Improved Panel Joint Test

The improved joint specimen was tested in compression and tension at temperatures of –65°F, room temperature, and 160°F. The stress levels were determined by strain gages and deflections were measured with dial gages and an extensometer. The sensors were located as shown in Figure 162.

4.2.4.1 Compression Testing — Representative loads for the 4.5-inch-wide specimen were:

Limit of active LFC = –8,000 pounds (1 g + 0.5 g)

Limit load = –13,333 pounds (2.5 g)

Ultimate load = –20,000 pounds (2.5 $g \times 1.5$)

The test specimen was loaded to more than the limit load but less than ultimate, so that the same specimen could be used for the whole series of testing.

Figures 163 through 166 show the strain gage results at room temperature. After the initial misfits had been aligned at the lower load levels, the load/strain relationships became straight lines. This indicated continuing elastic behavior with no apparent failure up to the maximum load applied.

The maximum strain of the titanium surface at the limit load of –13,333 pounds was -1.57×10^{-3} in./in. at strain gage 13. This is equivalent to a stress of –25,277 psi which extrapolates to a maximum stress of –37,916 psi at 20,000 pounds ultimate load, assuming a constant E value of 16.1×10^6. This is well below the compression yield strength of 132,000 psi for 6A1 4V titanium alloy used.

On the composite side of the panel, the maximum compressive strain at the limit load of –13,333 pounds was -1.73×10^{-3} at gages 18 and 20; the equivalent maximum stress was –14,013 psi. This extrapolates to –21,020 psi at the ultimate load of –20,000 pounds, assuming a constant E value of 8.1×10^6.

The extensometer readings are plotted in Figure 167. They produced a smooth curve, which showed a compression of –0.007 inch over the 1.0-inch gage length at the limit load of 2.5 g or –13,333 pounds. By subtracting the titanium strain at this load, it can be deduced that the gap filler was compressed by 0.006 inch. The LFC system is only designed to be effective up to + 1.5 g or a –8,000-pound load on the test specimen. At this load, the extensometer reading was –0.0056. Subtracting the titanium strain, the gap filler would be compressed by 0.006 – 0.001, or 0.005 inch. Assuming a value of 0.3 for the Poisson's ratio for the filler, the outward bulge is not sufficient to cause transition from laminar to turbulent flow over the surface, and would be acceptable.

The dial gage readings of lateral deflections of the titanium surface are listed in Figure 2. At the 1.5-g (–8,000-pound) design limit for LFC, the step at the joint was 0.001 inch; this is acceptable.

The wave depth h at an 8,000-pound load was 0.0035 – (0.0023 – 0.0001)/2 = 0.0023 inch over a wavelength λ of 13.0 inches. This is an h/λ value of 0.000177 in the direction of the leading edge or front spar. However, the wavelength in the airflow direction would depend on the sweep angle 'λ' so that the effective wavelength 'λ_e' = $\lambda_o/\sin$ or the effective h/λ_e would be $0.000177 \times 0.5 = \lambda/0.0000885$ for the test panel. This is far below the waviness that would cause transition. Figures 30 through 34 and Figure 168 show the strains and deflections under tensile loading at – 65°F, while Figure 20 and Figures 35 through 38 show the results at 160°F. All of these readings show no unusual behavior and are no higher than the corresponding room temperature readings discussed previously.

4.2.4.2 Tension Testing — The undamaged specimen used for compression testing was also used for tension testing. The specimen was loaded to 7,000 pounds, which exceeded the tensile limit load of 5,333 pounds, at room temperature and at 160°F. Finally, the specimen was loaded to the ultimate tensile load of 8,000 pounds at – 65°F.

The strain gage readings for the testing at room temperature and at 160°F are plotted in Figures 39 through 42 and 169 through 172. At these temperatures, the maximum strain at the composite surface was 0.00148 in./in. which corresponds to a stress of 12,000 psi at gage 8. The maximum strain at the titanium surface was 0.00051 in./in., equivalent to 8,211 psi, at gage 3. Both stresses are low for these materials at limit load.

The extensometer readings are shown in Figures 43 and 44. The maximum gap at limit load was 0.057 inch at 160°F. This is acceptable because LFC is not functional under negative g conditions.

The strain gage results at – 65°F are shown in Figures 45 through 47. Gages 11, 13, 15, 17, and 19 on the lower titanium surface (Figure 45) and gages 10, 12, and 16 on the upper composite surface (Figure 47) show a sudden increase in strain levels at a 6,000-pound load. Since there were no apparent failures, the specimen was cut open for an internal inspection. No signs of failure could be found. This confirmed that the specimen withstood loading in compression and tension at all three temperatures without failure.

It was concluded that the sudden change was due to relative movement at the bolts attaching the specimen to the simulated rib supports. The hole clearance at the bolts had allowed movement when the rib reactions exceeded the friction clamping that results from bolt tightening.

Contraction of the composite material at – 65°F would result in a reduction of the bolt clamping force. This is why the loads did not occur during testing at room temperature and at 160°F. Figures 45 and

47 show that strain subsequently increased at about the same rate as before the slippage. This showed that the joint specimen was continuing to transfer the tension loading.

Despite this event, the stress levels at - 65°F were not excessive at the ultimate tension load of 8,000 pounds. The maximum strain at the composite surface was 0.004 in./in., indicating a maximum composite stress of 32,400 psi, well below its ultimate strength. The maximum strain at the titanium surface was 0.0013 in./in., which corresponded to a very low stress of 21,320 psi.

The dial gage readings are shown in Figures 18, 19, and 173. The center gage readings show that unacceptable step-heights of 0.0063 and 0.0079 inch had occurred without load following testing at room temperature and 160°F. Since no failures had occurred, this could only have been caused by panel movement due to bolt clearance. This confirmed that the bolt clearances were too large.

This page intentionally left blank

SECTION 5
CONCLUSIONS AND RECOMMENDATIONS

5.1 CONCLUSIONS

5.1.1 Sliding-Joint Concept

The sliding-joint concept, although meeting the requirements of strength and panel deflections, has the following disadvantages:

1. A step can occur at the joint because of the tolerances needed to insert the long bolts and obtain a sliding fit.
2. The cost of the machined parts aligning the panels against a strong mold and drilling the long bolt holes with close tolerance would be high compared with costs of fabricating the three-rib joints.
3. The large fittings needed to contain the sliding bolts would result in a weight penalty relative to the alternative three-rib joint.

5.1.2 Three-Rib Concept

The final three-rib splice was most successful in meeting the design objectives for chordwise joints between removable LFC panels. The test specimen met all of the compression and tension load requirements at –65°F, room temperature, and 160°F without any indication of failure. It satisfied the requirements for waviness and smoothness across the joint under all conditions appropriate to the use of LFC. In addition, it overcame the disadvantages of the earlier three-rib design cited in Table 2.

The only concern was a slight residual step at the joint after tension testing. Subsequent analysis showed this to have been caused by differential panel movement allowed by hole clearances at the tie-bolts between the panels. This could be avoided in the future by having a closer fit to ensure that any differential panel movement could not exceed the maximum step height allowed for LFC panel joints. SLEVbolts could be used along the bolt row. The regular close-tolerance bolts would first be tightened to pull the panel ends together. Then, the expanding SLEVbolts would be used to avoid any differential panel movement. Both types of bolts would have tension loads between the panels.

It is believed that joints of this type would also satisfy the requirements of interchangeability and replacement in the field without use of shims or excessive hand fitting to ensure smoothness after installation.

The guiding principles followed in developing this joint design would be applicable to alternative LFC panel designs and should result in a satisfactory joint.

5.2 RECOMMENDATIONS

1. The bolts connecting the LFC panels should fit to a close tolerance. To facilitate this, it is recommended that metal bushings be used for the close-tolerance holes in the composite material. This would also minimize hole deflection under bearing loads and reduce the possibility of bolt bending.

2. Further development of the "gap filler/seal" system should be undertaken to ensure long life and easy replacement.

3. Although the final three-rib specimen withstood repeated loading in tension and compression at both normal and extreme temperatures, the joint needs to be tested under representative fatigue conditions before being used extensively in flight. The test specimen should have a representative wing leading edge shape and be subjected to the full spectrum of loading conditions, including aerodynamic loads and strain imposed by the main wing deflections.

4. A development program is needed for the spanwise joint. This could be combined with the task described in Item 3.

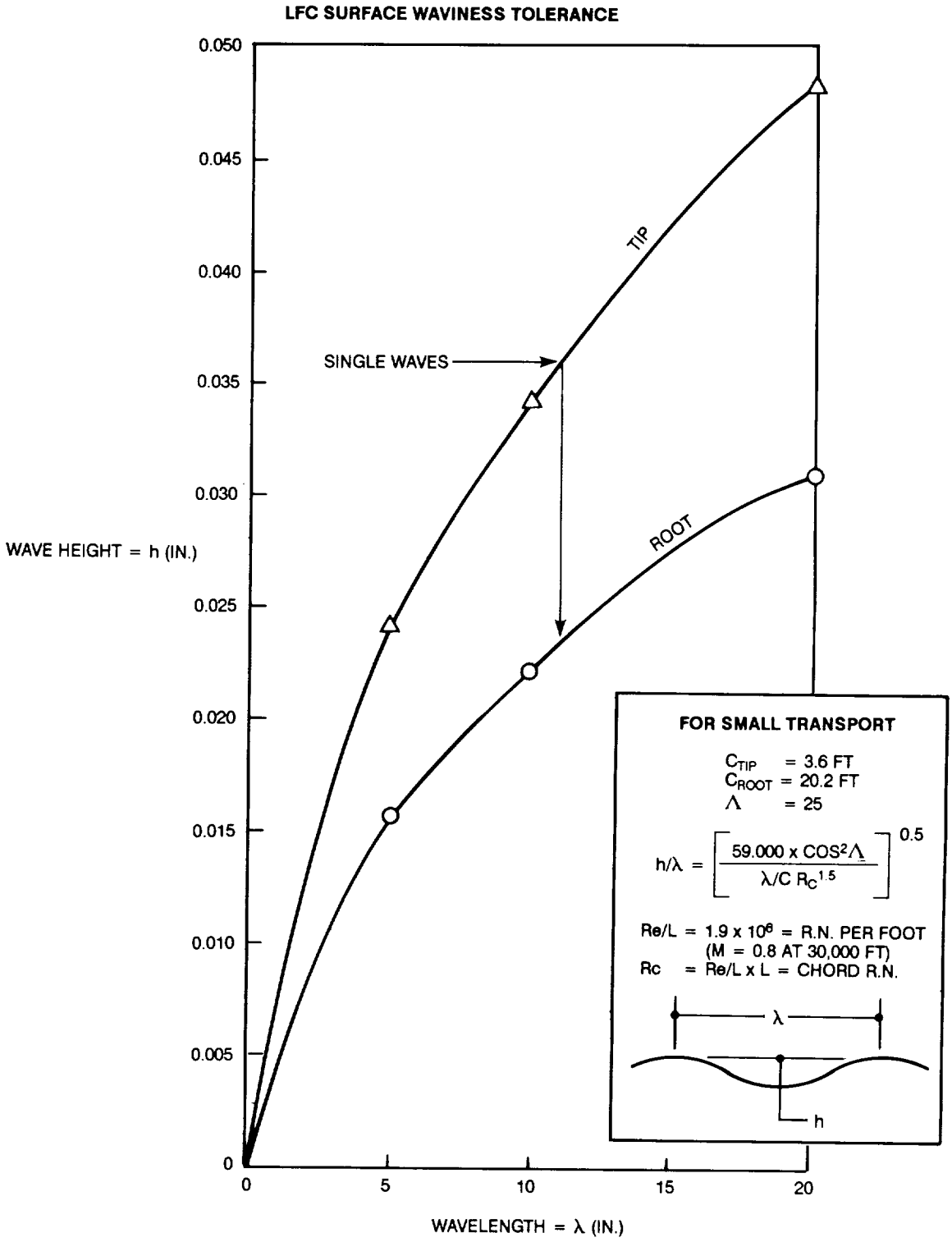

SOURCE: NASA CR NO. 178166

FIGURE 1. WAVE HEIGHT VERSUS WAVE LENGTH AT WING TIP AND ROOT TO AVOID TURBULENCE

LOAD (1,000 LB)	UPPER	CTR UPPER	CTR LOWER	LOWER
0	0	0	0	0
0.5	–0.0005	+0.0005	+0.0003	–0.0007
1	+0.0007	+0.0006	+0.0004	–0.0018
2	+0.0025	+0.0016	+0.0013	–0.0020
3	+0.0034	+0.0017	+0.0013	–0.0030
4	+0.0038	+0.0025	+0.0023	–0.0032
5	+0.0039	+0.0034	+0.0023	–0.0025
6	+0.0035	+0.0035	+0.0023	–0.0012
7	+0.0028	+0.0035	+0.0023	0
8	+0.0023	+0.0035	+0.0023	+0.0011
9	+0.0016	+0.0044	+0.0024	+0.0022
10	+0.0010	+0.0045	+0.0024	+0.0031
11	+0.0005	+0.0045	+0.0027	+0.0042
12	0	+0.0045	+0.0033	+0.0050
13	–0.0005	+0.0045	+0.0033	+0.0060
14	–0.0014	+0.0055	+0.0033	+0.0072
15	–0.0020	+0.0055	+0.0034	+0.0085
16	–0.0028	+0.0064	+0.0034	+0.0096
0	–0.0038	+0.0022	+0.0025	+0.0021

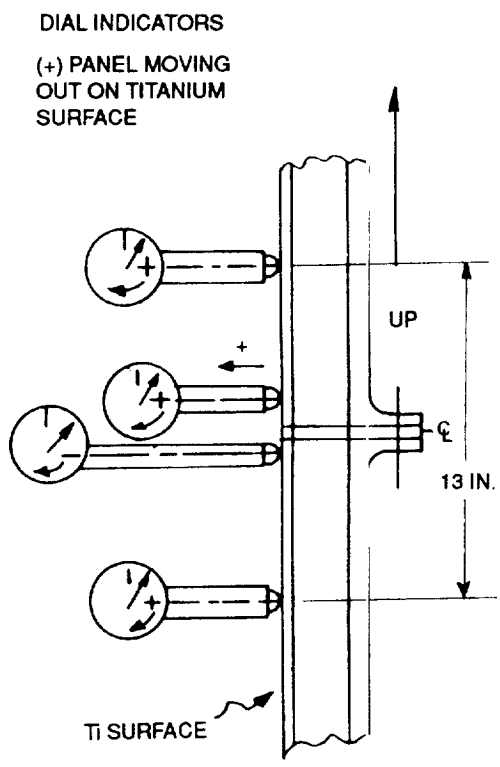

FIGURE 2. DIAL GAGE READINGS FOR MODIFIED JOINT PANEL IN COMPRESSION AT ROOM TEMPERATURE

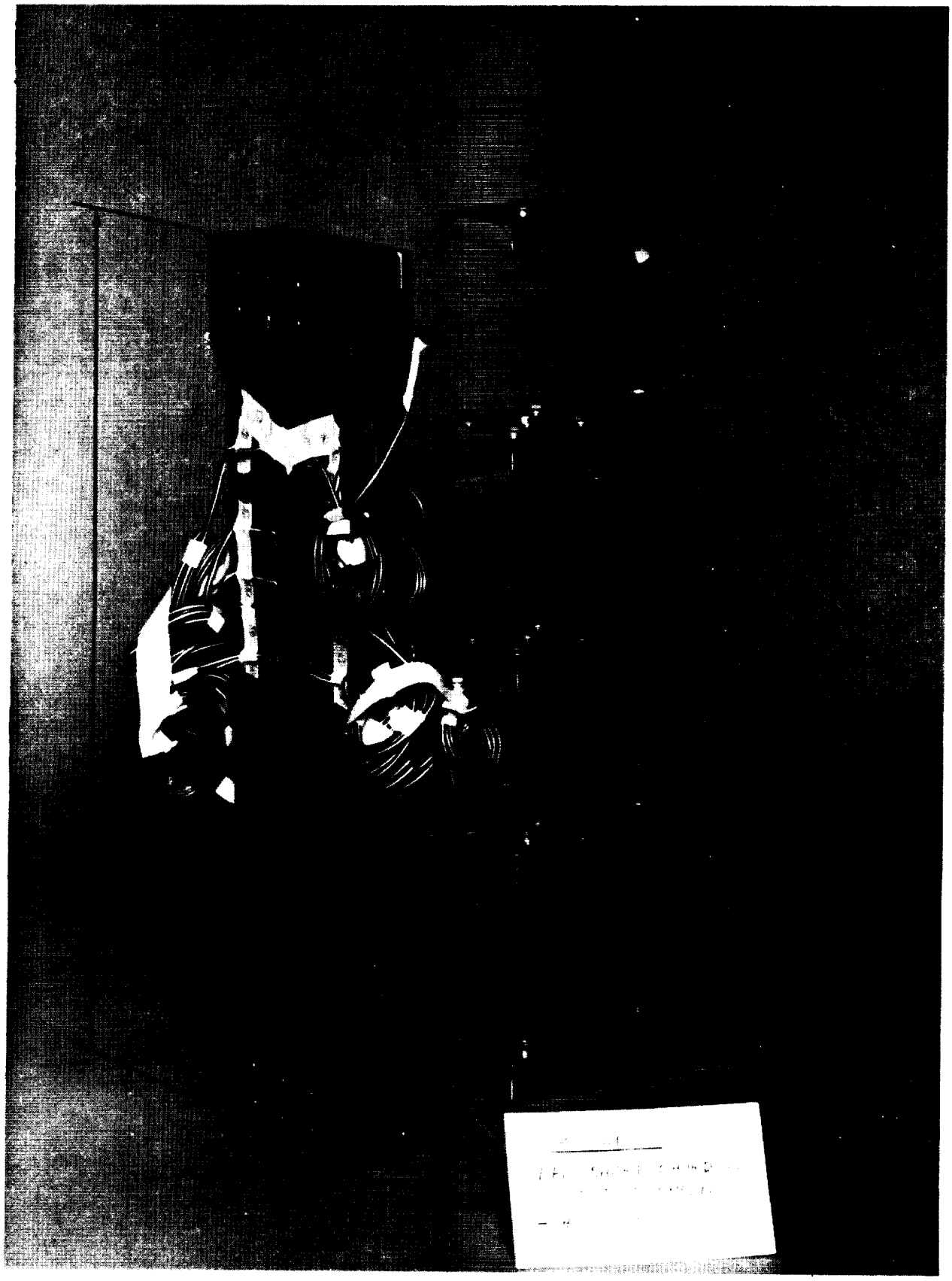

FIGURE 3. THREE-RIB JOINT — TITANIUM SIDE

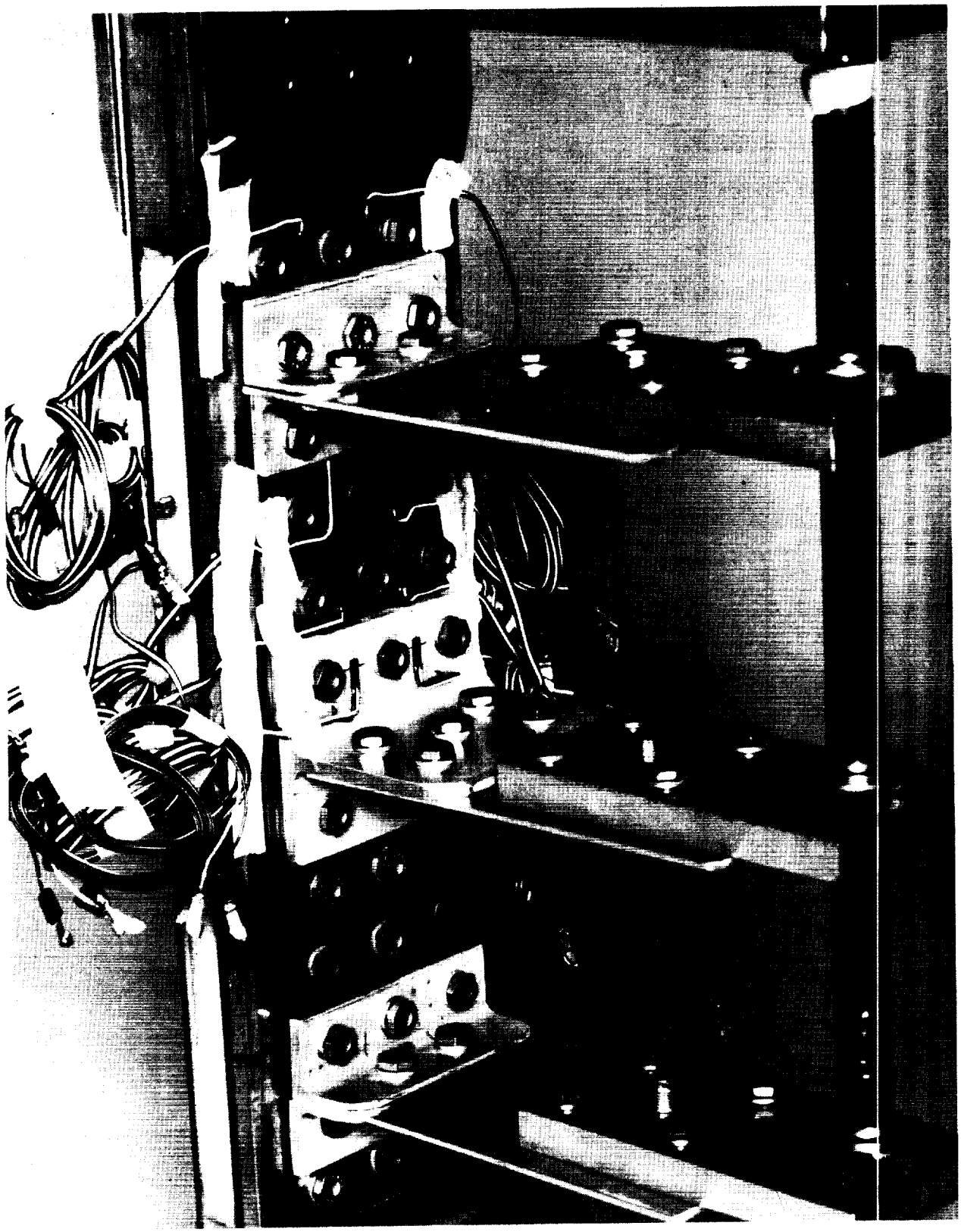

FIGURE 4. THREE-RIB JOINT — COMPOSITE SIDE

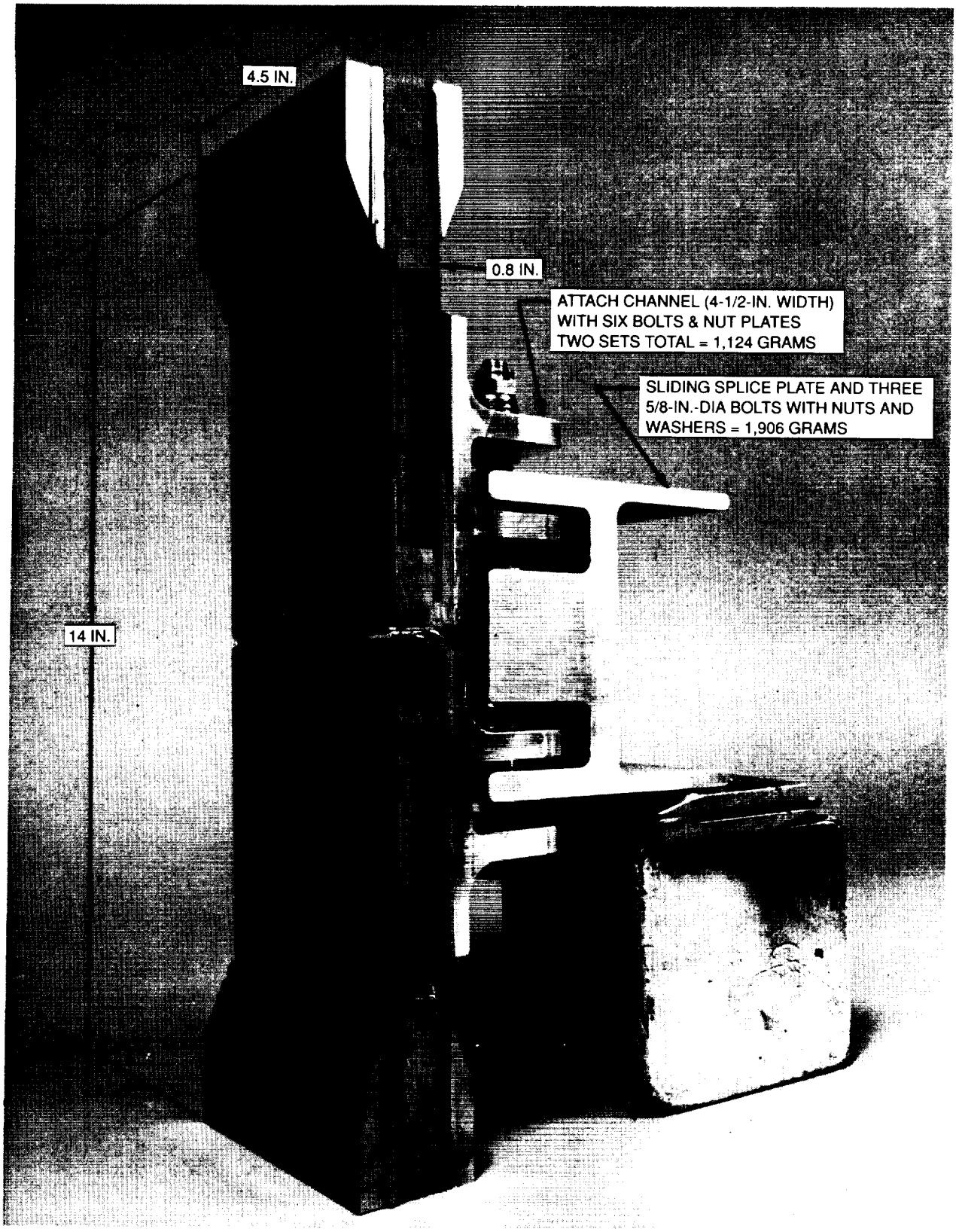

FIGURE 5. SMALL SLIDING JOINT

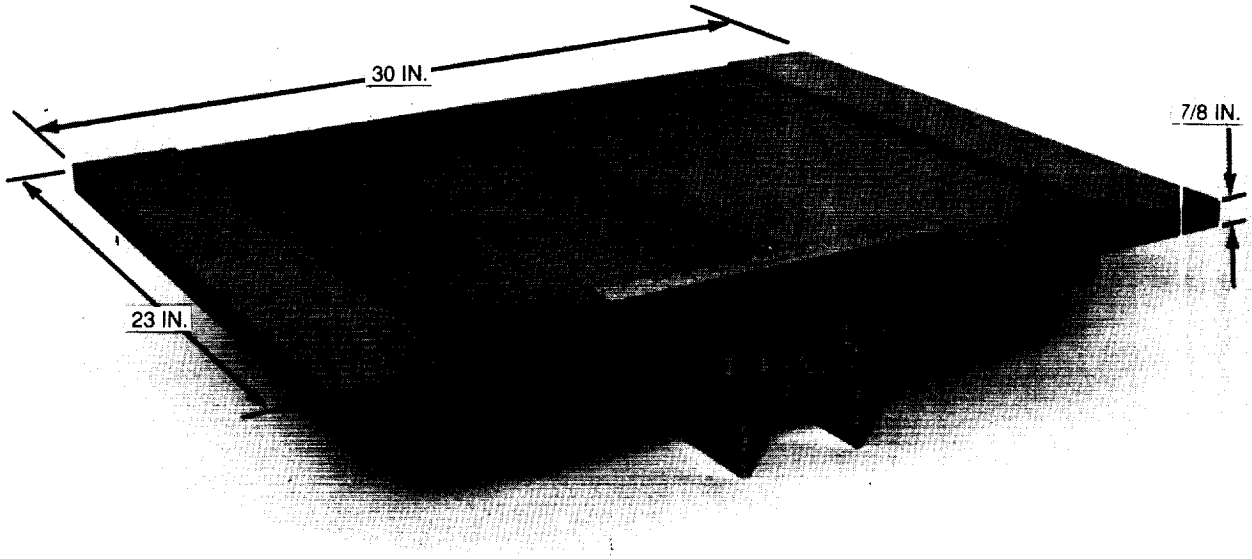

FIGURE 6. LARGE SLIDING JOINT — TITANIUM SIDE

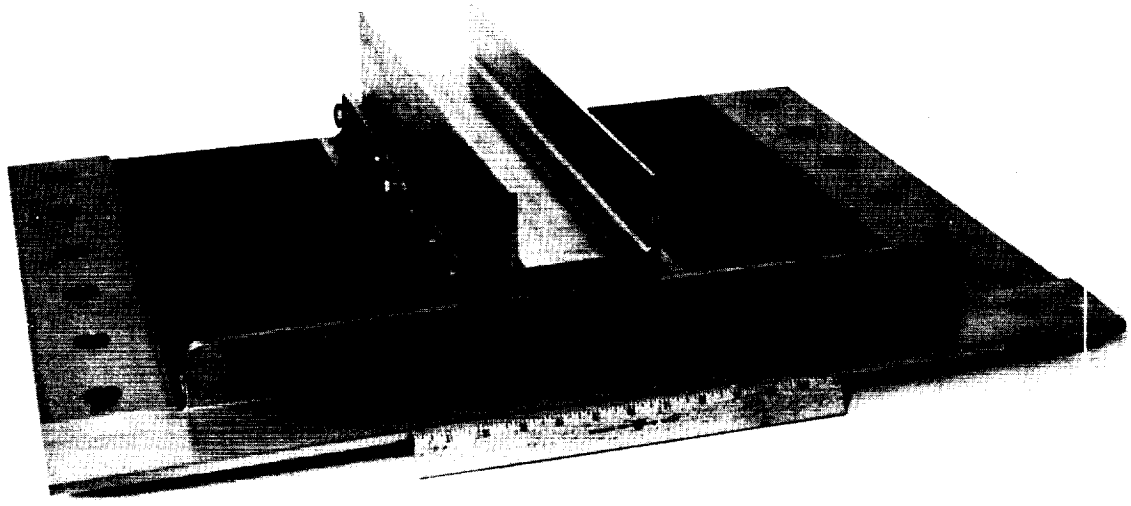

FIGURE 7. LARGE SLIDING JOINT — COMPOSITE SIDE

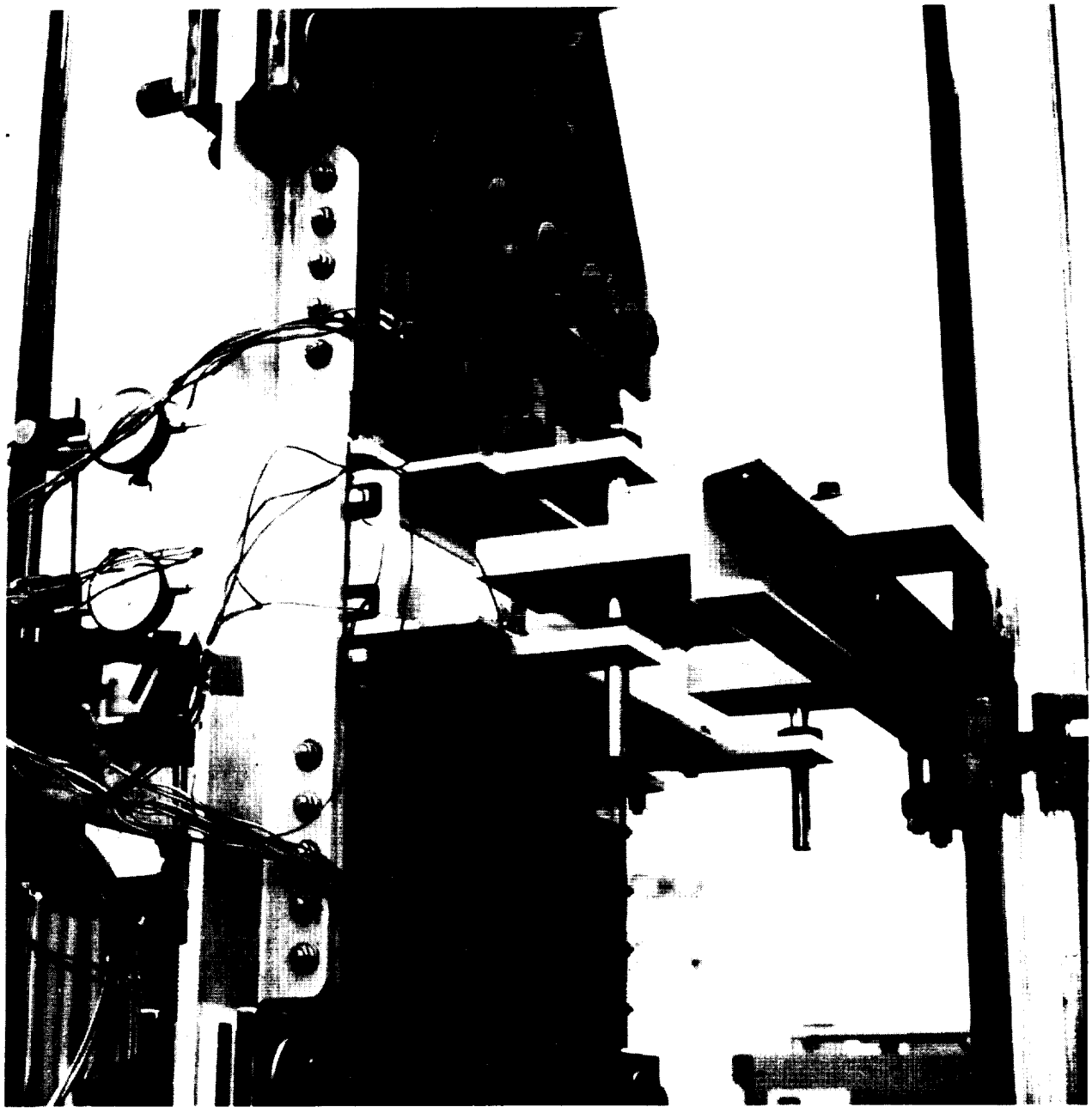

FIGURE 8. LARGE SLIDING JOINT — TEST JIG FOR TENSION

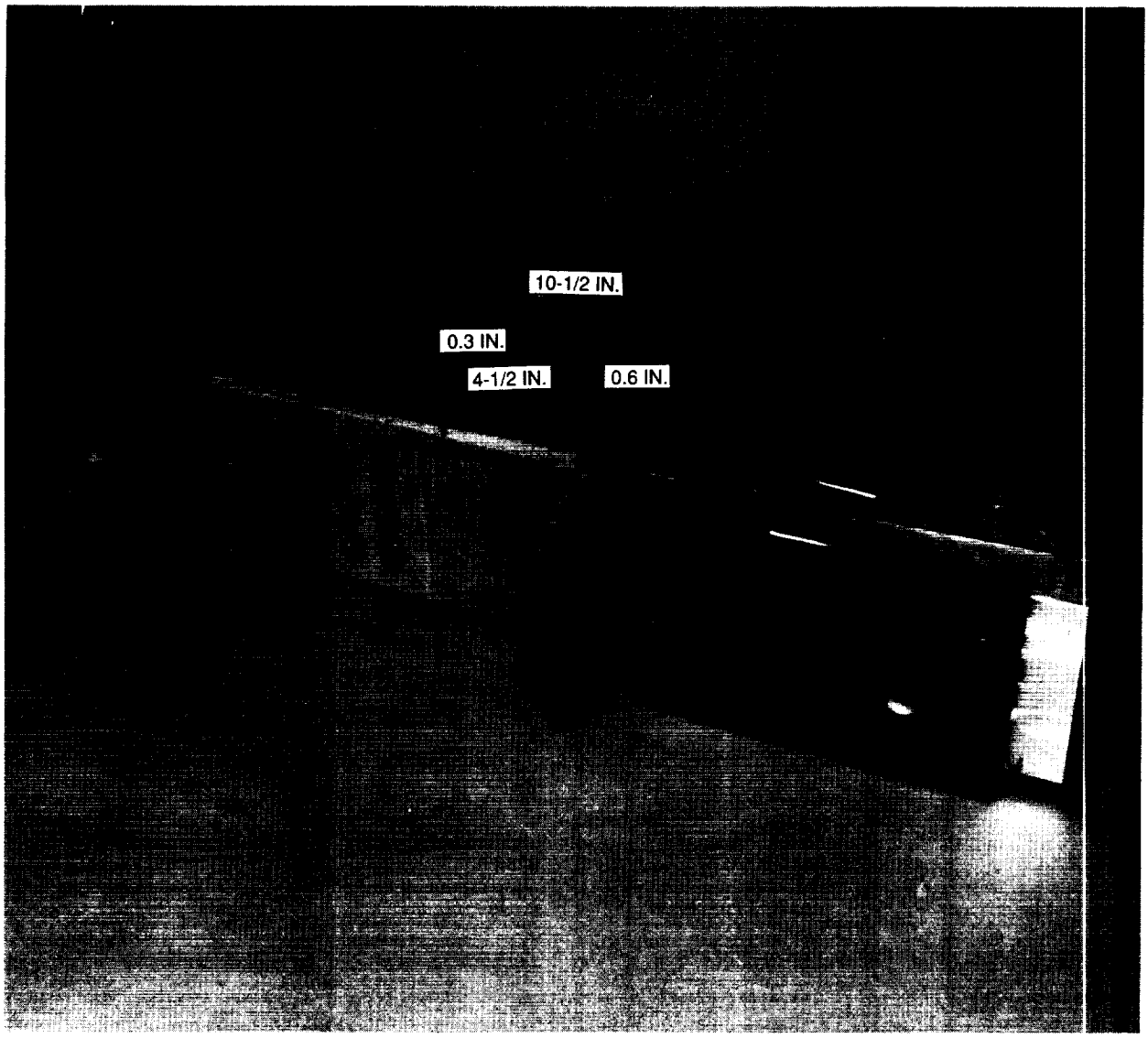

FIGURE 9. COMPOSITE TAPERED JOINT — BACK-TO-BACK ANGLES

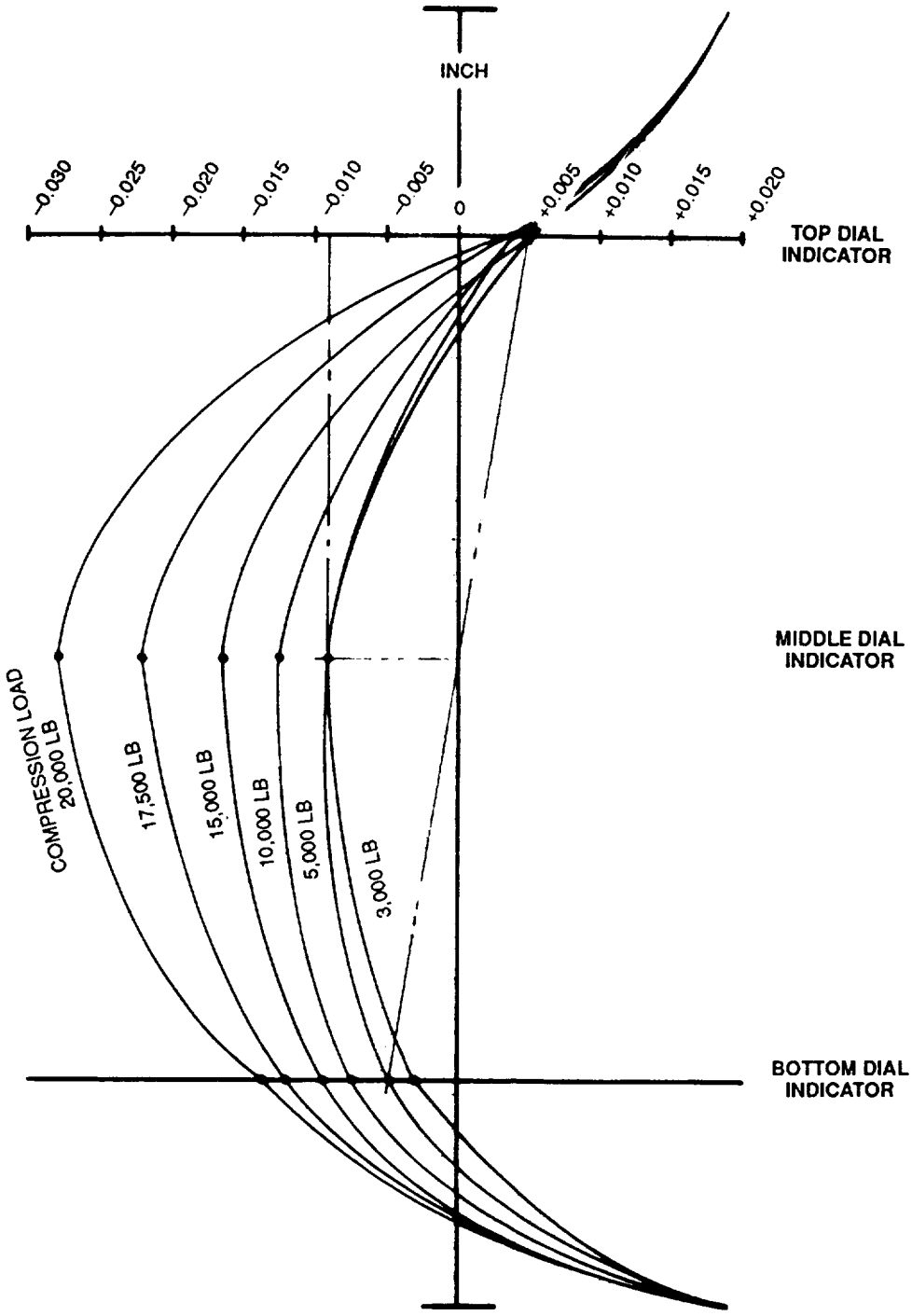

NOTE: 18-1/2 INCHES TOTAL LENGTH. 12-INCH SPAN BETWEEN TOP AND BOTTOM INDICATORS.

FIGURE 10. DIAL INDICATOR READINGS

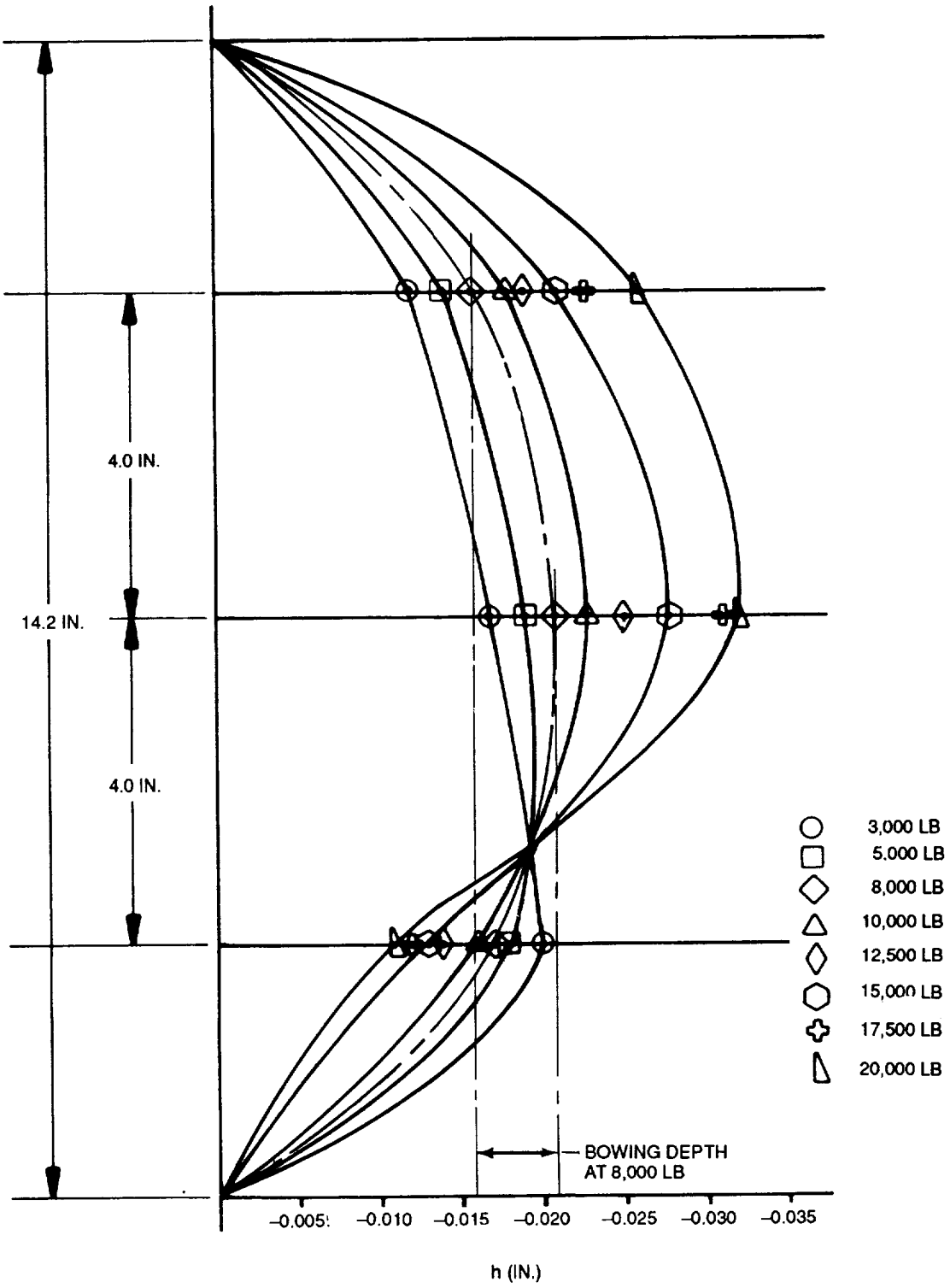

FIGURE 11. DIAL INDICATOR READINGS — SLIDING-JOINT SMALL PANEL COMPRESSION AT ROOM TEMPERATURE

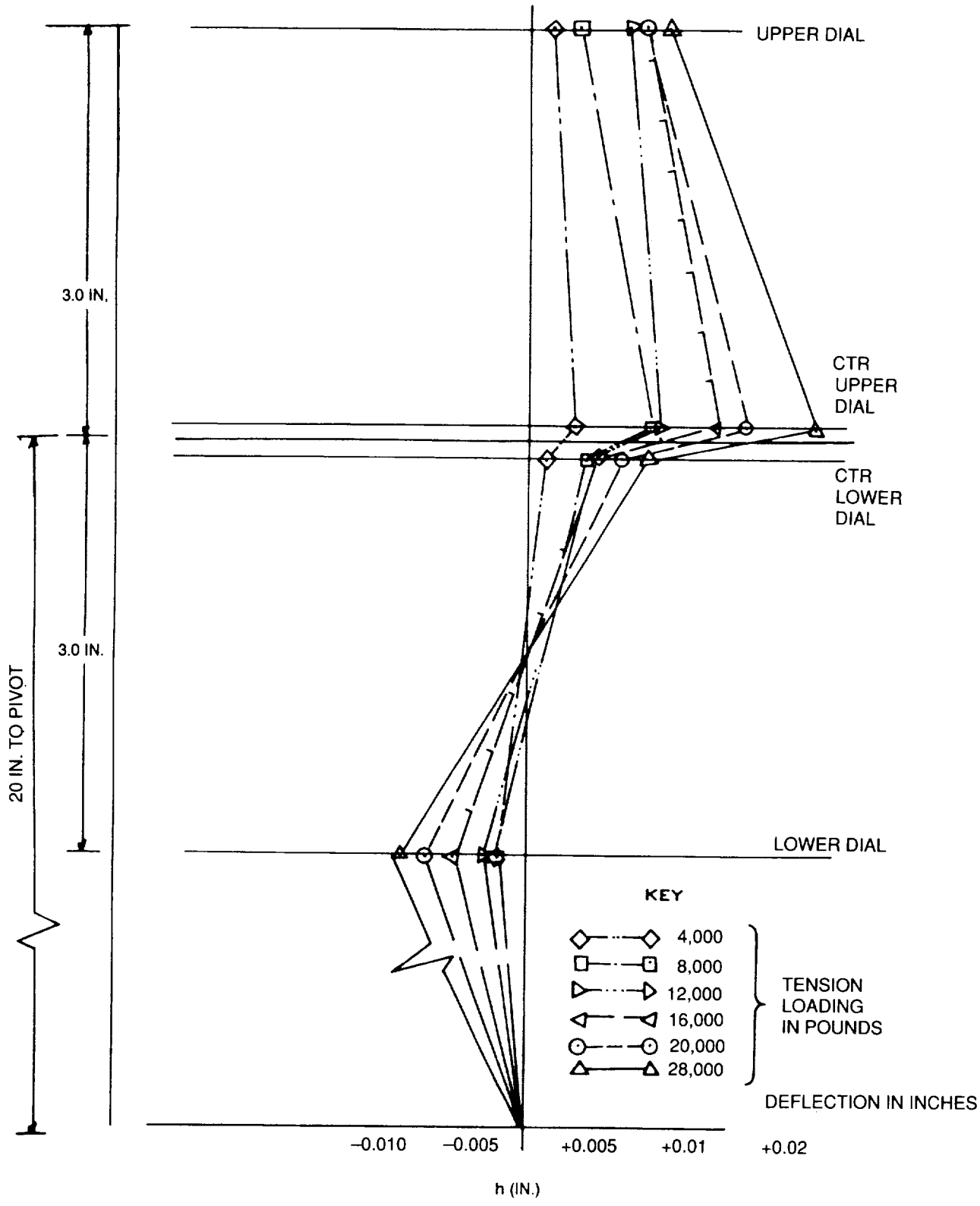

FIGURE 12. DIAL INDICATOR READING — TENSION TEST FOR THE LARGE SLIDING JOINT AT ROOM TEMPERATURE, RUN NO. 2 (WITH ADDITIONAL RIB CONSTRAINT)

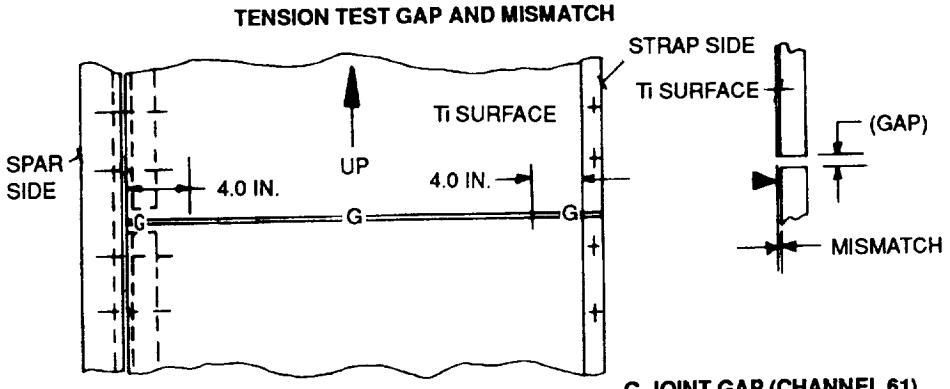

MISMATCH

LOAD (1,000 LB)	SPAR SIDE (IN.)	STRAP SIDE (IN.)
0	0.004	0.002
4	0.003	0.001
8	0.003	0.0015
12	0.004	0.002
16	0.006	0.0015
20	0.009	0.0015
24	0.008	0.0015
28.2	0.013	0.0015
0	0.002	0.000

G-JOINT GAP (CHANNEL 61)

LOAD (1,000 LB)	SPAR SIDE (IN.)	STRAP SIDE (IN.)	CENTER (EXTENSOMETER)
0	0.008	0.004	0
4	0.012	0.006	0.0059
8	0.014	0.008	0.0131
12	0.018	0.010	0.0198
16	0.025	0.012	0.0282
20	0.032	0.0135	0.0370
24	0.042	0.017	0.04470
27.8	—	—	0.0529
28.2	0.0445	0.017	0.080
0	0.010	0.006	0.0091

FIGURE 13. ROOM TEMPERATURE TEST RESULTS OF THE LARGE SLIDING-JOINT PANEL ASSEMBLY (24 BY 30 IN.)

LOAD (1,000 LB)	UPPER	CTR UPPER	CTR LOWER	LOWER
0	0	0	0	0
4	+0.0005	+0.0012	+0.0002	–0.0030
8	+0.0065	+0.0075	+0.0039	–0.0040
12	+0.0070	+0.0098	+0.0051	–0.0040
16	+0.0082	+0.0133	+0.0069	–0.0062
18	+0.0092	+0.0151	+0.0077	–0.0078
20	+0.0100	+0.0167	+0.0086	–0.0086
22	+0.0106	+0.0184	+0.0096	–0.0090
24	+0.0112	+0.0205	+0.0105	–0.0090
26	+0.0120	+0.0216	+0.0121	–0.0090
28	+0.0128	+0.0233	+0.0128	–0.0090
0	+0.003	+0.0037	+0.0029	+0.0010

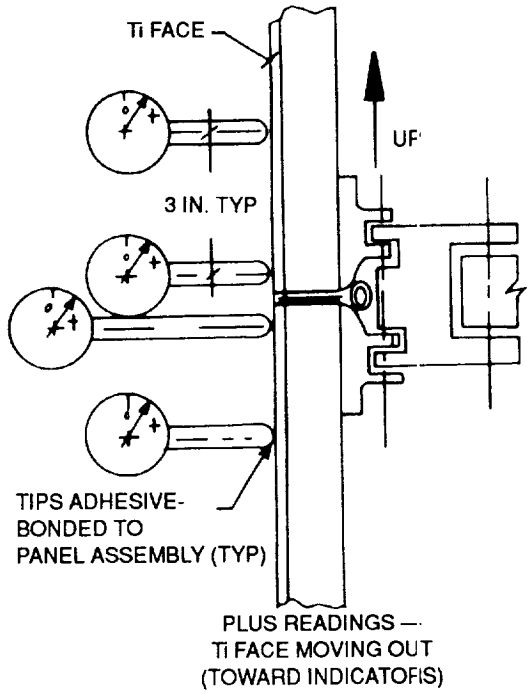

FIGURE 14. TENSION TEST FOR LARGE SLIDING-JOINT PANEL ASSEMBLY (24 BY 30 IN.) AT COLD (–65°F) CONDITION (WITH ADDITIONAL RIB CONSTRAINT)

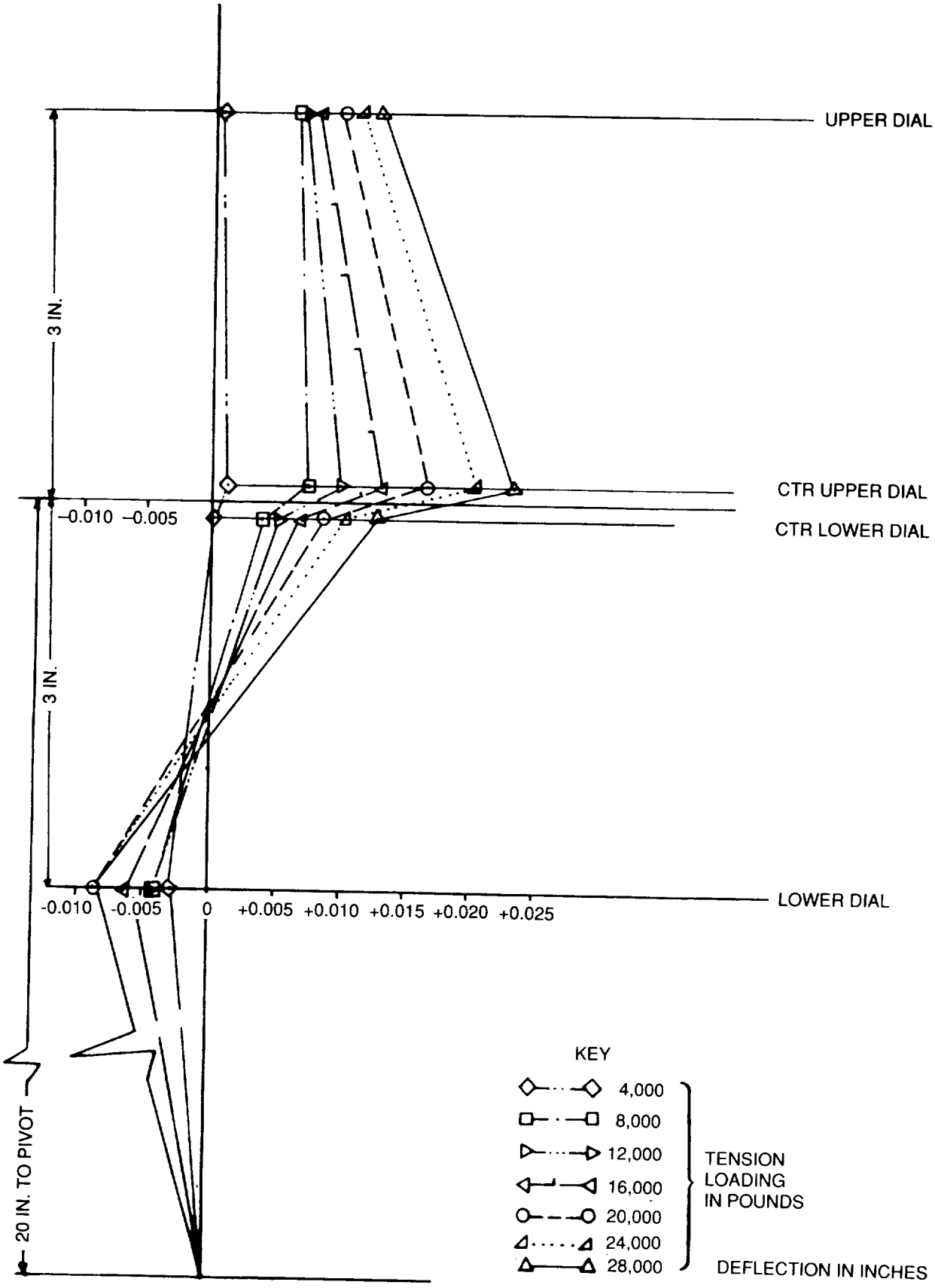

FIGURE 15. DIAL INDICATOR READING — TENSION TEST FOR THE LARGE SLIDING JOINT AT COLD (–65°F) CONDITION (WITH ADDITIONAL RIB CONSTRAINT)

LOAD (1,000 LB)	UPPER	CTR UPPER	CTR LOWER	LOWER
0	0	0	0	0
4	+0.0010	+0.0033	+0.0023	–0.001
8	+0.0060	+0.0082	+0.0056	–0.001
12	+0.0060	+0.0099	+0.0063	–0.0015
16	+0.0070	+0.0121	+0.0071	–0.0034
18	+0.0076	+0.0132	+0.0075	–0.0040
20	+0.0080	+0.0143	+0.0080	–0.0050
22	+0.0082	+0.0153	+0.0084	–0.0055
24	+0.0090	+0.0166	+0.0089	–0.0065
26	+0.0090	+0.0177	+0.0096	–0.0070
28	+0.0100	+0.0192	+0.0102	–0.0078
0	+0.0010	–0.0012	+0.0013	+0.003

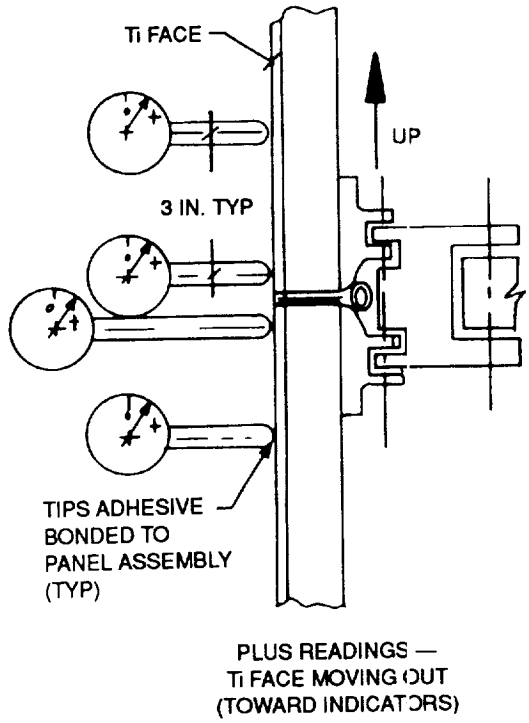

FIGURE 16. HOT(+165°F) DIAL INDICATOR READINGS TENSION TEST FOR THE LARGE SLIDING-JOINT PANEL ASSEMBLY (24 BY 30 IN.) (WITH ADDITIONAL RIB CONSTRAINT)

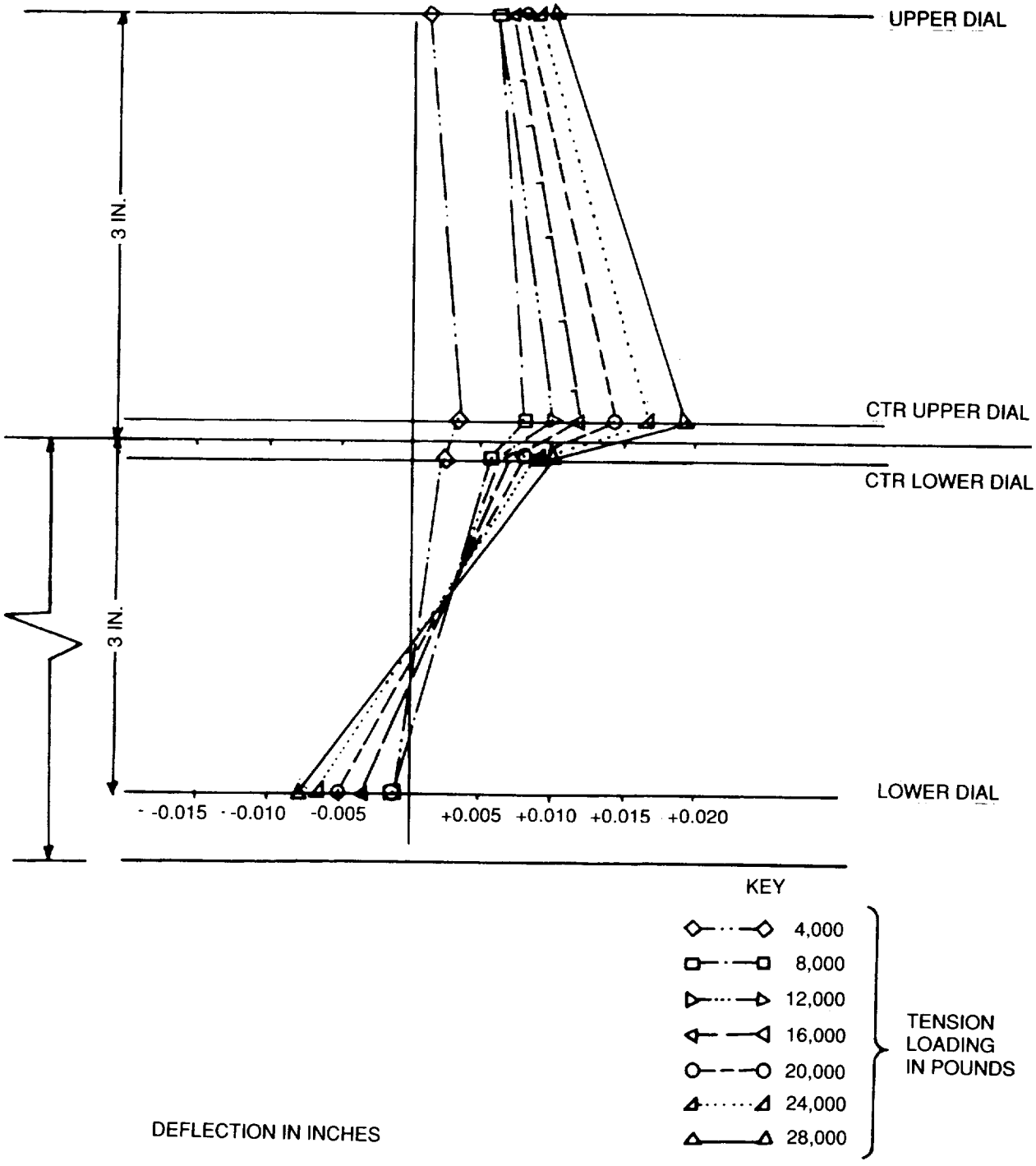

FIGURE 17. DIAL INDICATOR READING — TENSION TEST FOR THE LARGE SLIDING JOINT AT HOT (+160°F) CONDITION (WITH ADDITIONAL RIB CONSTRAINT)

LOAD (1,000 LB)	UPPER	CTR UPPER	CTR LOWER	LOWER
0	0	0	0	0
0.5	+0.0062	+0.0009	–0.0022	–0.0040
1	+0.0066	+0.0018	–0.0022	–0.0052
2	+0.0086	+0.0042	–0.0017	–0.0050
3	+0.0030	+0.0068	–0.0014	–0.0035
4	+0.0032	+0.0085	–0.0011	–0.0040
5	+0.0028	+0.0004	–0.0004	–0.0042
6	+0.0018	+0.0005	+0.0009	–0.0050
7	–0.0008	+0.0008	+0.0014	–0.0050
0	–0.0060	+0.0048	–0.0015	+0.0080

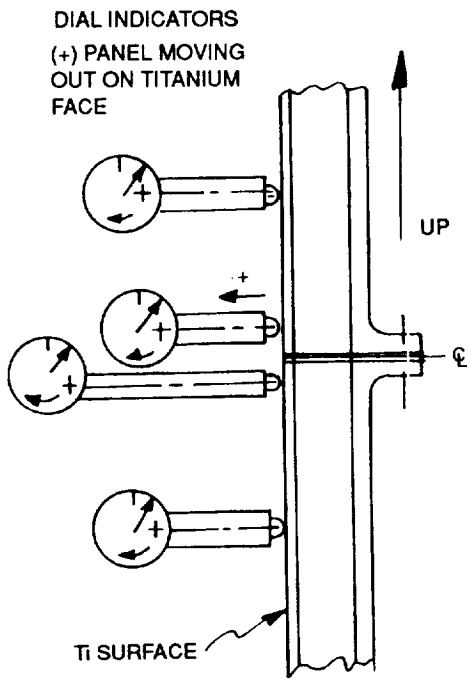

FIGURE 18. DIAL GAGE READINGS FOR MODIFIED JOINT PANEL IN TENSION AT +160°F

LOAD (1,000 LB)	UPPER	CTR UPPER	CTR LOWER	LOWER
0	0	0	0	0
0.5	+0.0050	+0.0006	–0.000	–0.0051
1		0	–0.0001	–0.0070
2	DIAL TIP ADHESIVE SEPARATED FROM Ti FACE	+0.0009	0	–0.0120
3		+0.0018	0	–0.0172
4		+0.0034	0	–0.0210
5		+0.0044	0	–0.0242
6		+0.0053	+0.0008	–0.0270
7		+0.0060	+0.0010	–0.0284
8		+0.0068	+0.0020	–0.0310
0		+0.0030	+0.0021	–0.0048

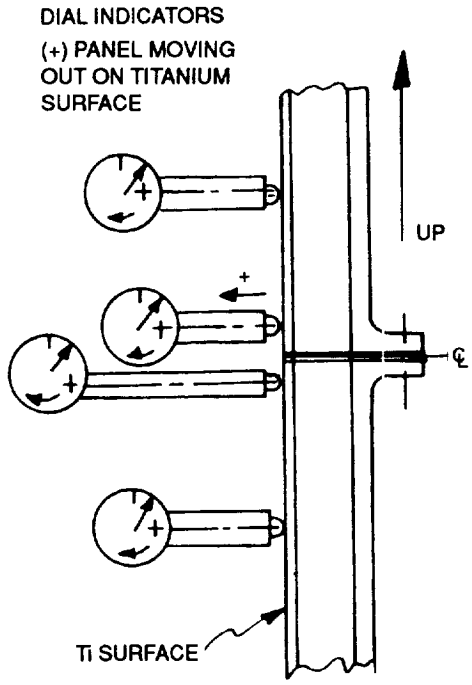

FIGURE 19. DIAL GAGE READINGS FOR MODIFIED JOINT PANEL IN TENSION AT –65°F

LOAD (1,000 LB)	UPPER	CTR UPPER	CTR LOWER	LOWER
0	0	0	0	0
0.5	–0.0015	0	0	–0.0020
1	+0.0022	0	0	–0.0025
2	+0.0033	+0.0003	0	–0.0035
3	+0.0037	+0.0009	0	–0.0030
4	+0.0039	+0.0009	+0.0001	–0.0025
5	+0.0039	+0.0010	+0.0002	–0.0020
6	+0.0037	+0.0019	+0.0003	–0.0010
7	+0.0032	+0.0021	+0.0004	0
8	+0.0030	+0.0020	+0.0003	+0.0004
9	+0.0026	+0.0029	+0.0004	+0.0010
10	+0.0022	+0.0029	+0.0013	+0.0020
0	+0.0008	+0.0006	+0.0005	+0.0015

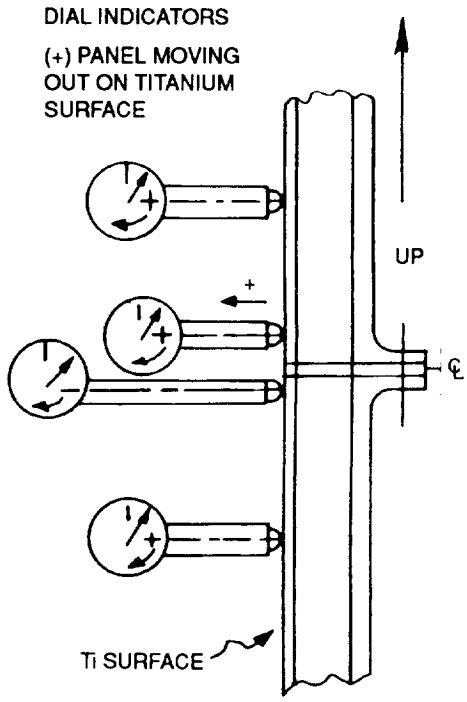

FIGURE 20. DIAL GAGE READINGS FOR MODIFIED JOINT PANEL IN COMPRESSION AT +160°F

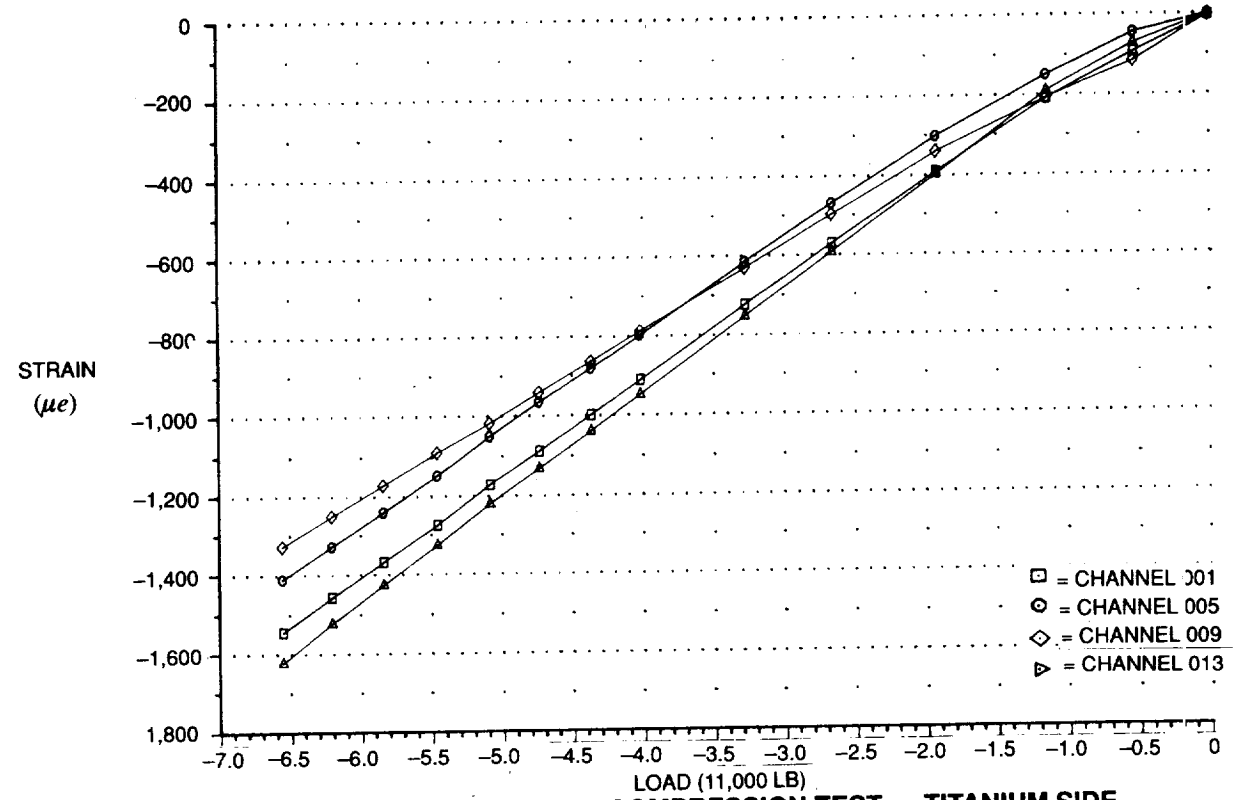

FIGURE 21. ROOM TEMPERATURE COMPRESSION TEST — TITANIUM SIDE, LARGE SLIDING JOINT — STRAIN GAGE READING

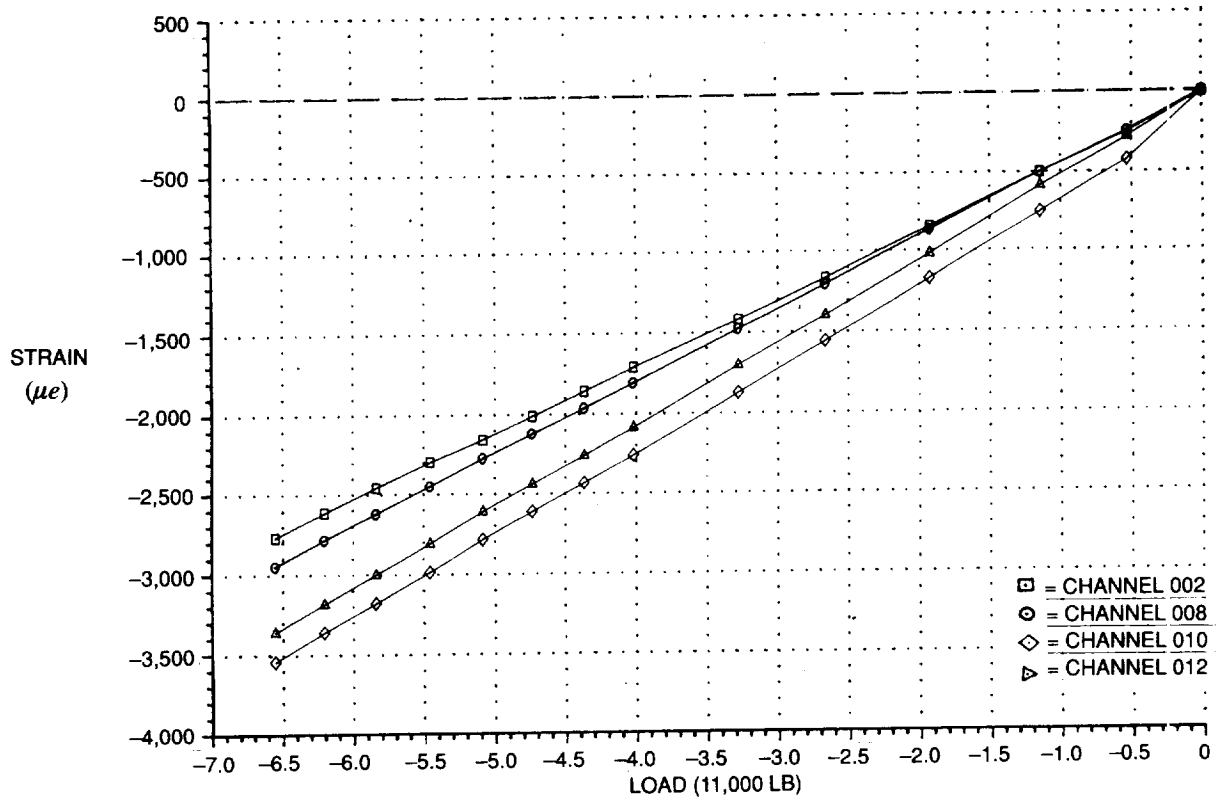

FIGURE 22. ROOM TEMPERATURE COMPRESSION — COMPOSITE SIDE, LARGE SLIDING JOINT — STRAIN GAGE READING

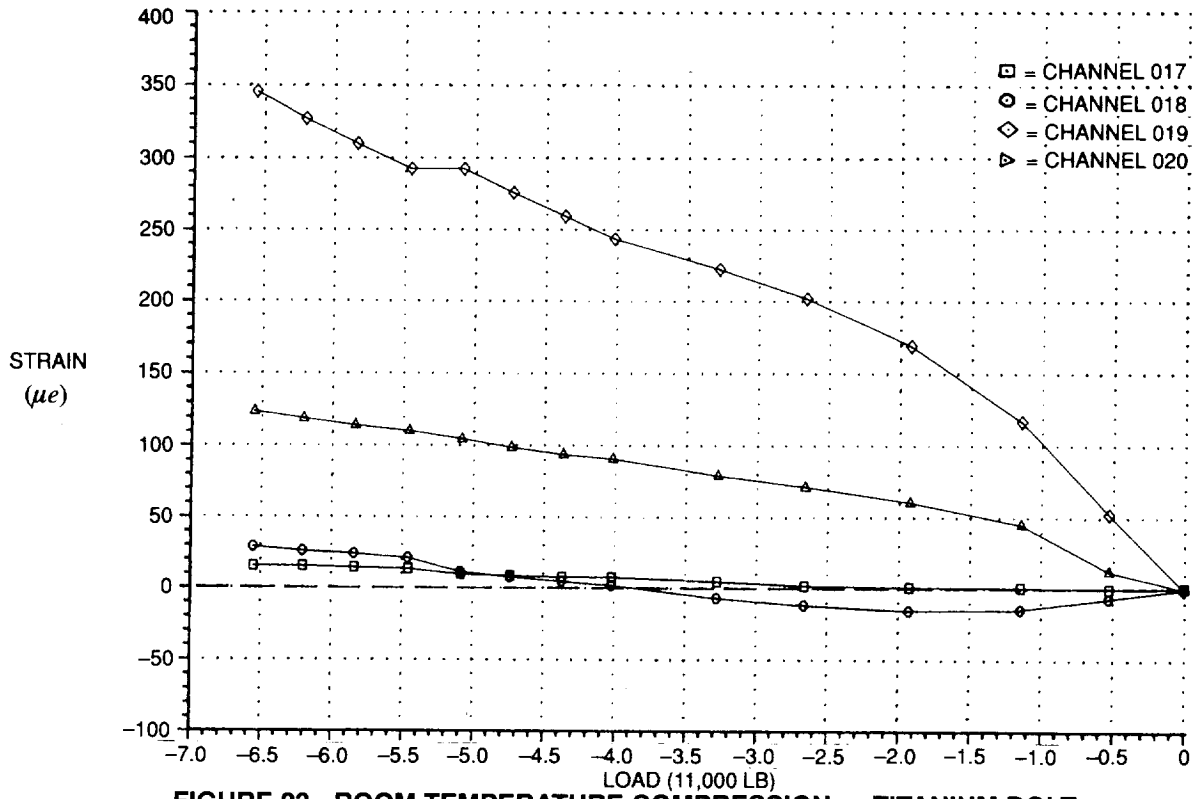

FIGURE 23. ROOM TEMPERATURE COMPRESSION — TITANIUM BOLT, LARGE SLIDING JOINT — STRAIN GAGE READING

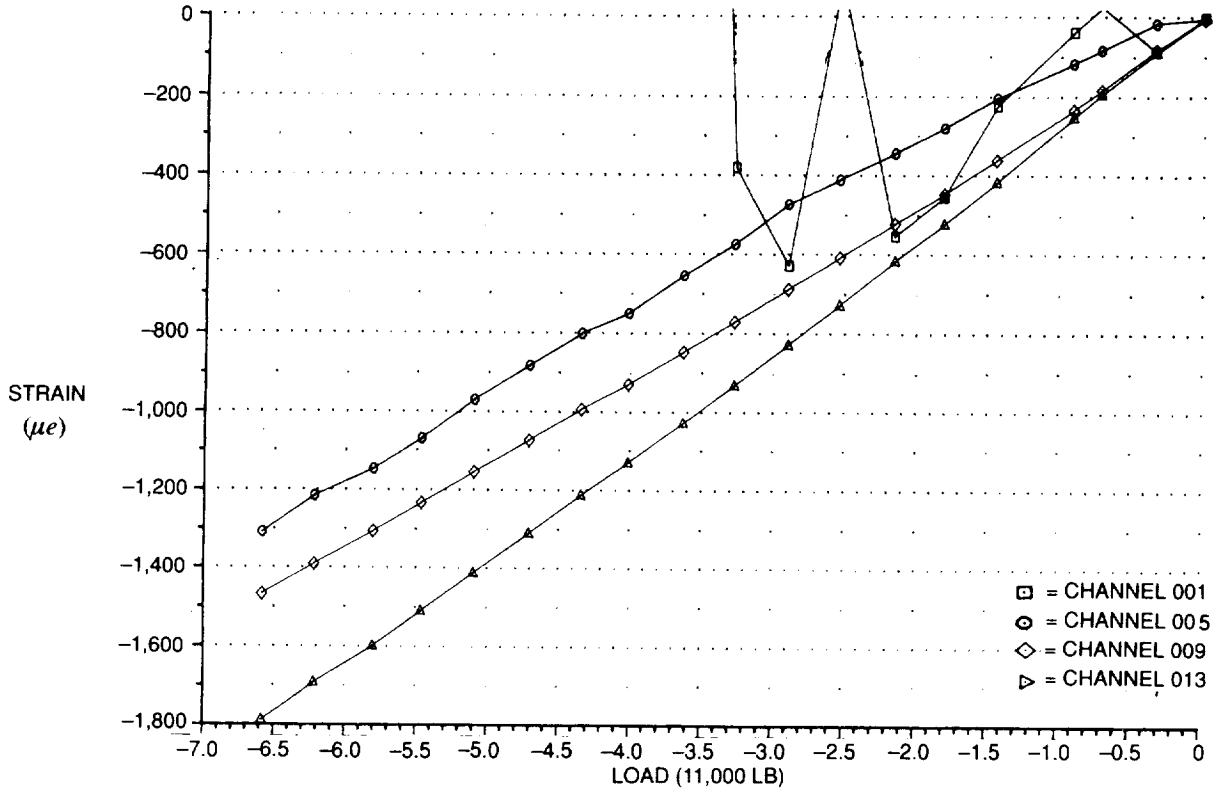

FIGURE 24. COLD COMPRESSION (–65°F) — TITANIUM SIDE, LARGE SLIDING JOINT — STRAIN GAGE READING

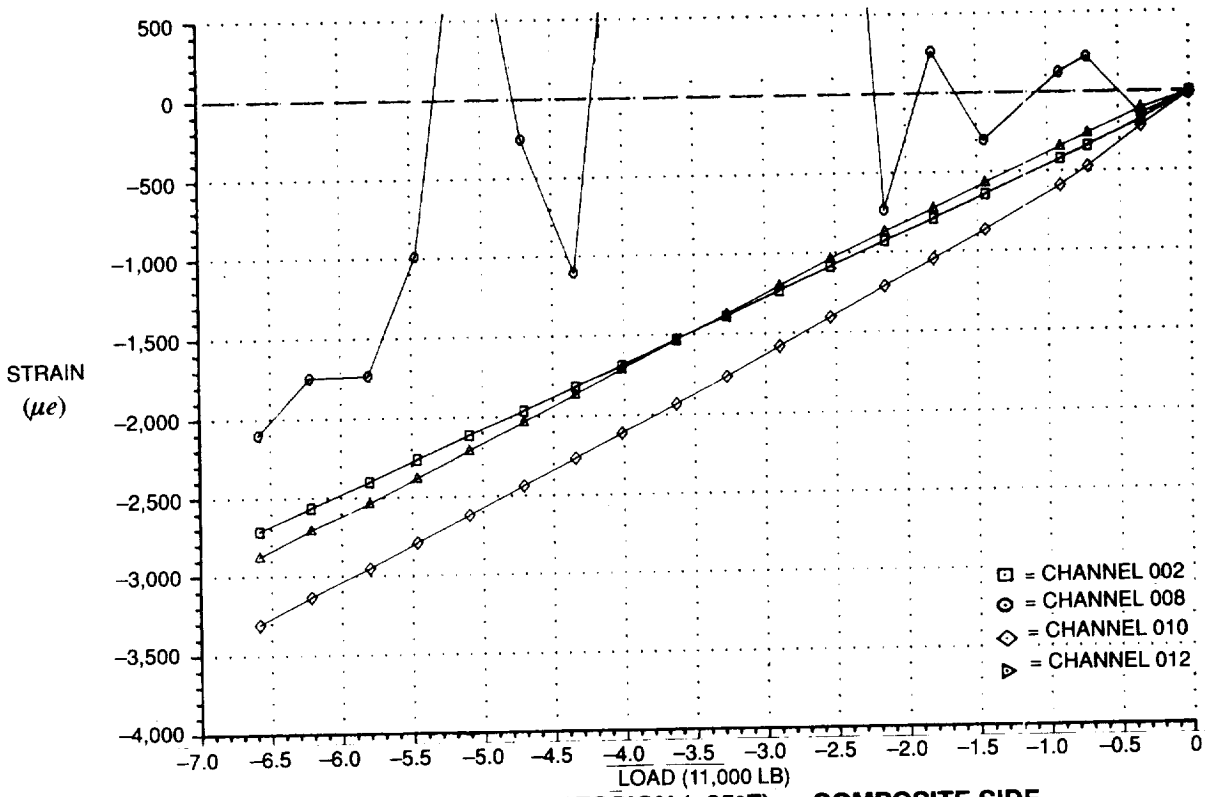

FIGURE 25. COLD COMPRESSION (–65°F) — COMPOSITE SIDE, LARGE SLIDING JOINT — STRAIN GAGE READING

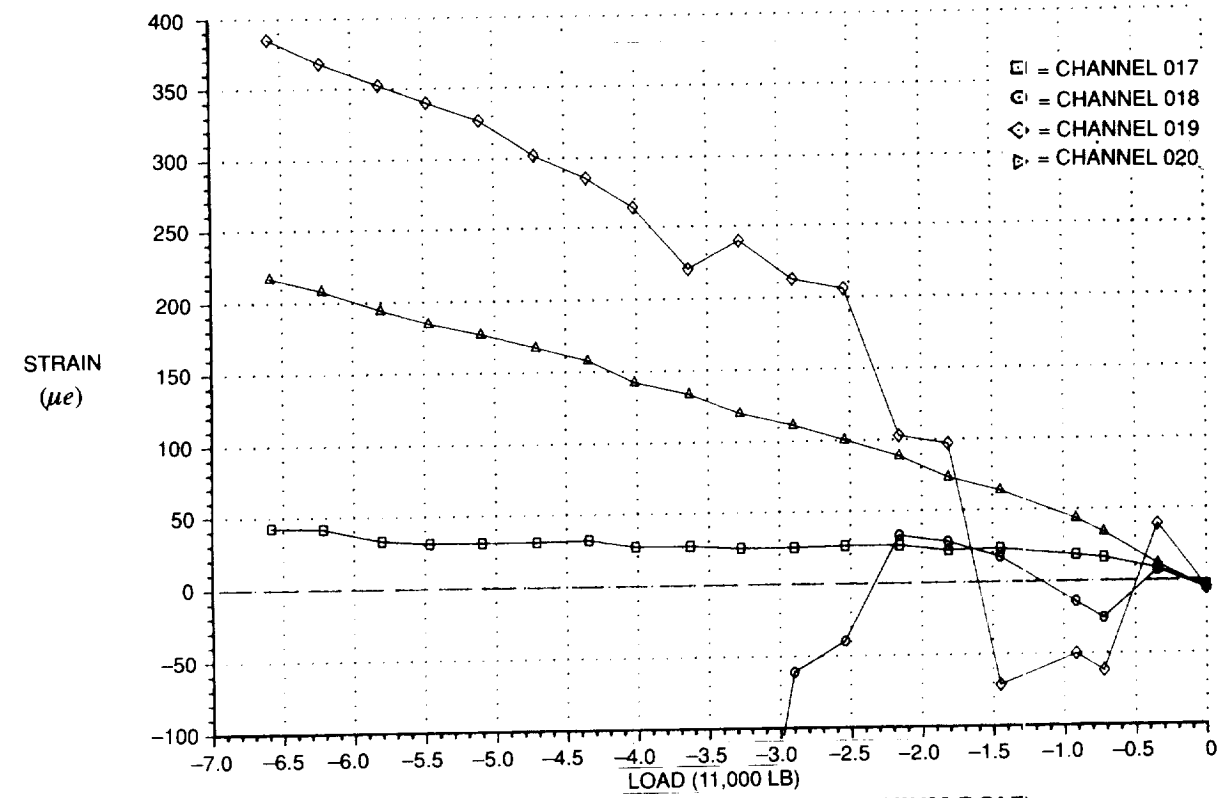

FIGURE 26. COLD COMPRESSION (–65°F) — TITANIUM BOLT, LARGE SLIDING JOINT — STRAIN GAGE READING

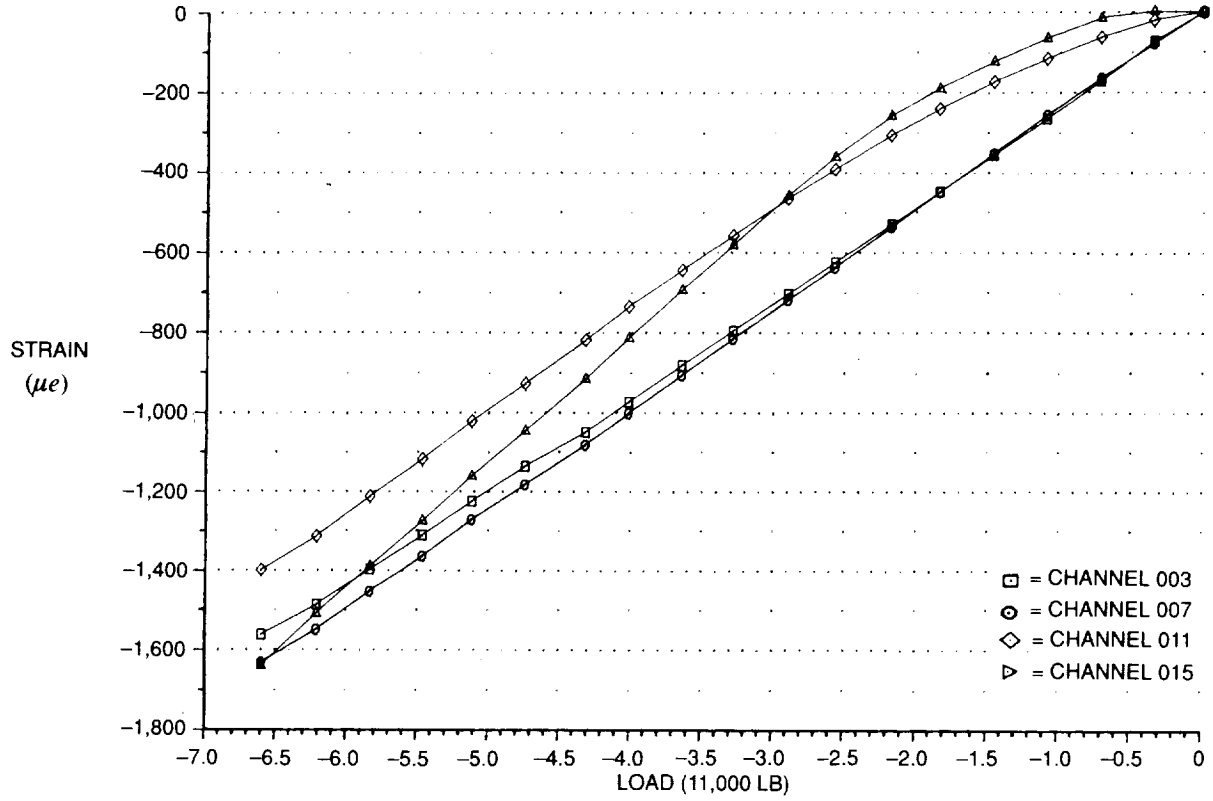

FIGURE 27. HOT COMPRESSION (160°F) — TITANIUM SIDE, LARGE SLIDING JOINT — STRAIN GAGE READING

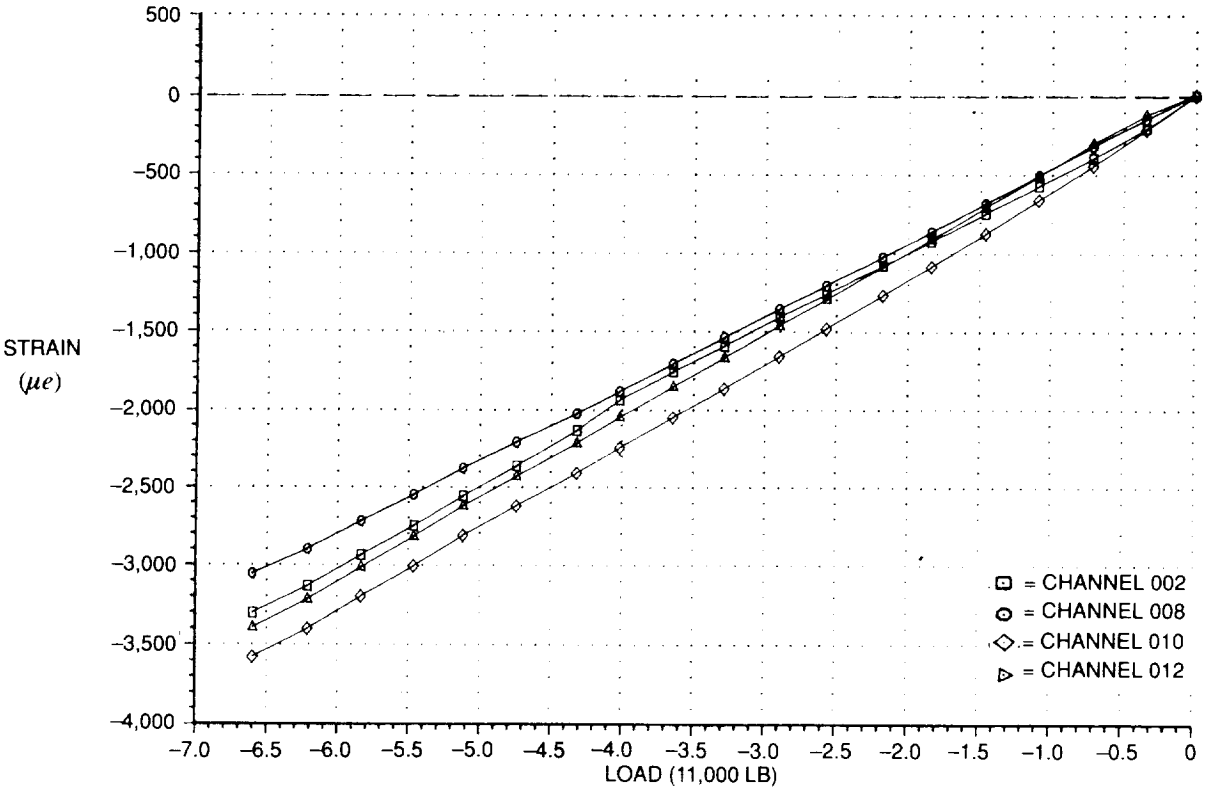

FIGURE 28. HOT COMPRESSION (160°F) — COMPOSITE SIDE, LARGE SLIDING JOINT — STRAIN GAGE READING

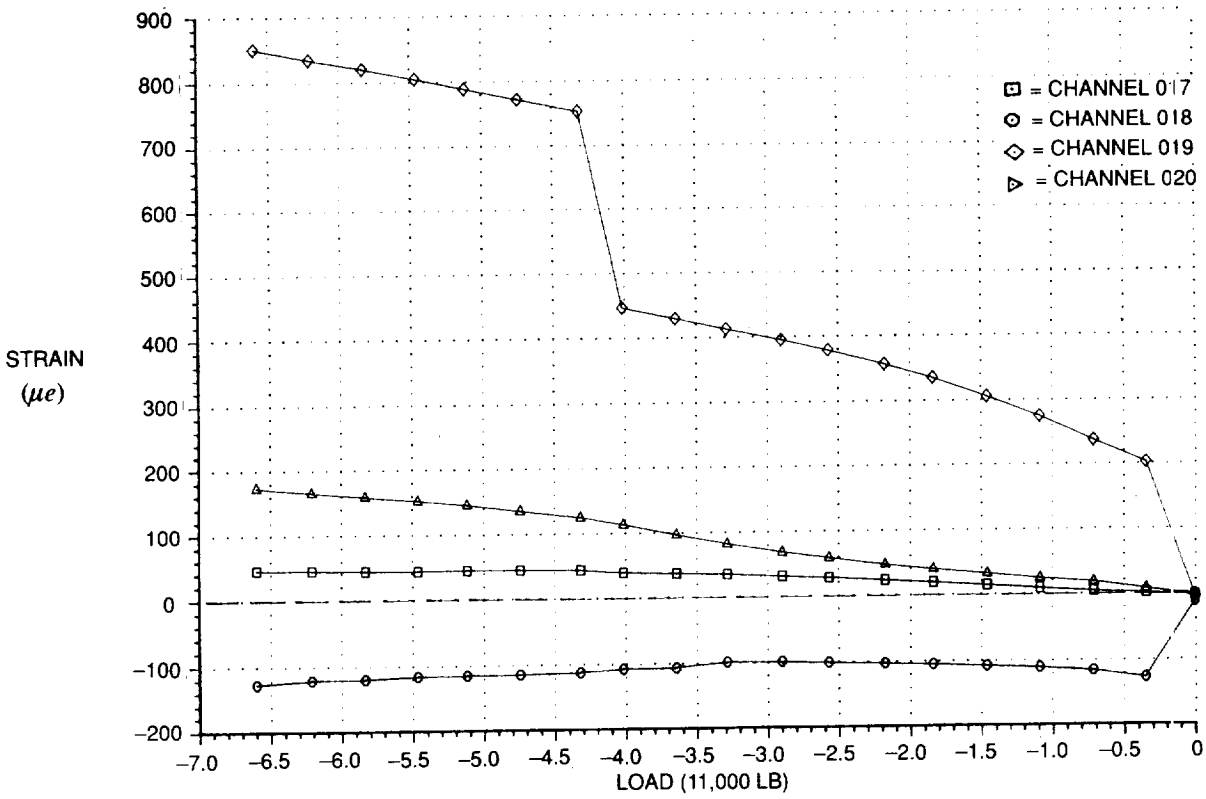

FIGURE 29. HOT COMPRESSION (160°F) — TITANIUM BOLT, LARGE SLIDING JOINT — STRAIN GAGE READING

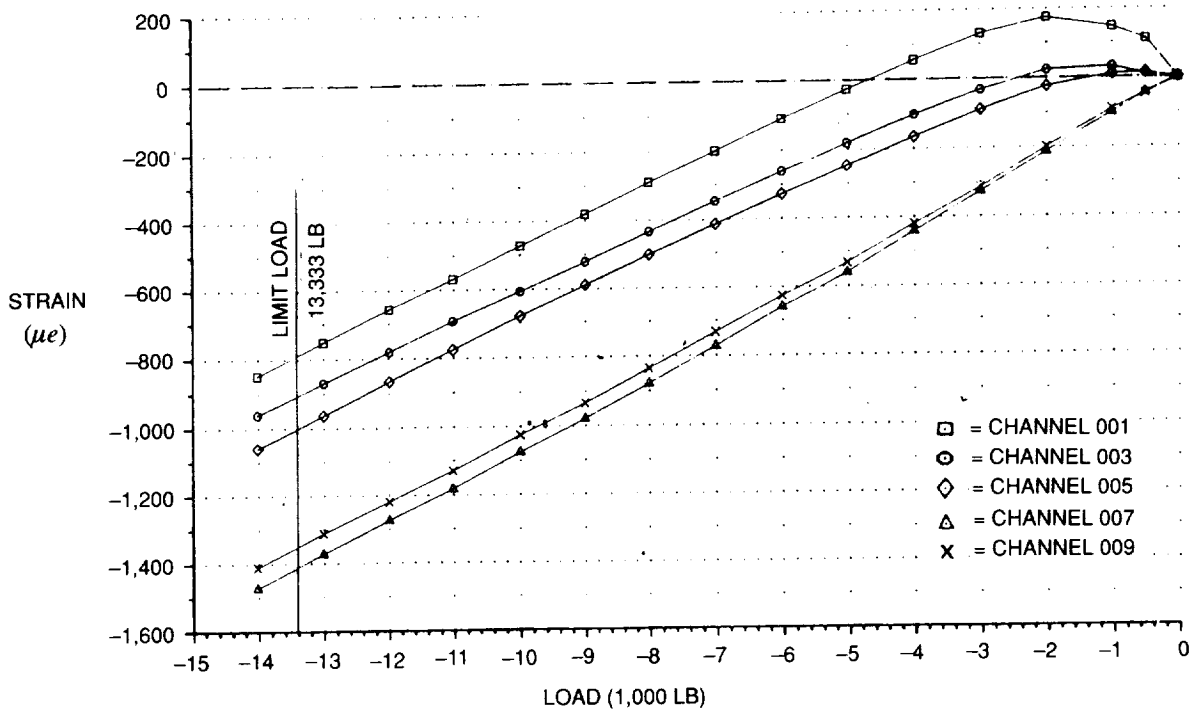

FIGURE 30. MODIFIED JOINT COMPRESSION TEST AT –65°F — STRAIN GAGE READINGS

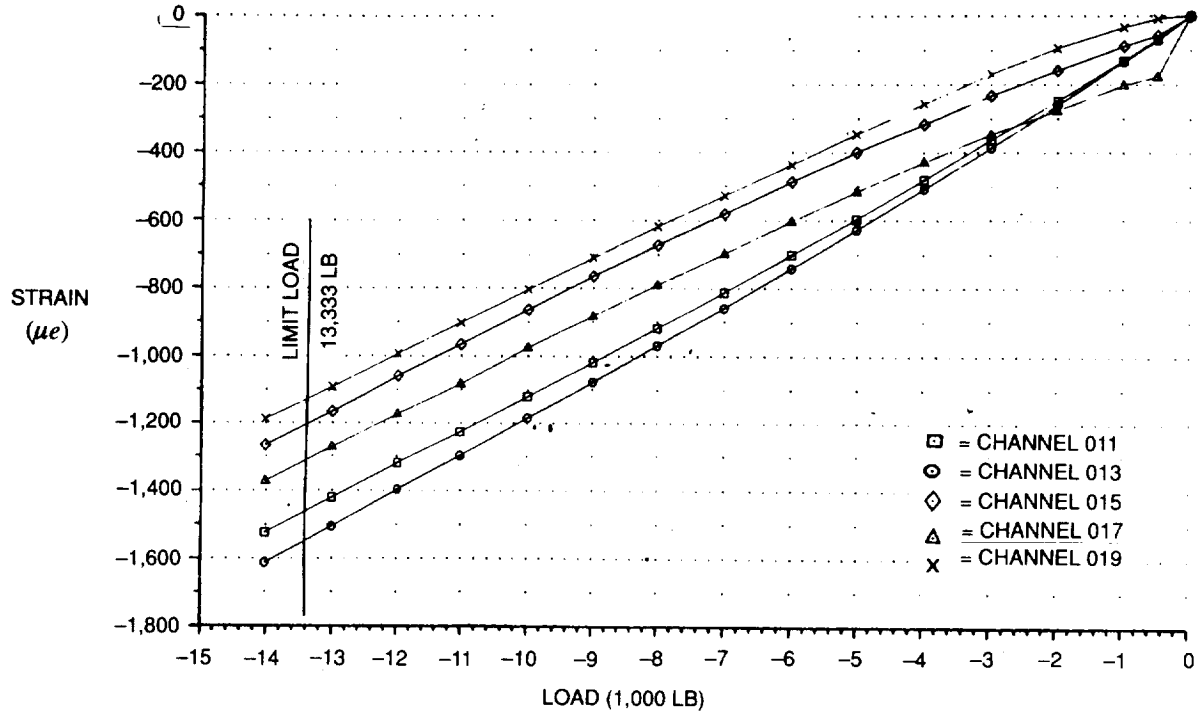

FIGURE 31. MODIFIED JOINT COMPRESSION TEST AT –65°F — STRAIN GAGE READINGS

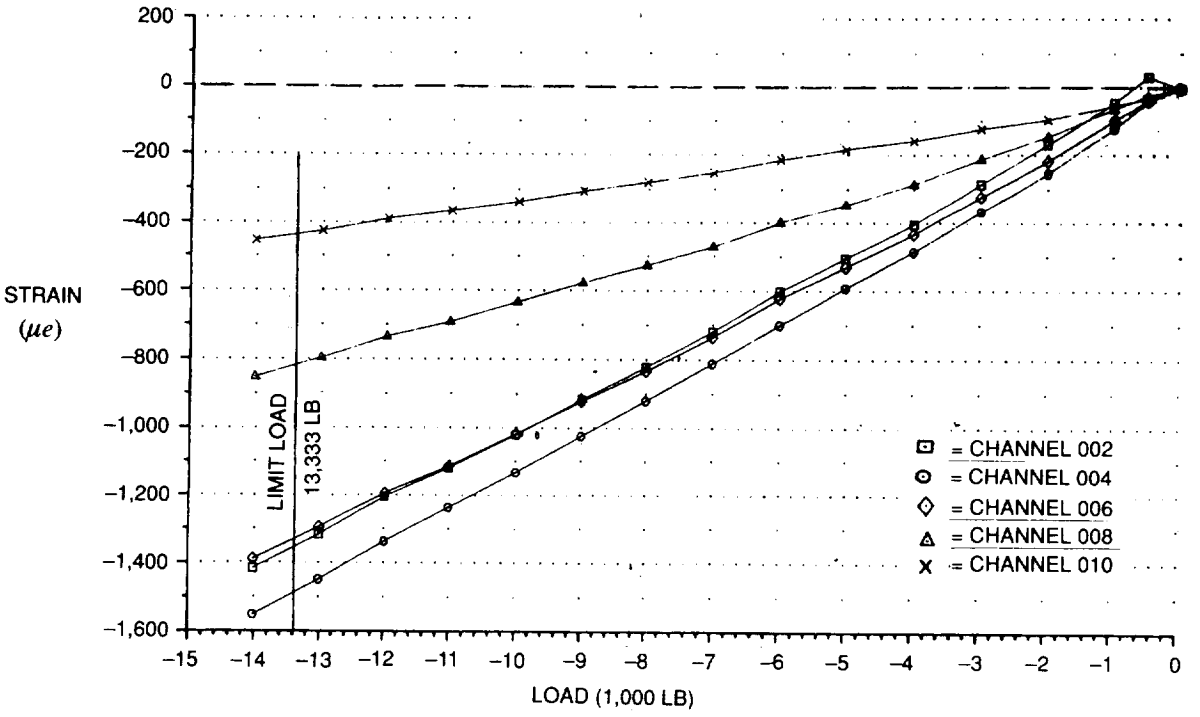

FIGURE 32. MODIFIED JOINT COMPRESSION TEST AT –65°F — STRAIN GAGE READINGS

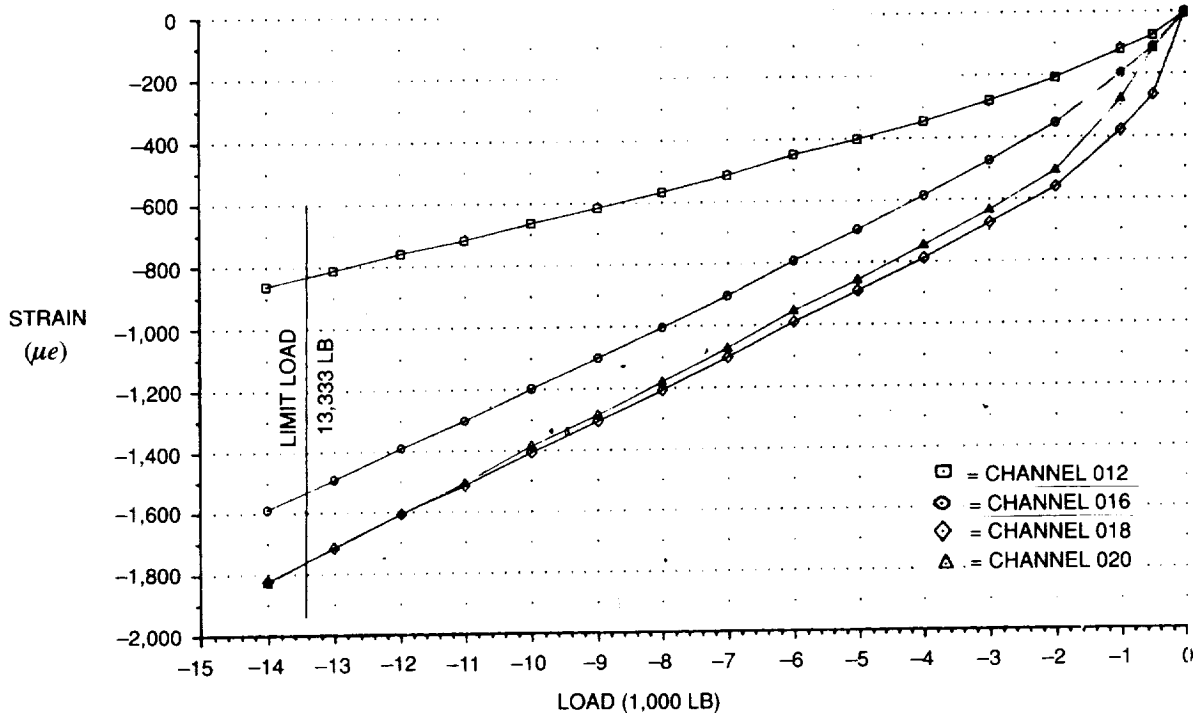

FIGURE 33. MODIFIED JOINT COMPRESSION TEST AT –65°F — STRAIN GAGE READINGS

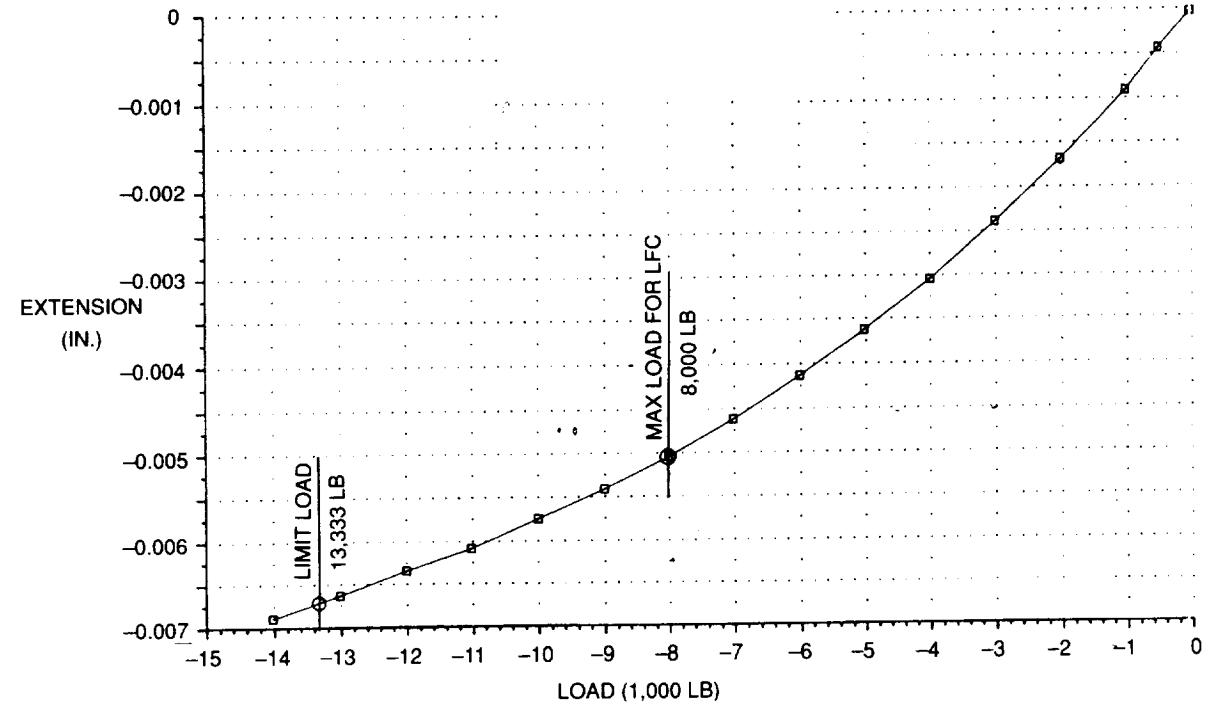

FIGURE 34. MODIFIED JOINT COMPRESSION TEST AT –65°F — EXTENSOMETER READINGS

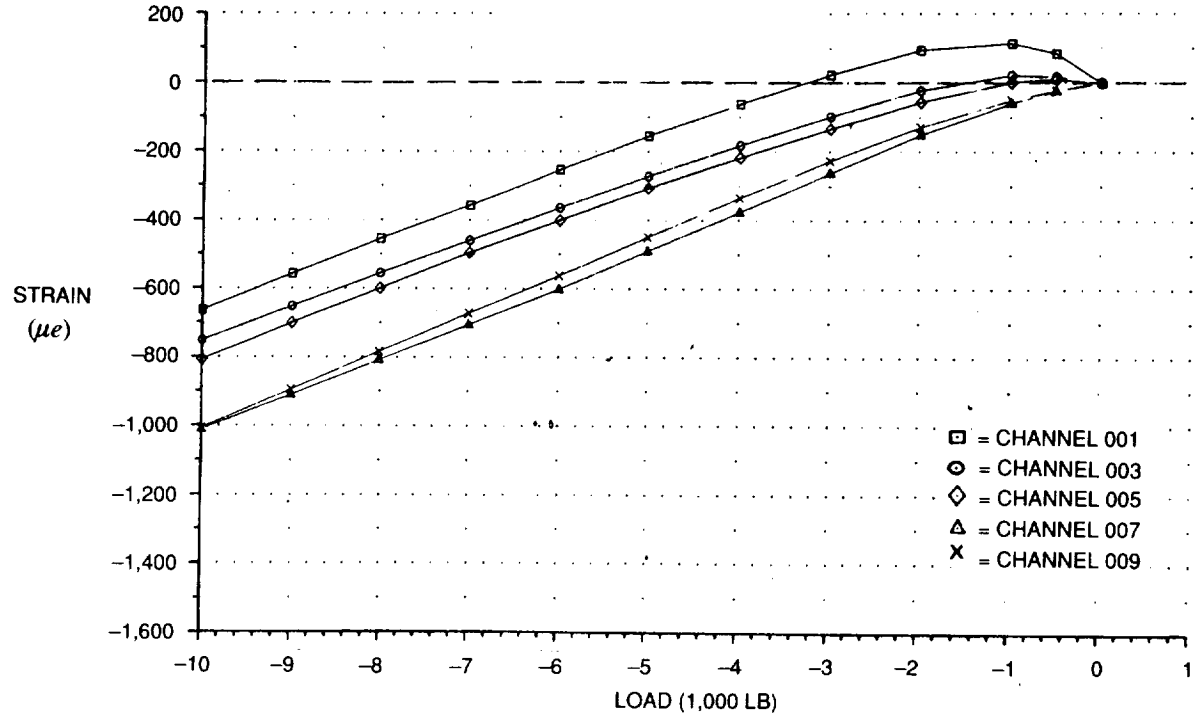

FIGURE 35. MODIFIED JOINT COMPRESSION TEST AT 160°F — STRAIN GAGE READINGS

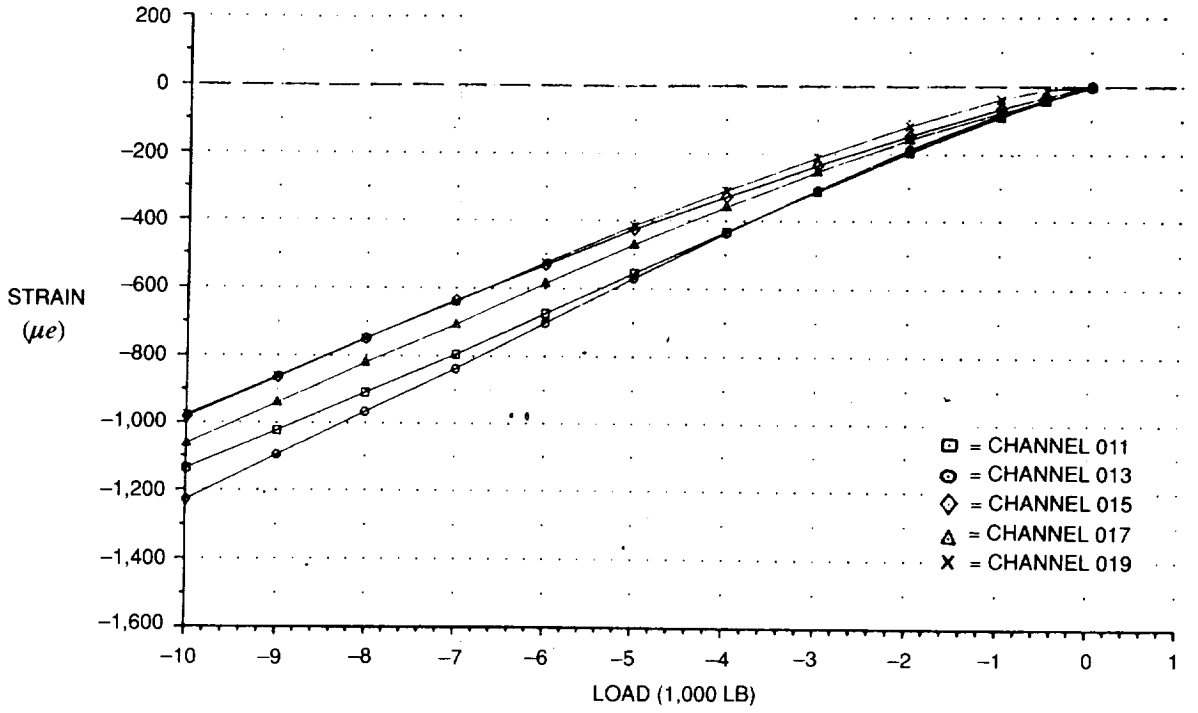

FIGURE 36. MODIFIED JOINT COMPRESSION TEST AT 160°F — STRAIN GAGE READINGS

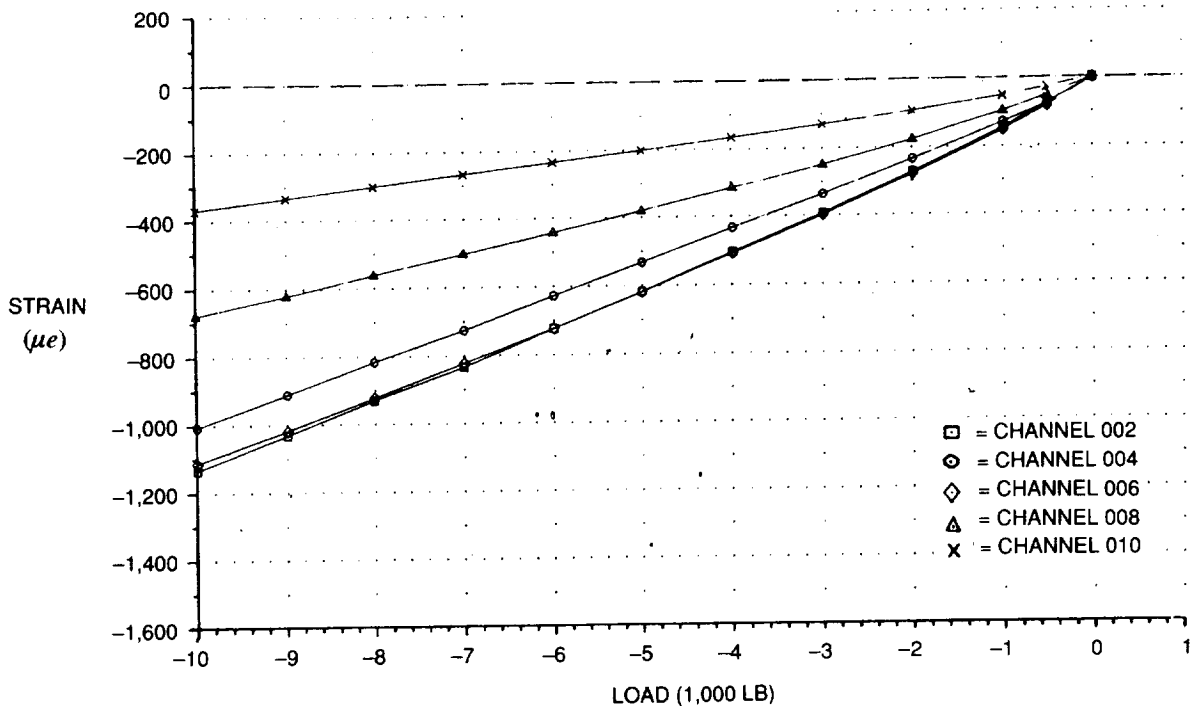

FIGURE 37. MODIFIED JOINT COMPRESSION TEST AT 160°F — STRAIN GAGE READINGS

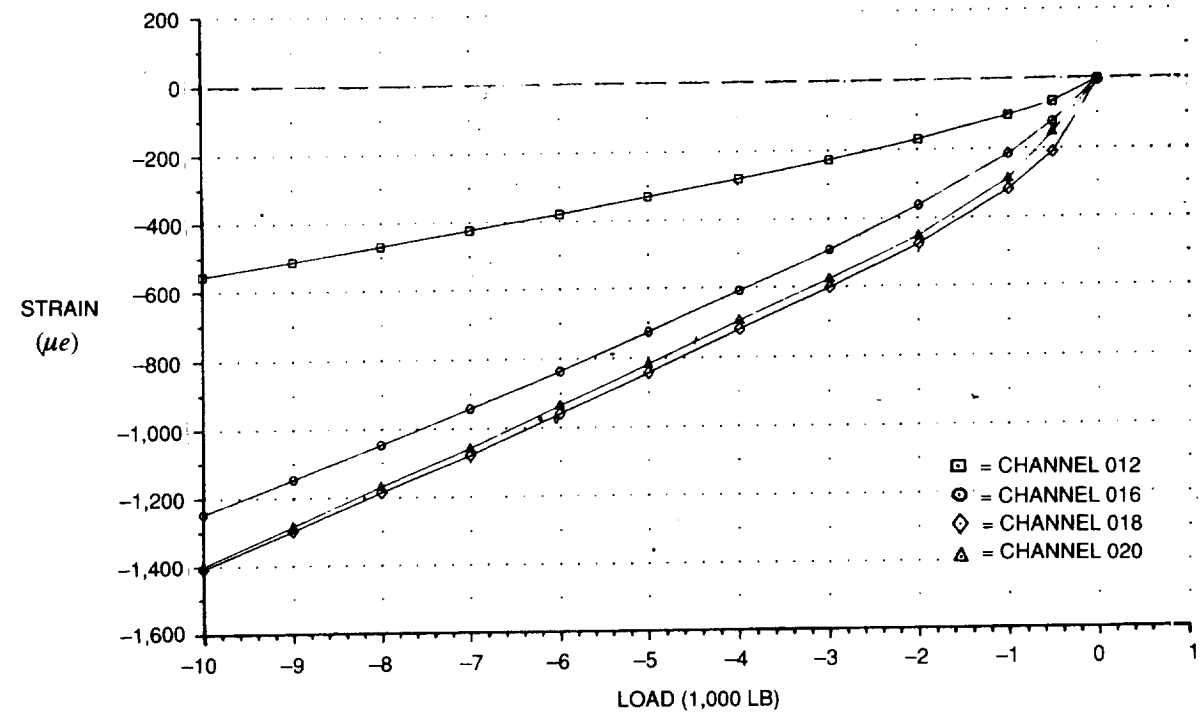

FIGURE 38. MODIFIED JOINT COMPRESSION TEST AT 160°F — STRAIN GAGE READINGS

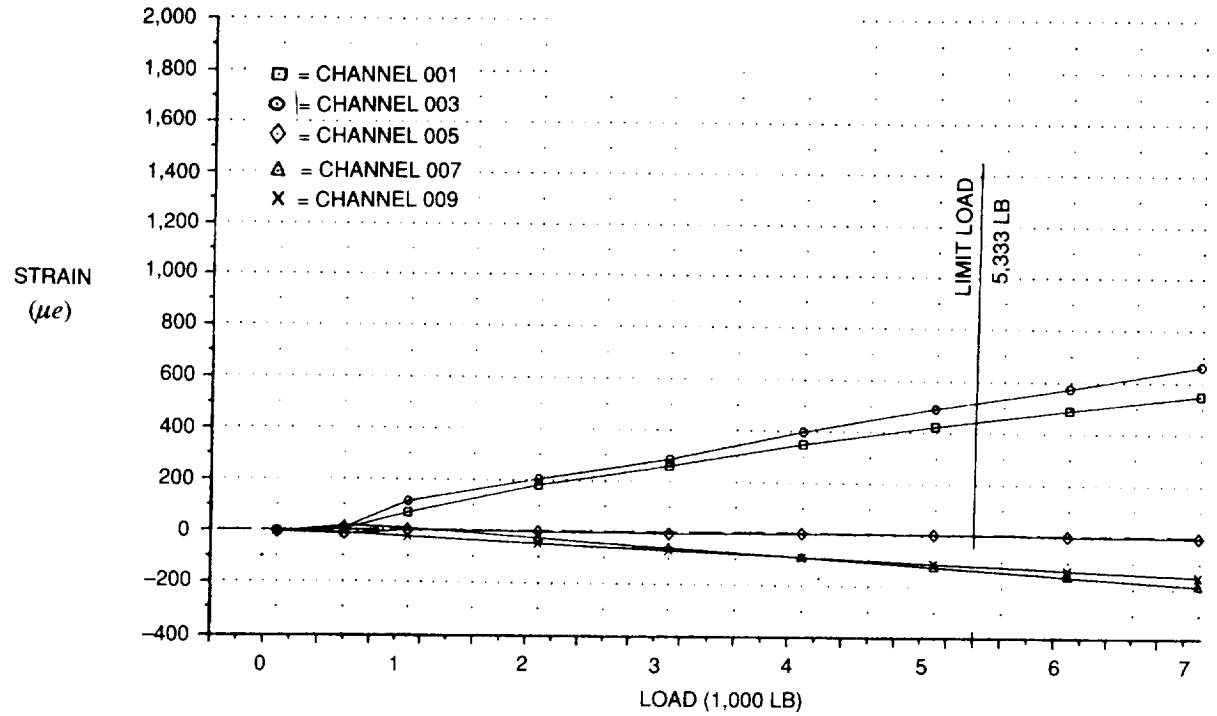

FIGURE 39. MODIFIED JOINT TENSION TEST AT 160°F — STRAIN GAGE READINGS

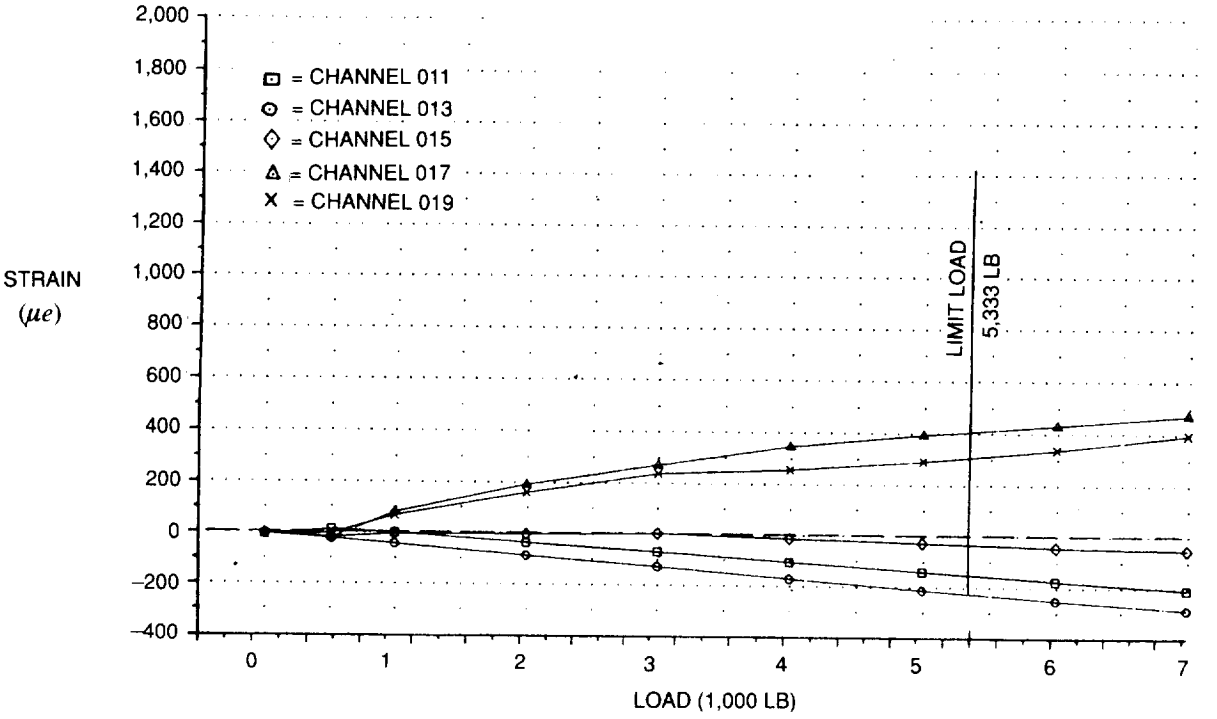

FIGURE 40. MODIFIED JOINT TENSION TEST AT 160°F — STRAIN GAGE READINGS

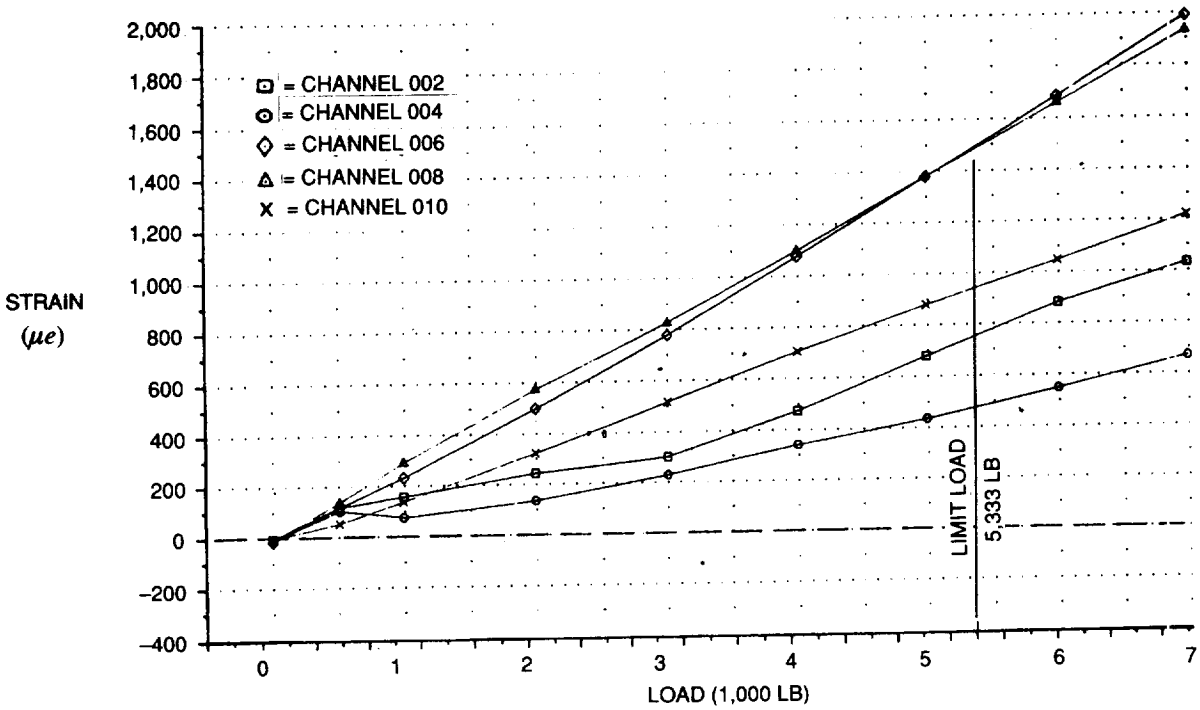

FIGURE 41. MODIFIED JOINT TENSION TEST AT 160°F — STRAIN GAGE READINGS

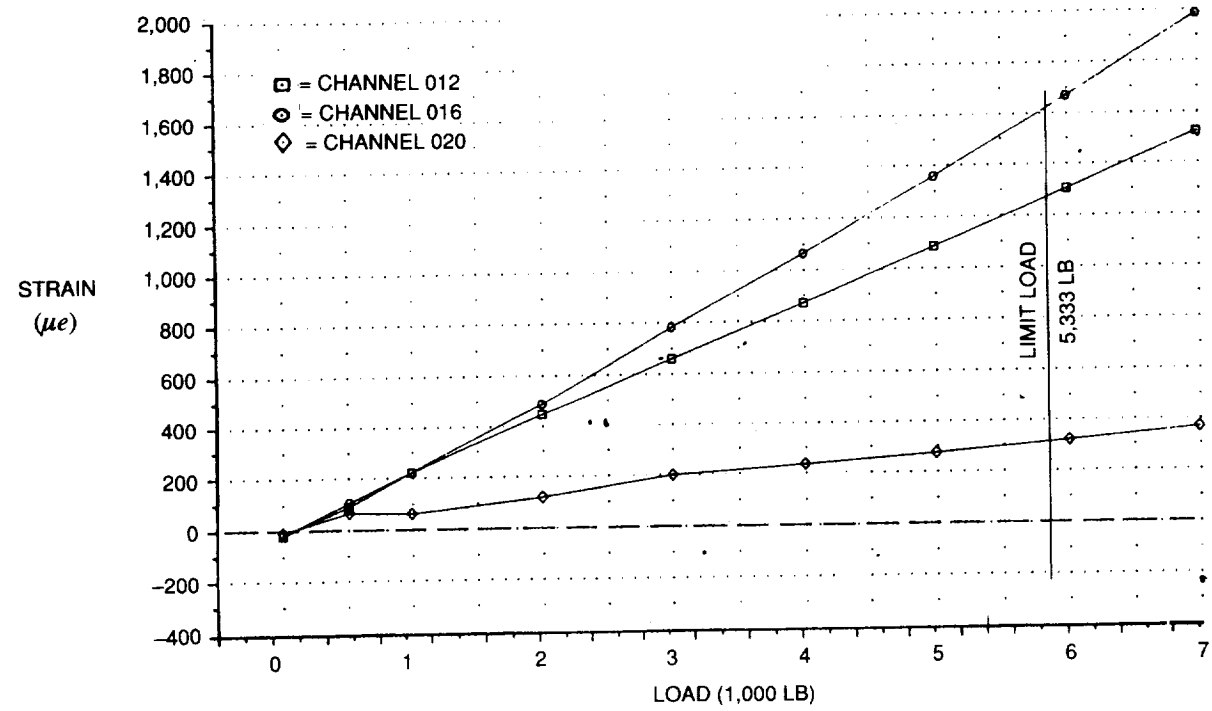

FIGURE 42. MODIFIED JOINT TENSION TEST AT 160°F — STRAIN GAGE READINGS

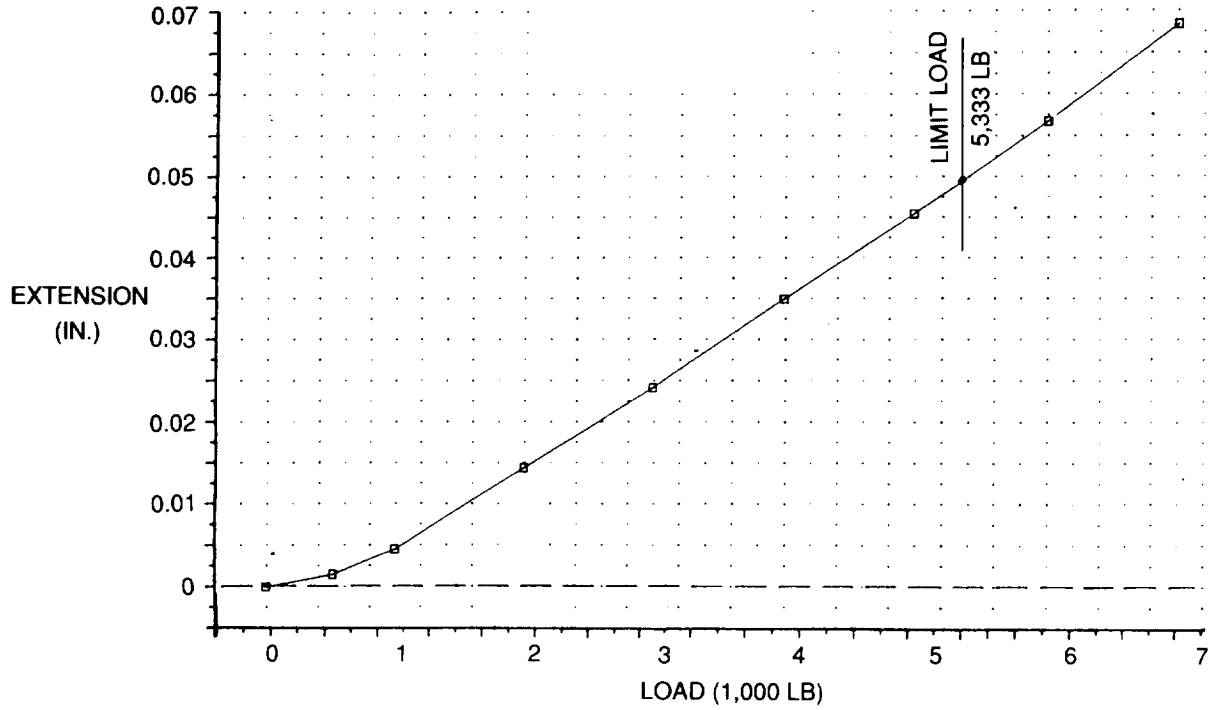

FIGURE 43. MODIFIED JOINT TENSION TEST AT ROOM TEMPERATURE — EXTENSOMETER READING

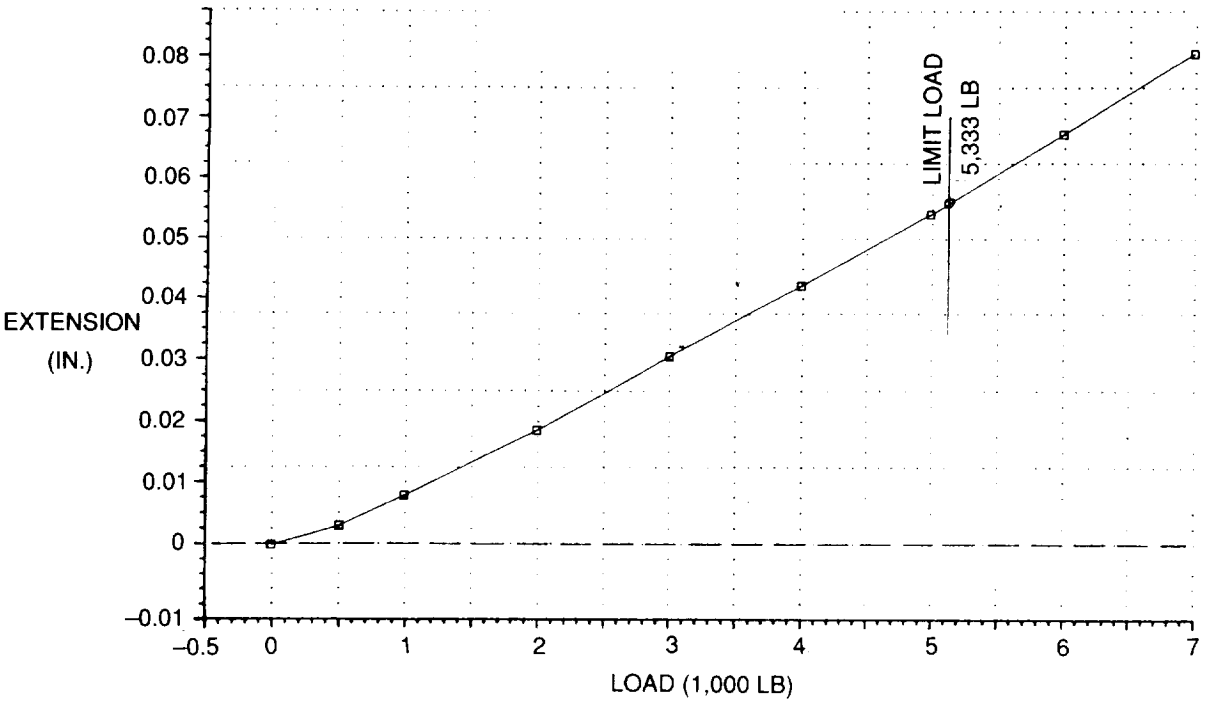

FIGURE 44. MODIFIED JOINT TENSION TEST AT 160°F — EXTENSOMETER READINGS

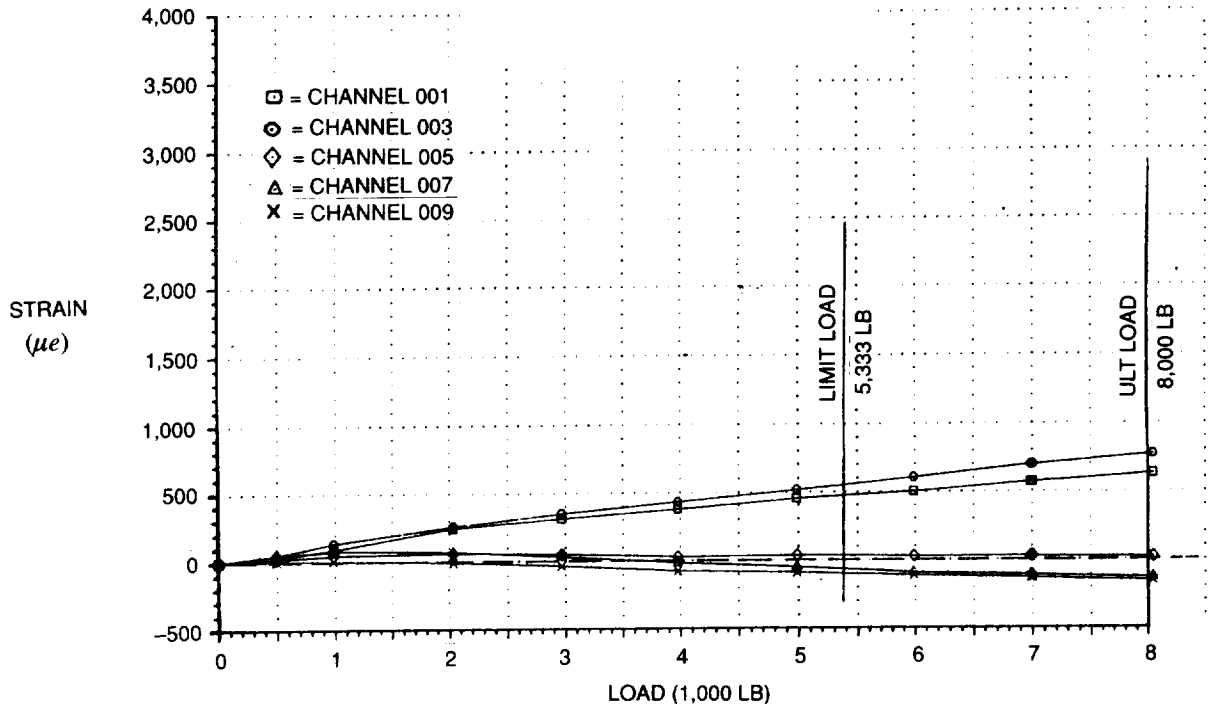

FIGURE 45. MODIFIED JOINT TENSION TEST AT –65°F — STRAIN GAGE READINGS

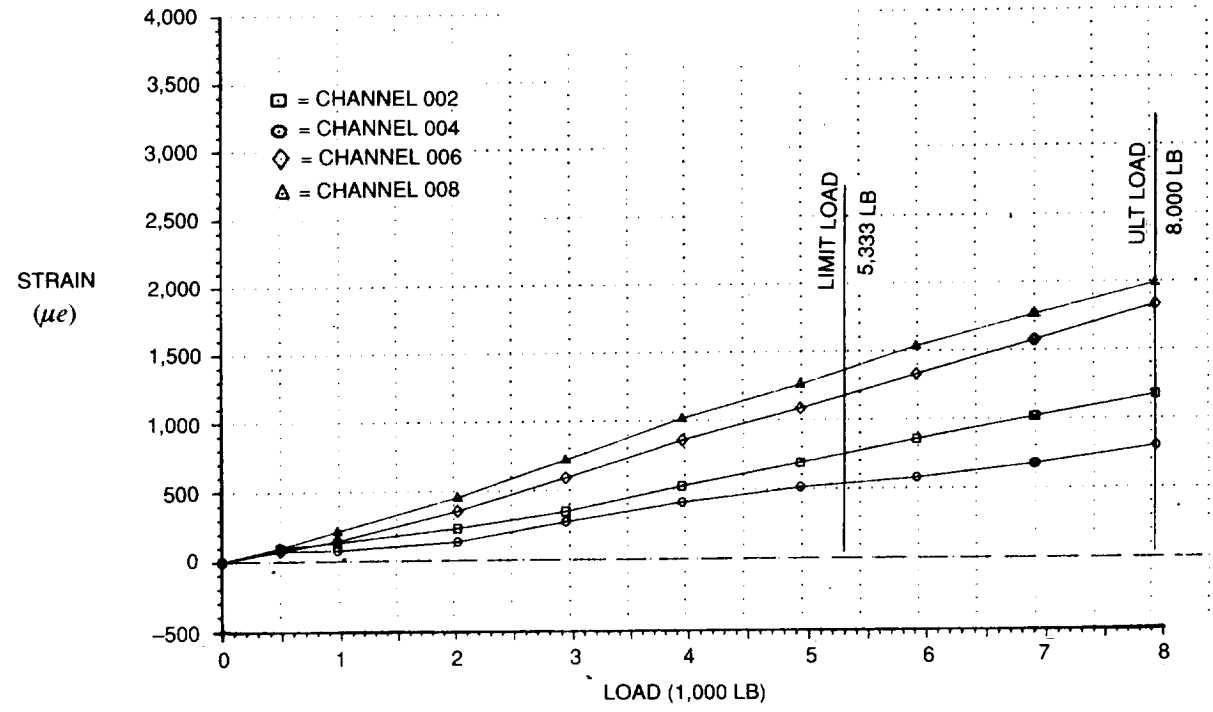

FIGURE 46. MODIFIED JOINT TENSION TEST AT –65°F — STRAIN GAGE READINGS

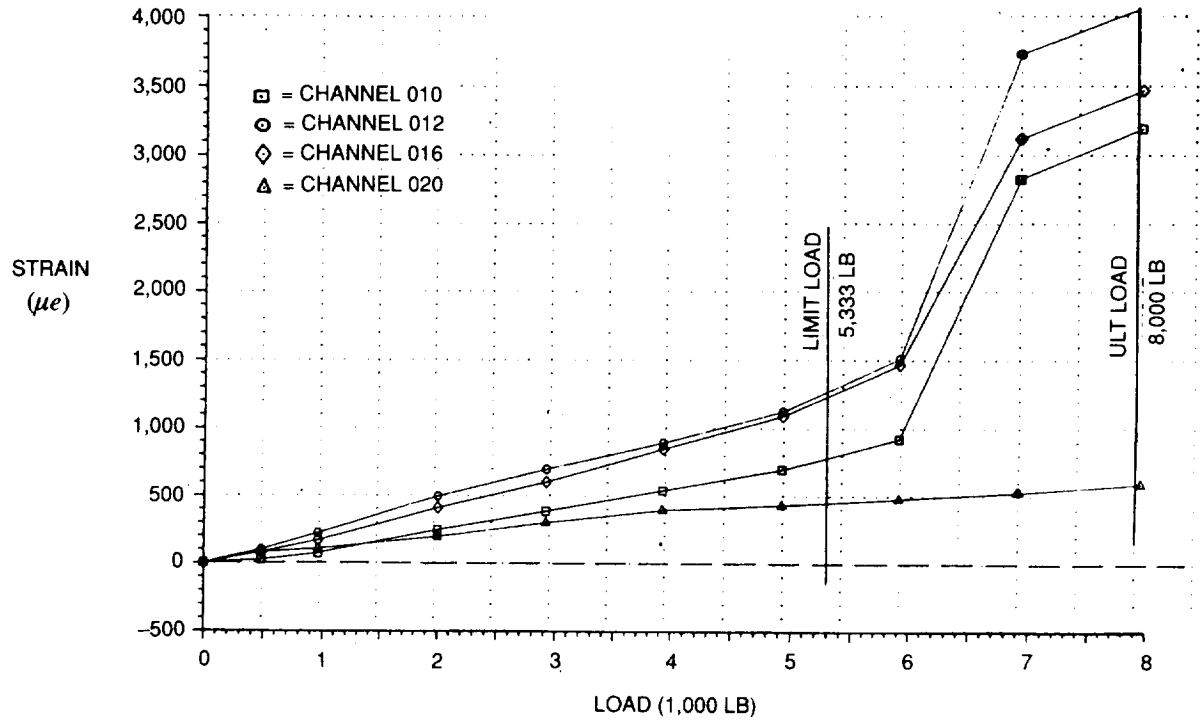

FIGURE 47. MODIFIED JOINT TENSION TEST AT –65°F — STRAIN GAGE READINGS

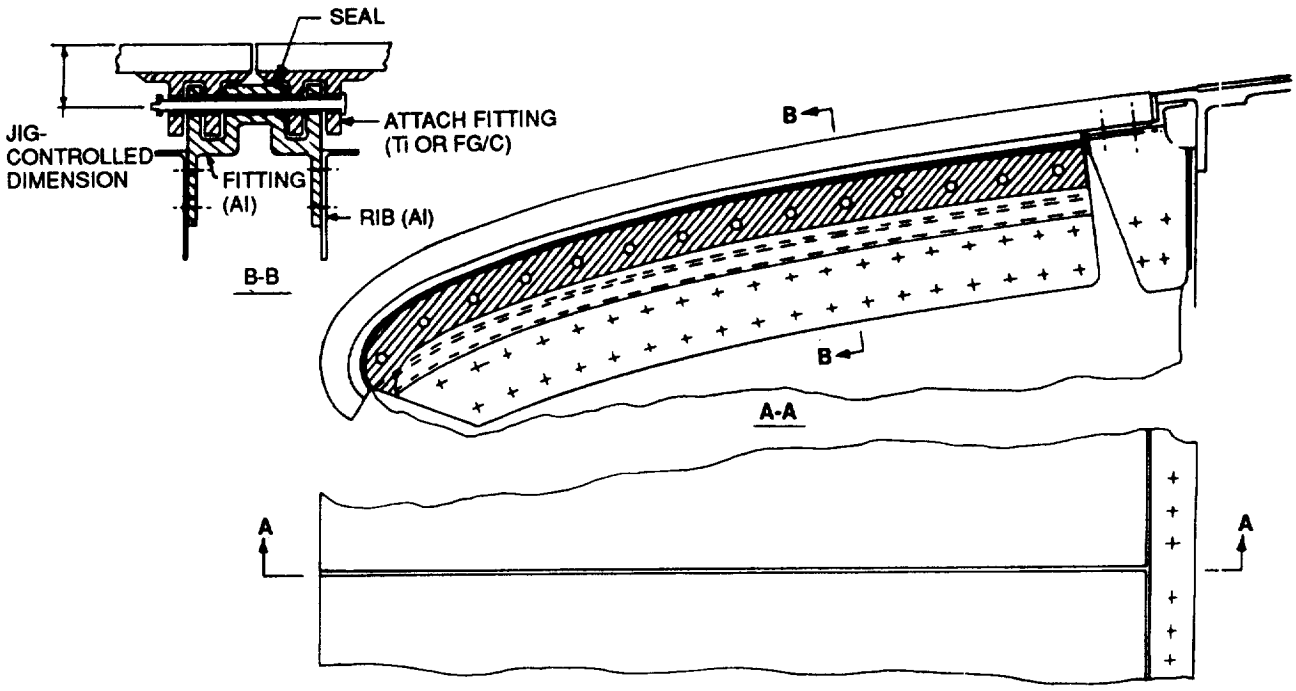

FIGURE 48. SLIDING CONCEPT

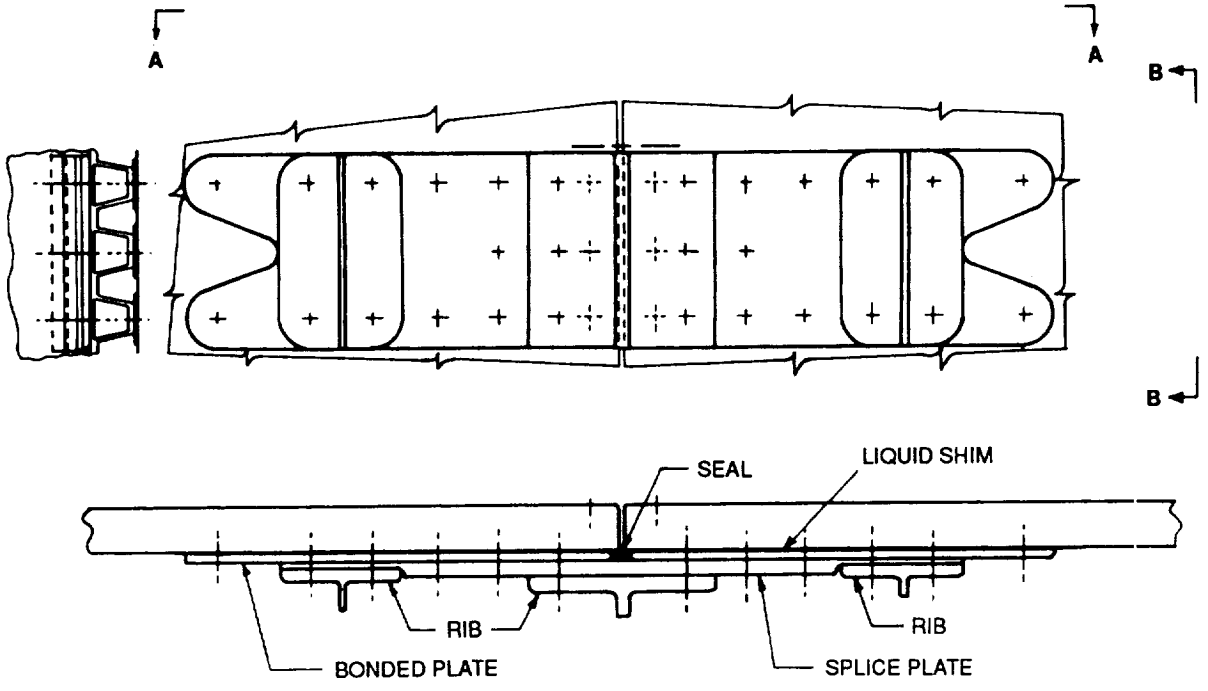

FIGURE 49. THREE-RIB CONCEPT

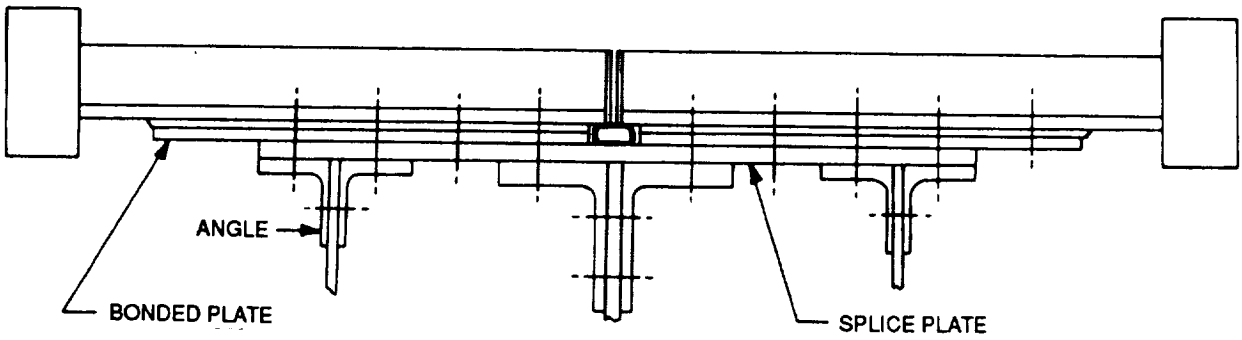

FIGURE 50. THREE-RIB CONCEPT WITH FLAT SPLICE PLATE

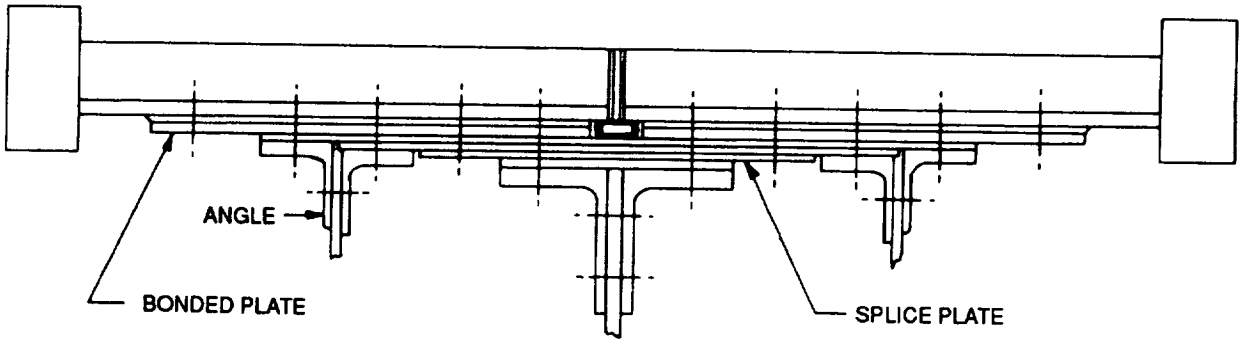

FIGURE 51. THREE-RIB CONCEPT WITH STEP-TAPERED SPLICE PLATE

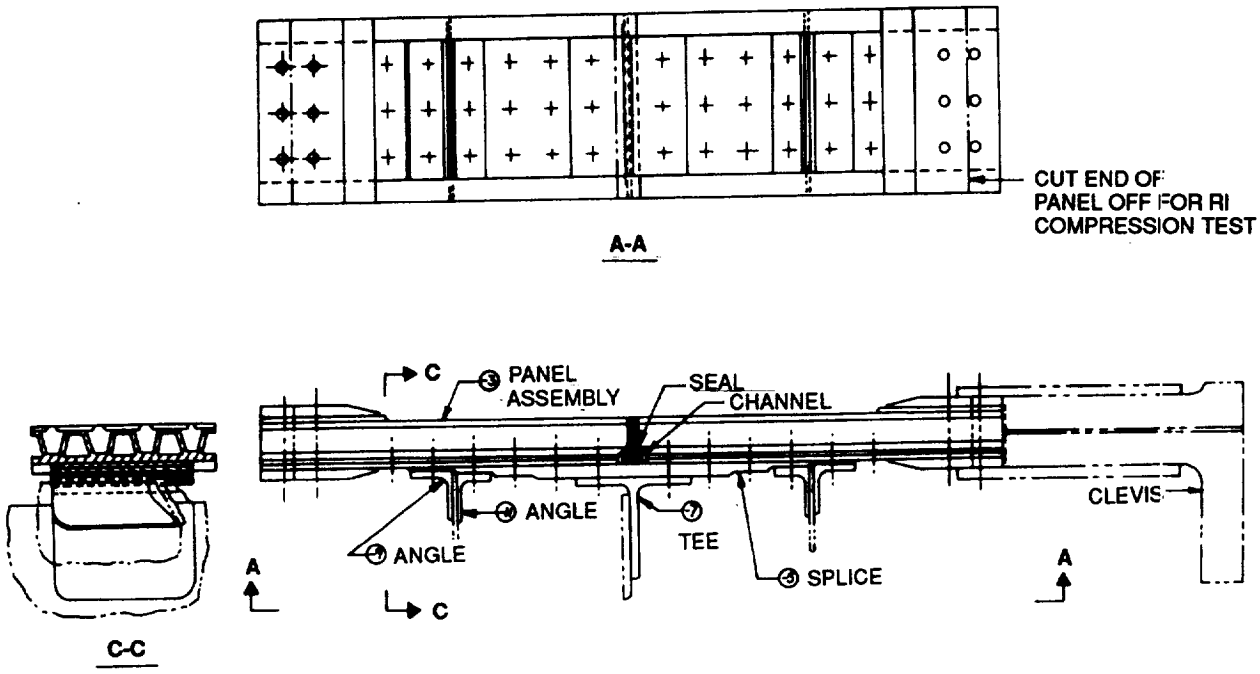

FIGURE 52. THREE-RIB JOINT TEST SPECIMEN

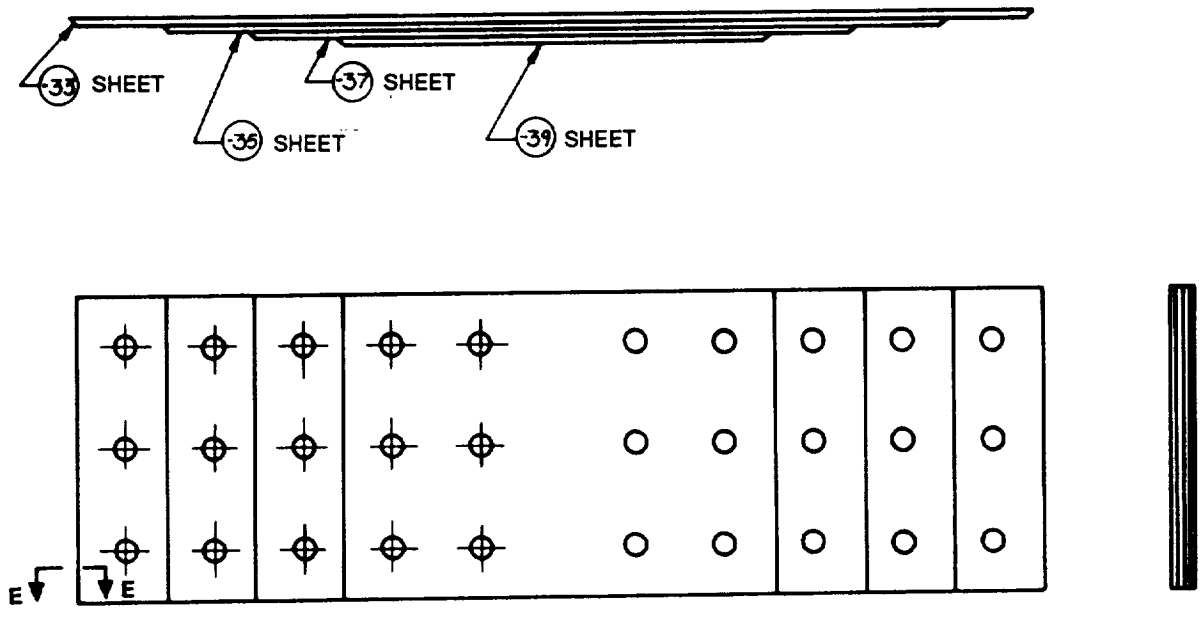

FIGURE 53. FOUR SHEETS OF TITANIUM BONDED TO FORM -5 TAPERED SPLICE PLATE

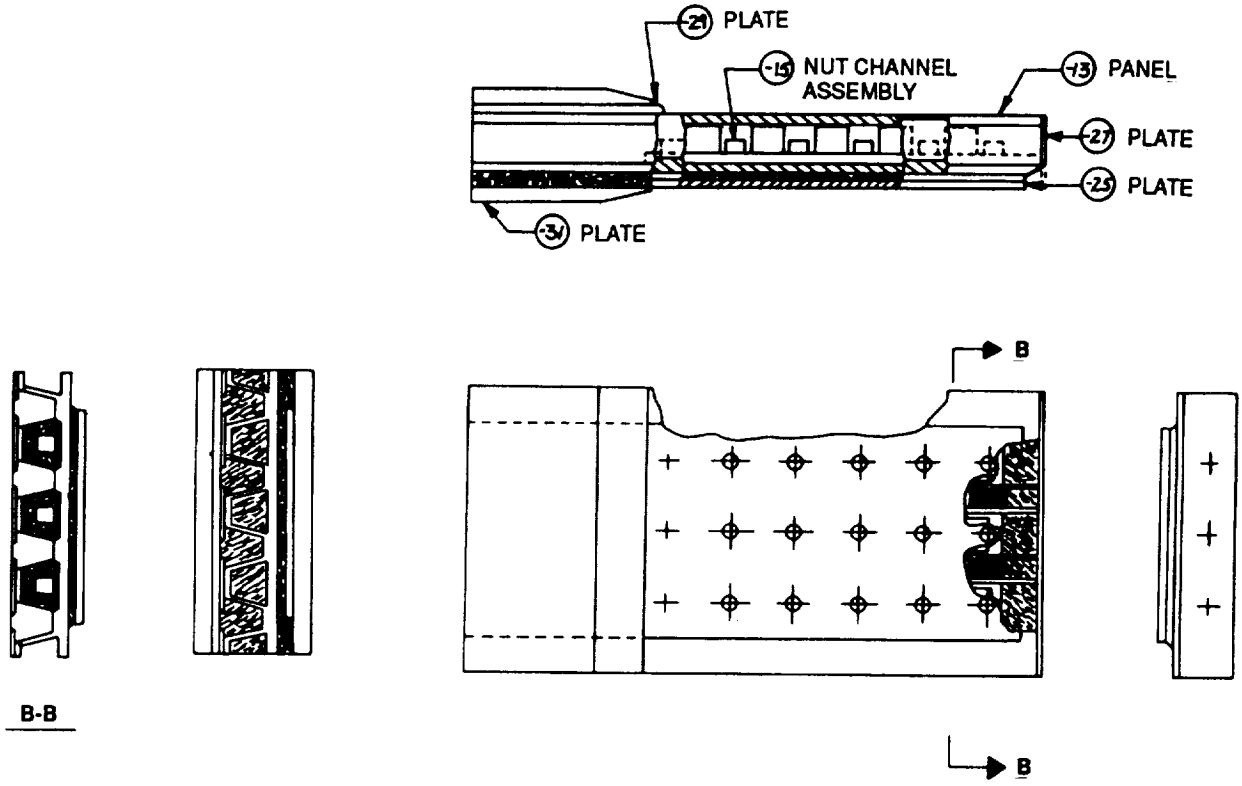

FIGURE 54. -3 PANEL ASSEMBLY

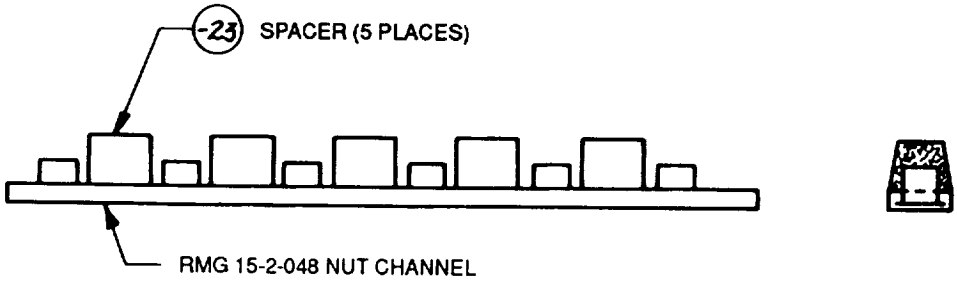

FIGURE 55. -15 NUT CHANNEL ASSEMBLY

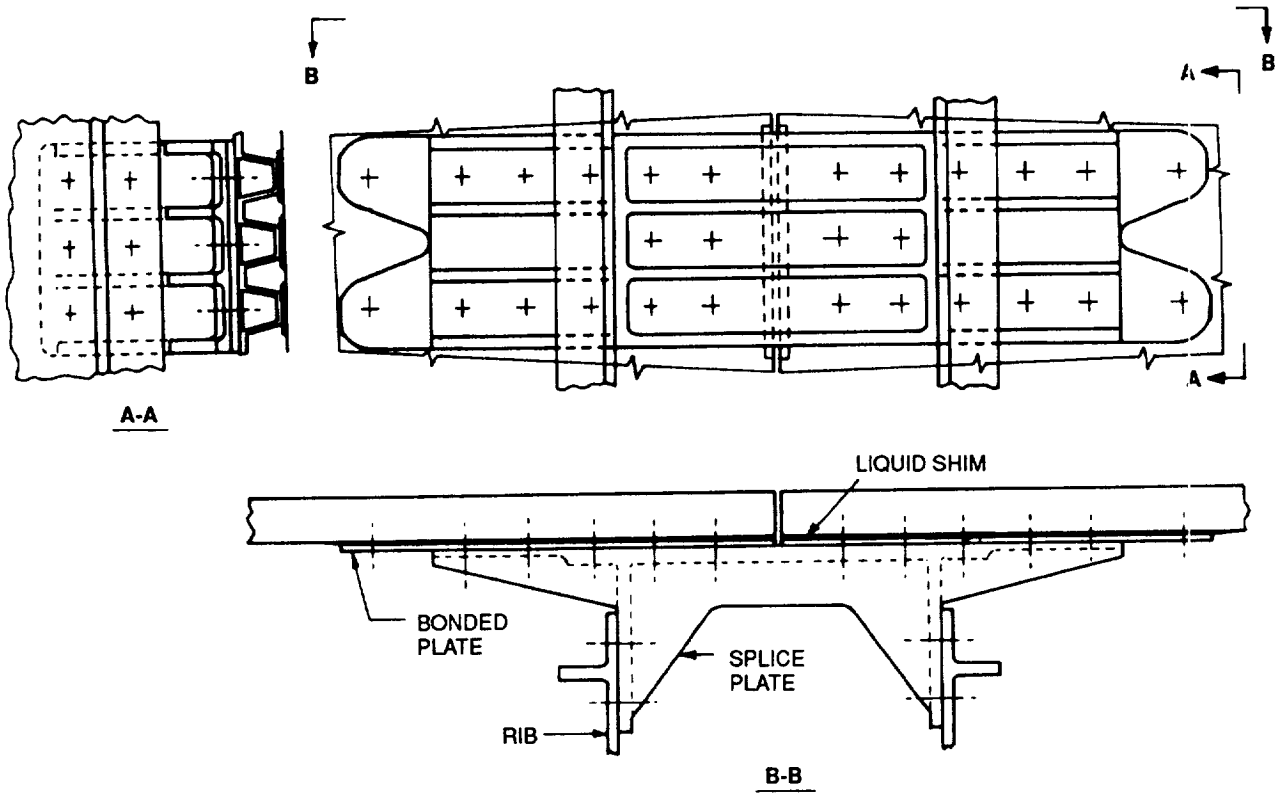

FIGURE 56. TWO-RIB CONCEPT

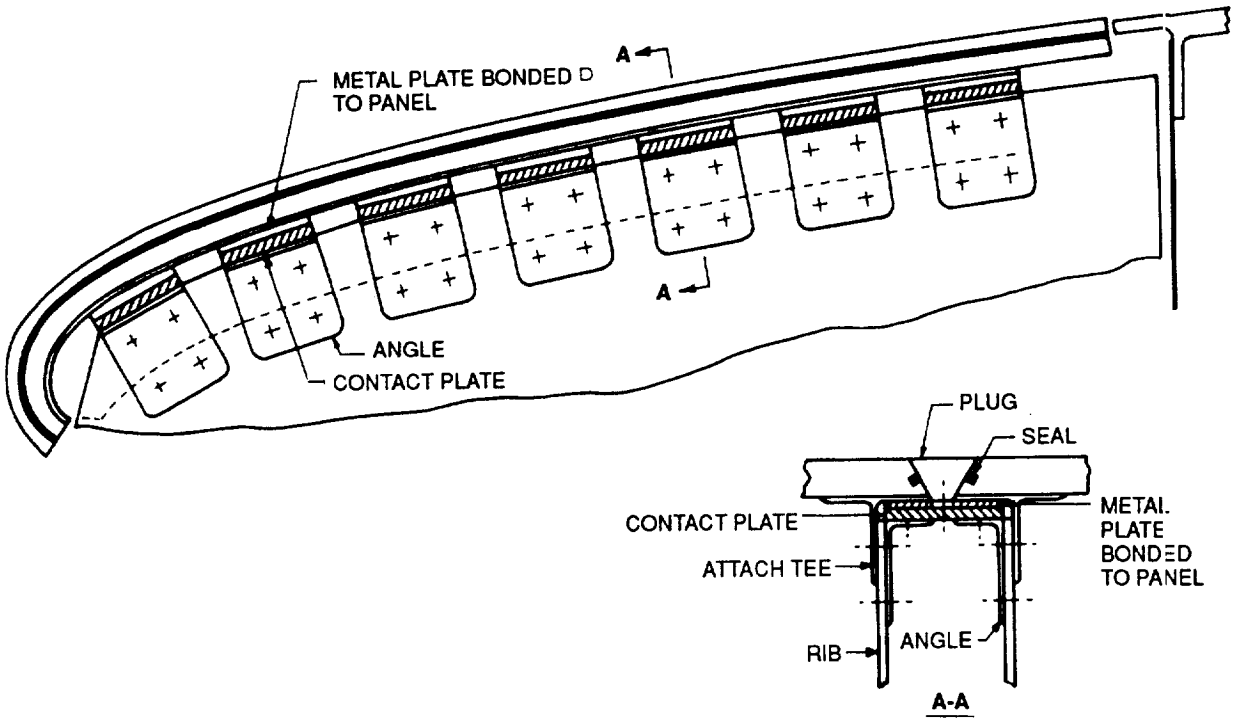

FIGURE 57. EXPANSION CONCEPT

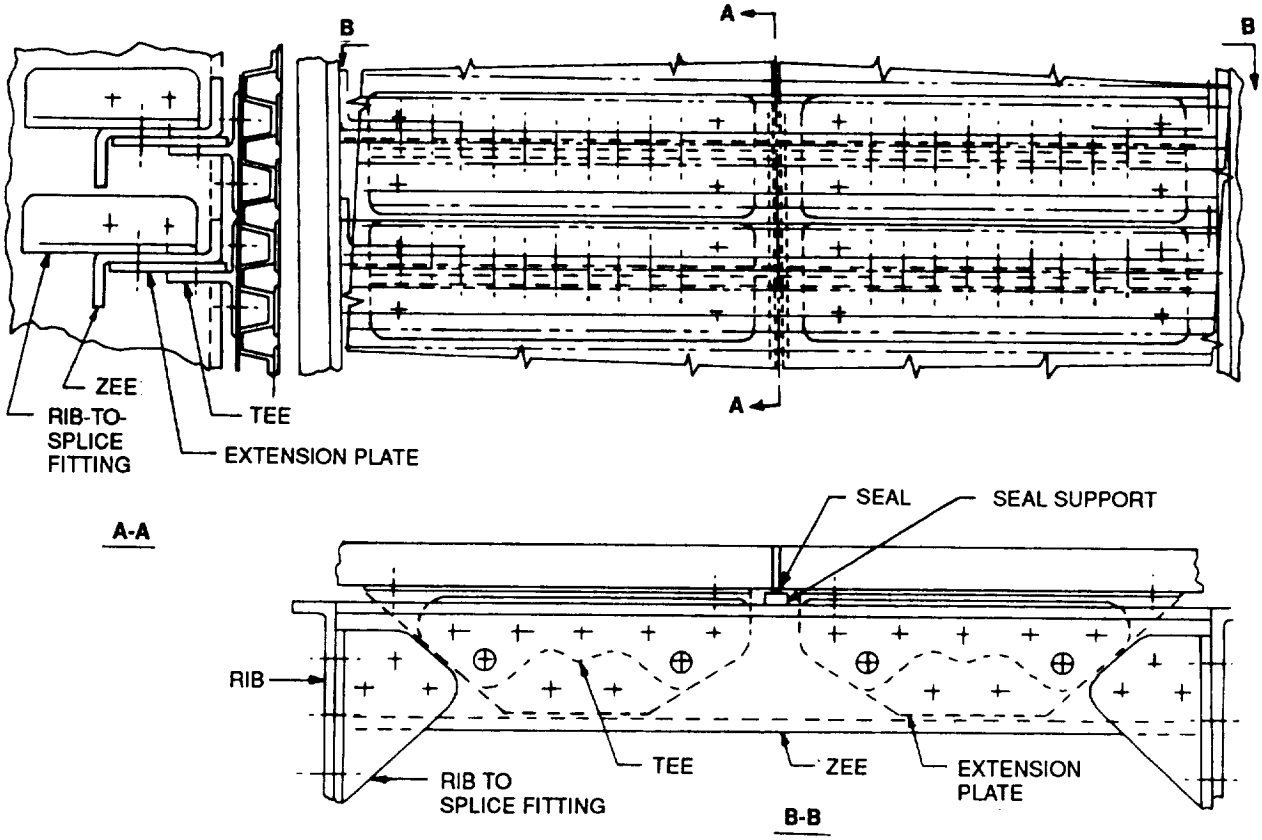

FIGURE 58. BLADE CONCEPT

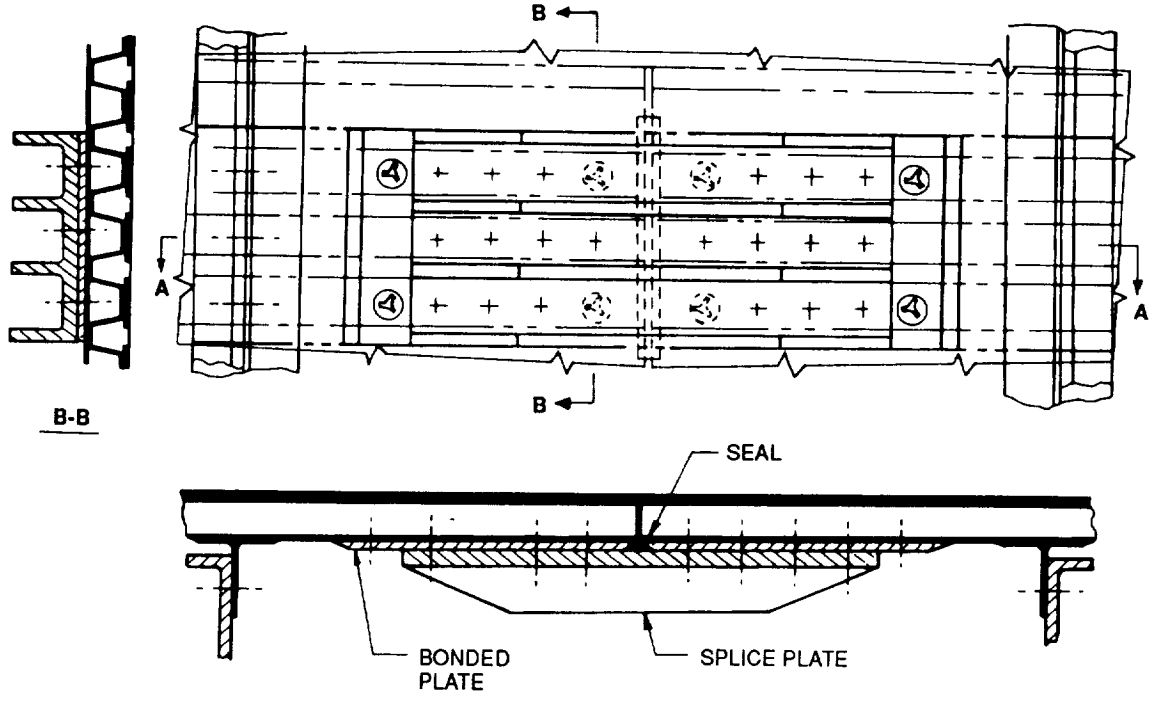

FIGURE 59. BEAM CONCEPT

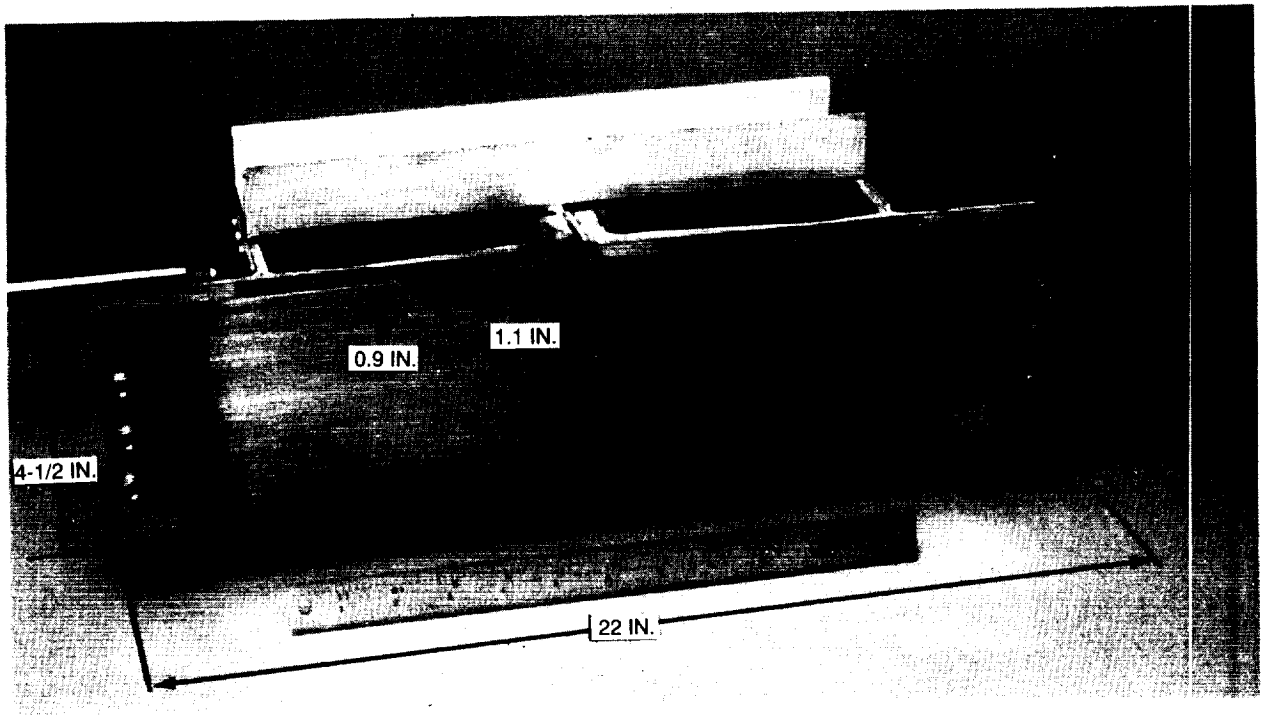

FIGURE 60. IMPROVED THREE-RIB DESIGN — TITANIUM SIDE

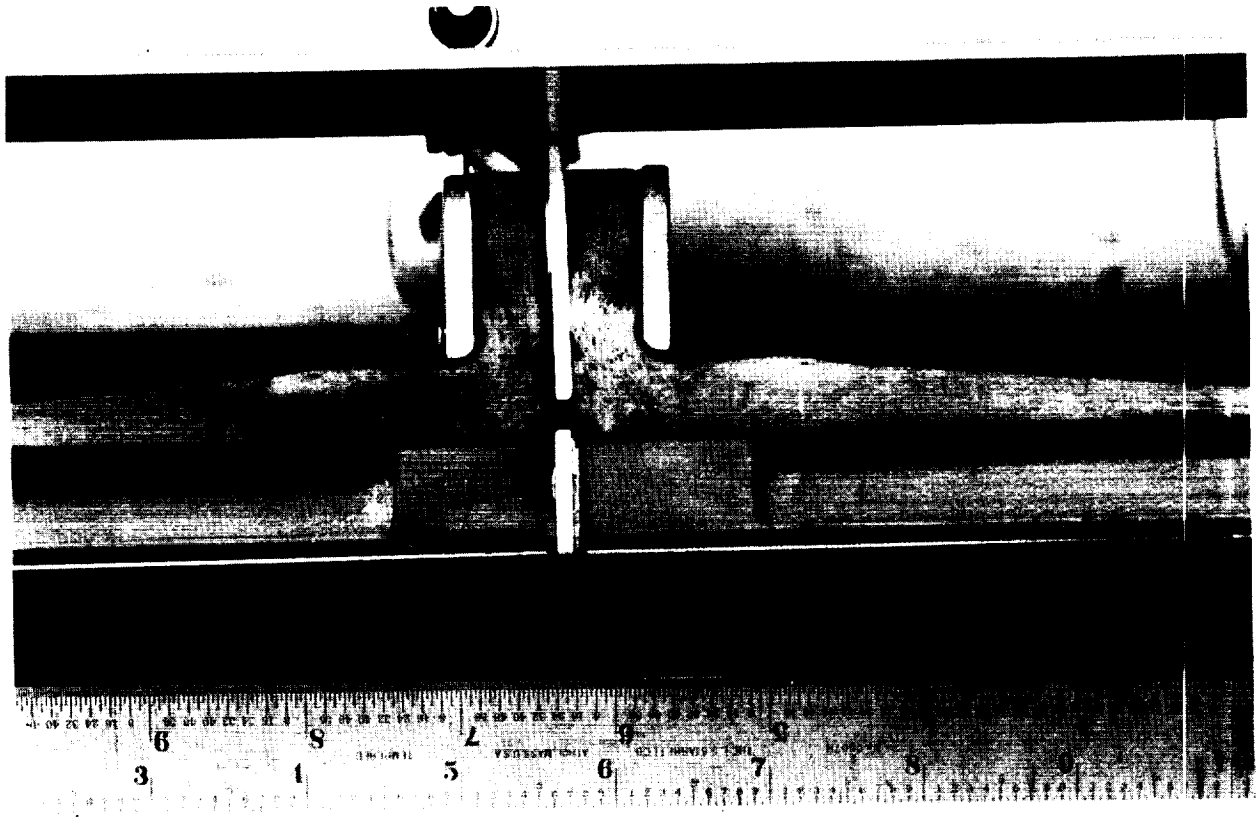

FIGURE 61. IMPROVED THREE-RIB DESIGN — CROSS SECTION

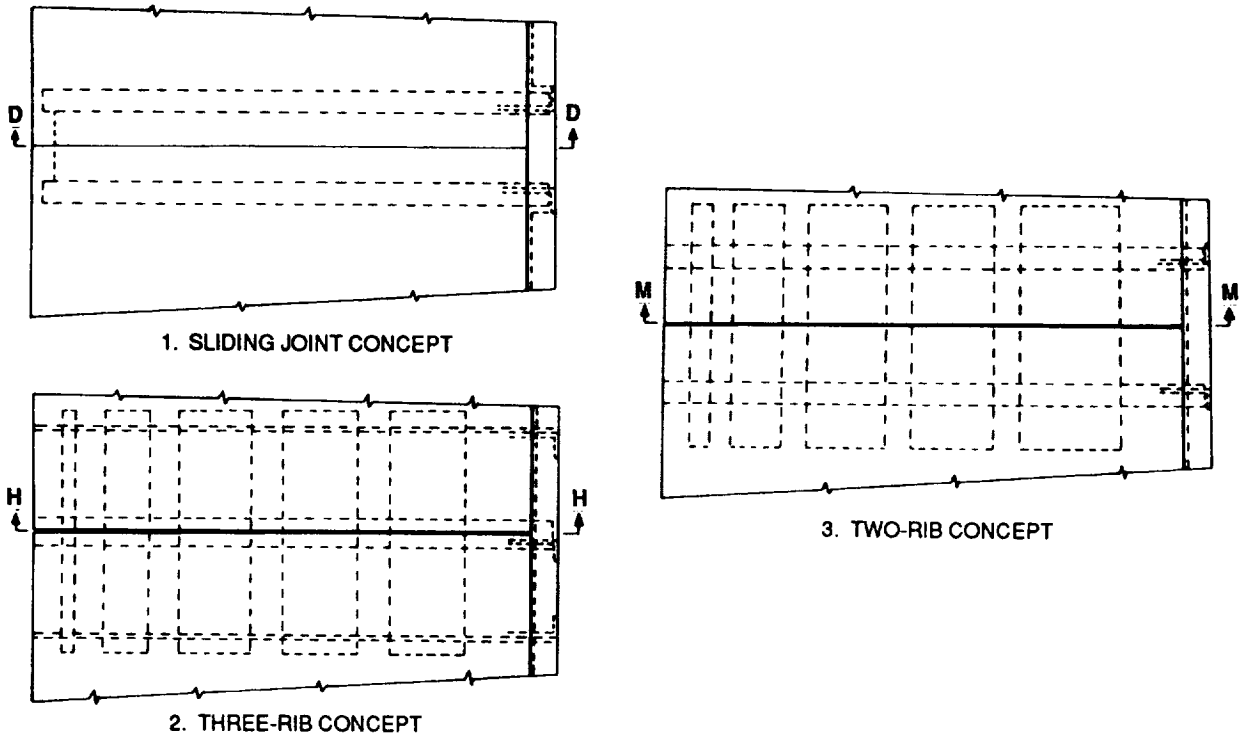

FIGURE 62. PLAN VIEWS OF CONCEPTS NO. 1 THROUGH 3

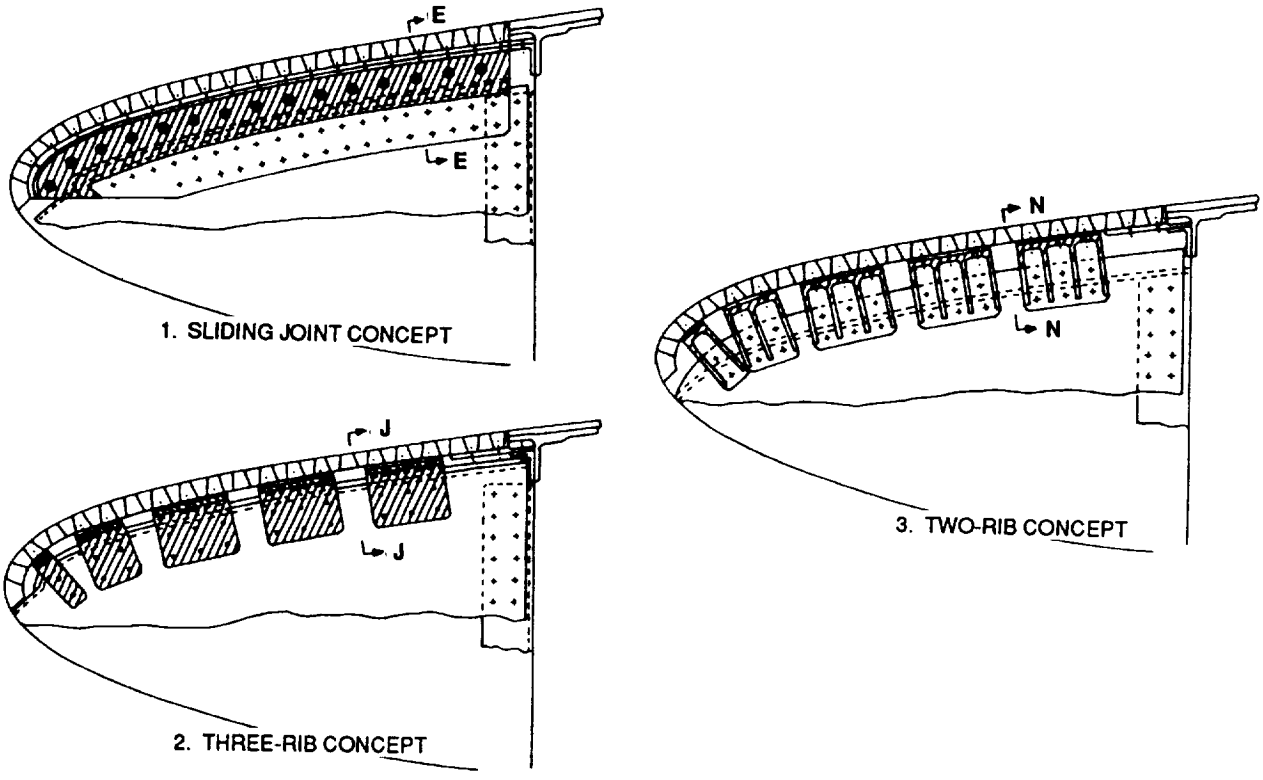

FIGURE 63. CROSS SECTIONS OF CONCEPTS NO. 1 THROUGH 3

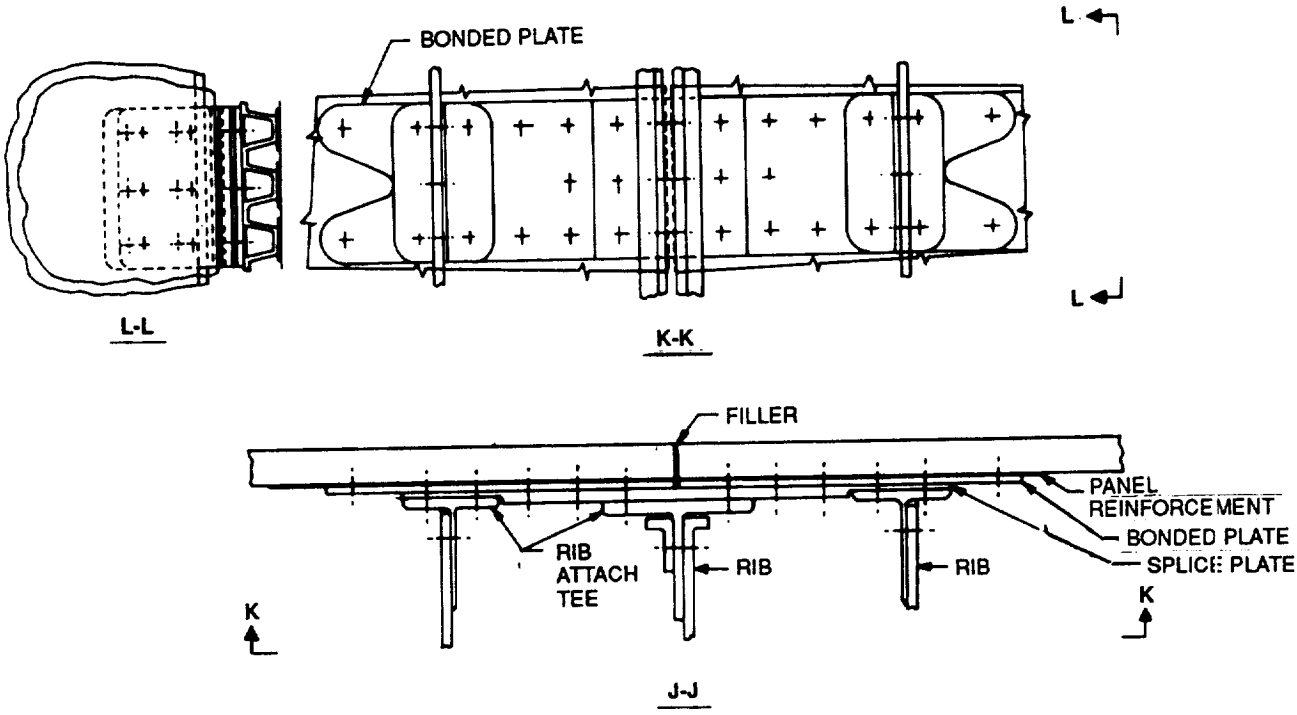

FIGURE 64. THREE-RIB CONCEPT

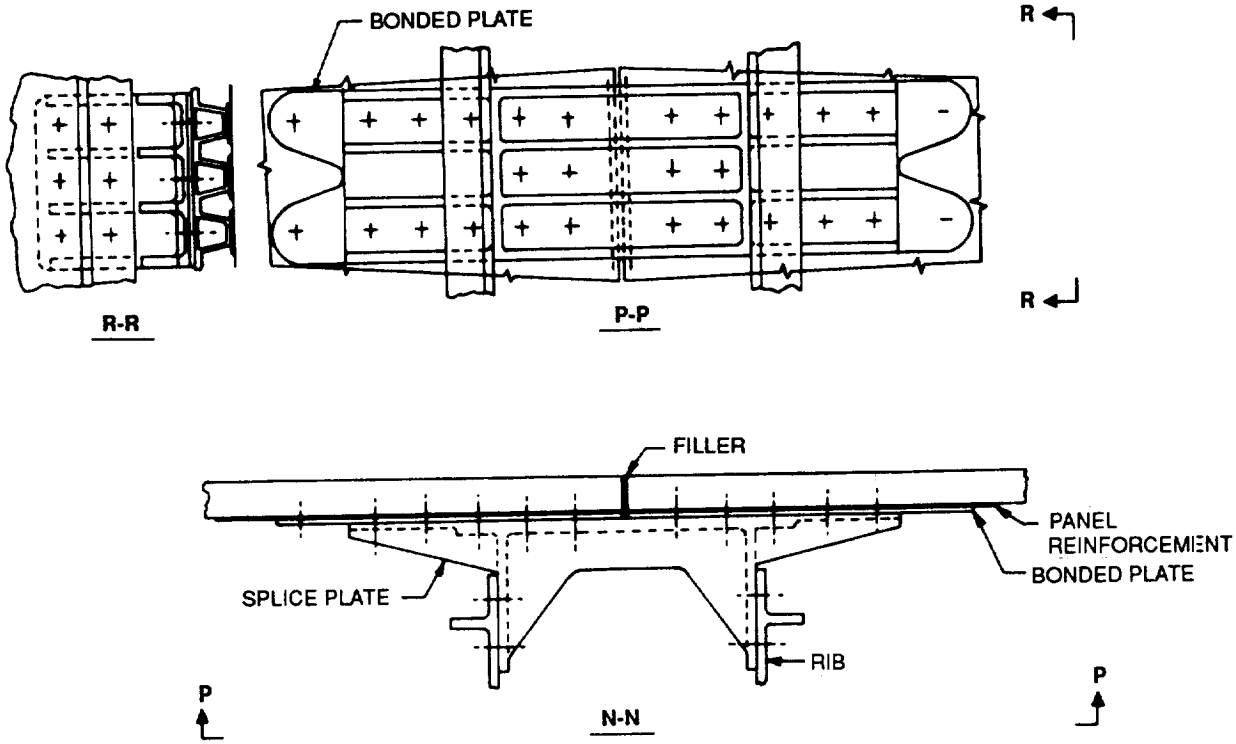

FIGURE 65. TWO-RIB CONCEPT

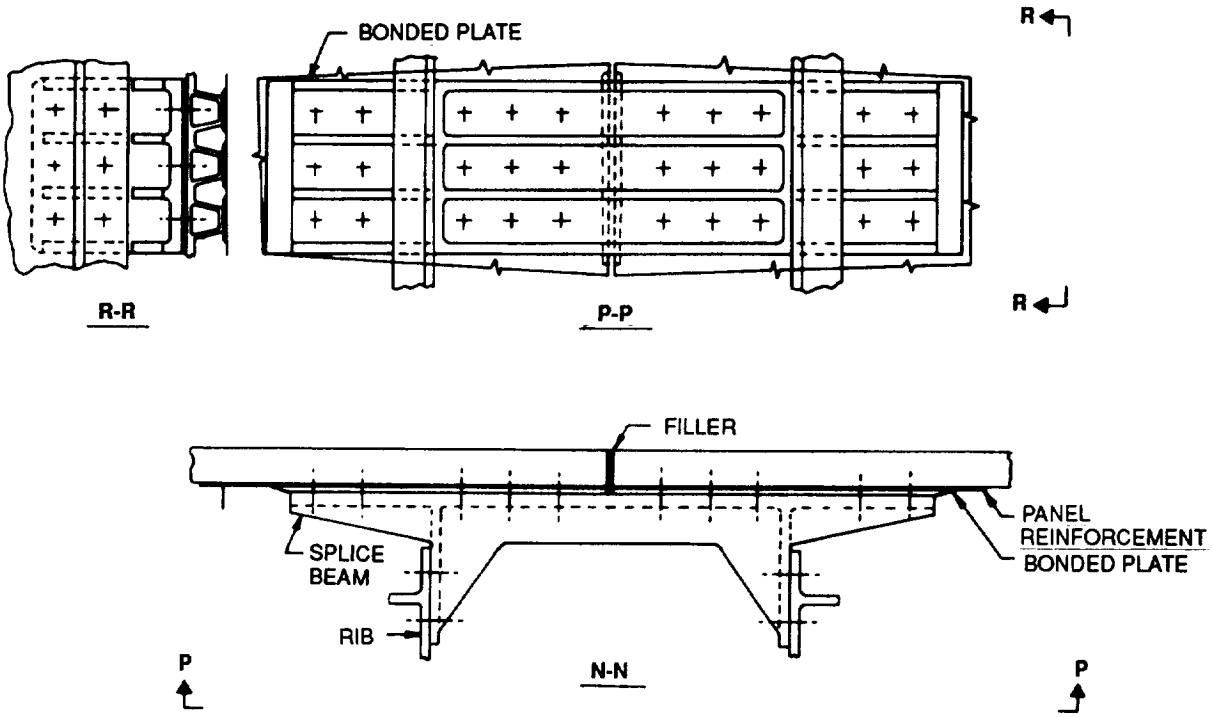

FIGURE 66. LENGTHENED TWO-RIB CONCEPT

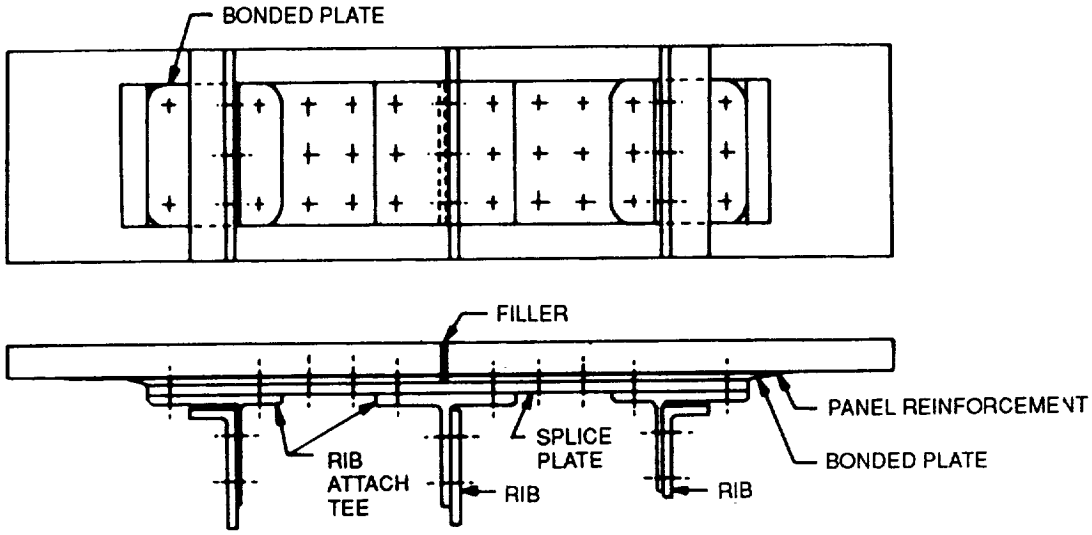

a. TENSION SHORT CHORDWISE SPECIMEN

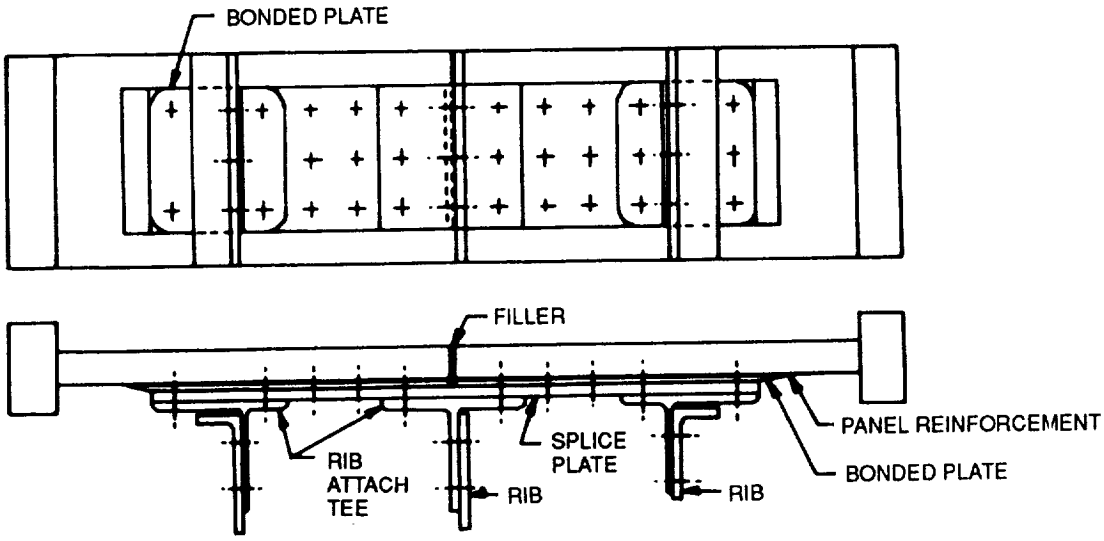

b. COMPRESSION SHORT CHORDWISE SPECIMEN

FIGURE 67. TENSION AND COMPRESSION SHORT CHORDWISE SPECIMENS FOR THREE-RIB CONCEPT

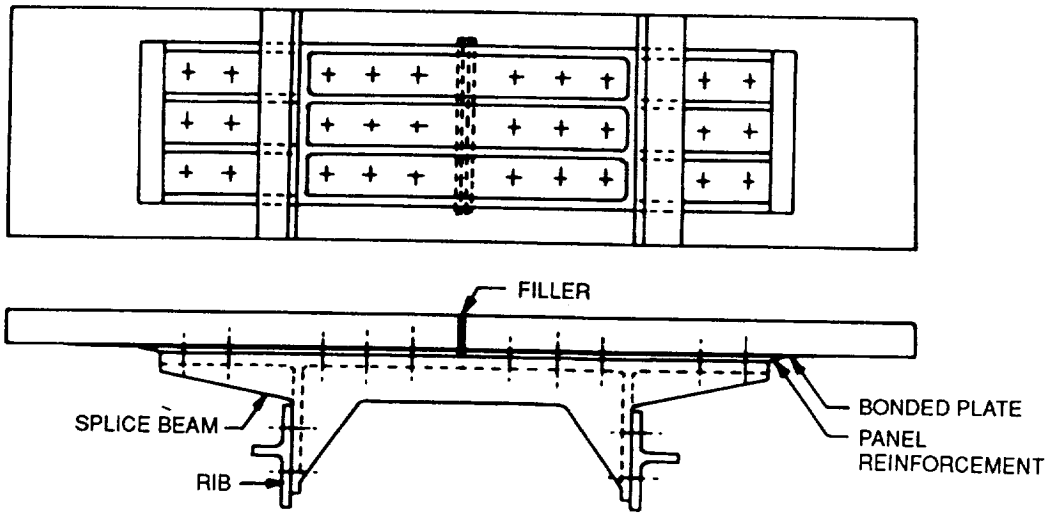

a. TENSION SHORT CHORDWISE SPECIMEN

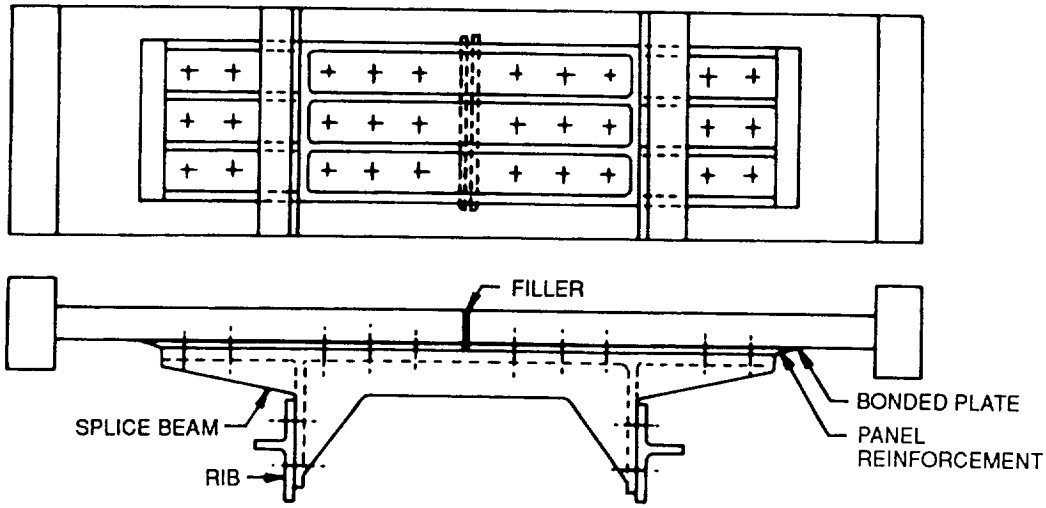

b. COMPRESSION SHORT CHORDWISE SPECIMEN

FIGURE 68. TENSION AND COMPRESSION SHORT CHORDWISE SPECIMENS FOR TWO-RIB CONCEPT

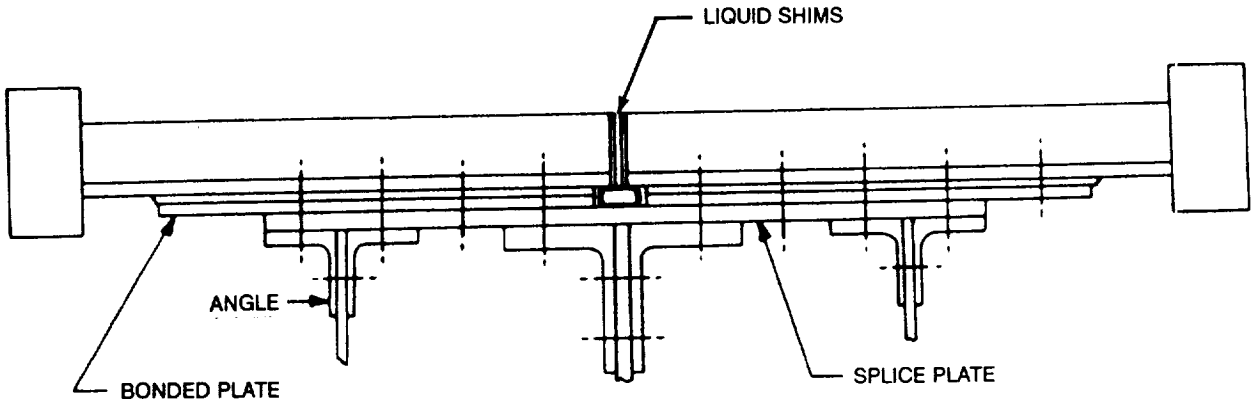

FIGURE 69. THREE-RIB CONCEPT WITH FLAT SPLICE PLATE AND LIQUID SHIM IN PLACE

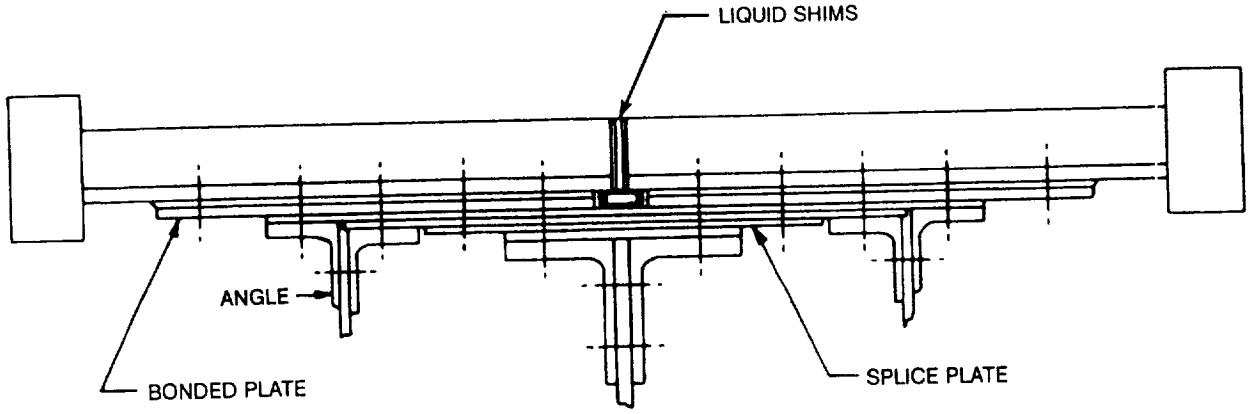

FIGURE 70. THREE-RIB CONCEPT WITH STEP-TAPERED SPLICE PLATE AND LIQUID SHIM IN PLACE

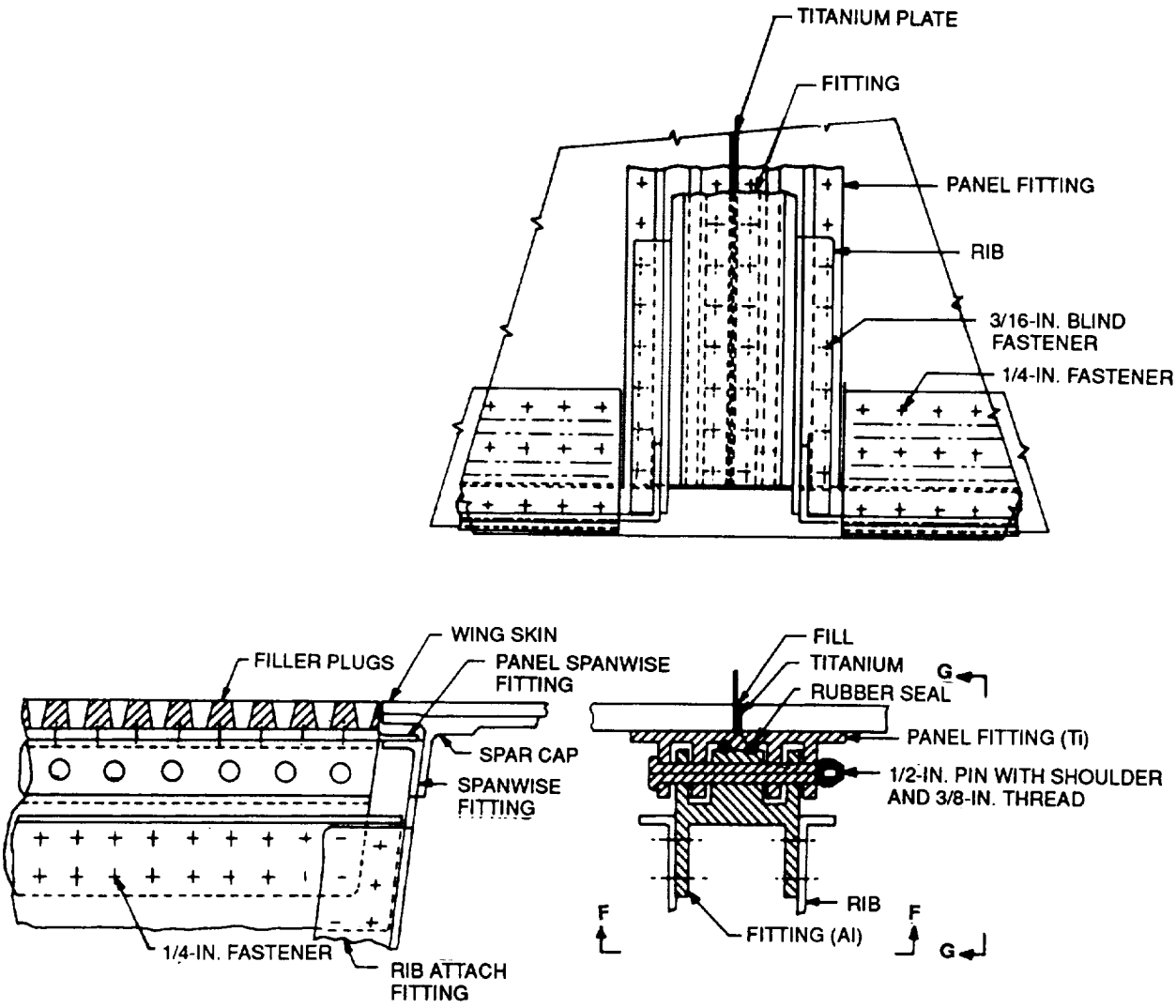

FIGURE 71. OVERALL ARRANGEMENT OF SLIDING CONCEPT

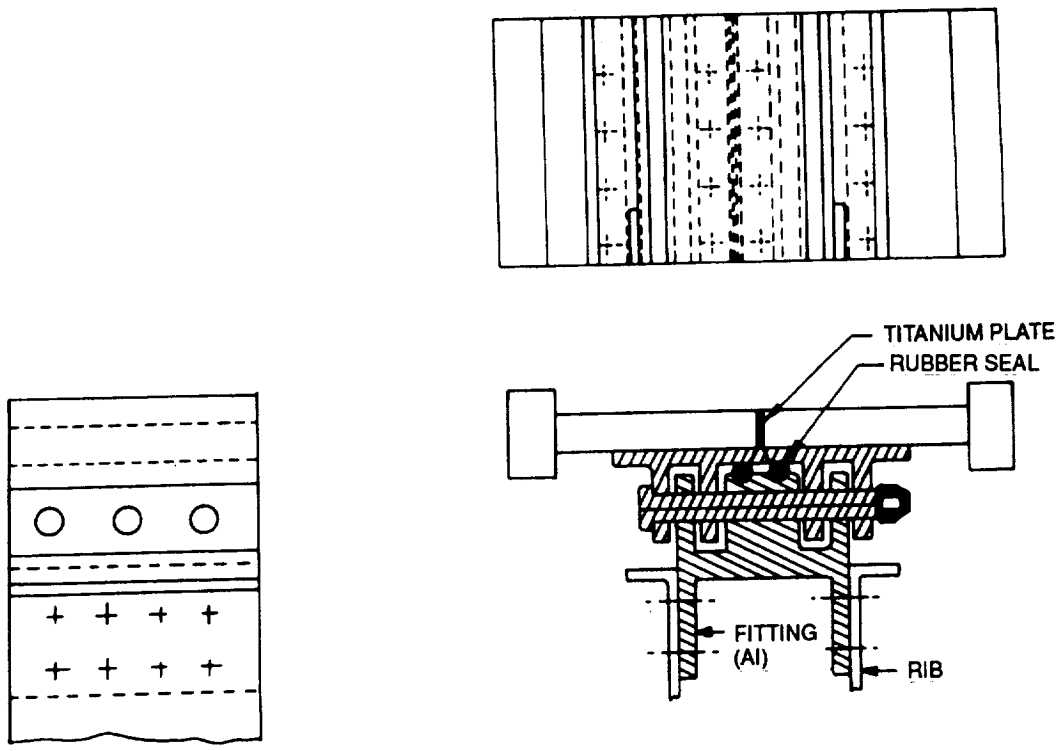

FIGURE 72. COMPRESSION SHORT CHORDWISE SPECIMEN FOR SLIDING CONCEPT

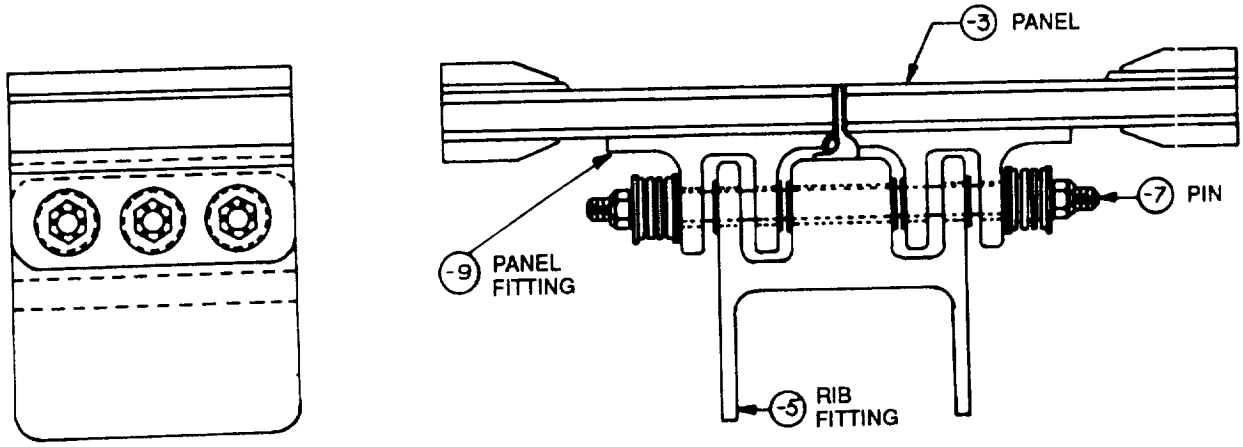

FIGURE 73. TEST PANEL FOR SLIDING CONCEPT DESIGN

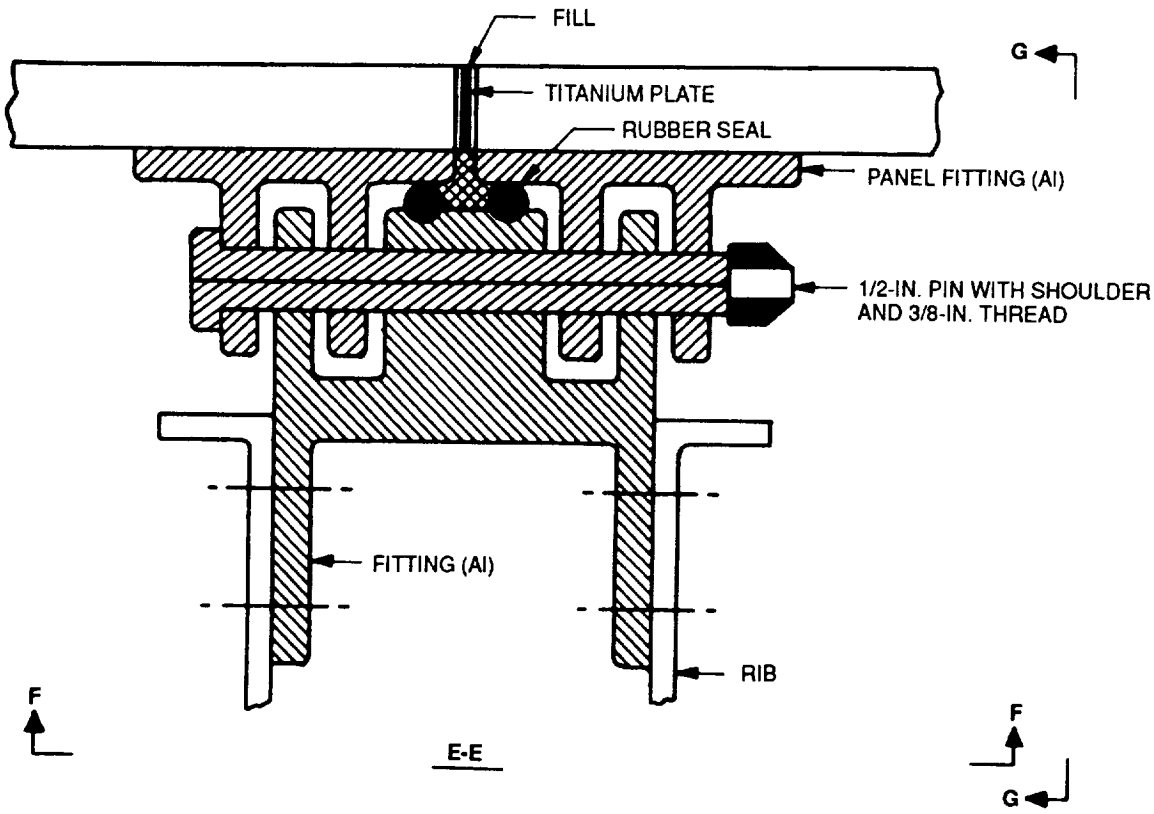

FIGURE 74. SLIDING CONCEPT

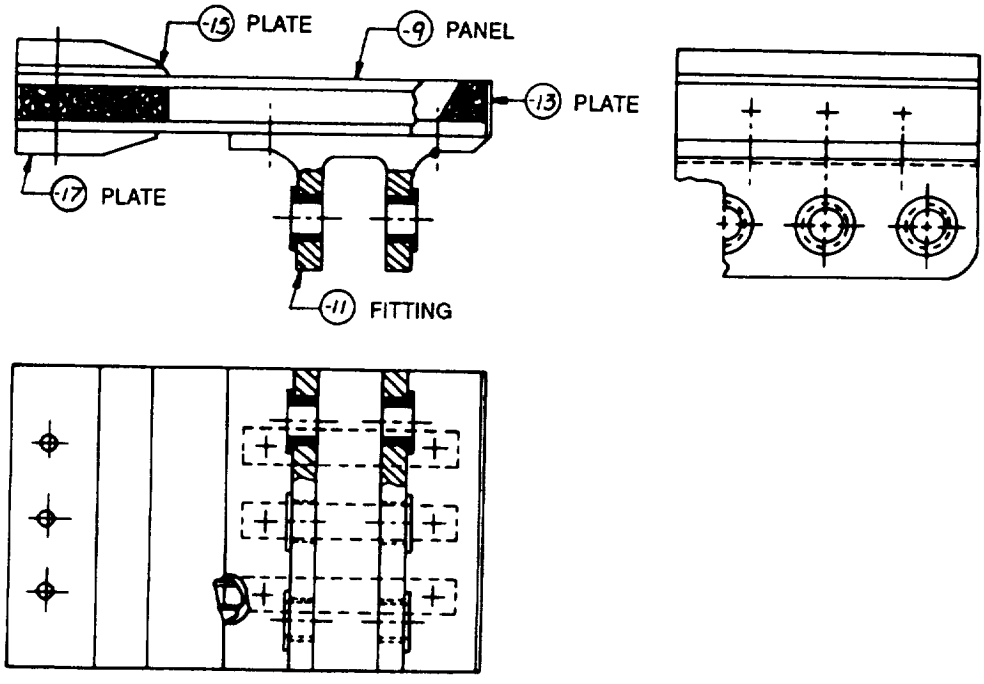

FIGURE 75. -3 PANEL ASSEMBLY — SMALL TEST SPECIMEN OF SLIDING-JOINT CONCEPT

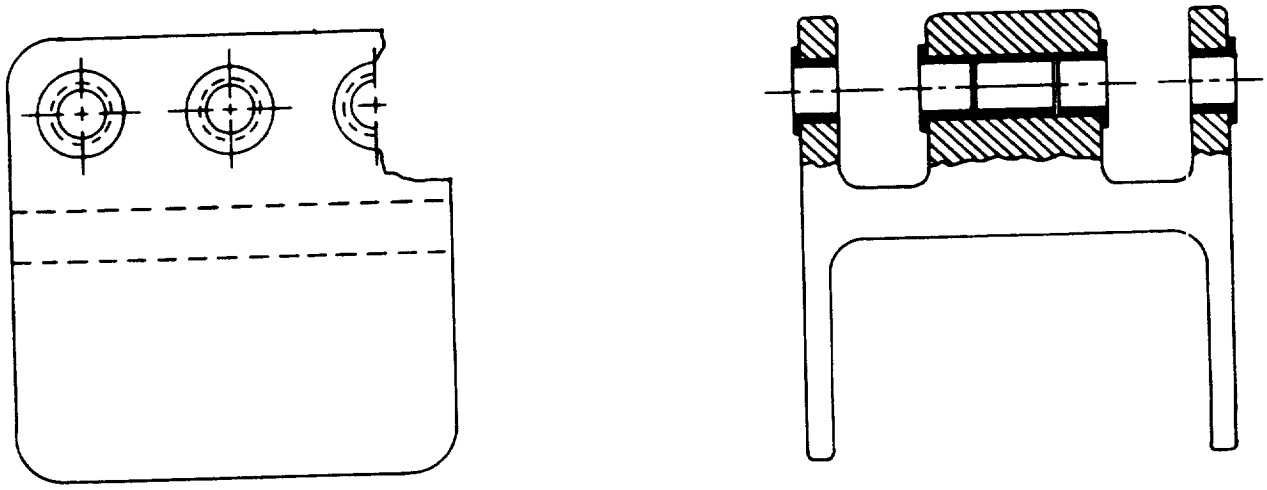

FIGURE 76. DETAILS OF -5 ALUMINUM-BRONZE BUSHINGS

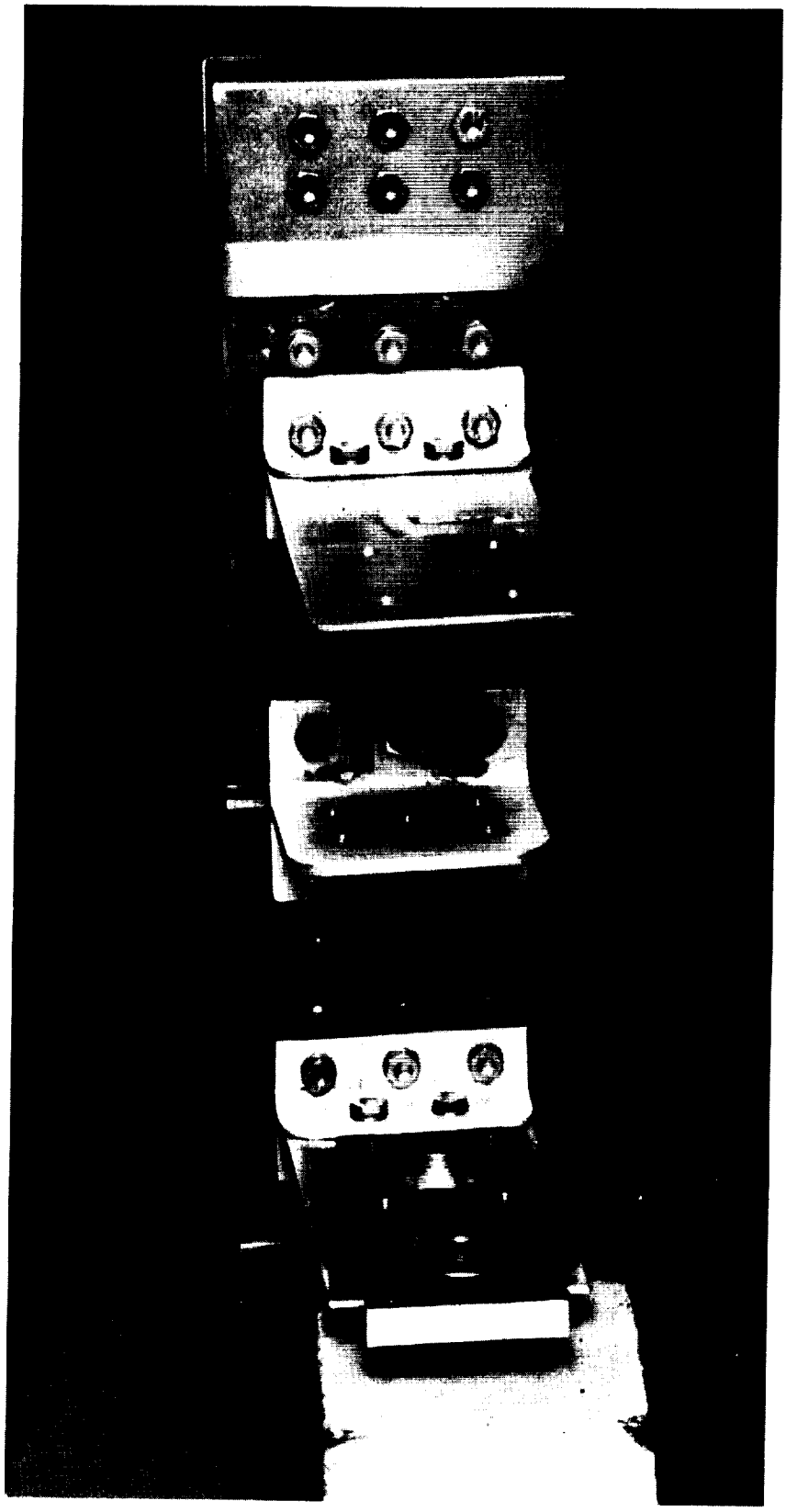

FIGURE 77. THREE-RIB CONCEPT — COMPOSITE SIDE

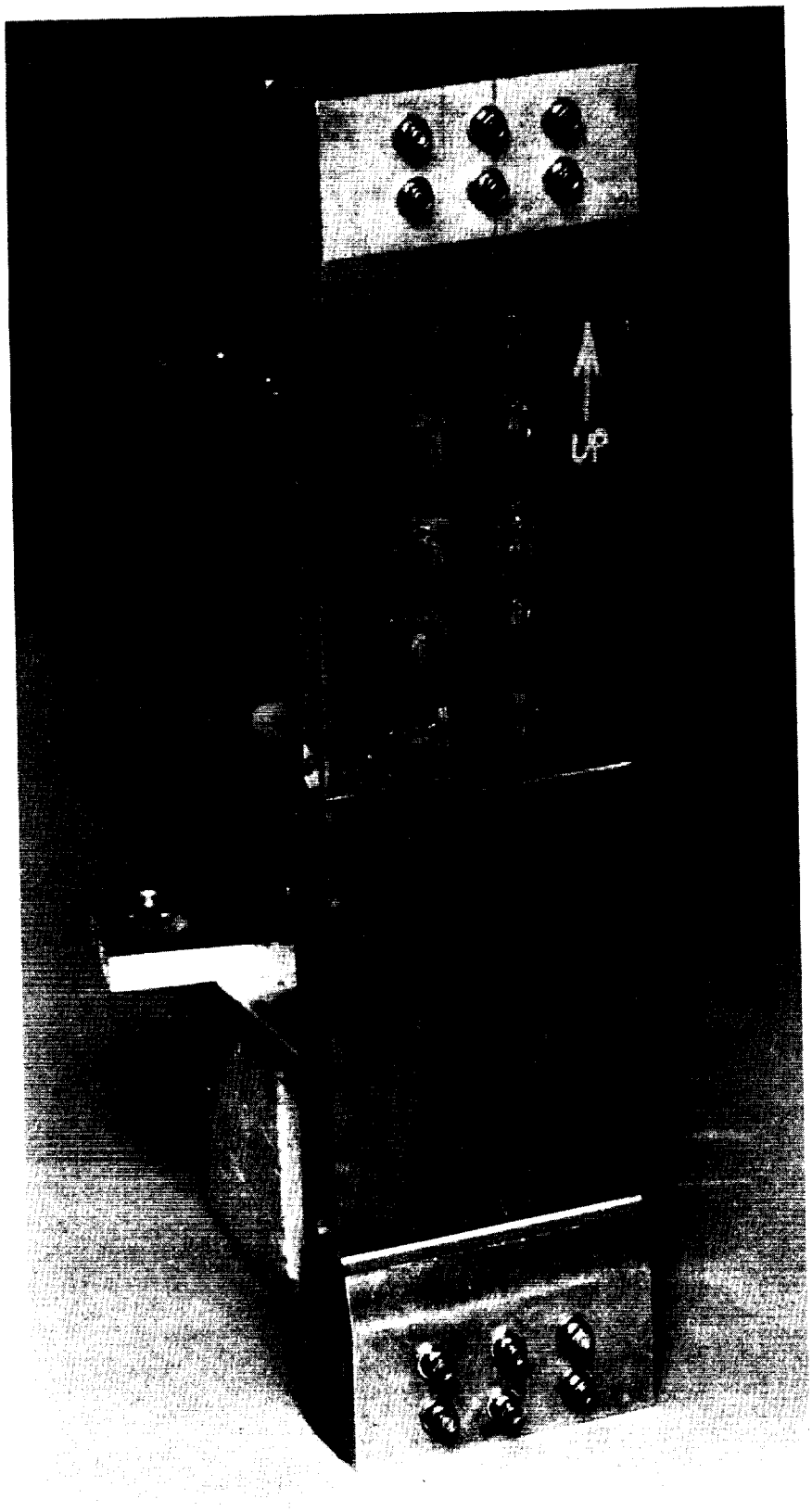

FIGURE 78. THREE-RIB CONCEPT — TITANIUM SIDE

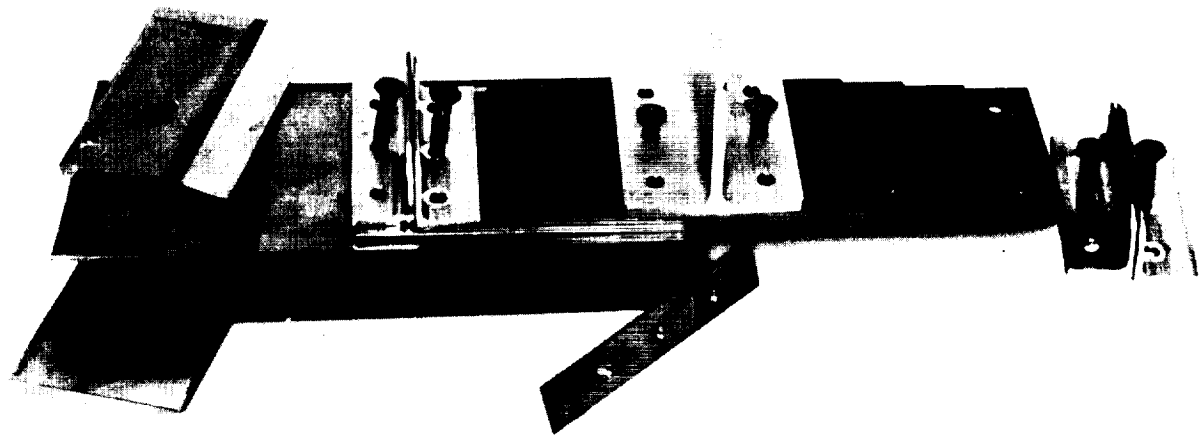

FIGURE 79. THREE-RIB JOINT CONCEPT SHOWING TAPERED SPLICE PLATES

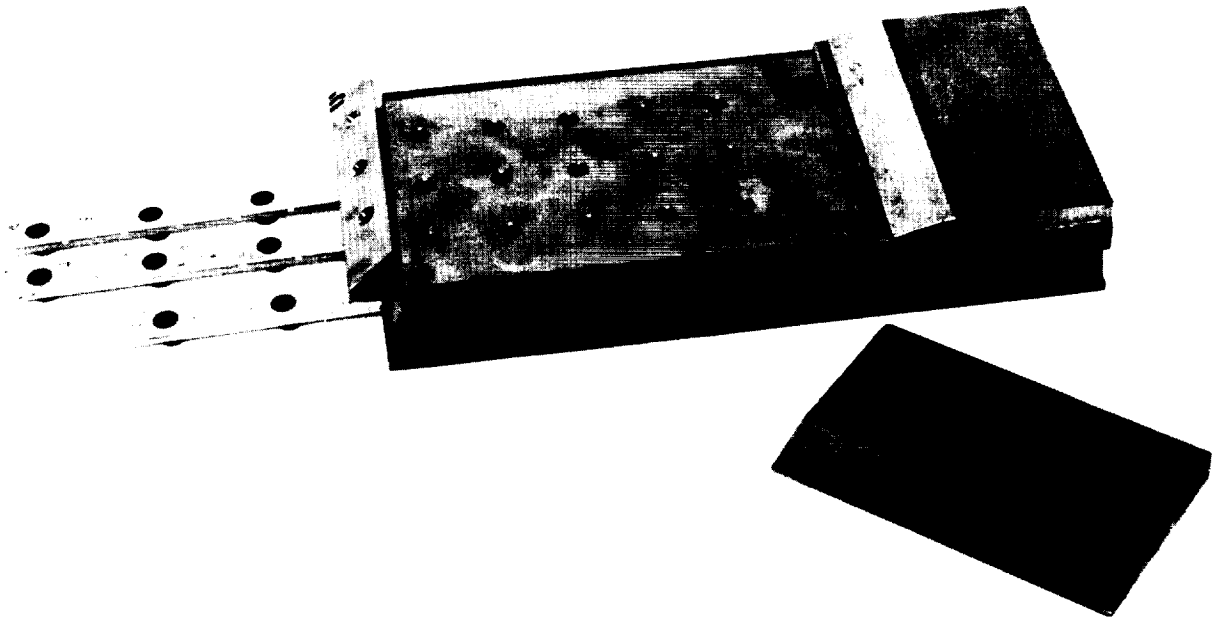

FIGURE 80. THREE-RIB JOINT CONCEPT SHOWING PANEL WITH NUT CHANNELS

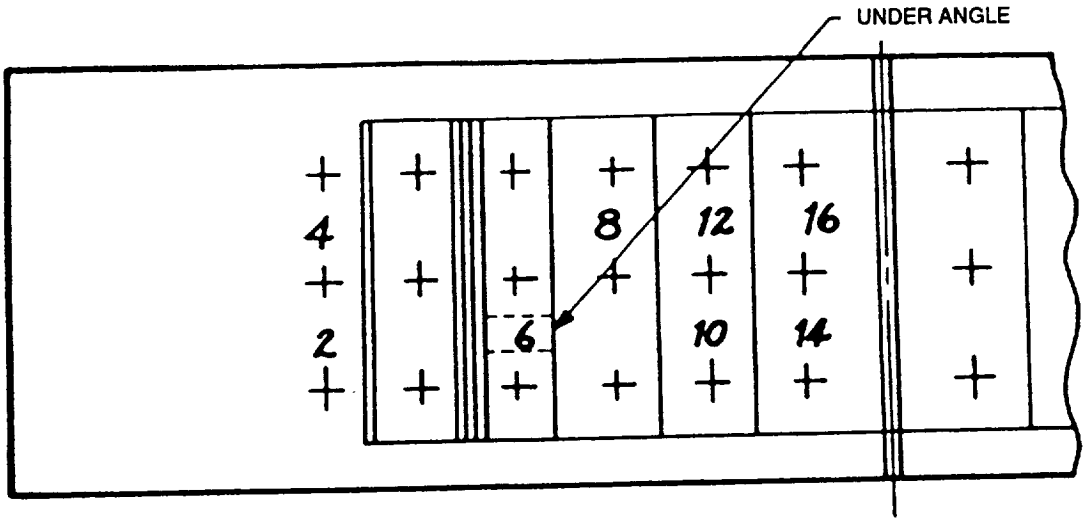

LOWER SURFACE

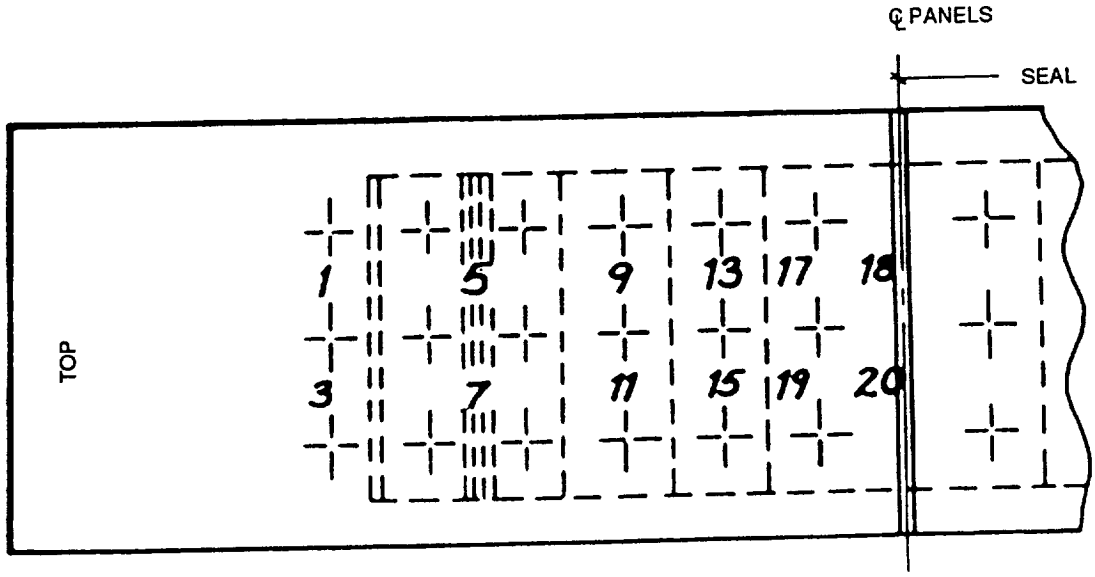

UPPER SURFACE (PERF TI)

STRAIN GAGE AS SHOWN (20 REQUIRED)

NOTE: LENGTH IS 18-1/2 INCHES

FIGURE 81. LOCATION OF STRAIN GAGES FOR THREE-RIB CONCEPT

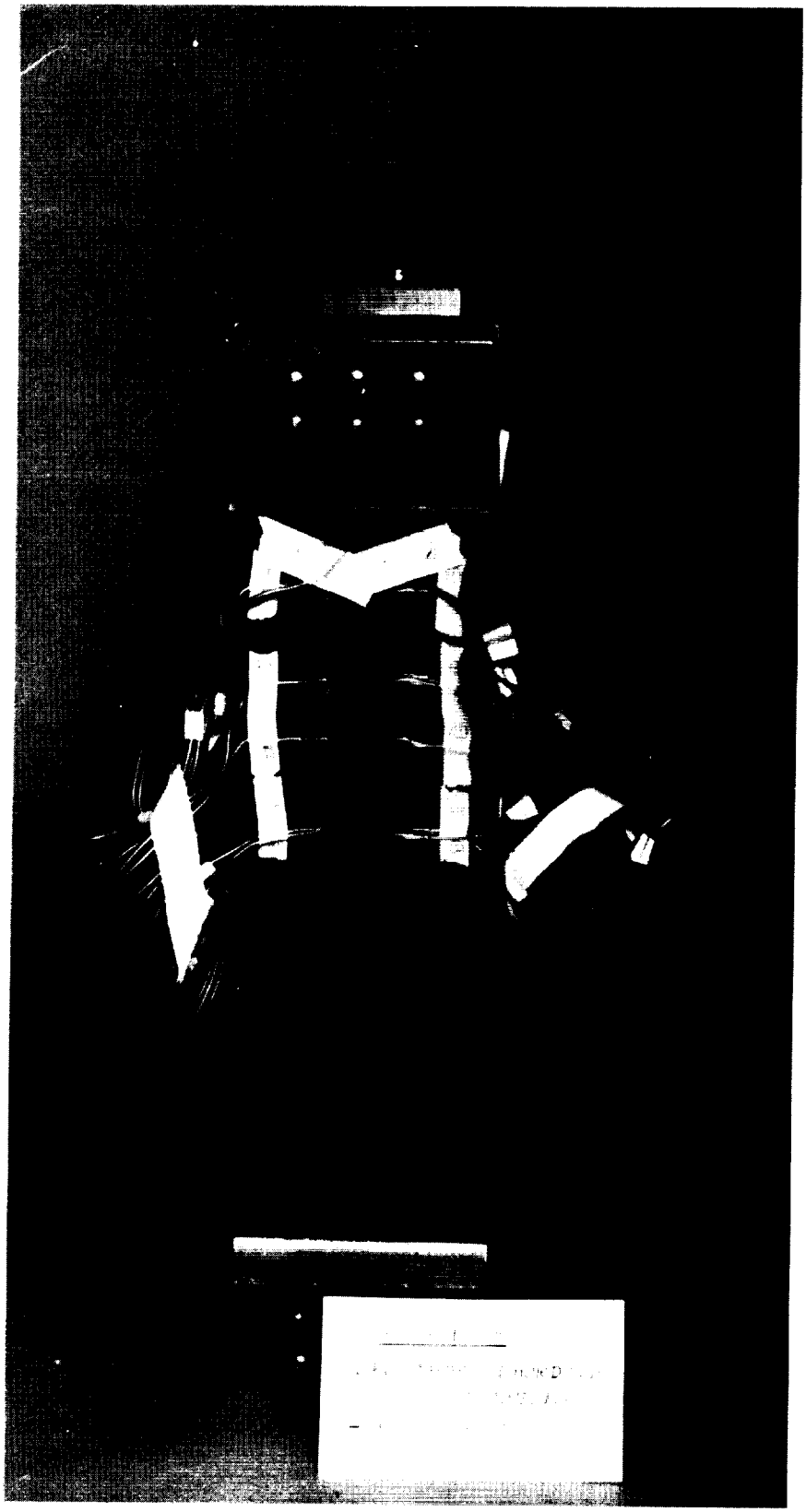

FIGURE 82. THREE-RIB CONCEPT — LFC SHORT CHORDWISE JOINT ASSEMBLY — FRONT VIEW OF TITANIUM FACE

FIGURE 83. THREE-RIB CONCEPT — LFC SHORT CHORDWISE JOINT ASSEMBLY — SIDE VIEW OF TITANIUM FACE

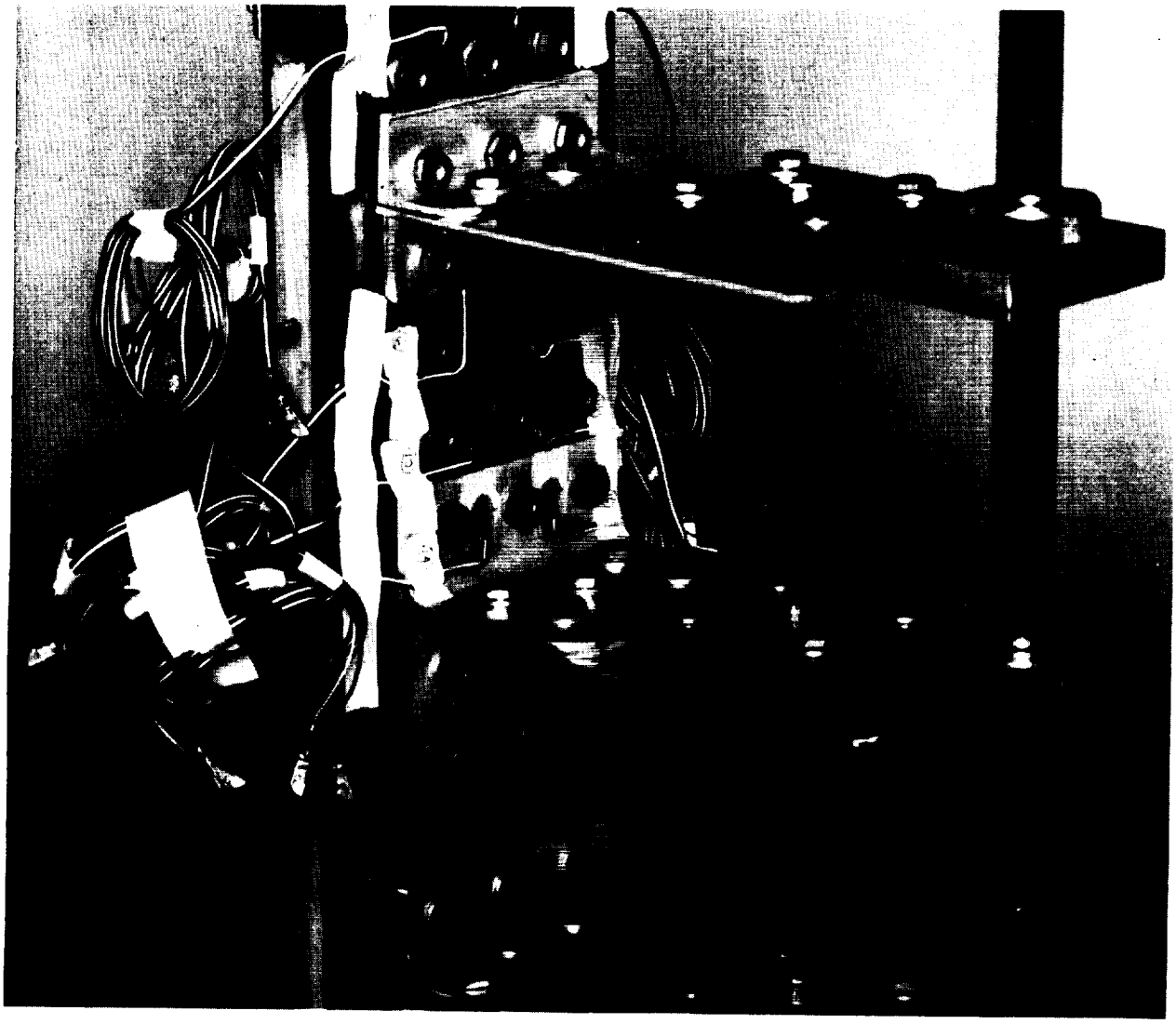

FIGURE 84. THREE-RIB CONCEPT — LFC SHORT CHORDWISE JOINT ASSEMBLY — CLOSE-UP VIEW OF COMPOSITE SIDE

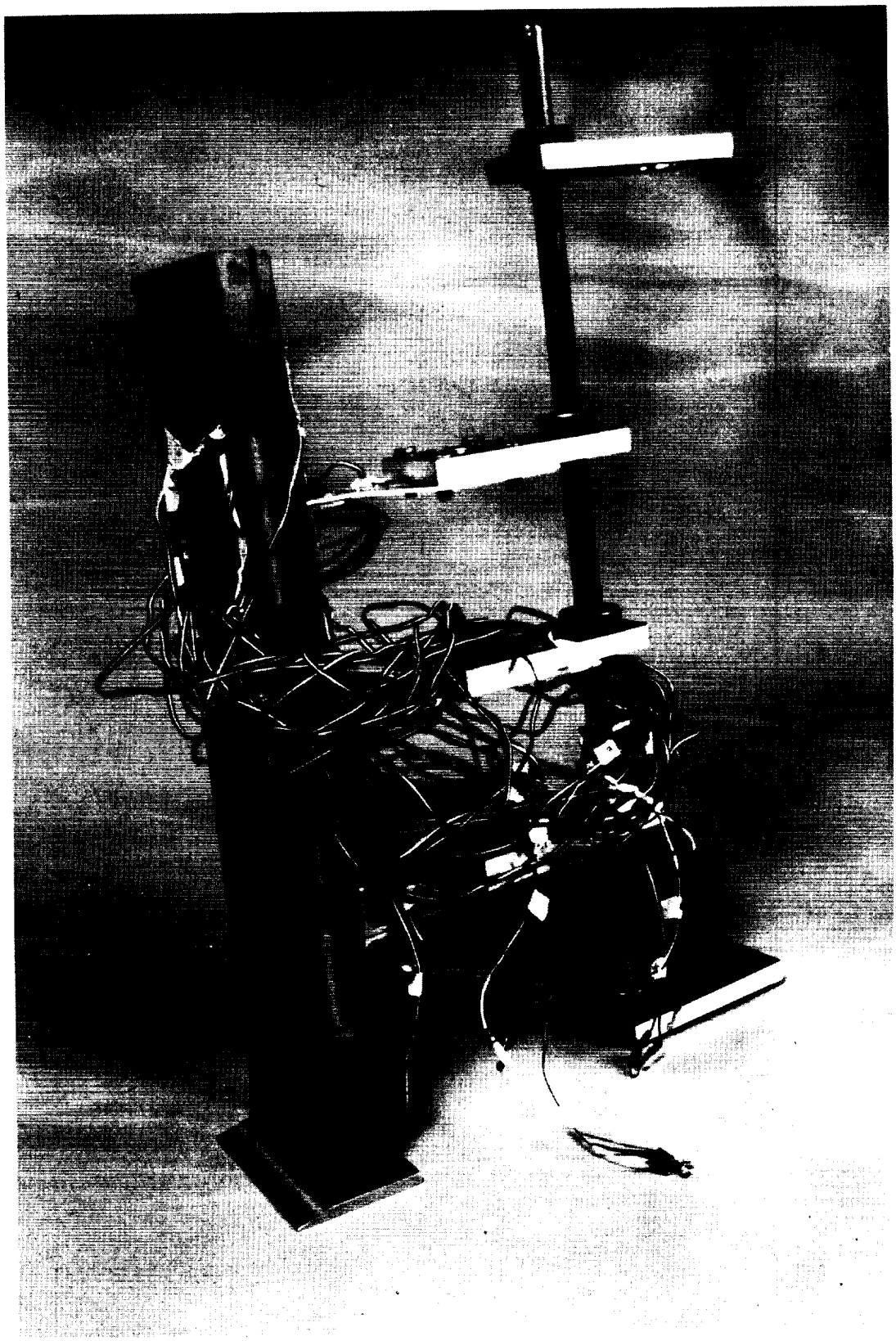

FIGURE 85. THREE-RIB CONCEPT (WITHOUT SEAL) AFTER TEST — NOTICE CENTER BOWING AT THE GAP

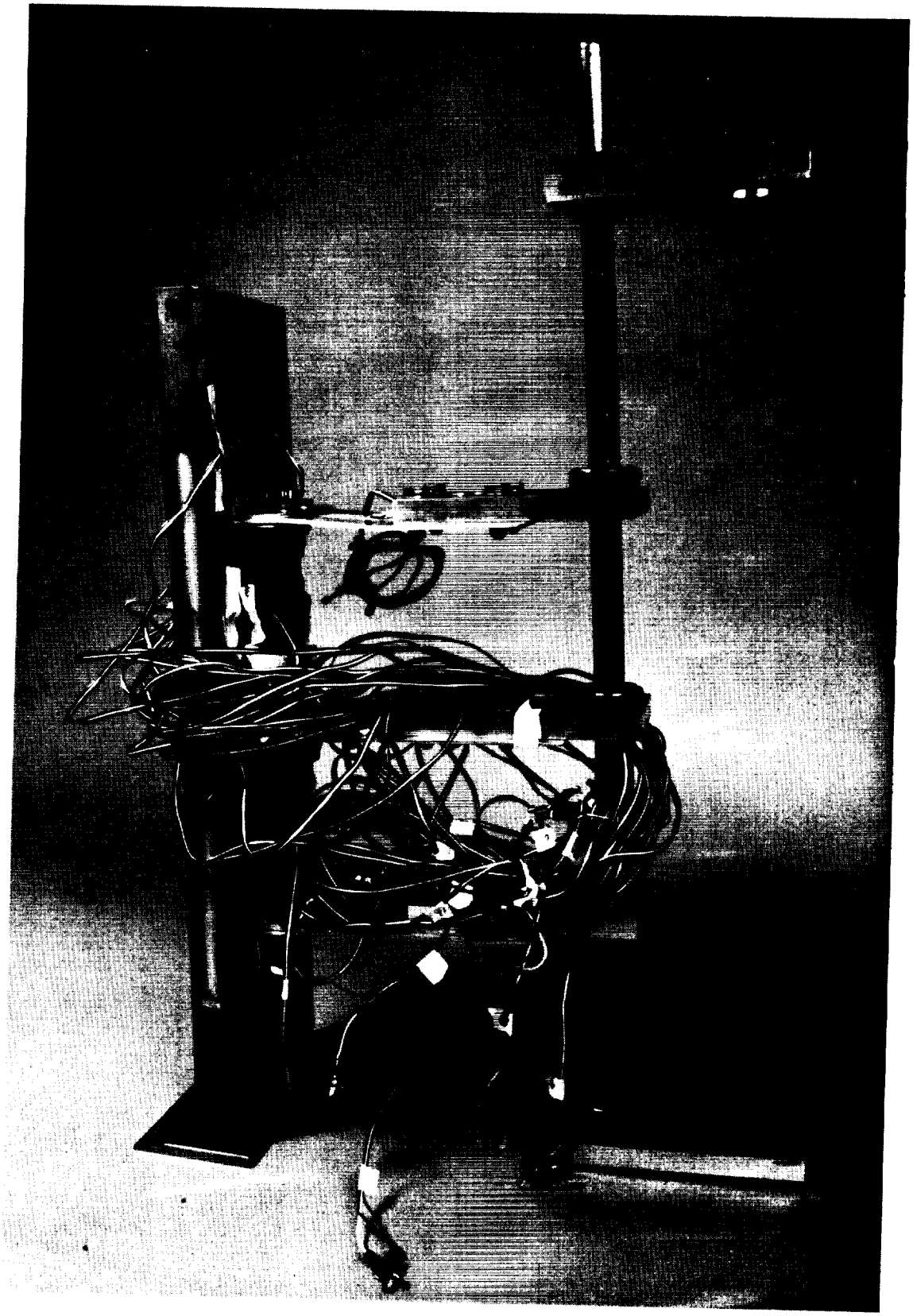

FIGURE 86. THREE-RIB CONCEPT (WITHOUT SEAL) AFTER TEST — NOTICE UPPER RIB BENDING

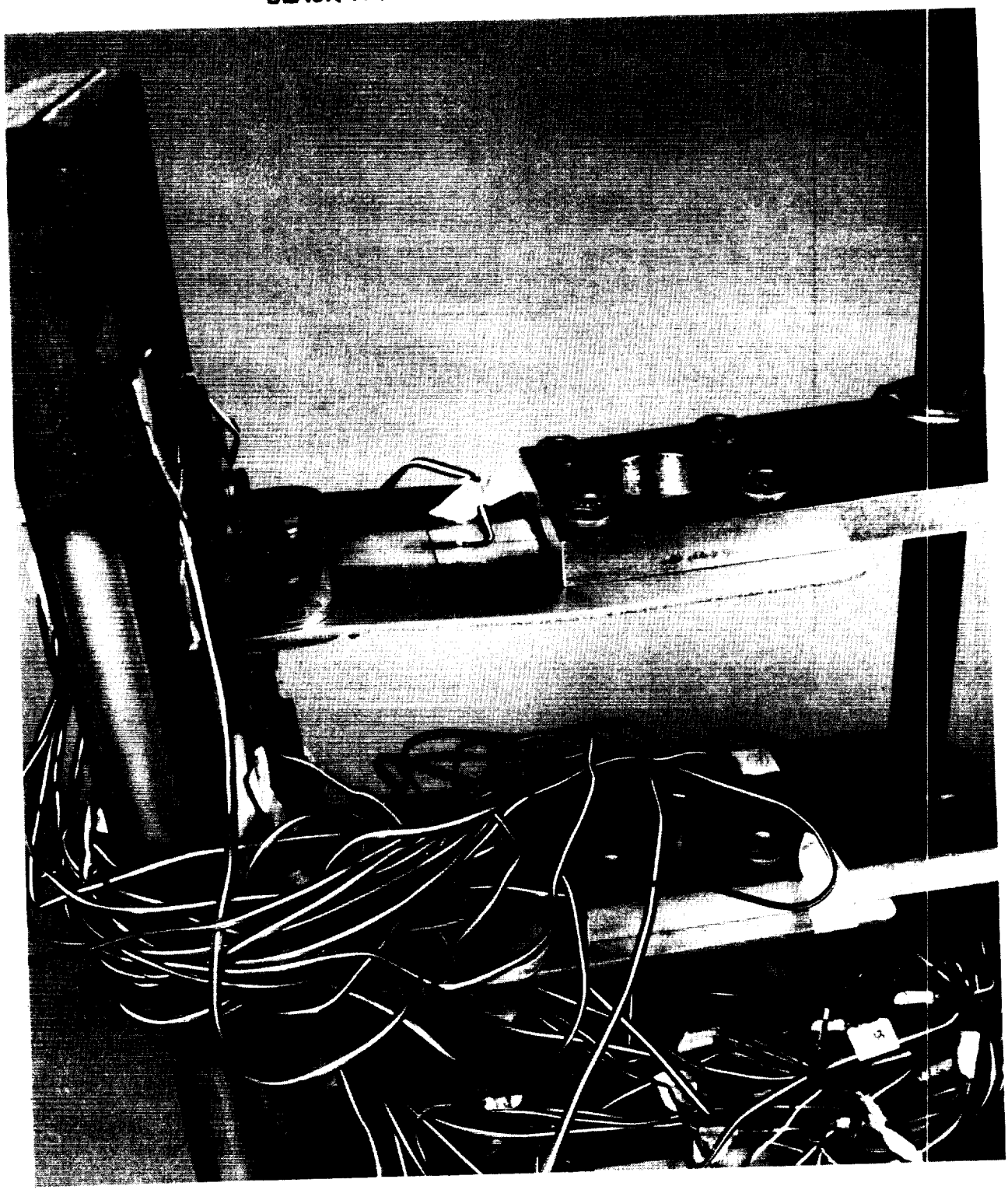

FIGURE 87. CLOSE-UP OF THREE-RIB CONCEPT SMALL TEST SPECIMEN

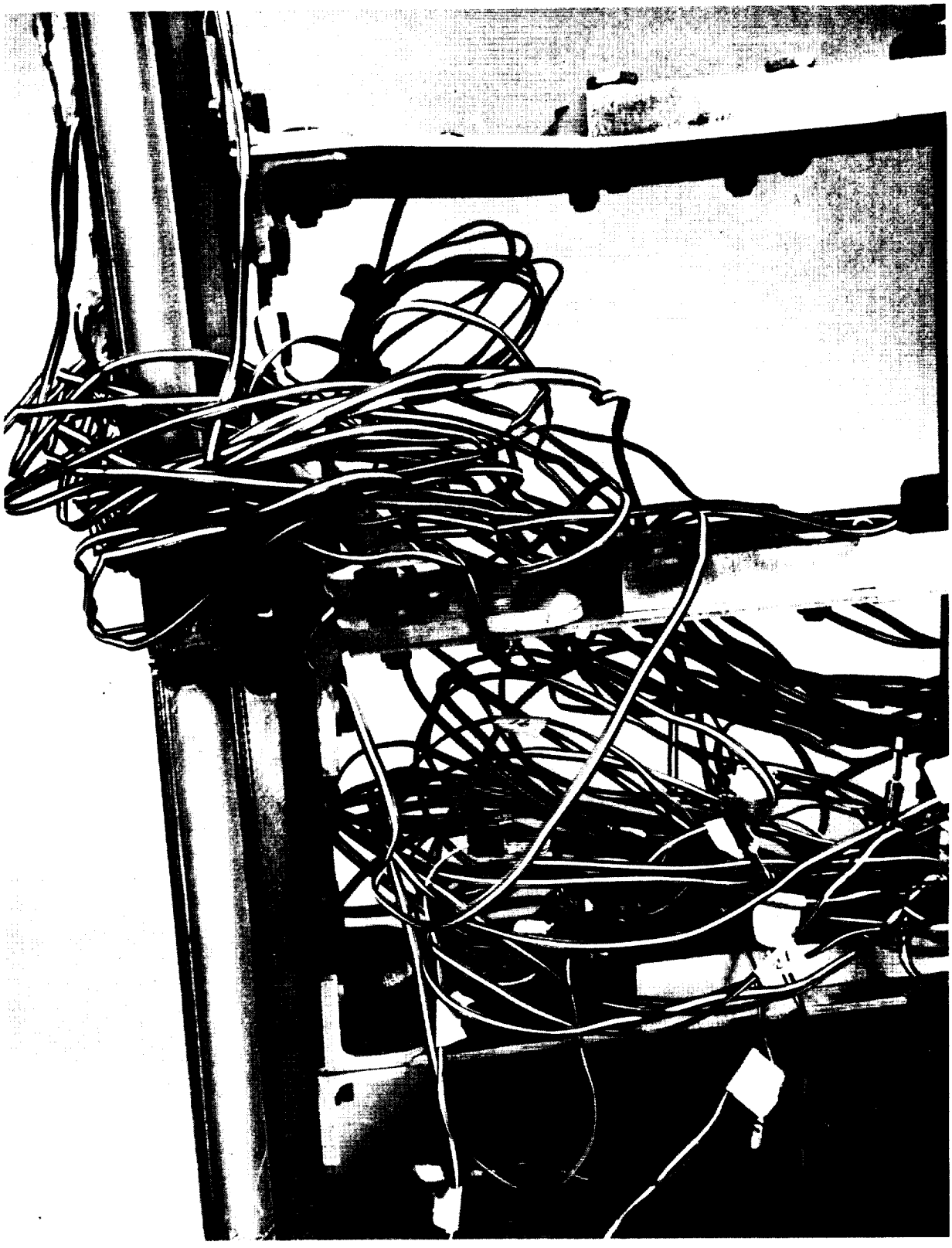

FIGURE 88. THREE-RIB CONCEPT — CLOSE-UP OF GAP WITH SEAL REMOVED

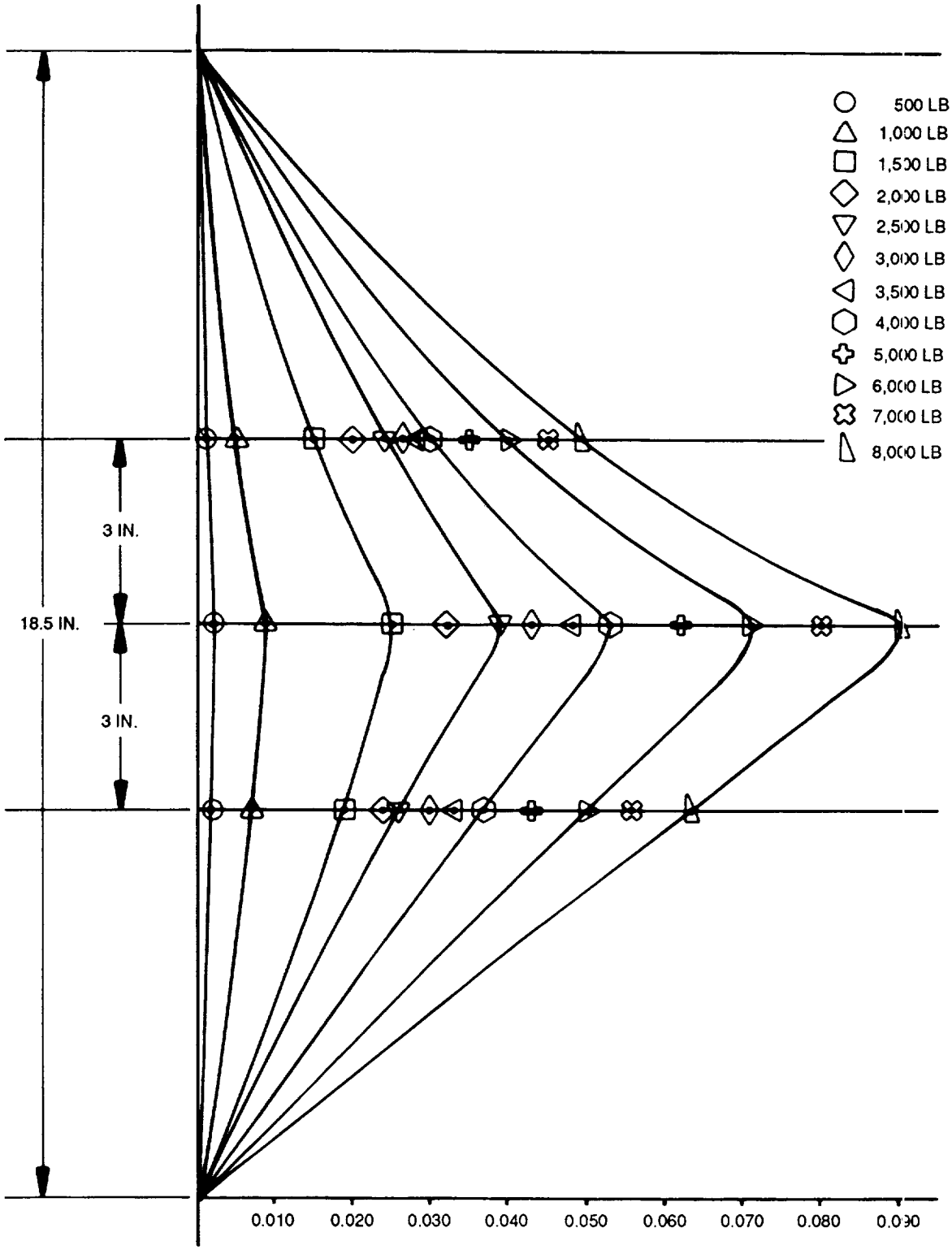

FIGURE 89. DIAL INDICATOR READINGS, THREE-RIB JOINT SMALL PANEL IN TENSION AT ROOM TEMPERATURE

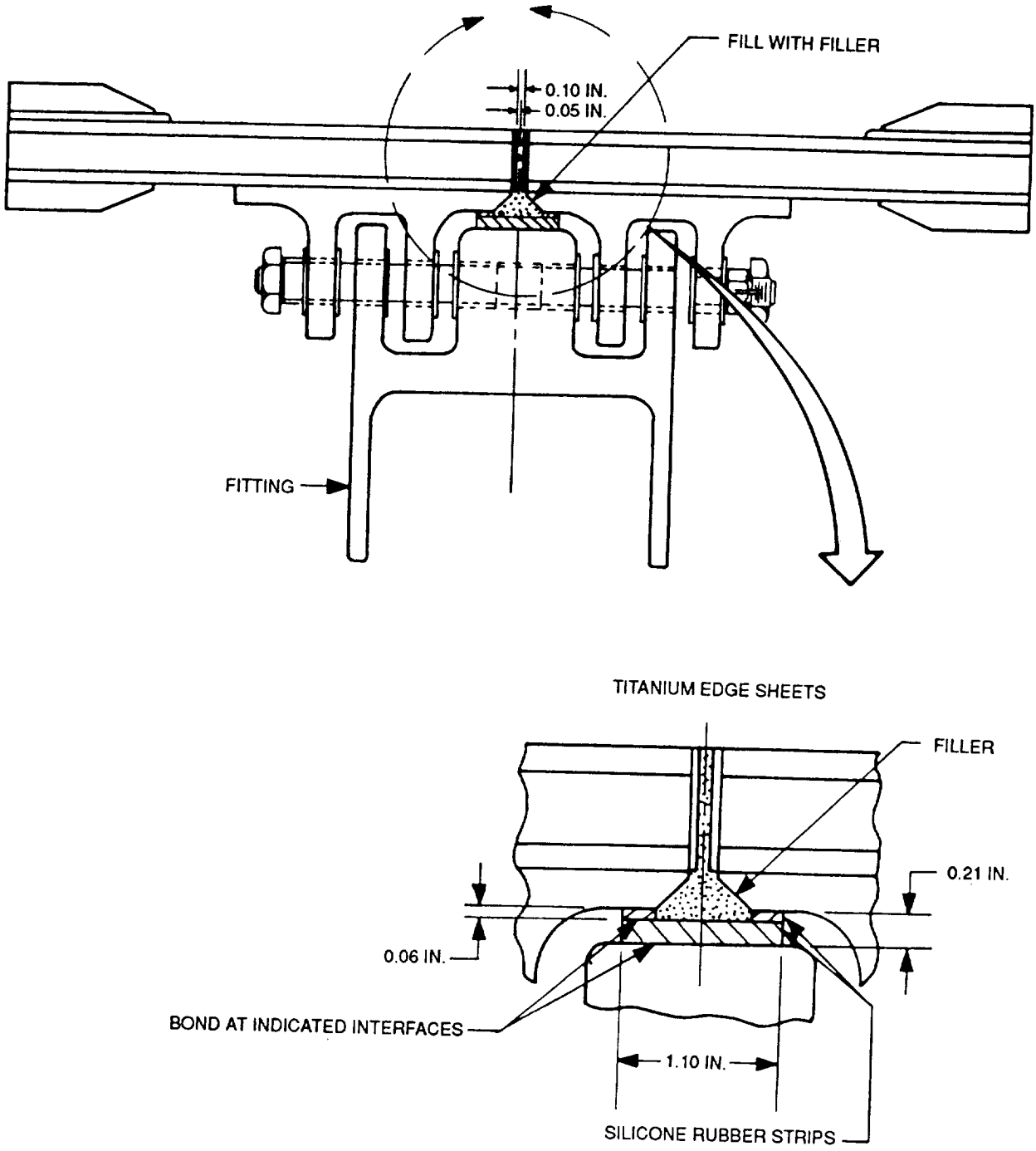

FIGURE 90. "NEW" SEAL MANAGEMENT

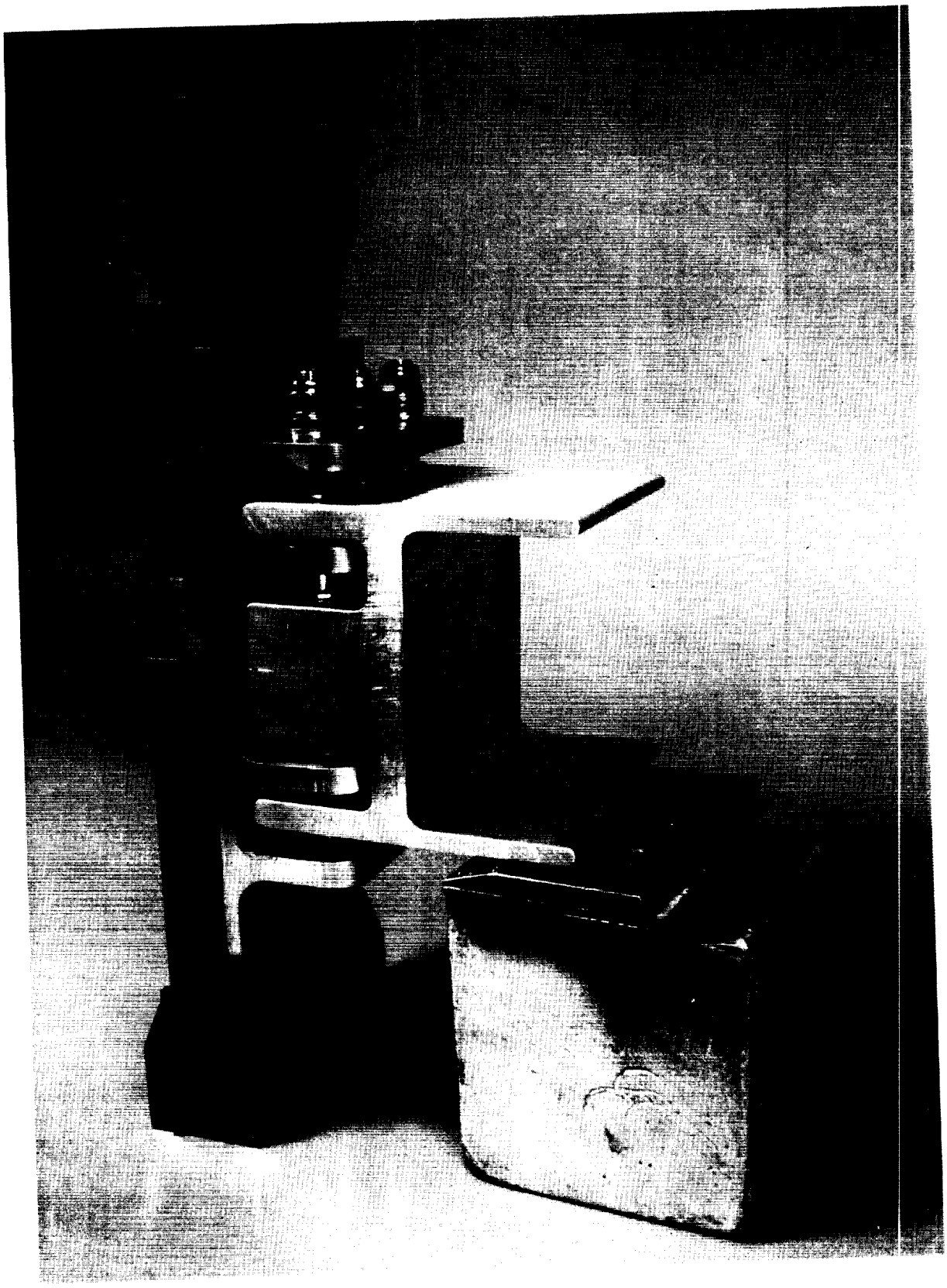

FIGURE 91. SLIDING JOINT SMALL TEST PANEL — THREE-QUARTER VIEW OF COMPOSITE SIDE

ORIGINAL PAGE
BLACK AND WHITE PHOTOGRAPH

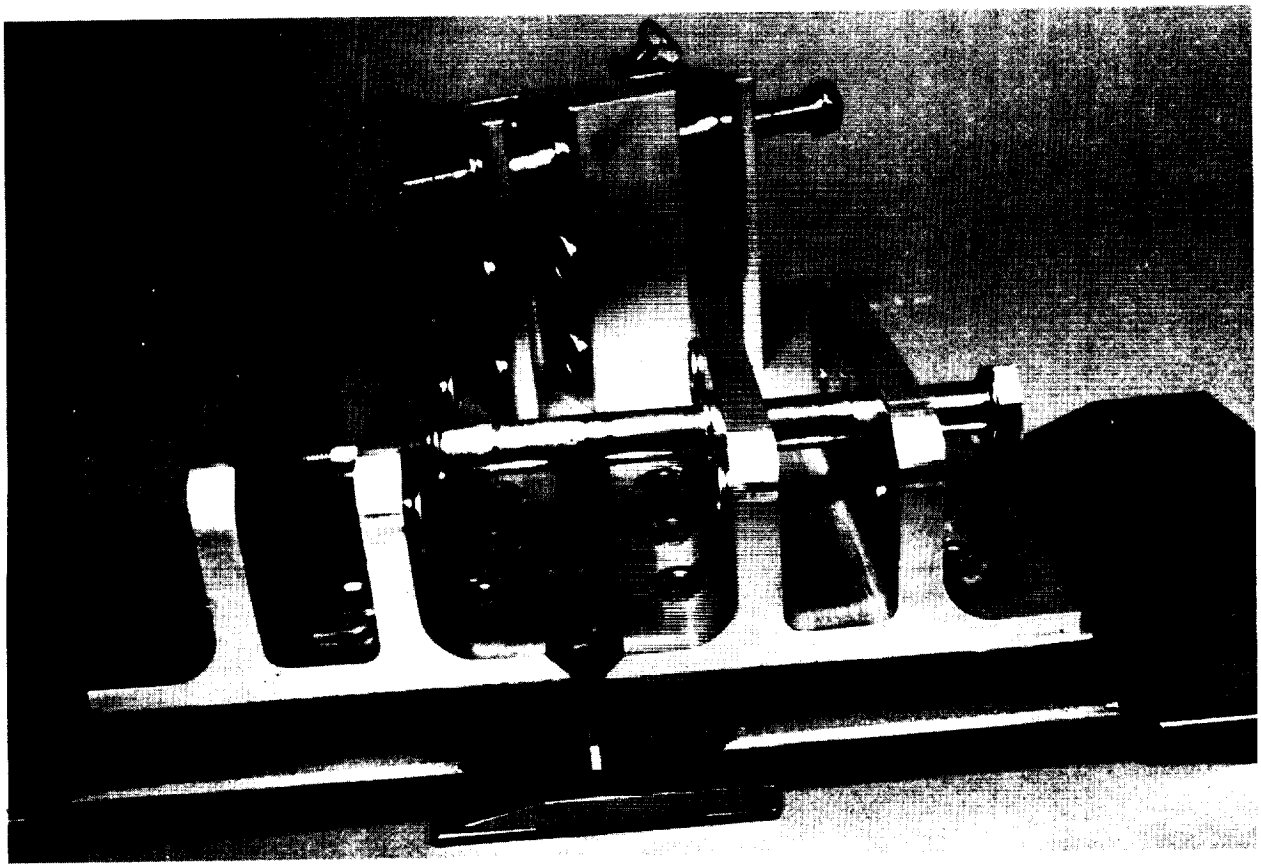

FIGURE 92. SLIDING JOINT SMALL TEST PANEL — CLOSE-UP OF COMPOSITE SIDE WITH RIB ATTACHMENT IN BACKGROUND

ORIGINAL PAGE
BLACK AND WHITE PHOTOGRAPH

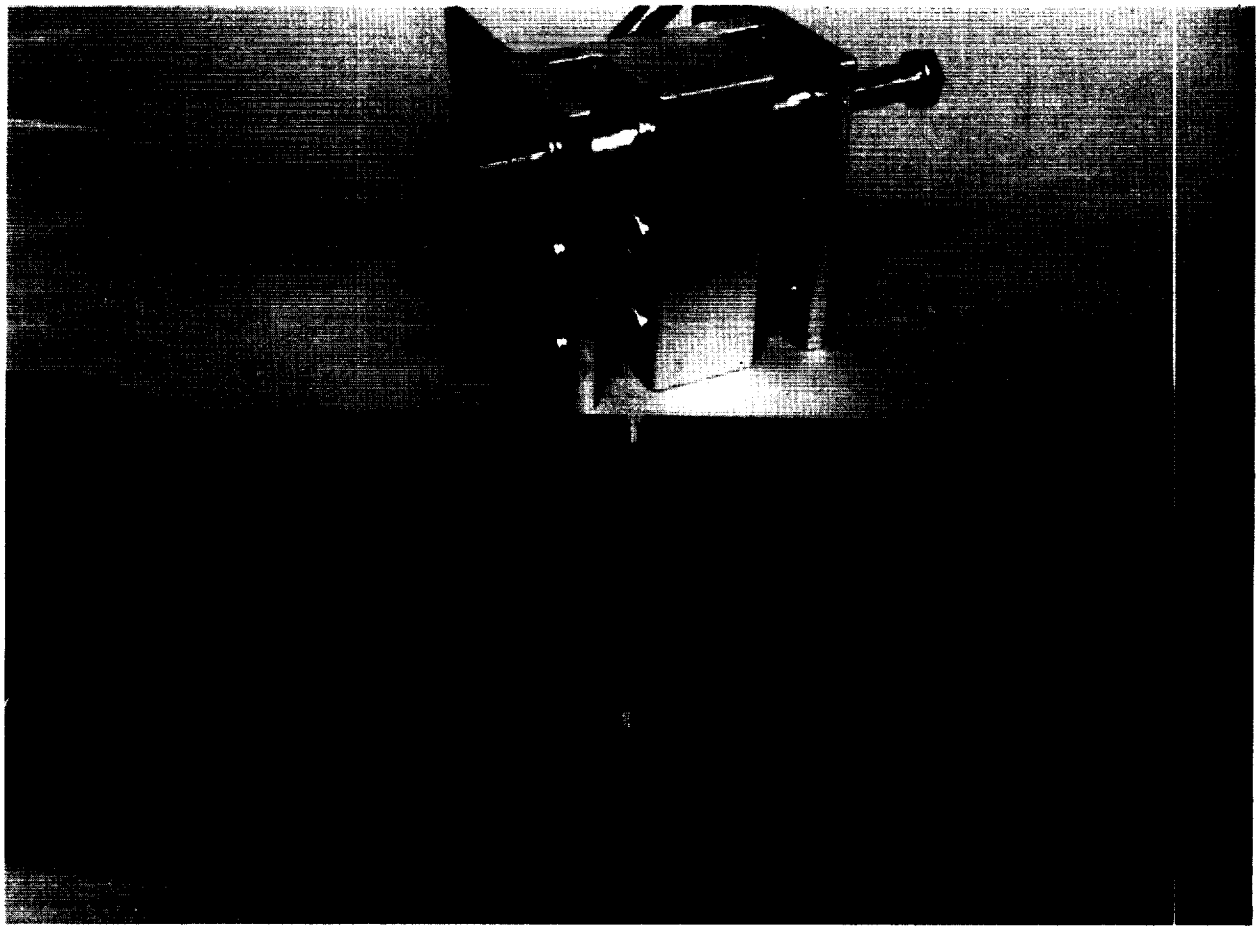

FIGURE 93. SLIDING JOINT SMALL TEST PANEL — VIEW OF TITANIUM SIDE — RIB ATTACH FITTING ON THE LEFT

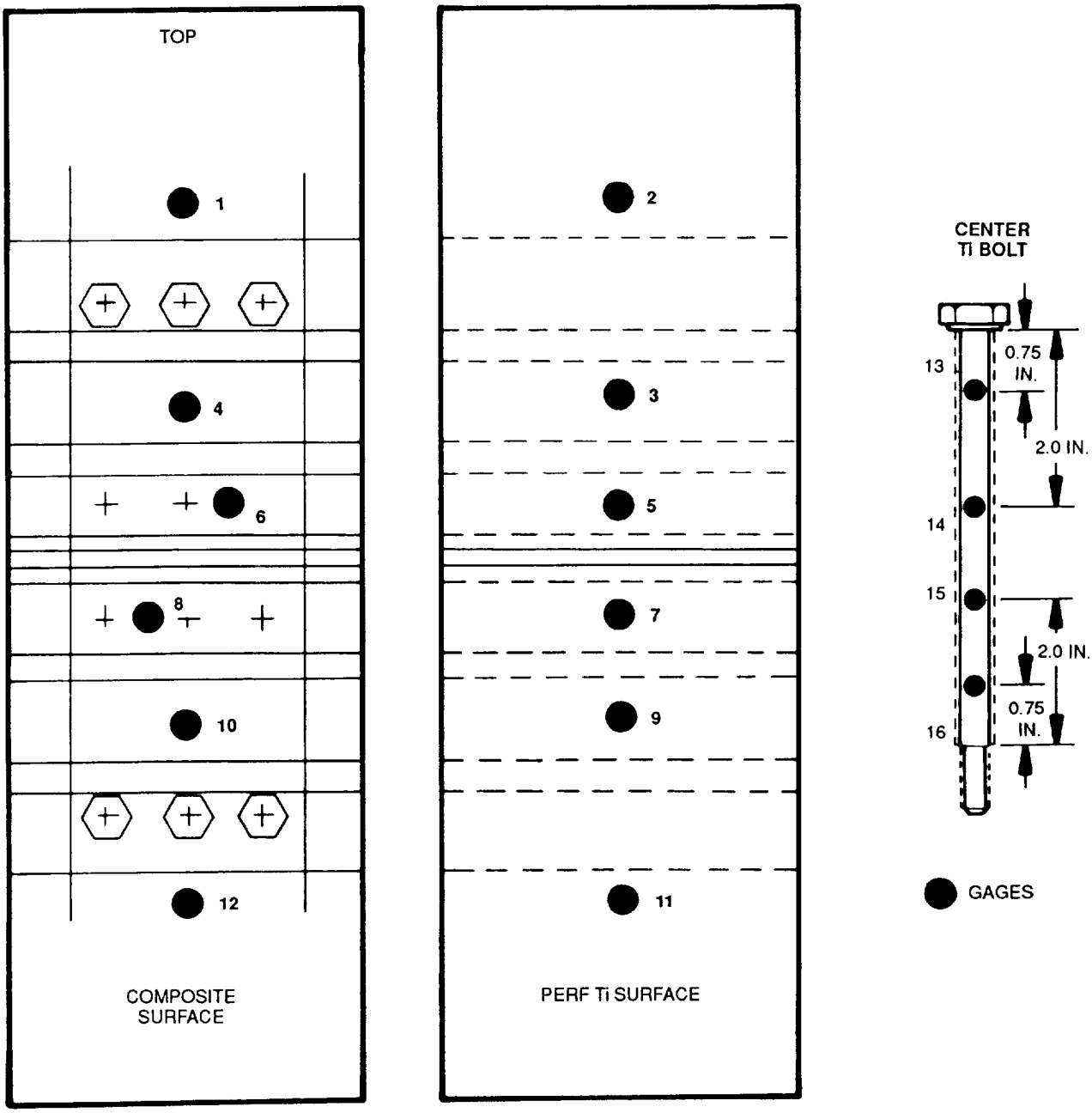

FIGURE 94. CHORDWISE SLIDING-JOINT TEST SPECIMEN

ORIGINAL PAGE
BLACK AND WHITE PHOTOGRAPH

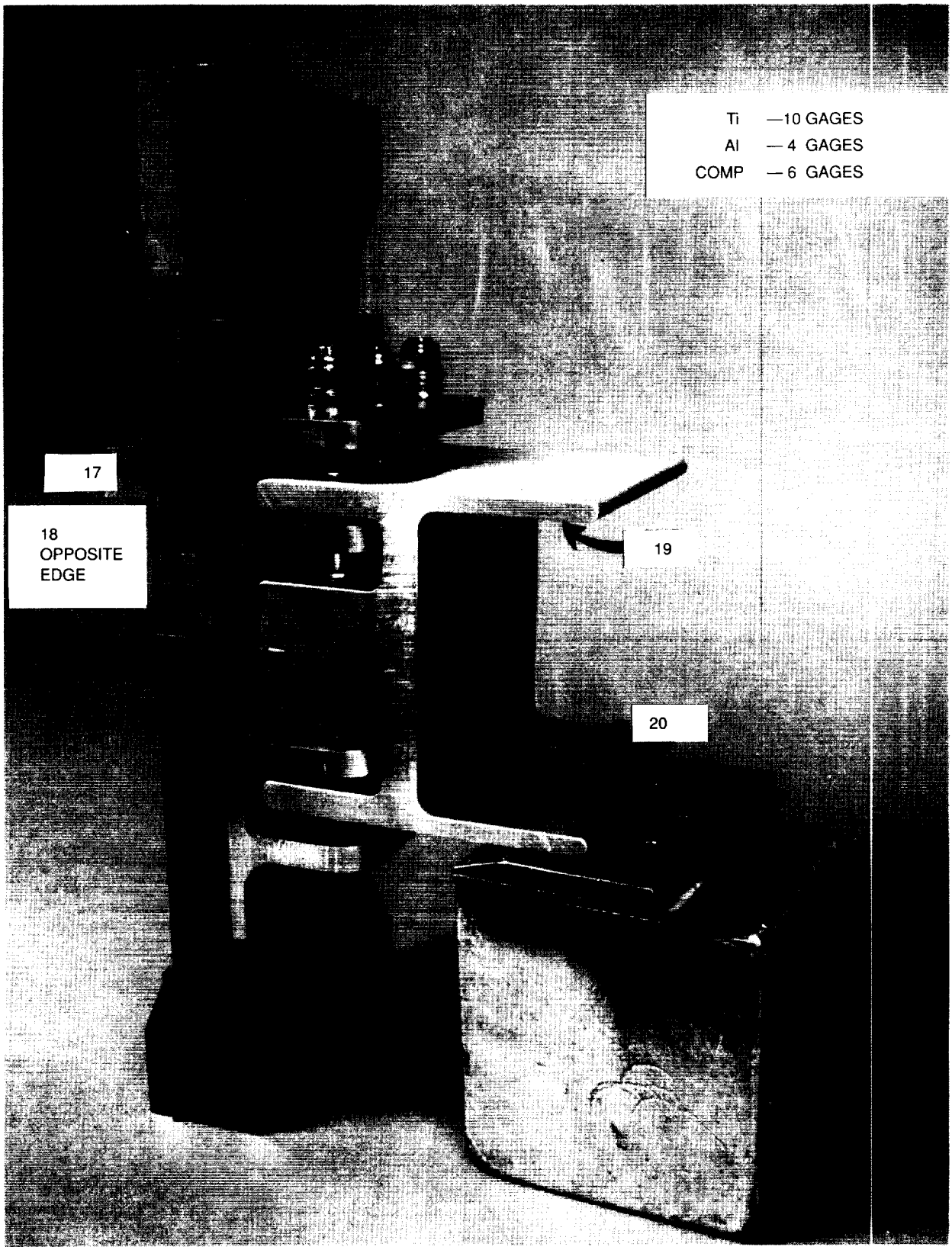

FIGURE 95. STRAIN GAGE LOCATIONS ON THE FITTING

ORIGINAL PAGE
BLACK AND WHITE PHOTOGRAPH

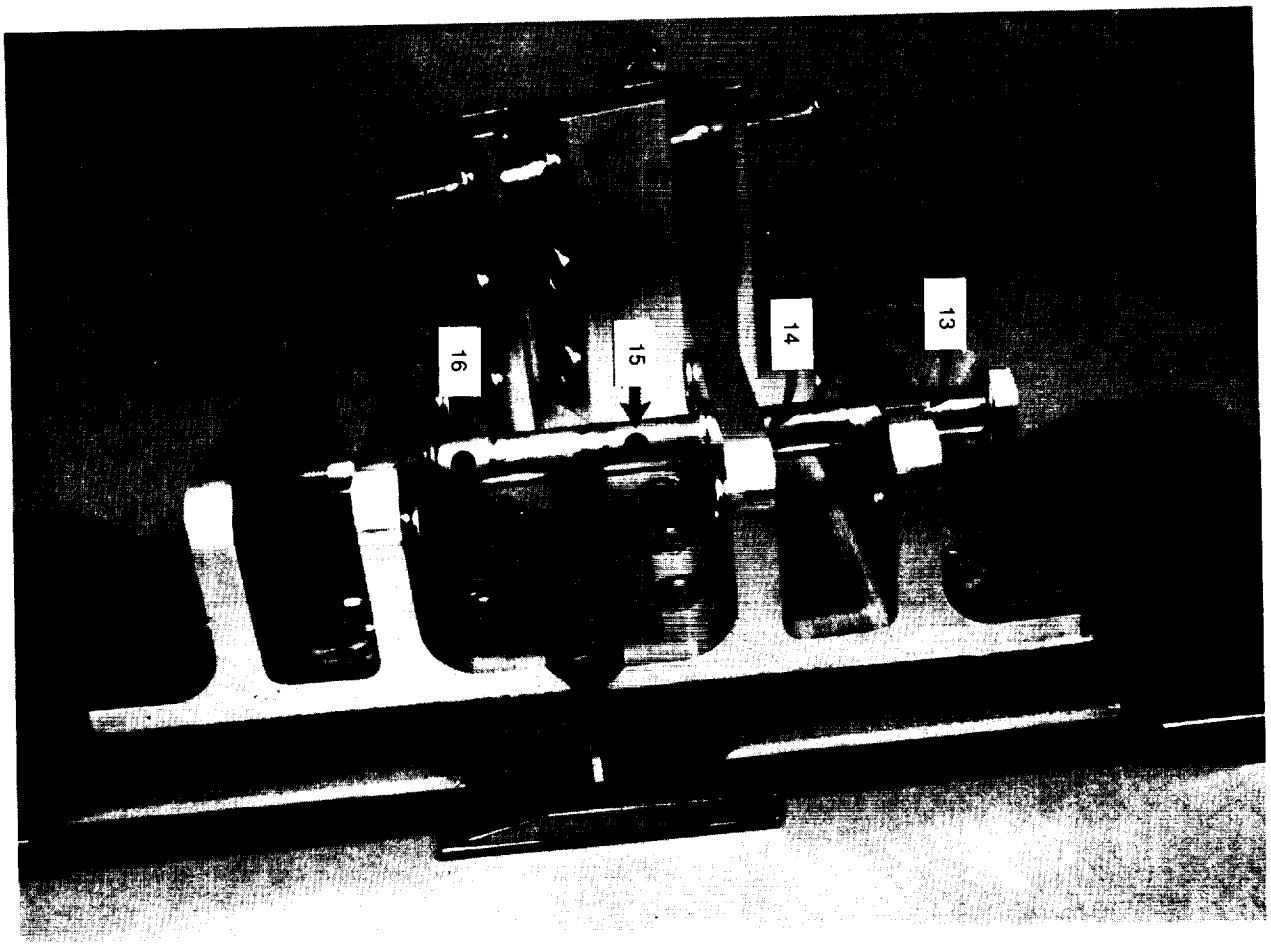

FIGURE 96. STRAIN GAGE LOCATIONS ON THE BOLT

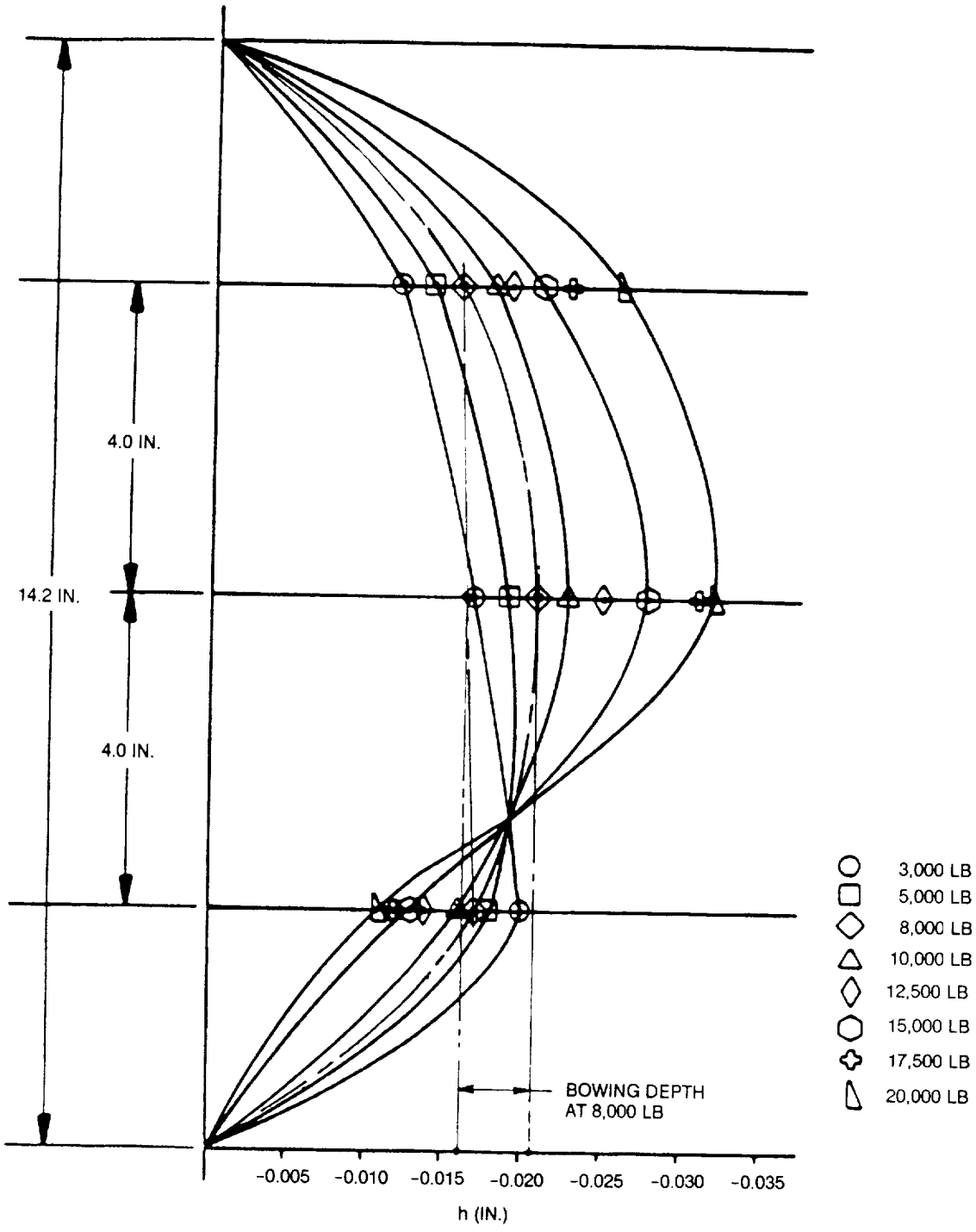

FIGURE 97. DIAL INDICATOR READINGS SLIDING JOINT SMALL PANEL COMPRESSION AT ROOM TEMPERATURE

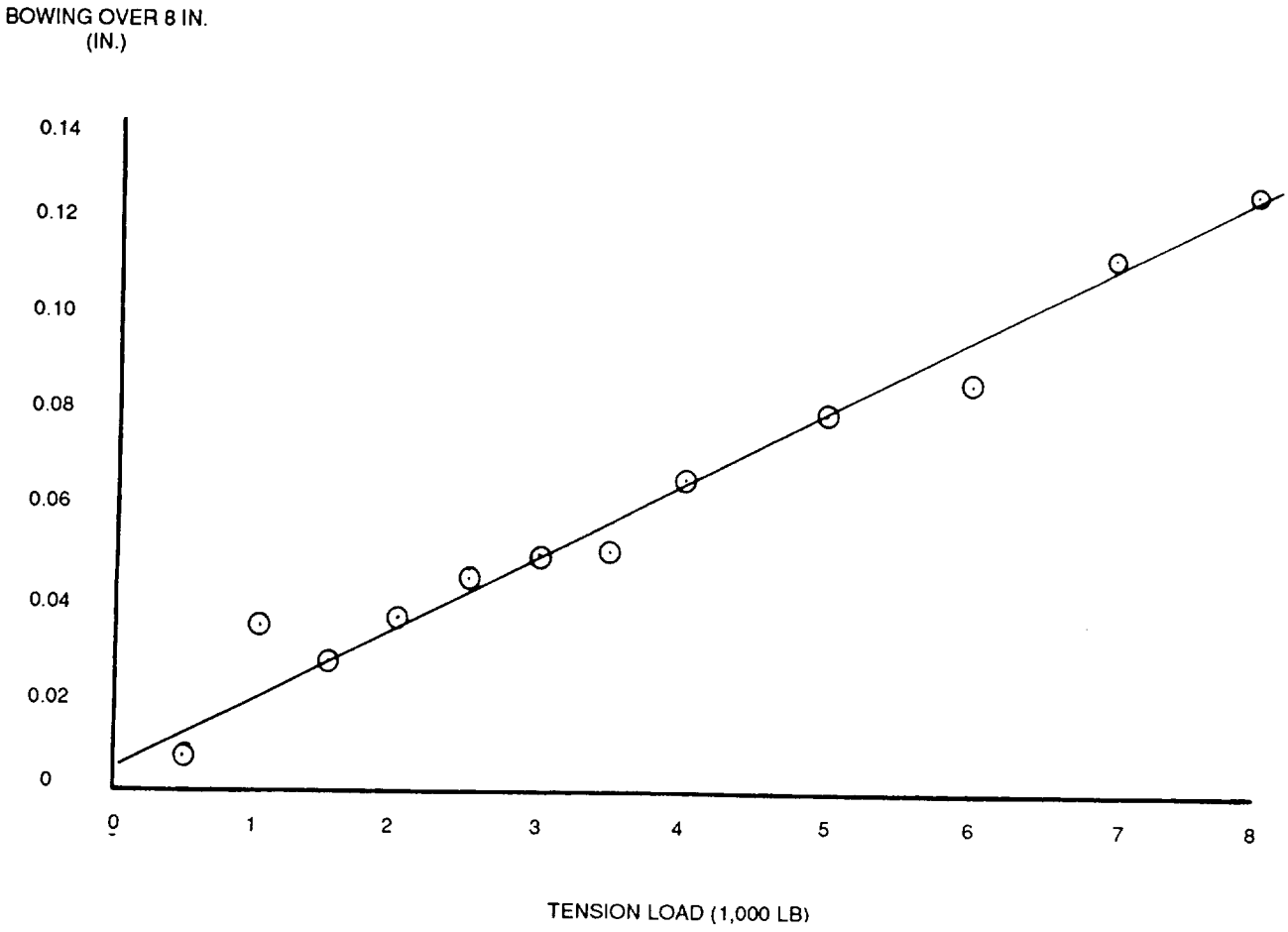

FIGURE 98. BOWING OF SLIDING JOINT IN TENSION

ORIGINAL PAGE
BLACK AND WHITE PHOTOGRAPH

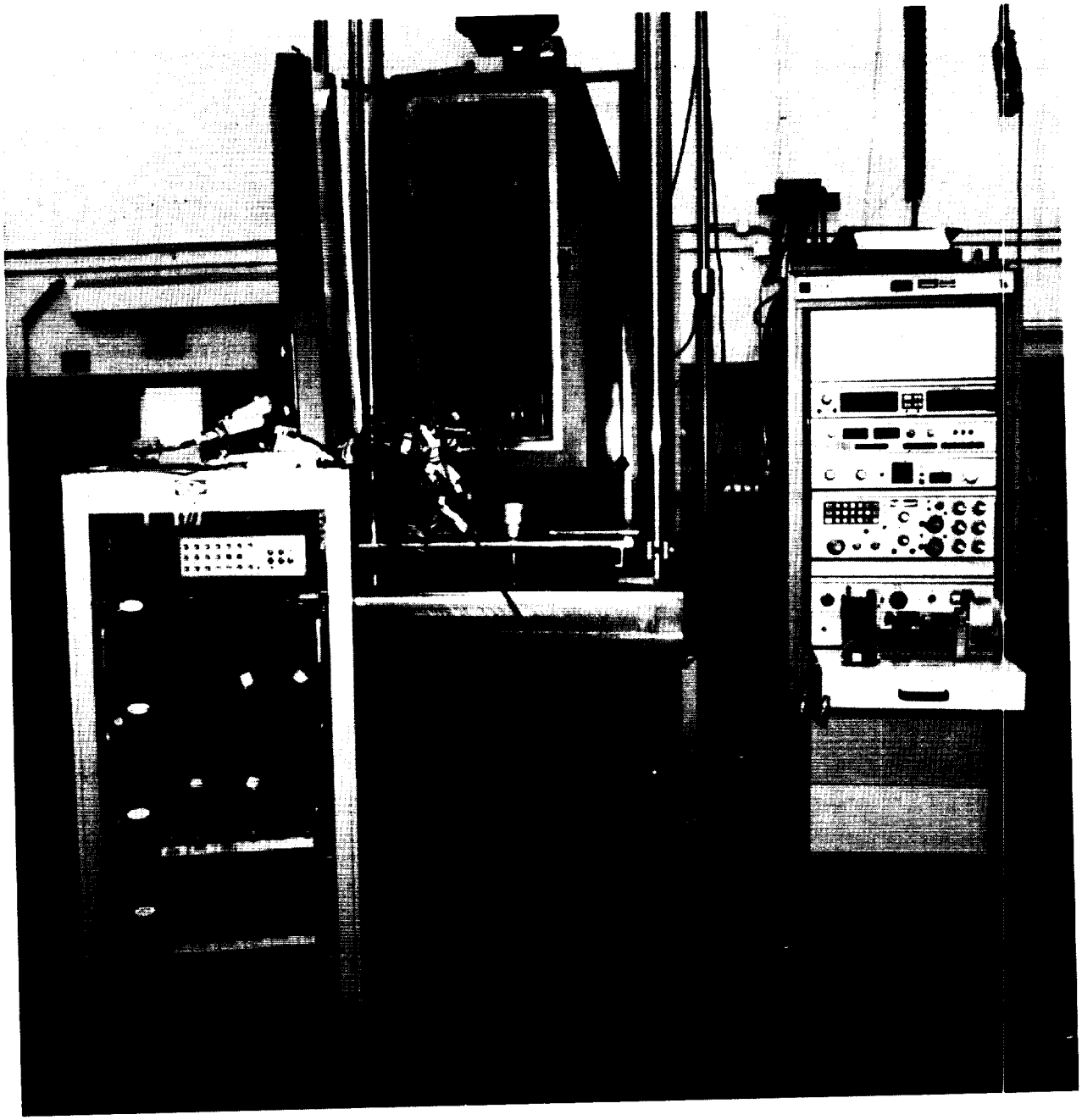

FIGURE 99. SMALL SLIDING JOINT IN ENVIRONMENTAL CHAMBER — TENSION TEST

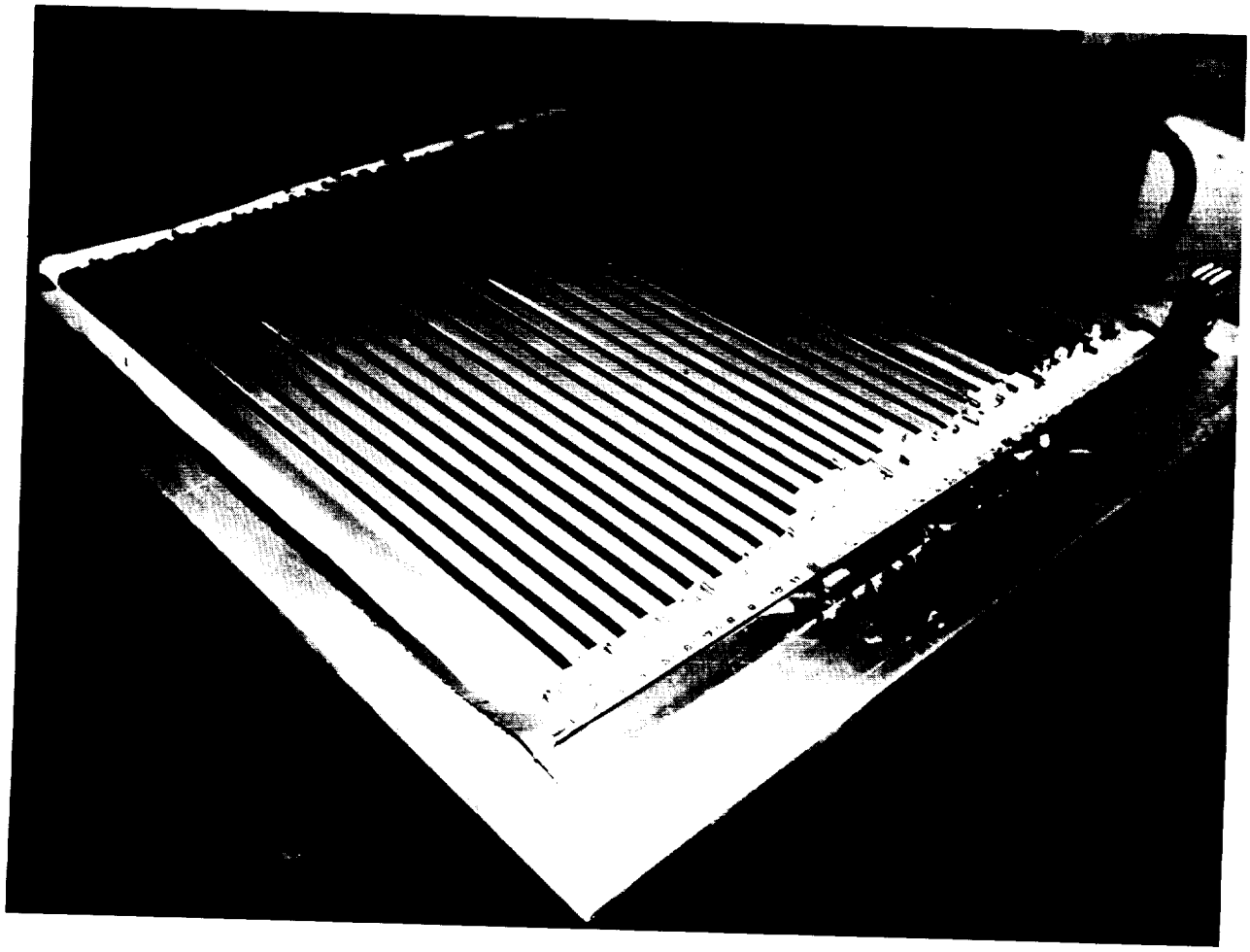

FIGURE 100. SLIDING JOINT PANEL

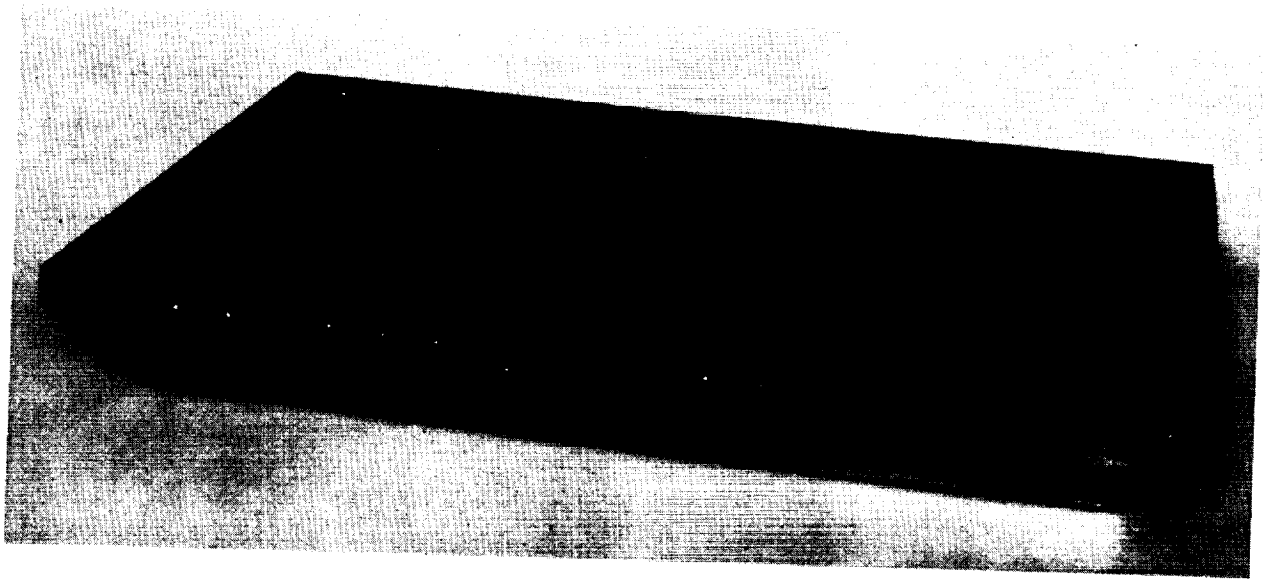

FIGURE 101. SLIDING JOINT LARGE TEST PANEL WITH TITANIUM END STRIP ADDED AT END OF FLUTES

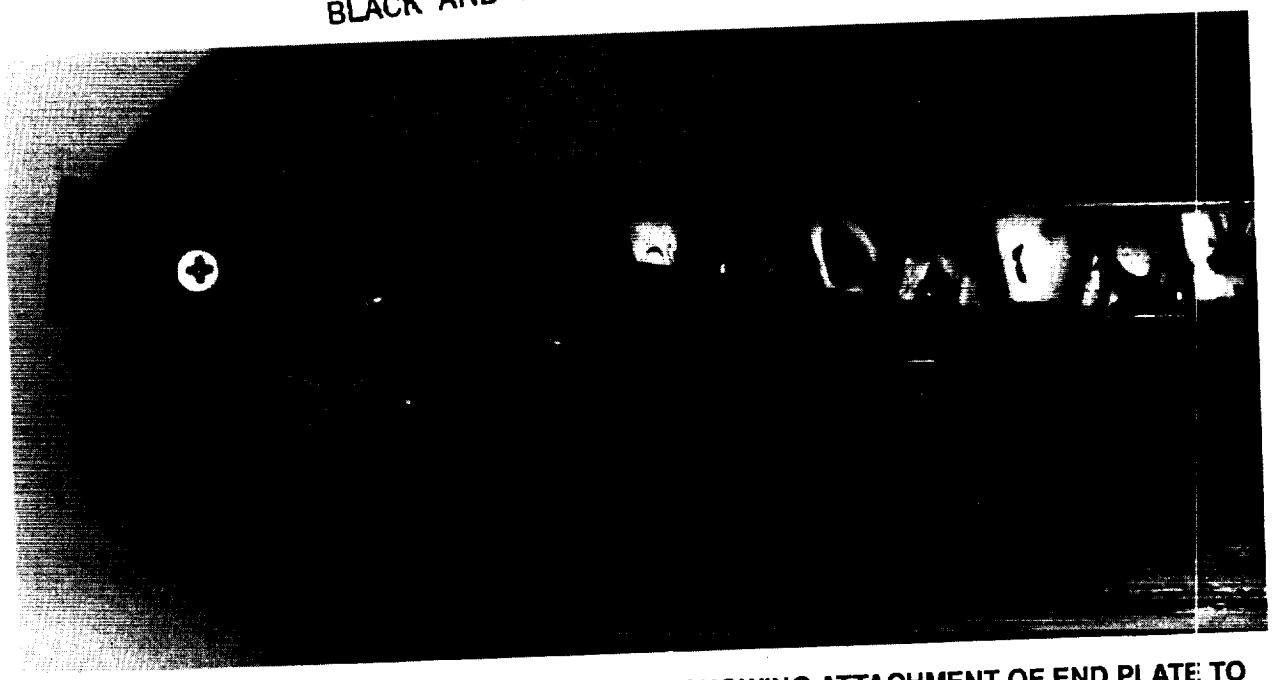

FIGURE 102. SLIDING JOINT LARGE TEST PANEL SHOWING ATTACHMENT OF END PLATE TO INACTIVE FLUTES

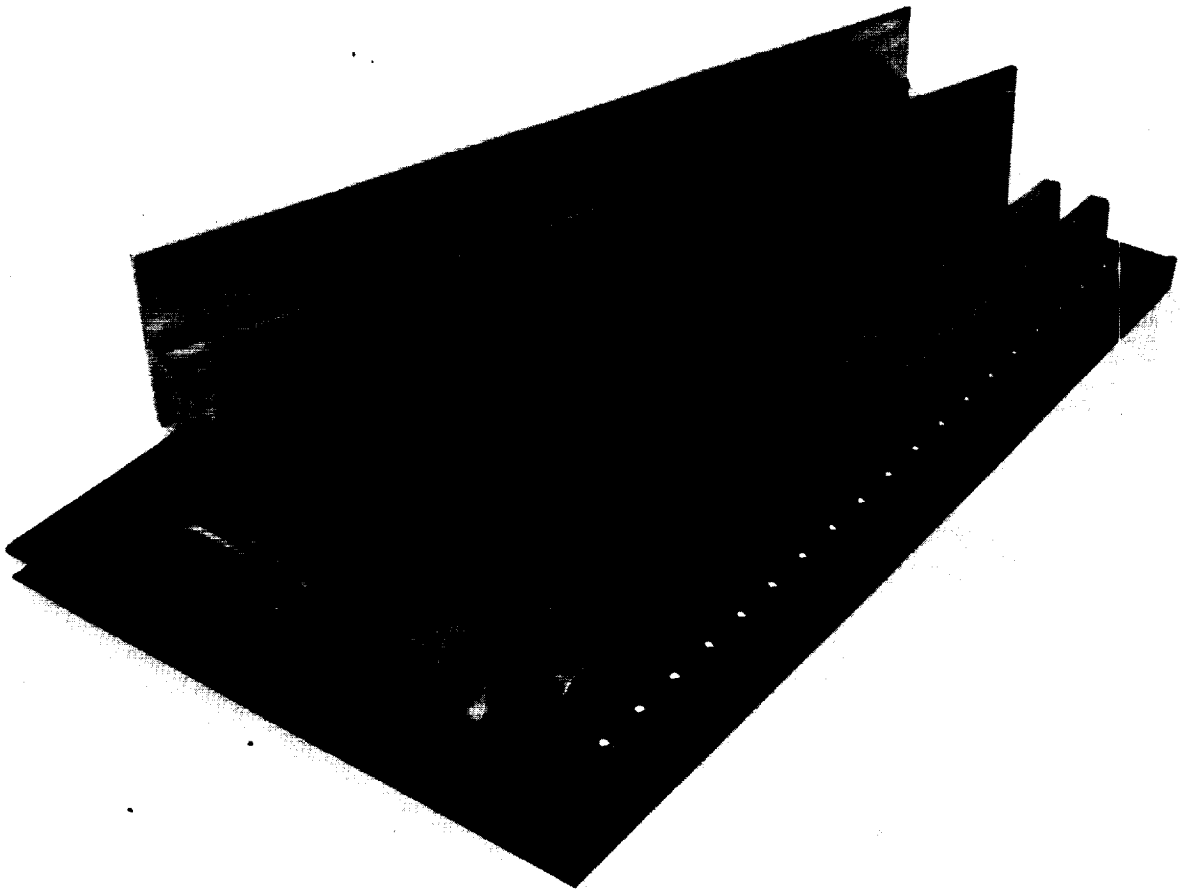

FIGURE 103. SLIDING JOINT LARGE TEST PANEL BEFORE BOLTS IN JOINT ARE DRILLED

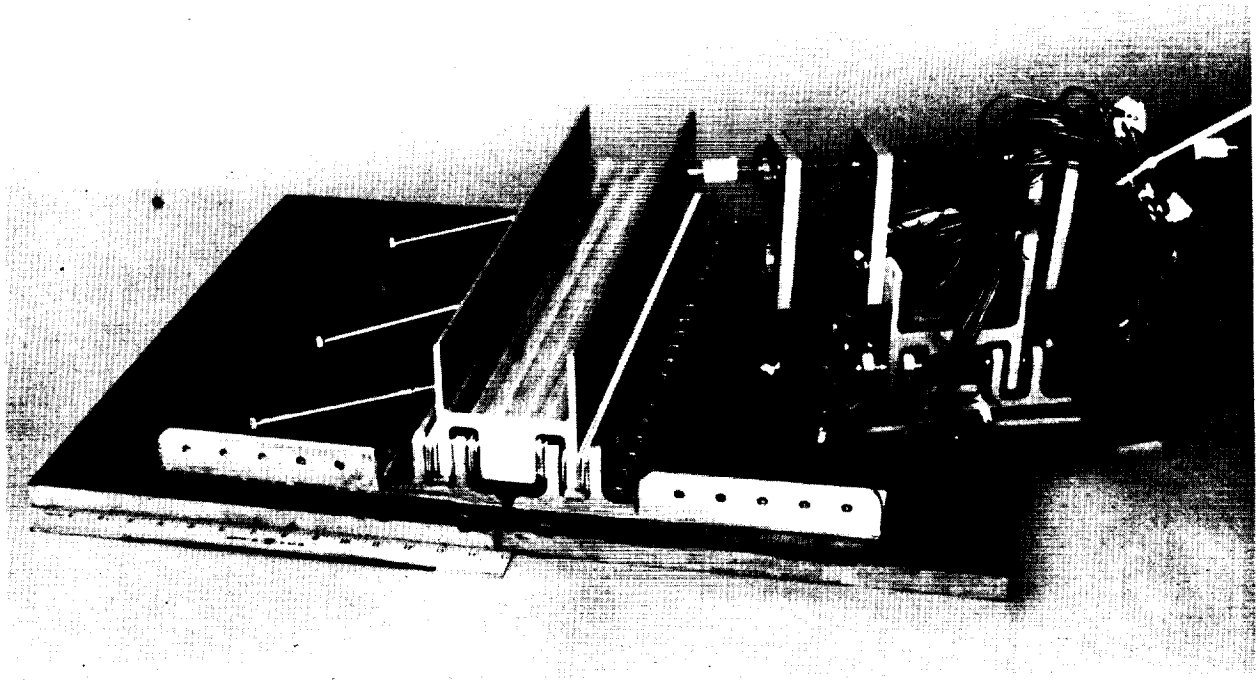

FIGURE 104. SLIDING JOINT LARGE TEST PANELS ASSEMBLED WITH SMALL TEST PANEL RESTING ON TOP

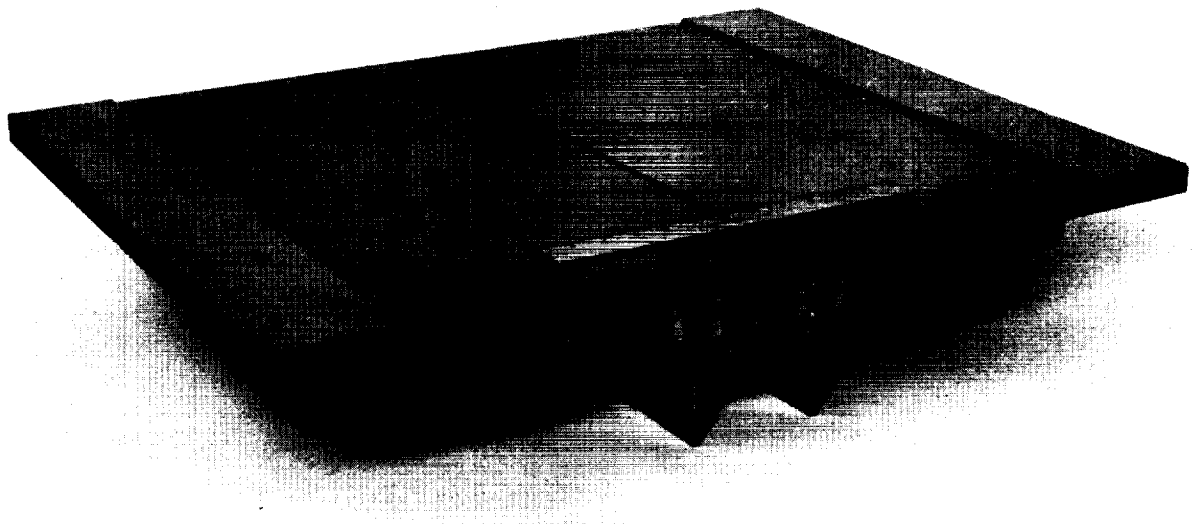

FIGURE 105. SLIDING JOINT LARGE PANEL — TITANIUM SIDE

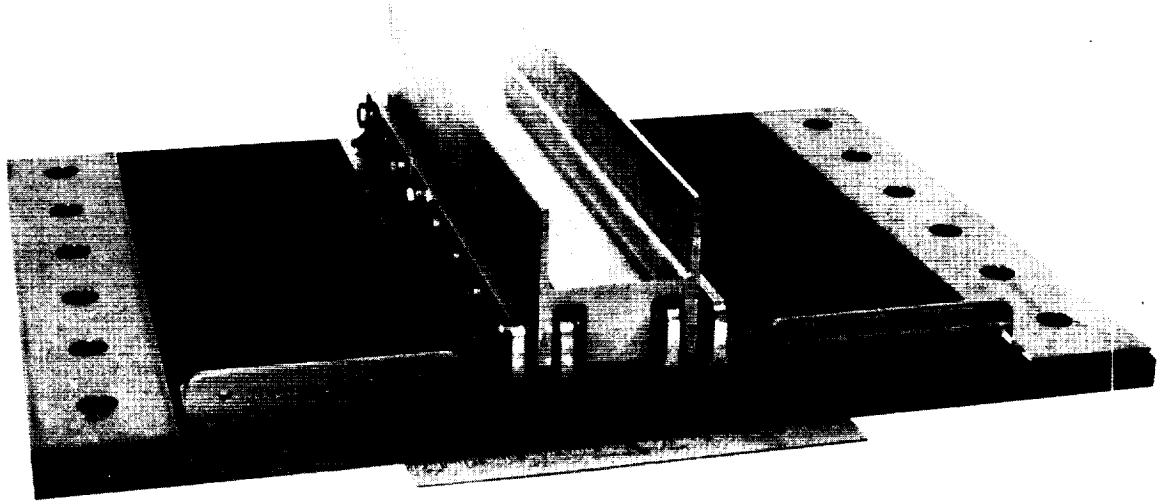

FIGURE 106. SLIDING JOINT LARGE PANEL — COMPOSITE SIDE

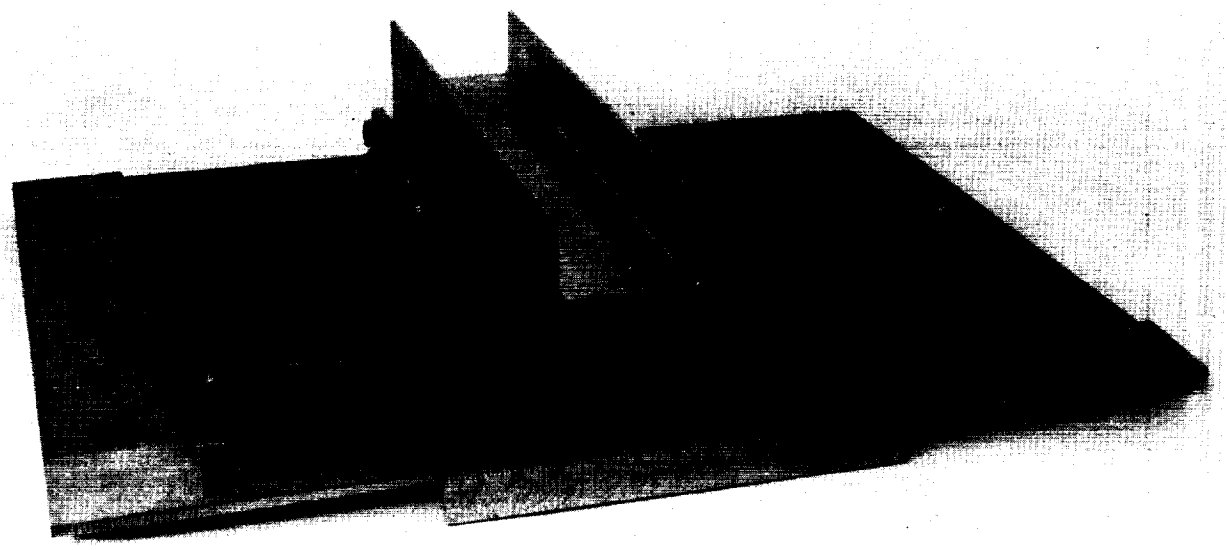

FIGURE 107. SLIDING JOINT LARGE PANEL WITH CONTINUOUS ANGLE ATTACHED

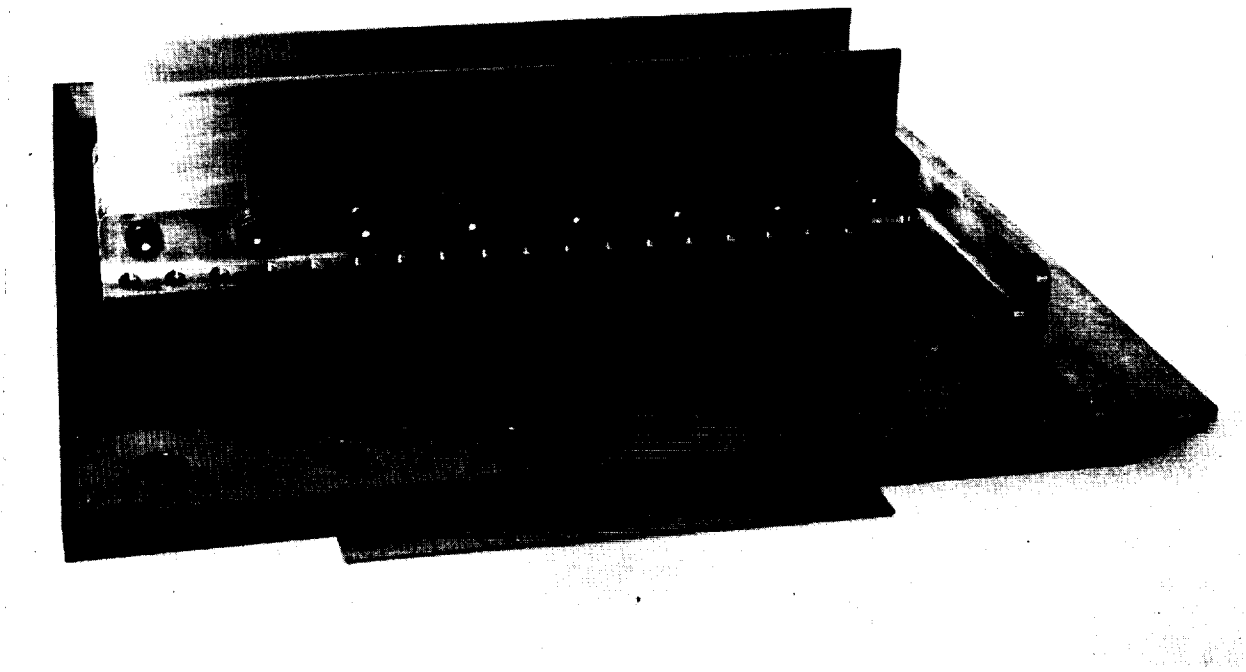

FIGURE 108. SLIDING JOINT LARGE PANEL — EDGE VIEW — SPANWISE FLUTES BARELY VISIBLE

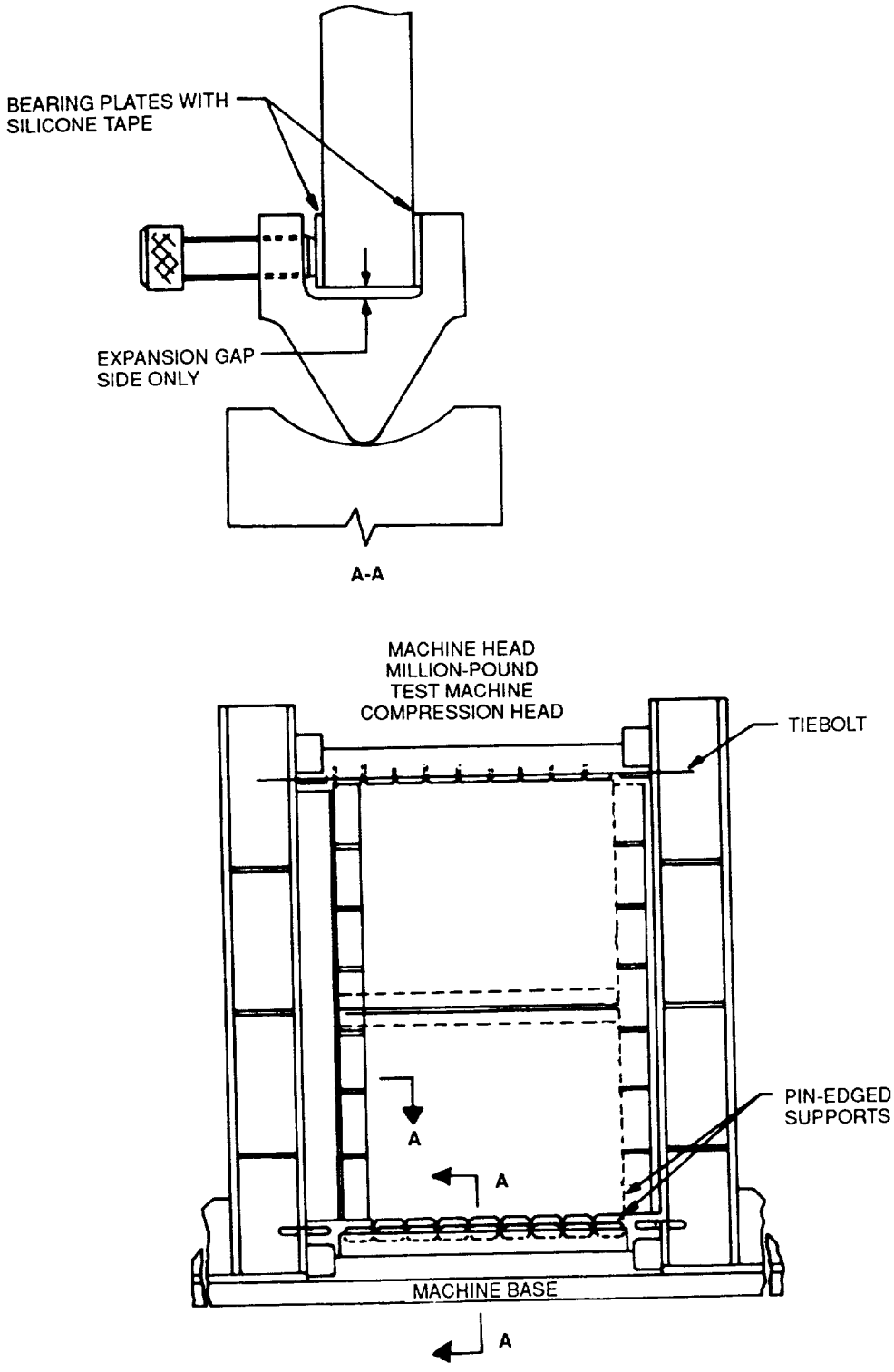

FIGURE 109. LARGE SLIDING-JOINT SPECIMEN TEST MILLION-POUND MACHINE

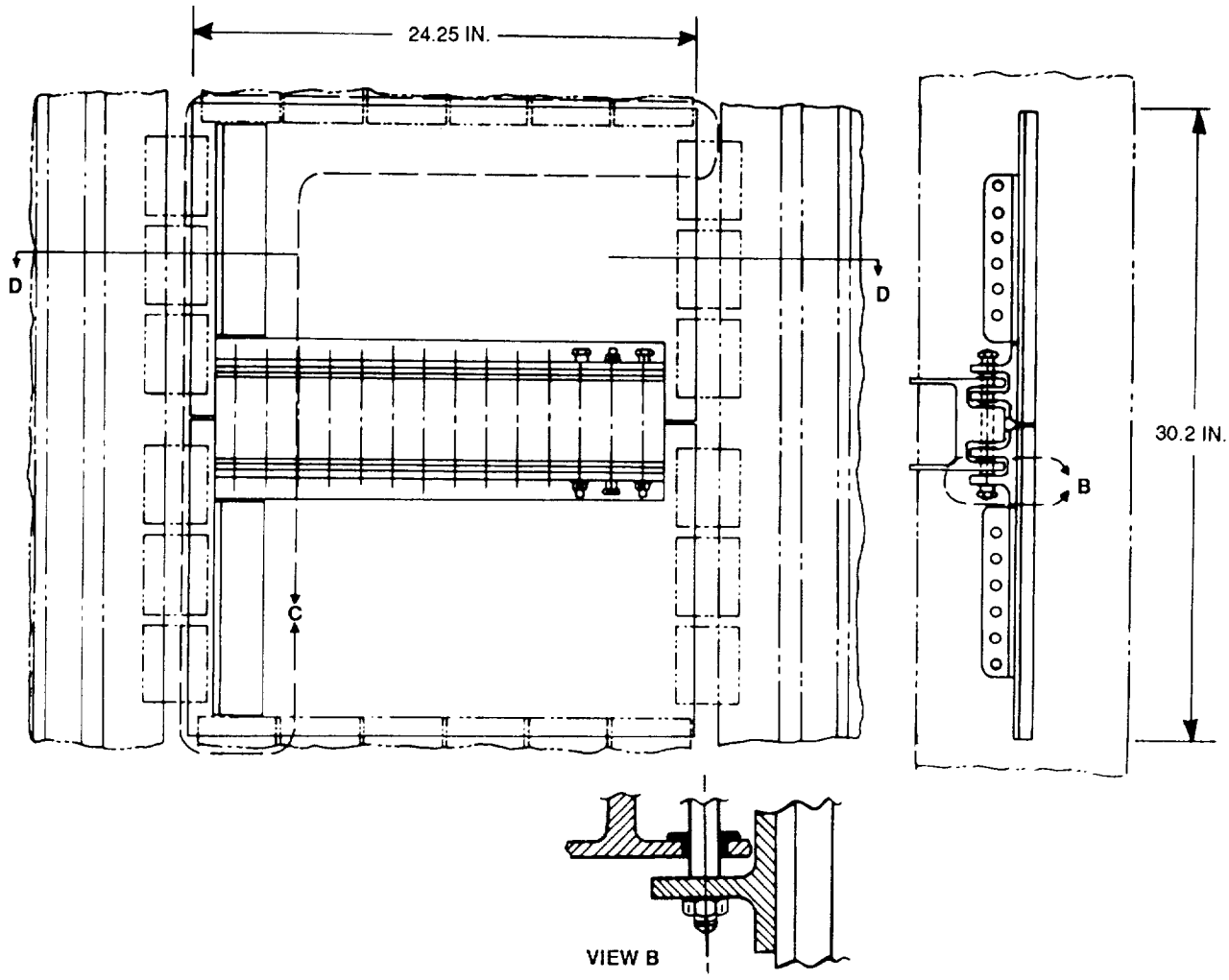

FIGURE 110. SLIDE-JOINT COMPRESSION PANEL TEST SETUP

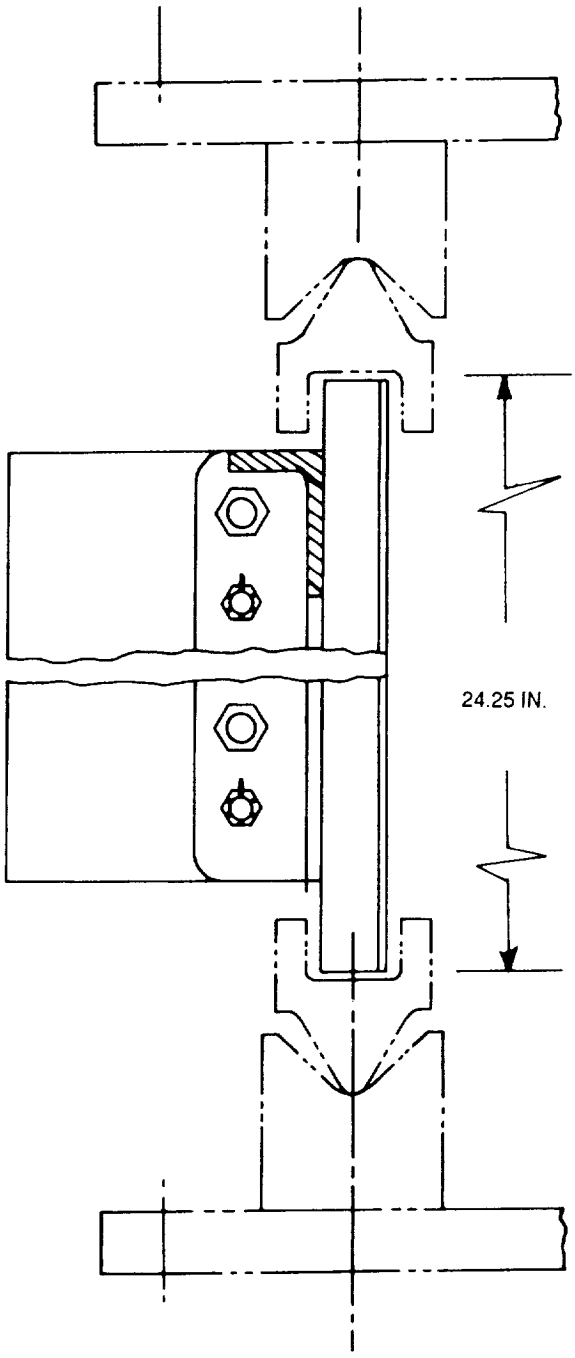

FIGURE 111. CROSS SECTION VIEW D-D OF FIGURE 110 ROTATED 90 DEGREES CLOCKWISE

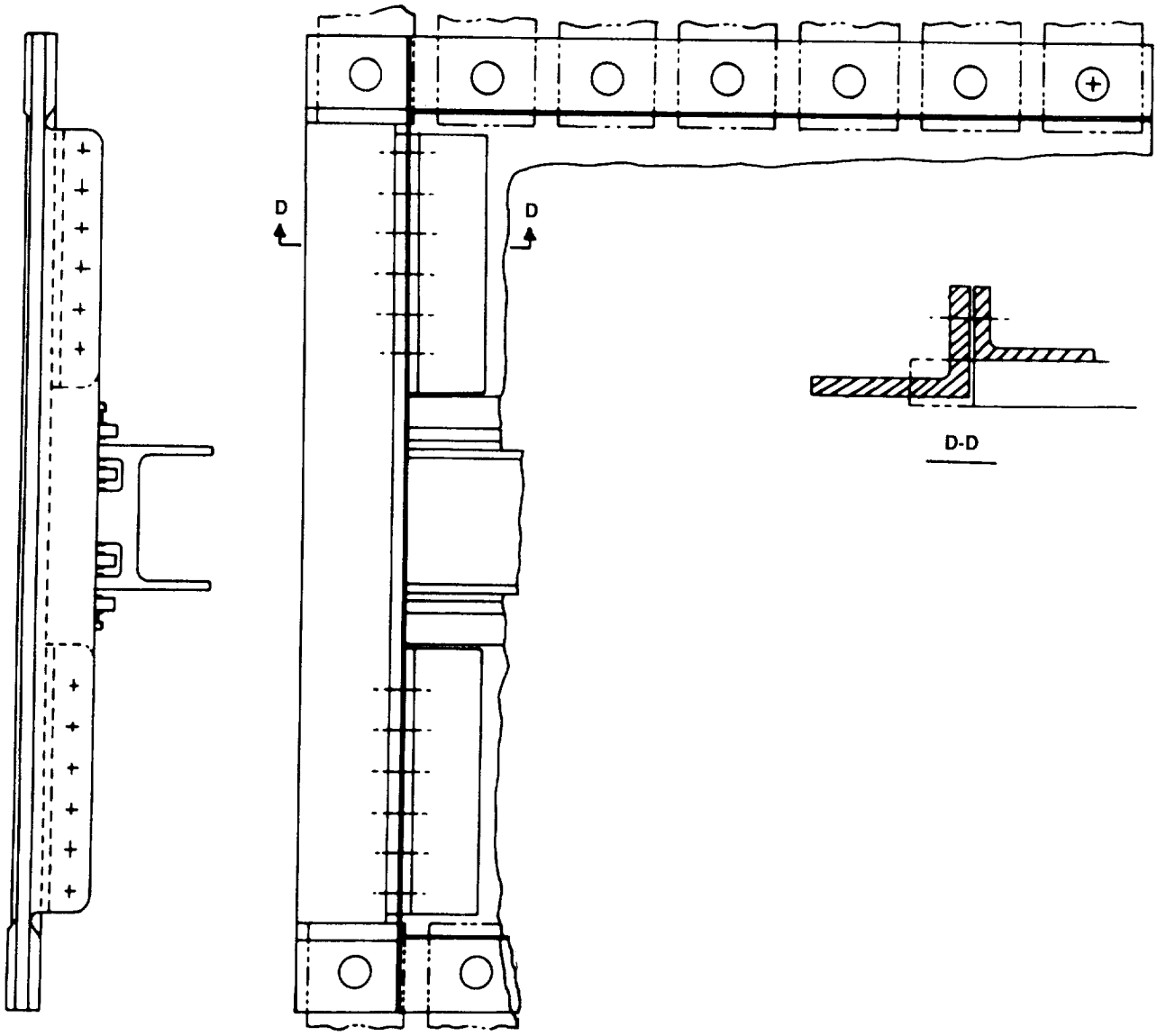

FIGURE 112. TENSION PANEL — VIEW C FROM FIGURE 61

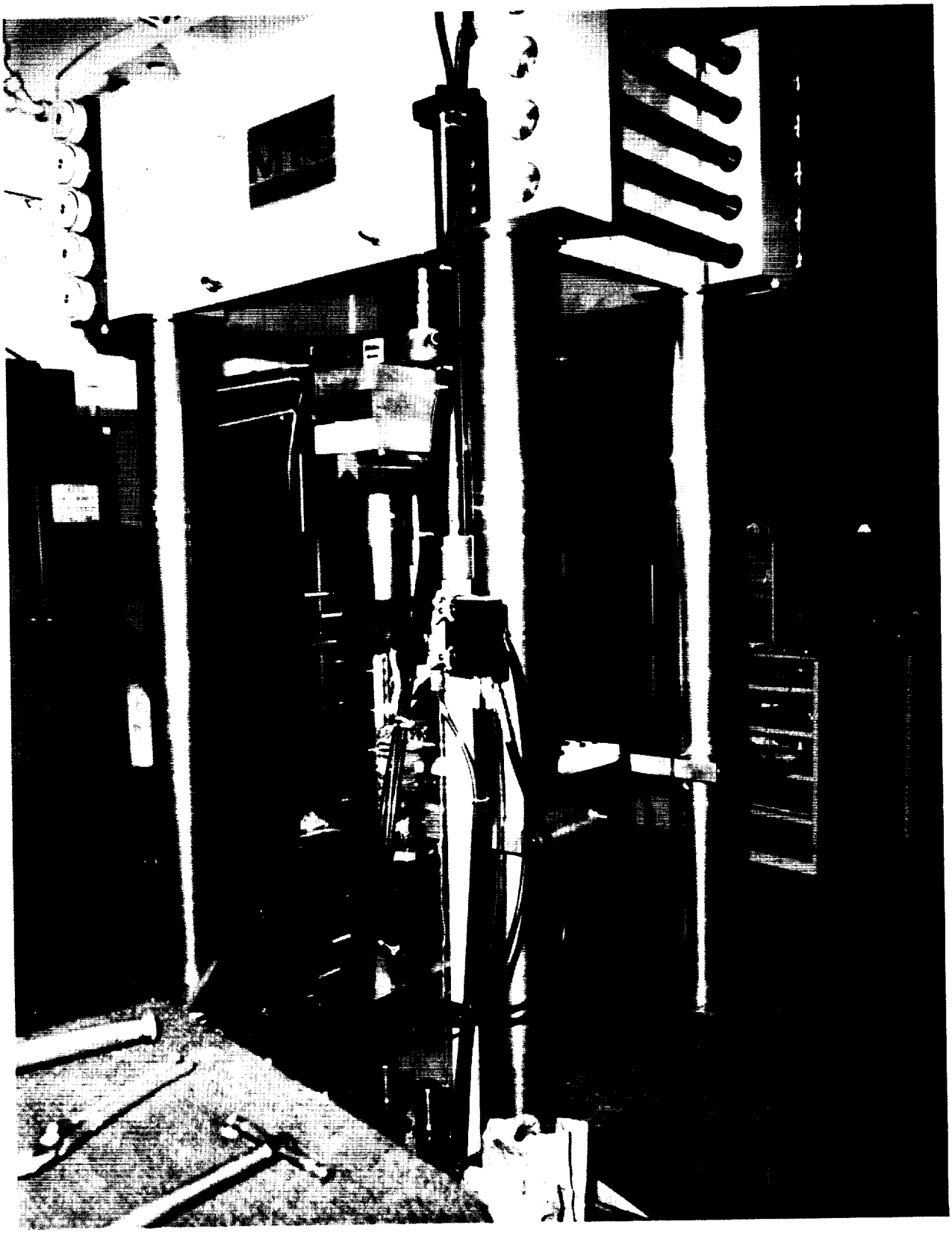

FIGURE 113. TEST SETUP FOR COMPRESSION TEST OF LARGE SLIDING-JOINT PANELS — ROOM TEMPERATURE CONDITION

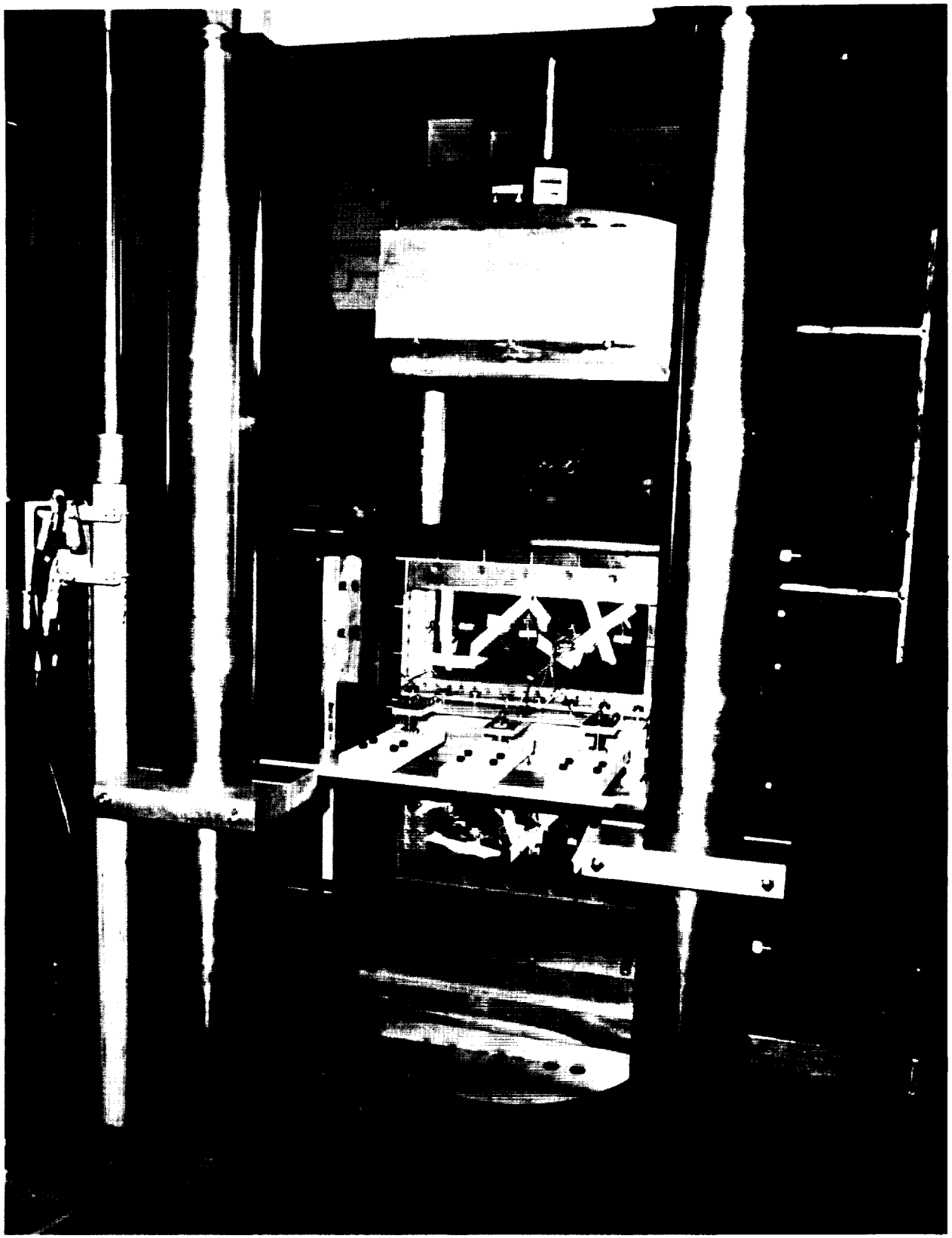

FIGURE 114. CLOSE-UP VIEW OF LARGE SLIDING-JOINT PANELS COMPRESSION TEST SETUP — ROOM TEMPERATURE CONDITION — COMPOSITE SIDE

FIGURE 115. SIDE VIEW OF LARGE SLIDING-JOINT PANELS COMPRESSION TEST SETUP — ROOM TEMPERATURE CONDITION — COMPOSITE SIDE

ORIGINAL PAGE
BLACK AND WHITE PHOTOGRAPH

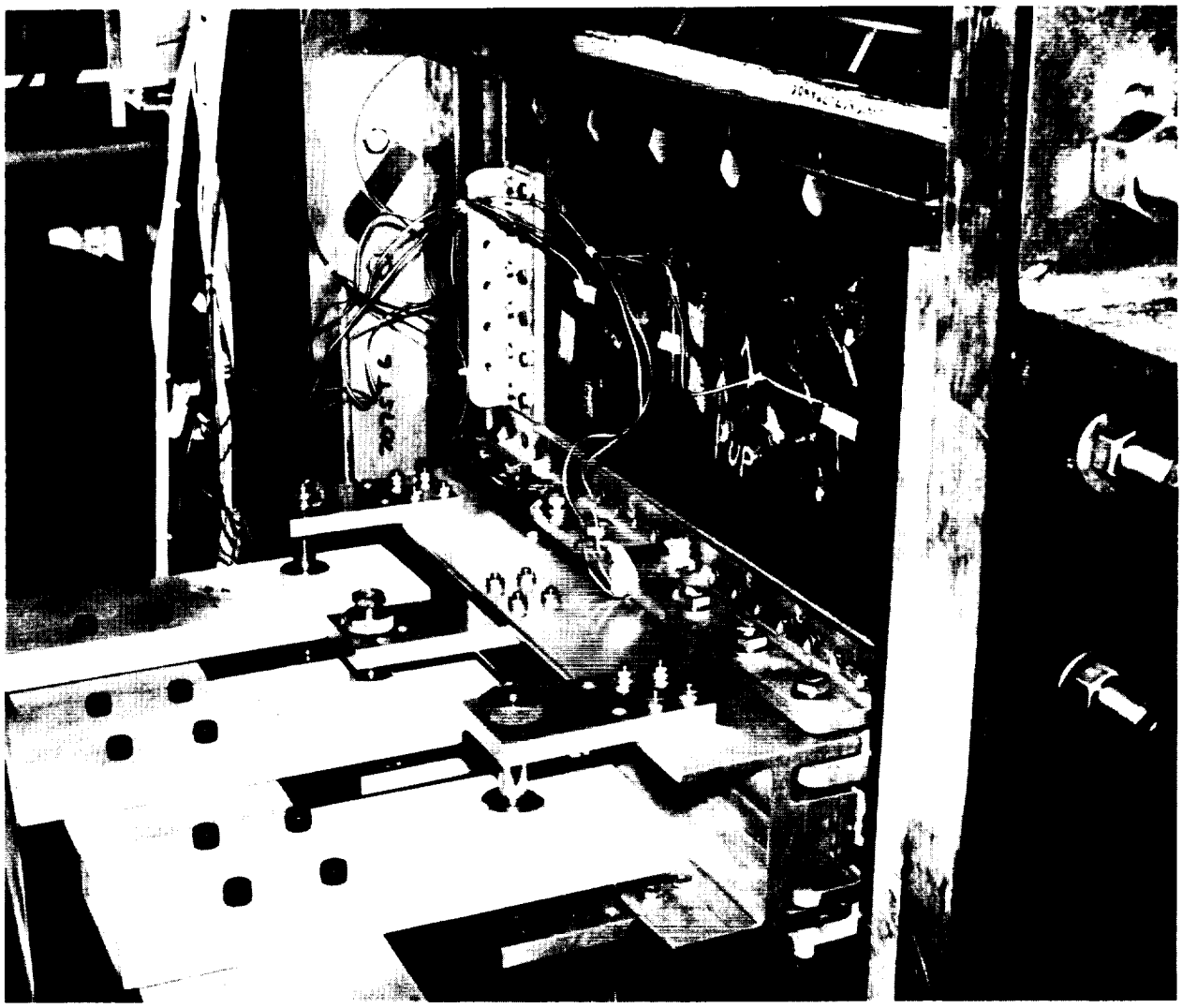

FIGURE 116. CLOSE-UP VIEW OF LARGE SLIDING-JOINT PANELS COMPRESSION TEST SETUP — ROOM TEMPERATURE CONDITION — COMPOSITE SIDE

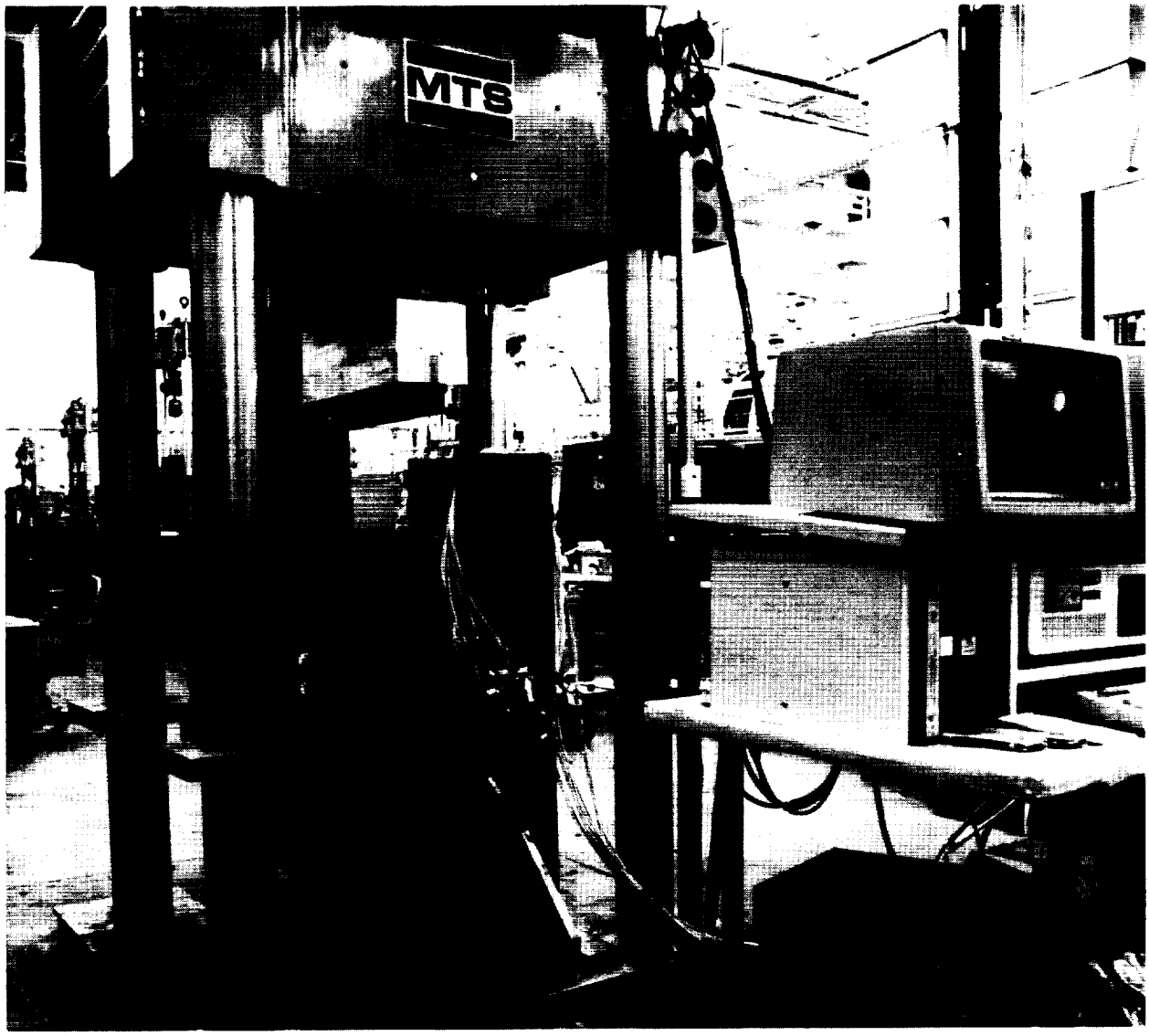

FIGURE 117. TEST SETUP FOR COMPRESSION TEST OF LARGE SLIDING-JOINT PANELS — ROOM TEMPERATURE CONDITION — TITANIUM SIDE

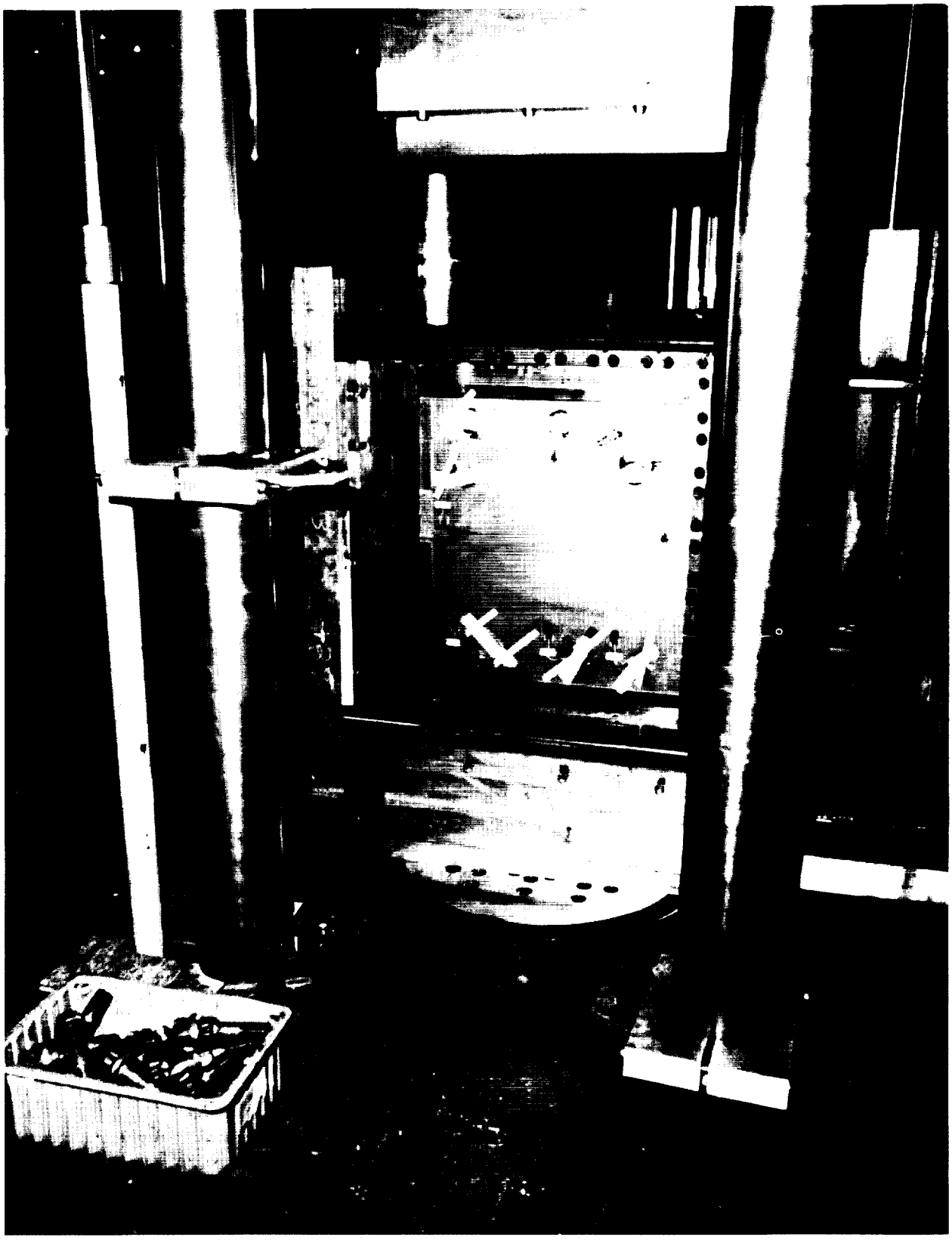

FIGURE 118. CLOSE-UP OF TEST SETUP FOR COMPRESSION TEST OF LARGE SLIDING-JOINT PANELS — ROOM TEMPERATURE CONDITION — TITANIUM SIDE

FIGURE 119. CLOSE-UP OF DIAL INDICATORS ON THE TITANIUM SIDE OF THE LARGE SLIDING-JOINT PANELS — ROOM TEMPERATURE CONDITION

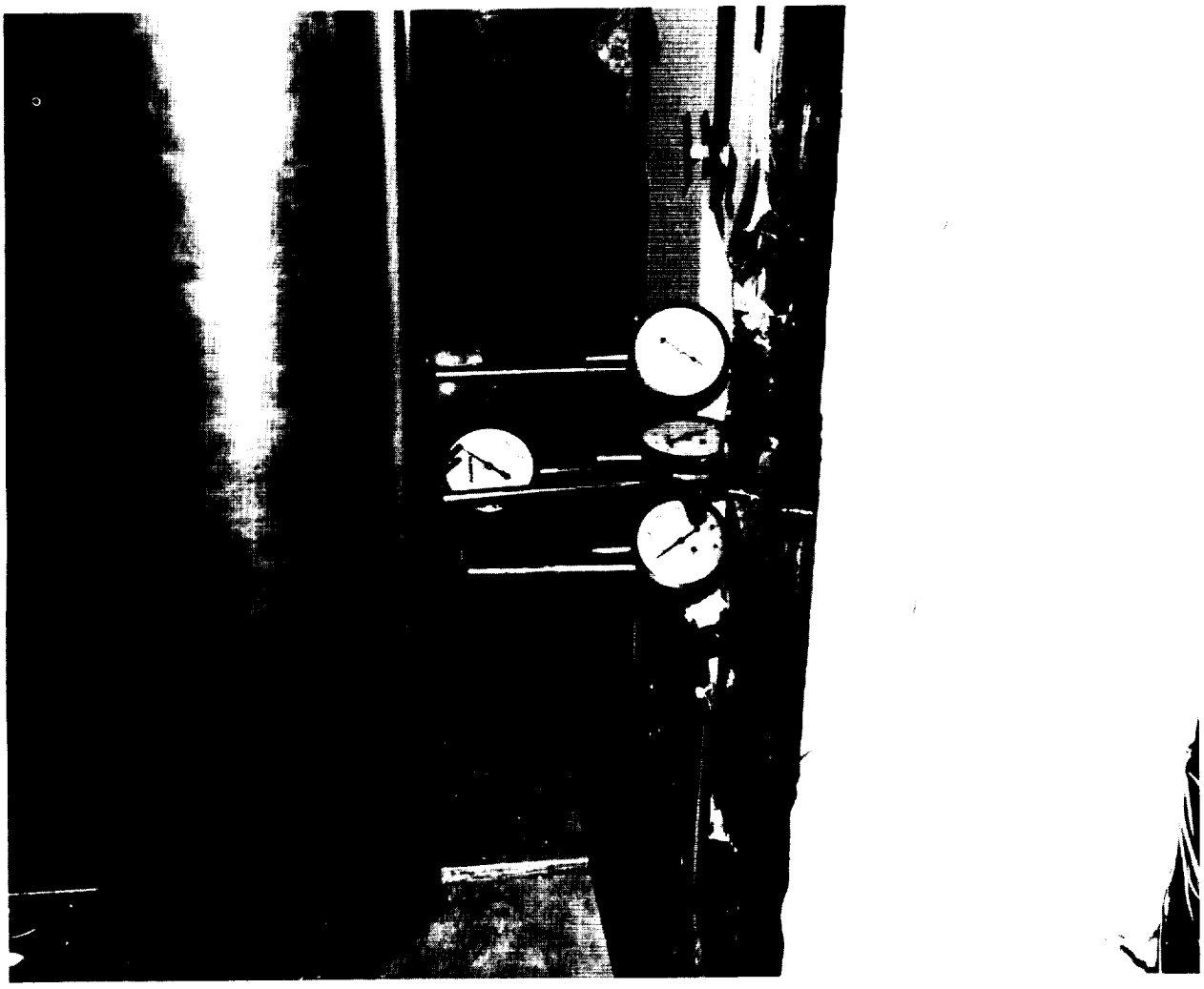

FIGURE 120. CLOSE-UP OF FOUR DIAL INDICATORS FOR THE HOT AND COLD CONDITIONS OF THE LARGE SLIDING-JOINT PANELS (THERMAL BOX IS WHITE)

FIGURE 121. THERMAL WHITE BOX IS CONNECTED TO HEATING/COOLING UNIT WITH INSULATED PIPES

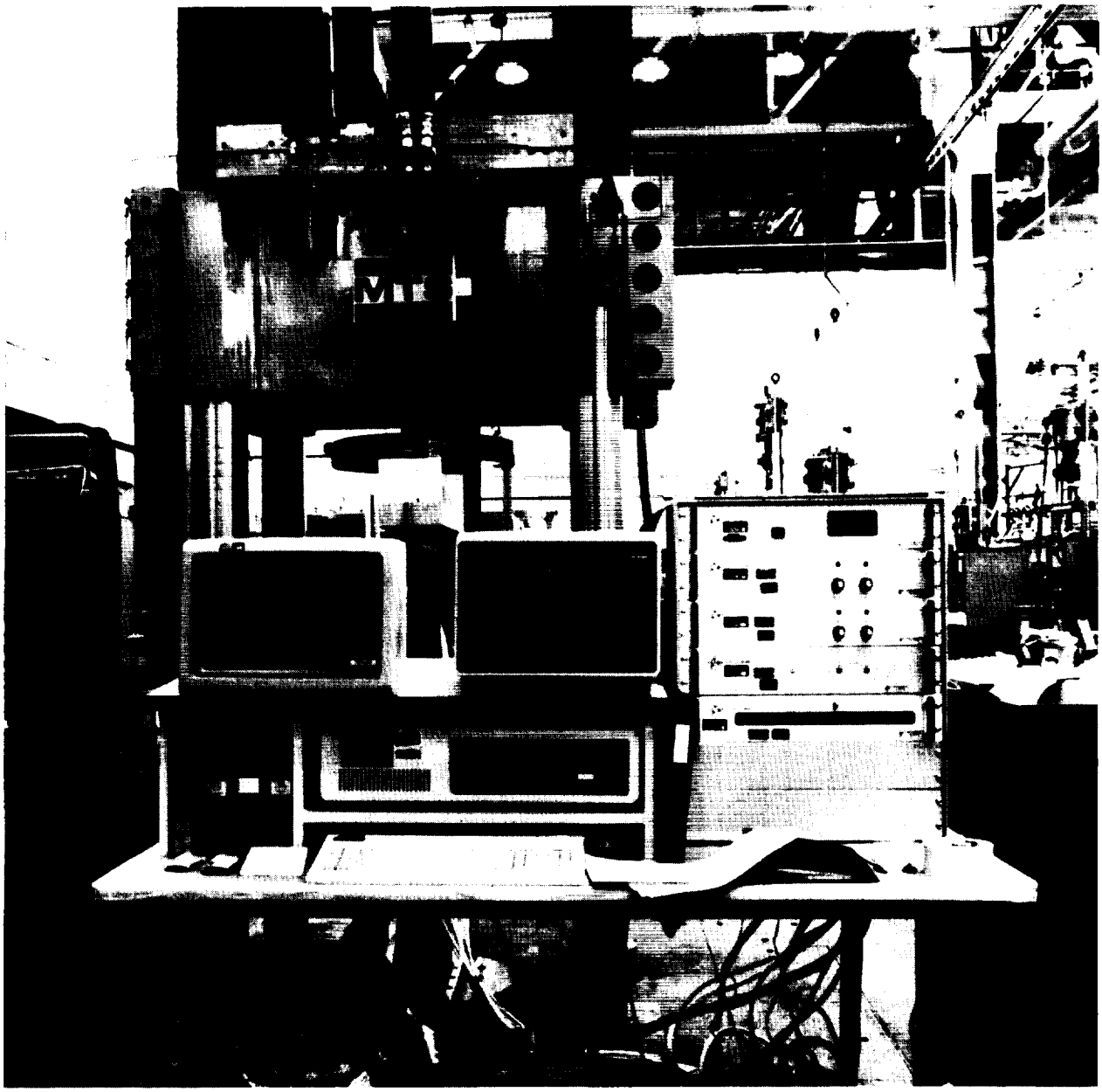

FIGURE 122. COMPUTER DATA CONTROL INSTRUMENTATION USED FOR RECORDING AND MONITORING STRAIN GAGES AND TEMPERATURES

LOAD (1,000 LB)	UPPER	CENTER	LOWER
0	0	0	0
4	–0.001	0	0
8	–0.001	–0.001	0
12	–0.001	–0.001	0
16	–0.002	–0.003	0
20	–0.002	–0.004	0
24	–0.0025	–0.0045	0
28	–0.0025	–0.0047	0
32	–0.0025	–0.0047	0
36	–0.0027	–0.0050	+0.001
40	–0.0023	–0.0048	+0.001
44	–0.0022	–0.0048	+0.0015
48	–0.0020	–0.0048	+0.0020

DIAL INDICATOR
READINGS TO
1.67 LOAD FACTOR

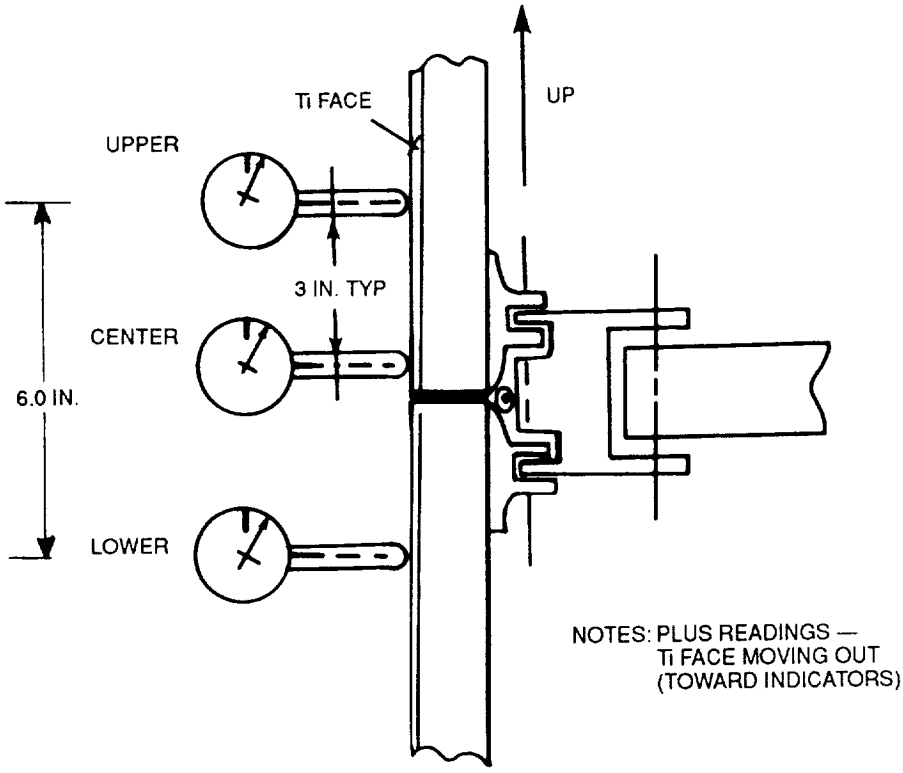

FIGURE 123. COMPRESSION TEST — J3 LARGE SLIDING JOINT

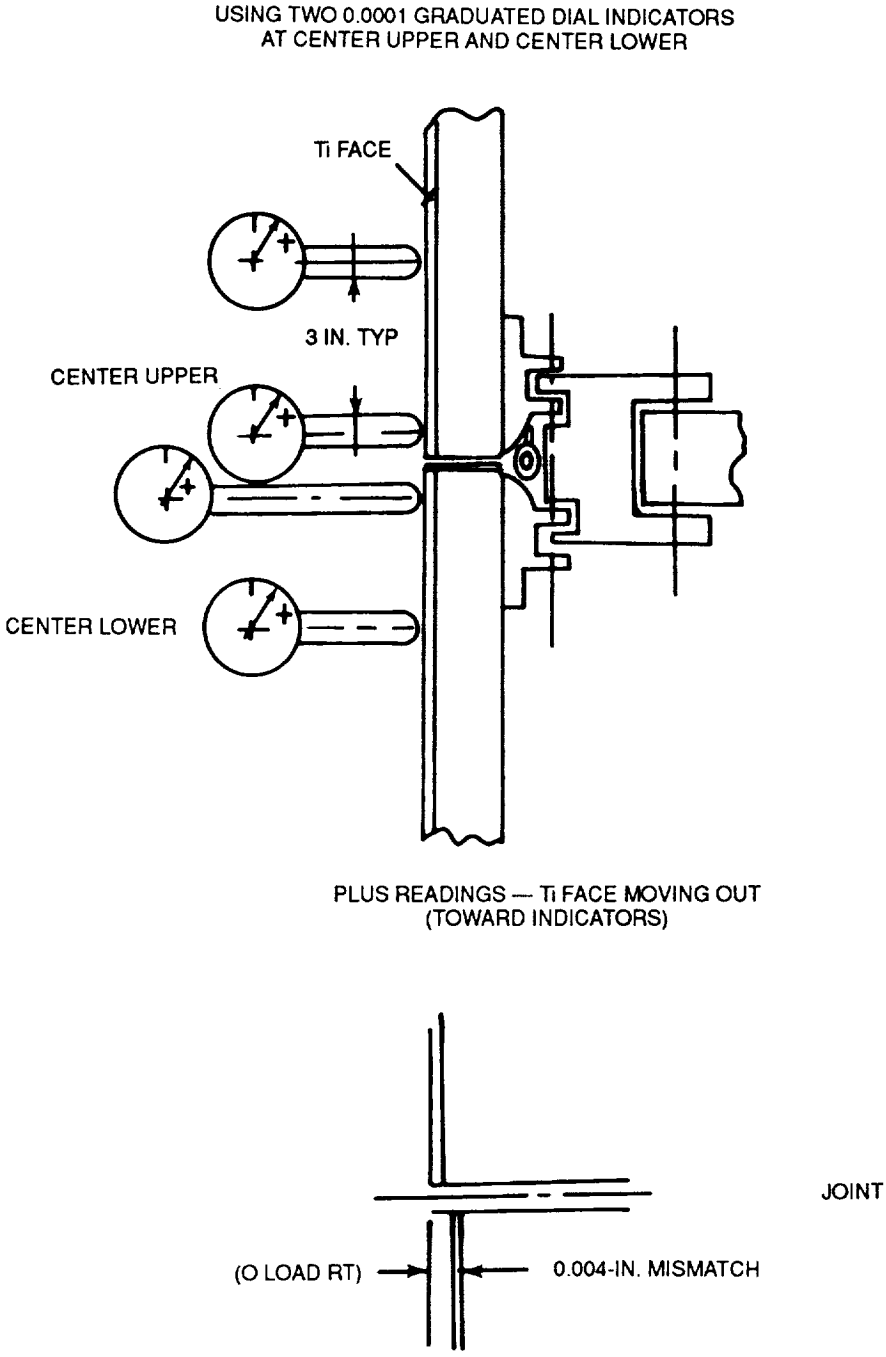

FIGURE 124. ADDITIONAL DIAL GAGES

LOAD (1,000 LB)	UPPER	CTR UPPER	CTR LOWER	LOWER
0	0	0	0	0
4	+0.0010	0	0	0
8	+0.0012	0	–0.0002	0
12	+0.0012	0	0	0
16	+0.0020	0	0	+0.0008
20	+0.0022	0	0	+0.0008
24	+0.0028	+0.0008	+0.0005	+0.0010
28	+0.0030	+0.0010	+0.0010	+0.0014
32	+0.0038	+0.0016	+0.0012	+0.0018
46	+0.0040	+0.0018	+0.0016	+0.0020
40	+0.0046	+0.0020	+0.0020	+0.0026
44	+0.0050	+0.0026	+0.0022	+0.0030
48	+0.0060	+0.0028	+0.0028	+0.0035
52	+0.0068	+0.0032	+0.0030	+0.0038
56	+0.0068	+0.0036	+0.0032	+0.0040
60	+0.0070	+0.0038	+0.0034	+0.0044
64	+0.0074	+0.0040	+0.0038	+0.0048
68	+0.0088	+0.0048	+0.0040	+0.0050
72	+0.0090	+0.0048	+0.0044	+0.0054
28.8	+0.0028	+0.0010	+0.0012	+0.0020
0	–0.0016*	0	0	0

*ADHESIVE DISBOND

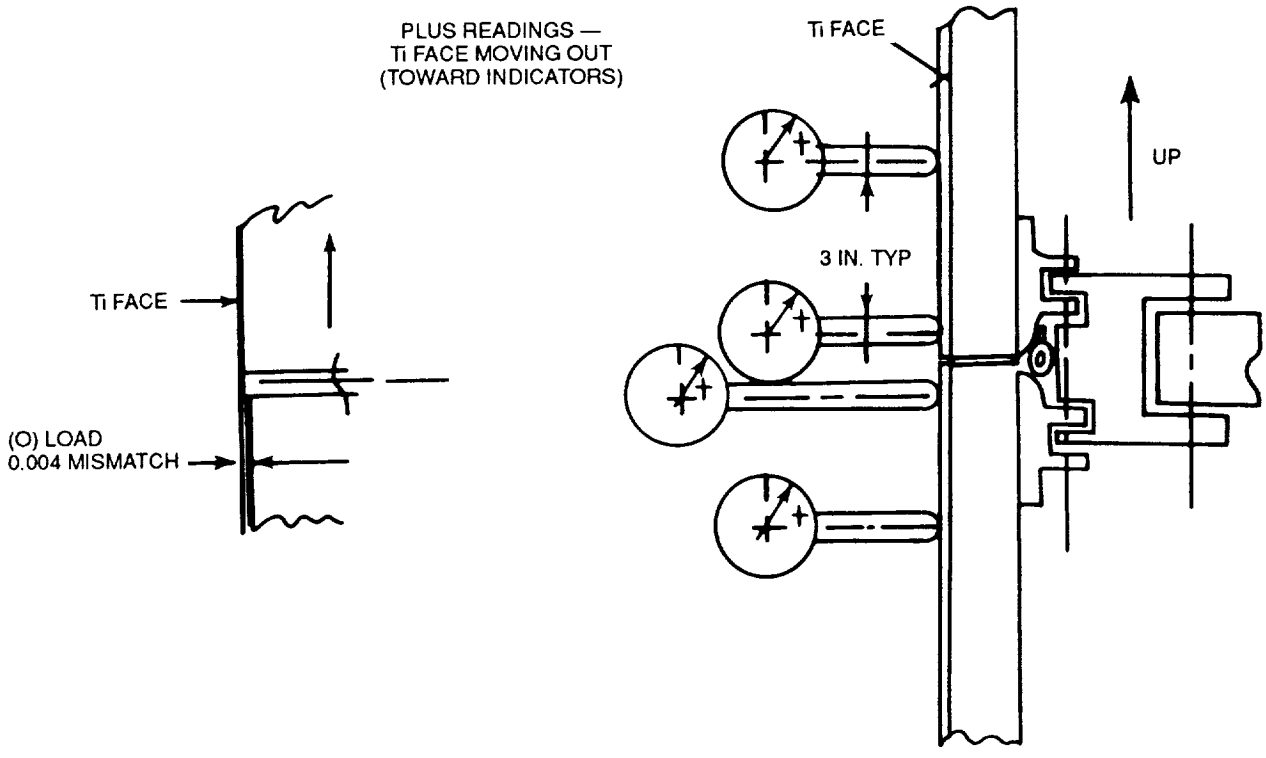

FIGURE 125. COLD (–65°F) DIAL INDICATOR READINGS

LOAD (1,000 LB)	UPPER	CTR UPPER	CTR LOWER	LOWER
0	0	0	0	0
4	0	0	0	0
8	+0.0005	–0.0005	–0.0004	–0.0002
12	+0.0018	–0.0005	0	0
16	+0.0025	–0.0003	0	0
20	+0.0032	–0.0002	+0.0002	0
24	+0.0040	0	+0.0002	+0.0002
28	+0.0050	+0.0002	+0.0008	+0.0008
32	+0.0052	+0.0002	+0.0010	+0.0010
36	+0.0060	+0.0008	+0.0012	+0.0015
40	+0.0070	+0.0010	+0.0016	+0.0020
44	+0.0078	+0.0014	+0.0020	+0.0022
48	+0.0090	+0.0020	+0.0026	+0.0030
52	+0.0100	+0.0025	+0.0030	+0.0036
56	+0.00118	+0.0032	+0.0038	+0.0044
60	+0.0130	+0.0038	+0.0044	+0.0040
64	+0.0140	+0.0042	+0.0050	+0.0054
68	+0.0150	+0.0048	+0.0056	+0.0062
72	+0.0162	+0.0050	+0.0062	+0.0070
28.8	+0.0080	+0.0015	+0.0022	+0.0030
0	0	0	+0.0002	+0.0006

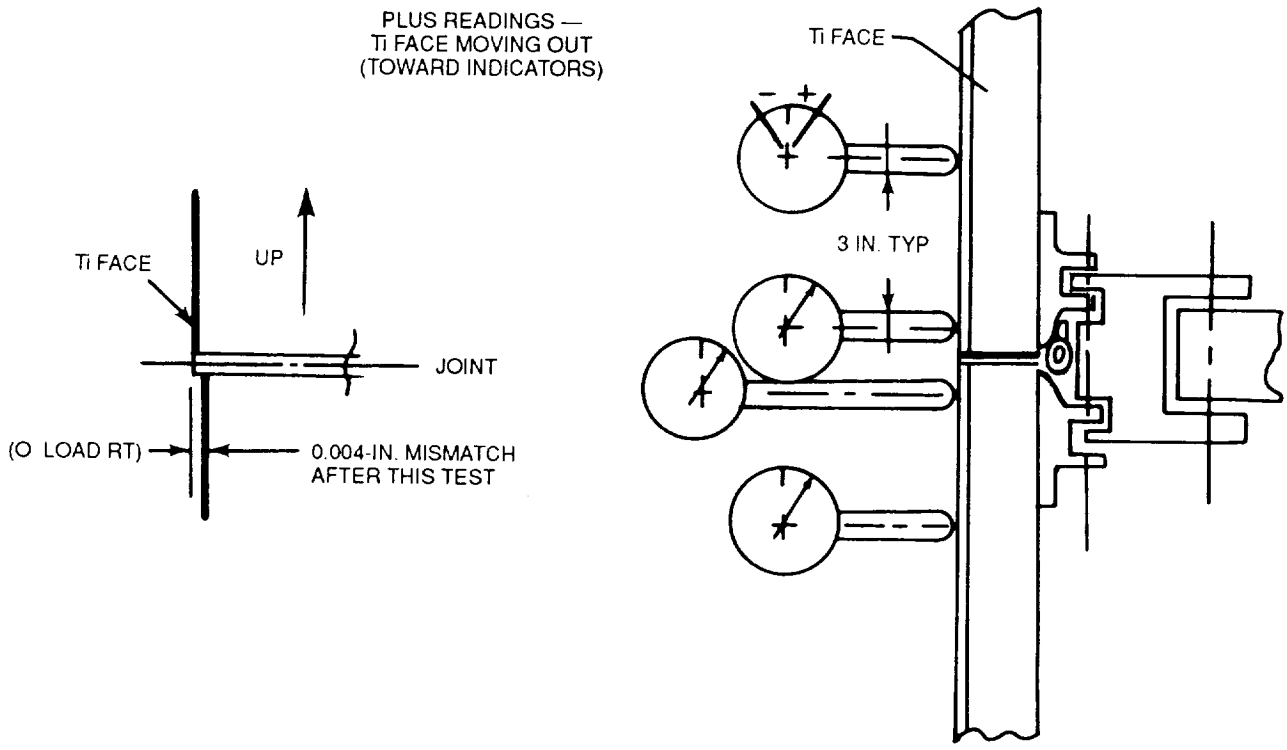

FIGURE 126. HOT (+165°F) DIAL INDICATOR READINGS

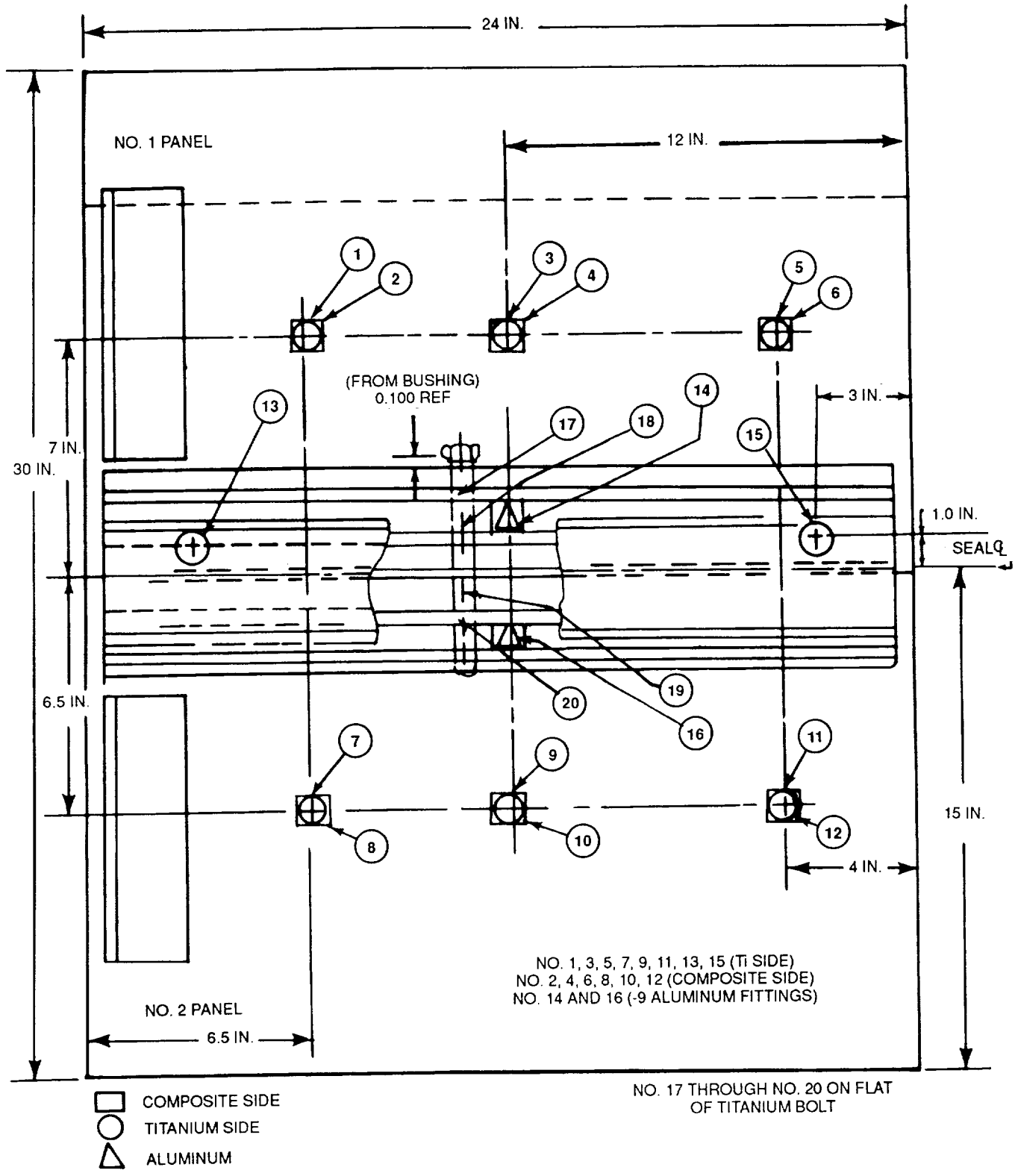

FIGURE 127. STRAIN GAGE LOCATIONS

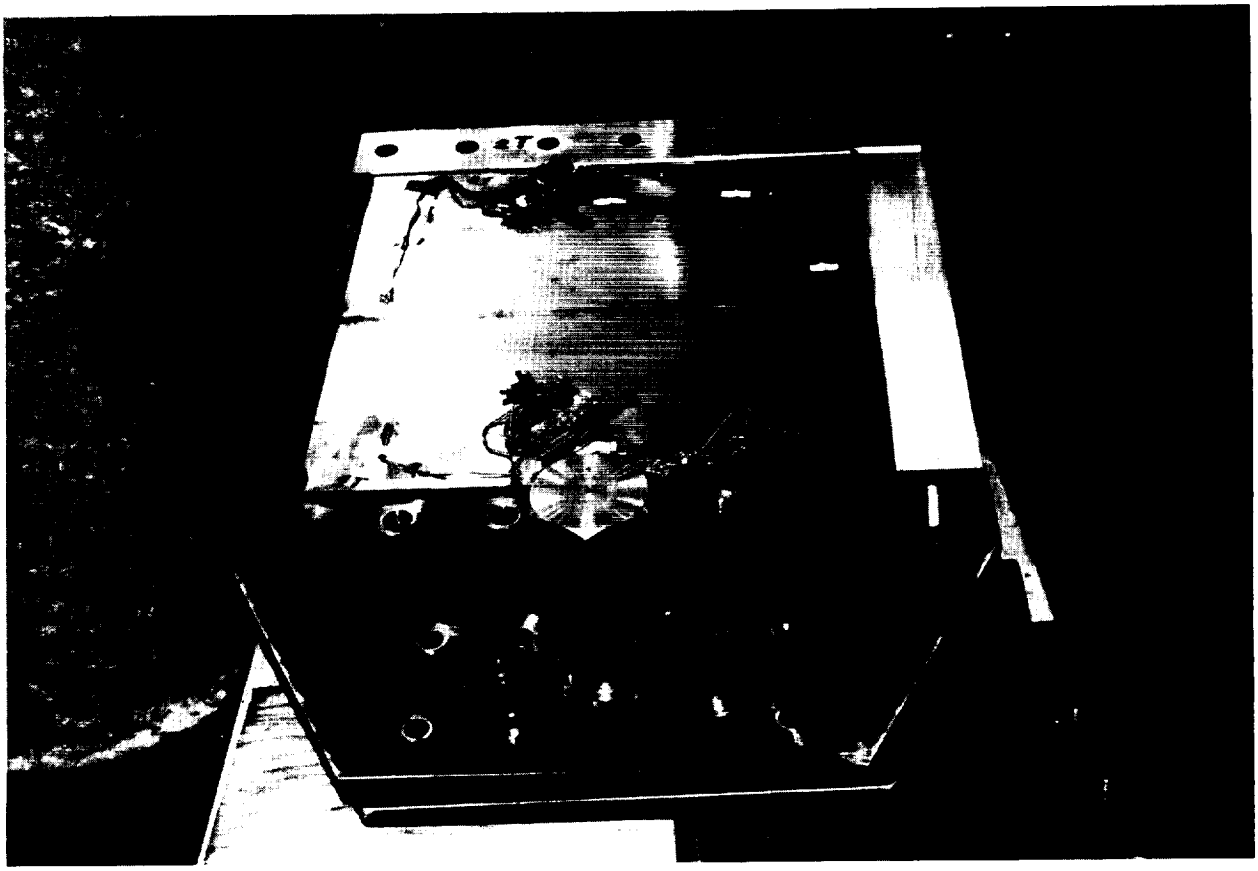

FIGURE 128. LARGE SLIDING-JOINT PANELS WITH TEST PLATES ADDED — FRONT VIEW

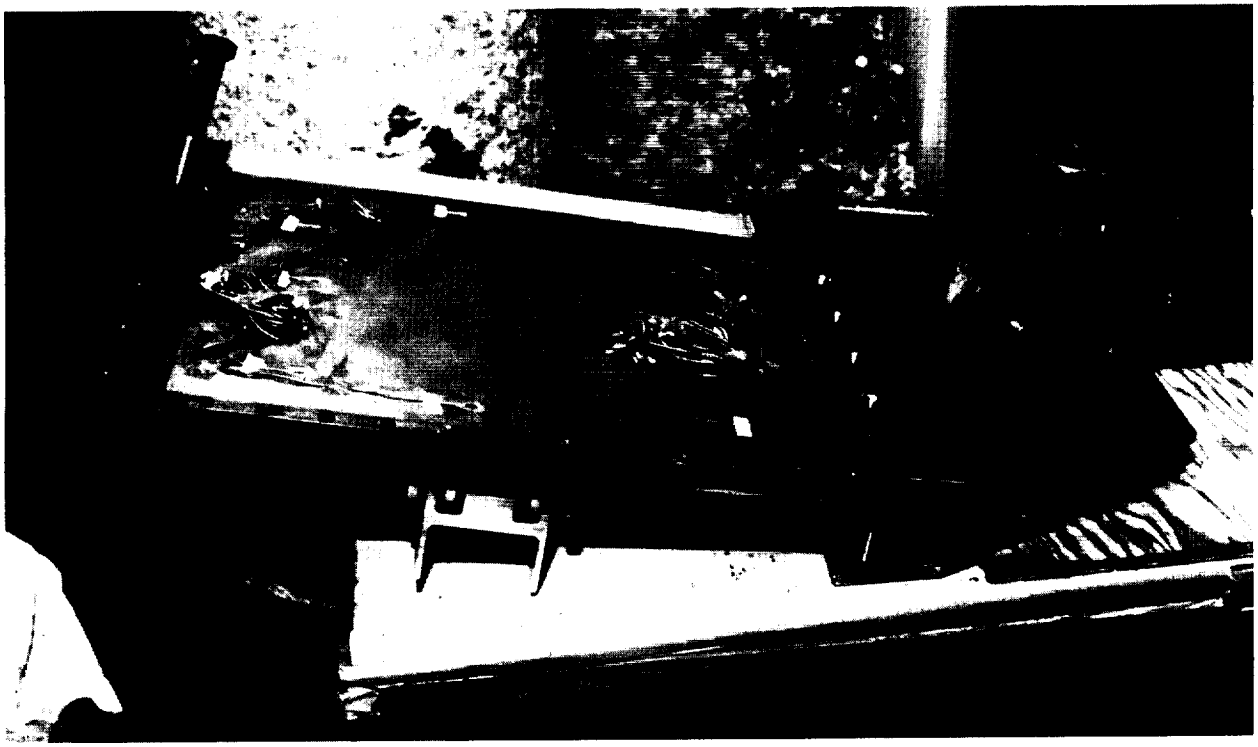

FIGURE 129. LARGE SLIDING-JOINT PANELS WITH TEST PLATES ADDED — SIDE VIEW

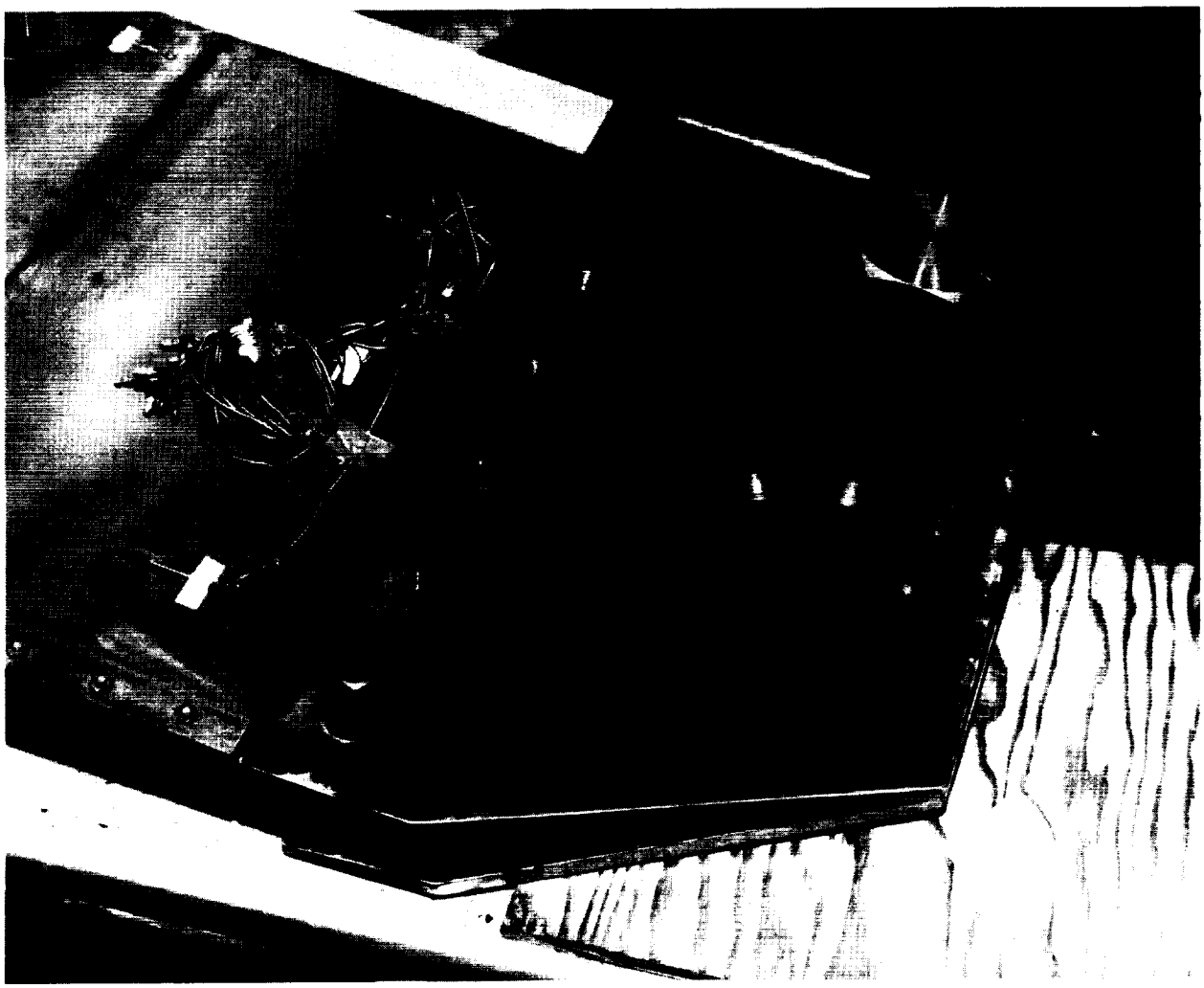

FIGURE 130. CLOSE-UP OF LARGE SLIDING-JOINT PANEL — WITH TEST END PLATES

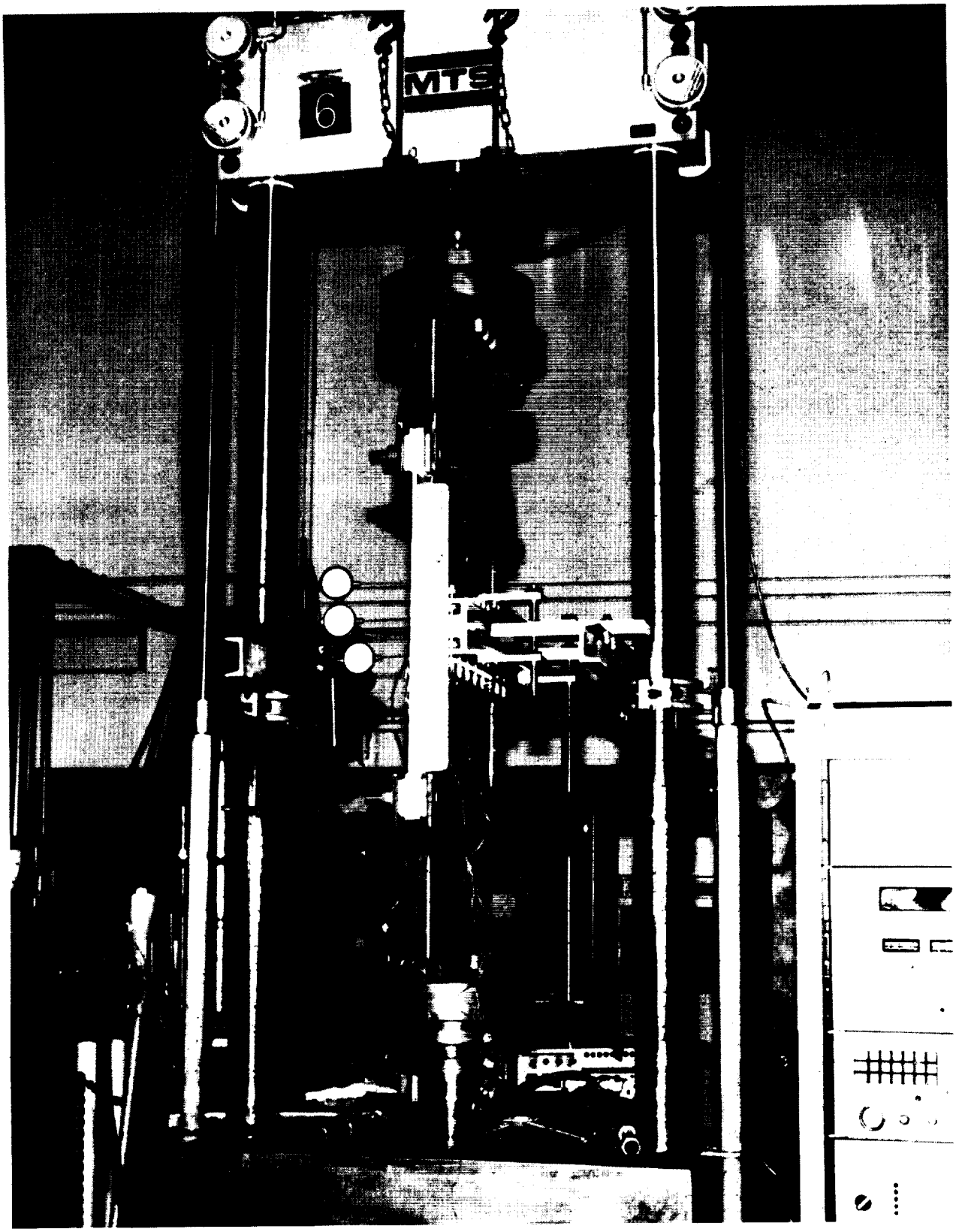

FIGURE 131. SLIDING-JOINT LFC PANELS READY FOR TENSION TESTING

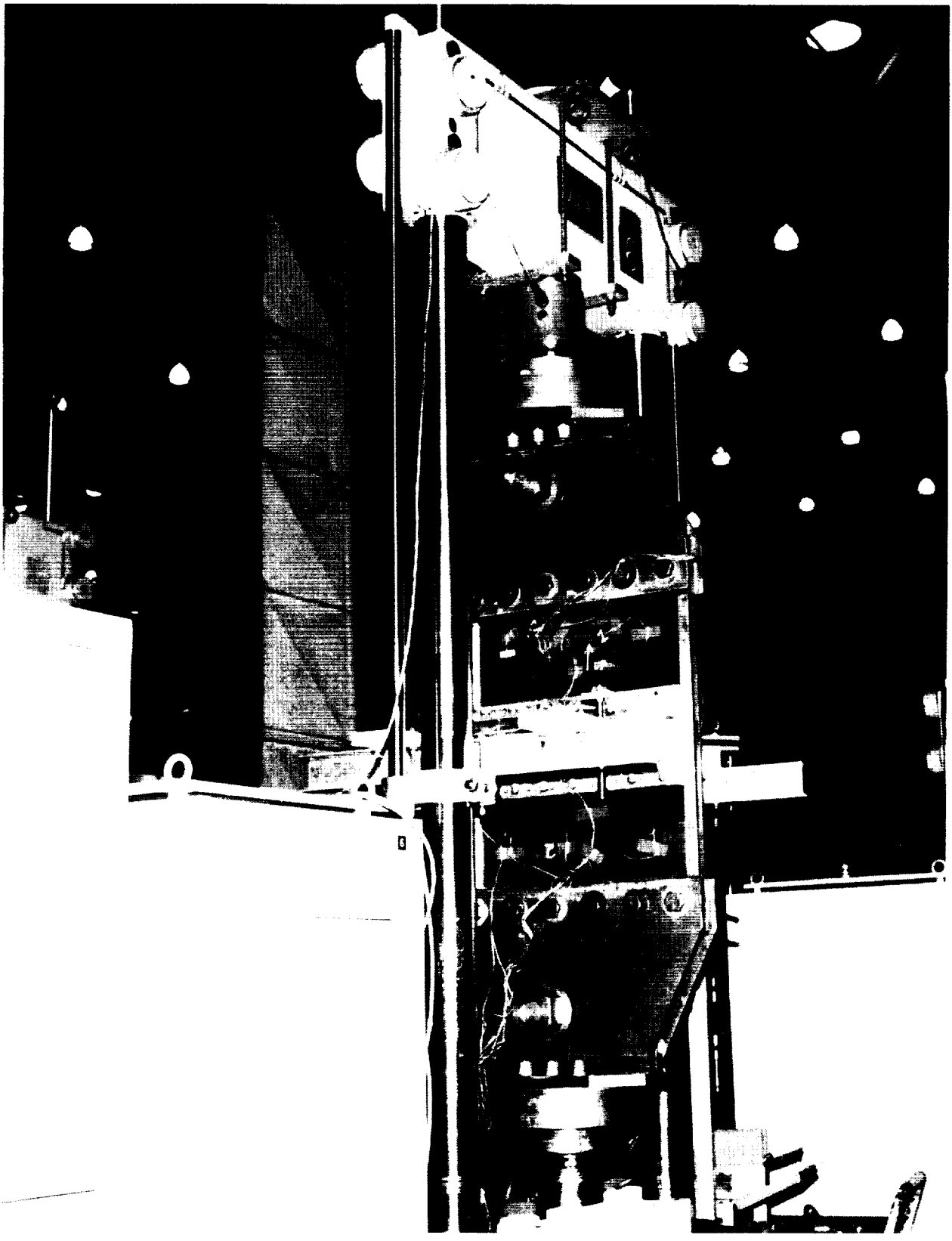

FIGURE 132. CLOSE-UP OF TENSION TEST SETUP OF LFC SLIDING-JOINT PANELS

FIGURE 133. TENSION TEST SETUP OF SLIDING-JOINT PANELS — LATERAL SUPPORT SIDE

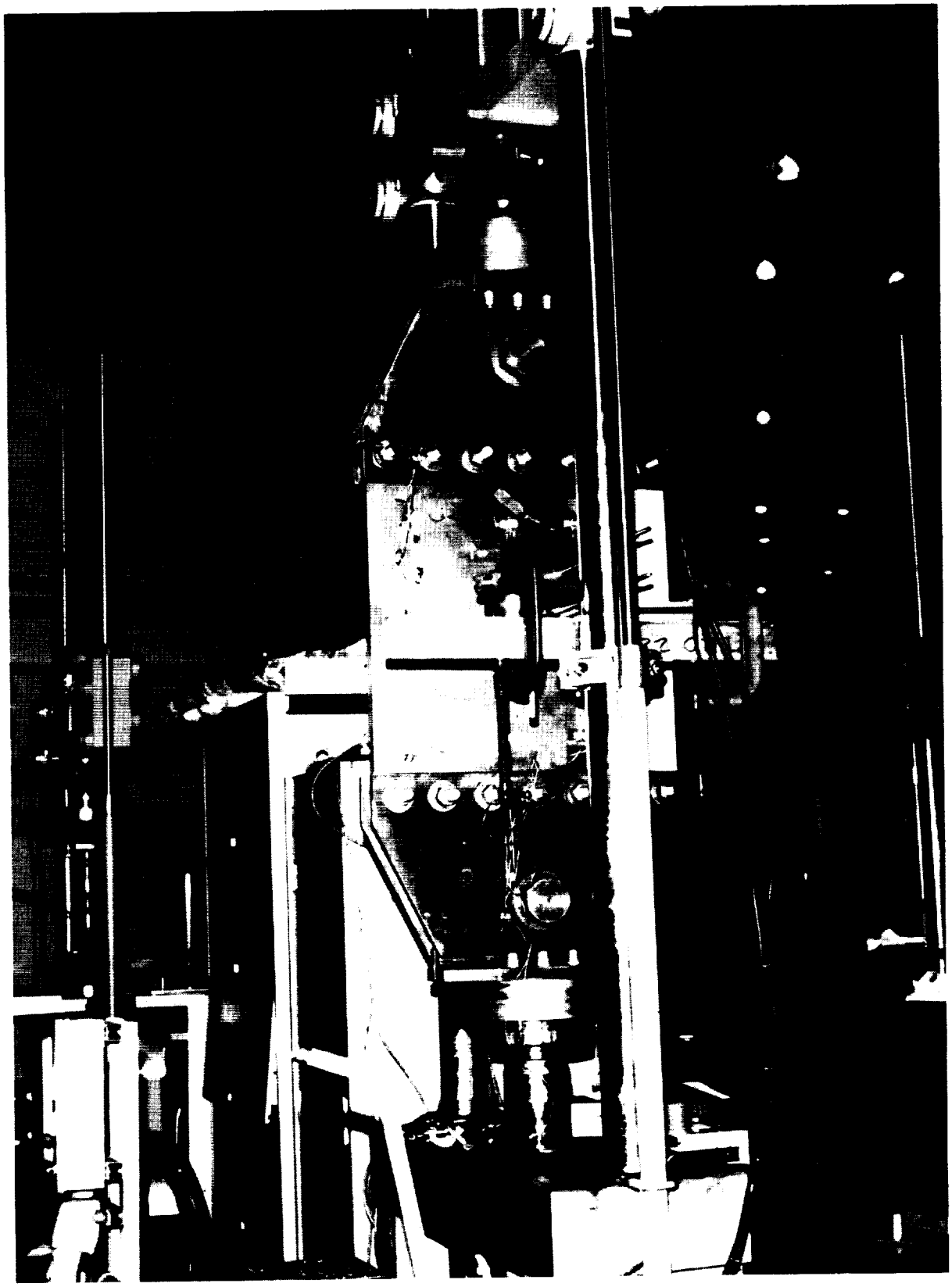

FIGURE 134. TENSION TEST SETUP OF SLIDING-JOINT PANELS — DIAL GAGE SIDE

ORIGINAL PAGE
BLACK AND WHITE PHOTOGRAPH

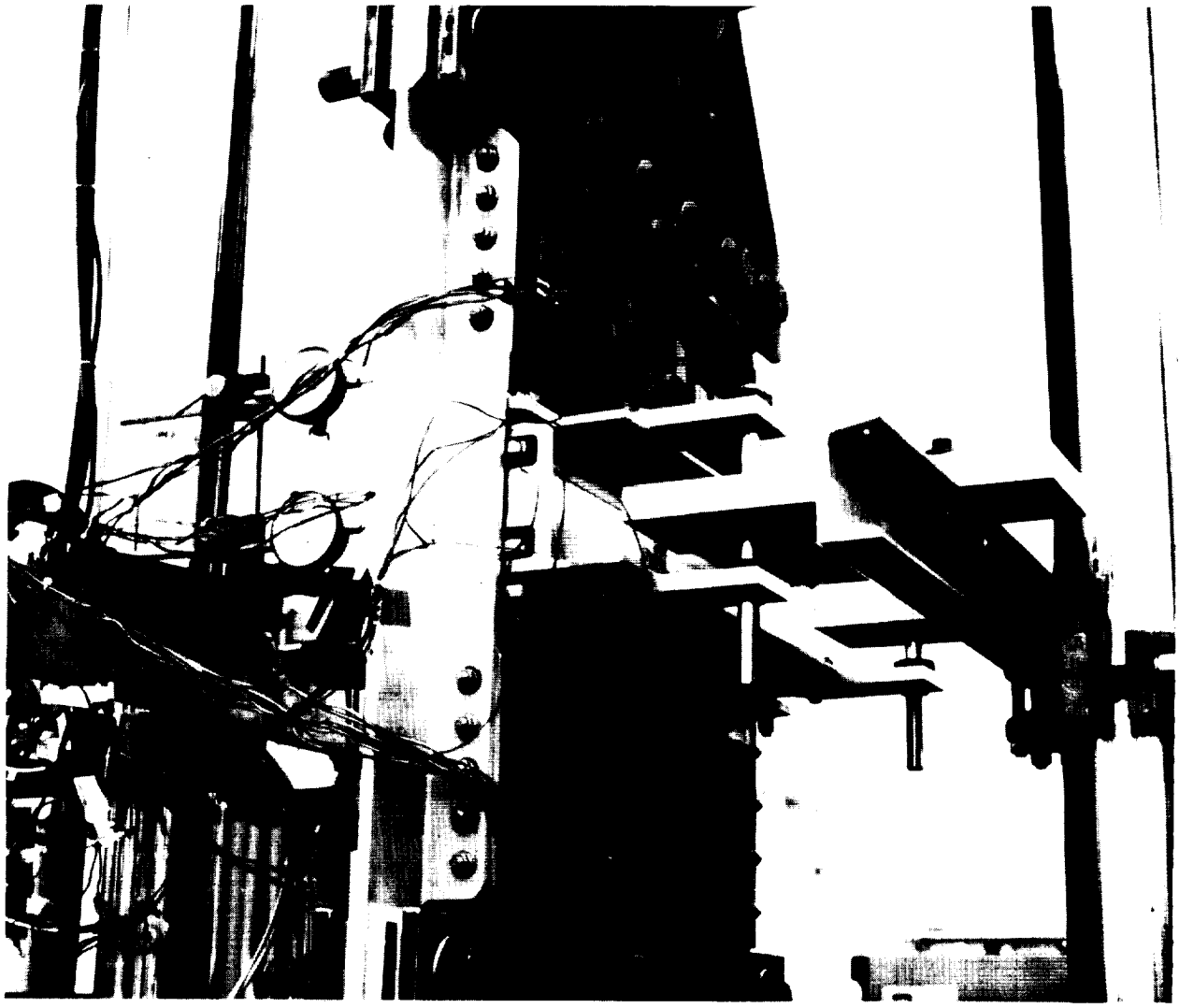

FIGURE 135. VIEW OF INITIAL RIB SUPPORTS WITH ONE ATTACHMENT TO THE VERTICAL COLUMN

ORIGINAL PAGE
BLACK AND WHITE PHOTOGRAPH

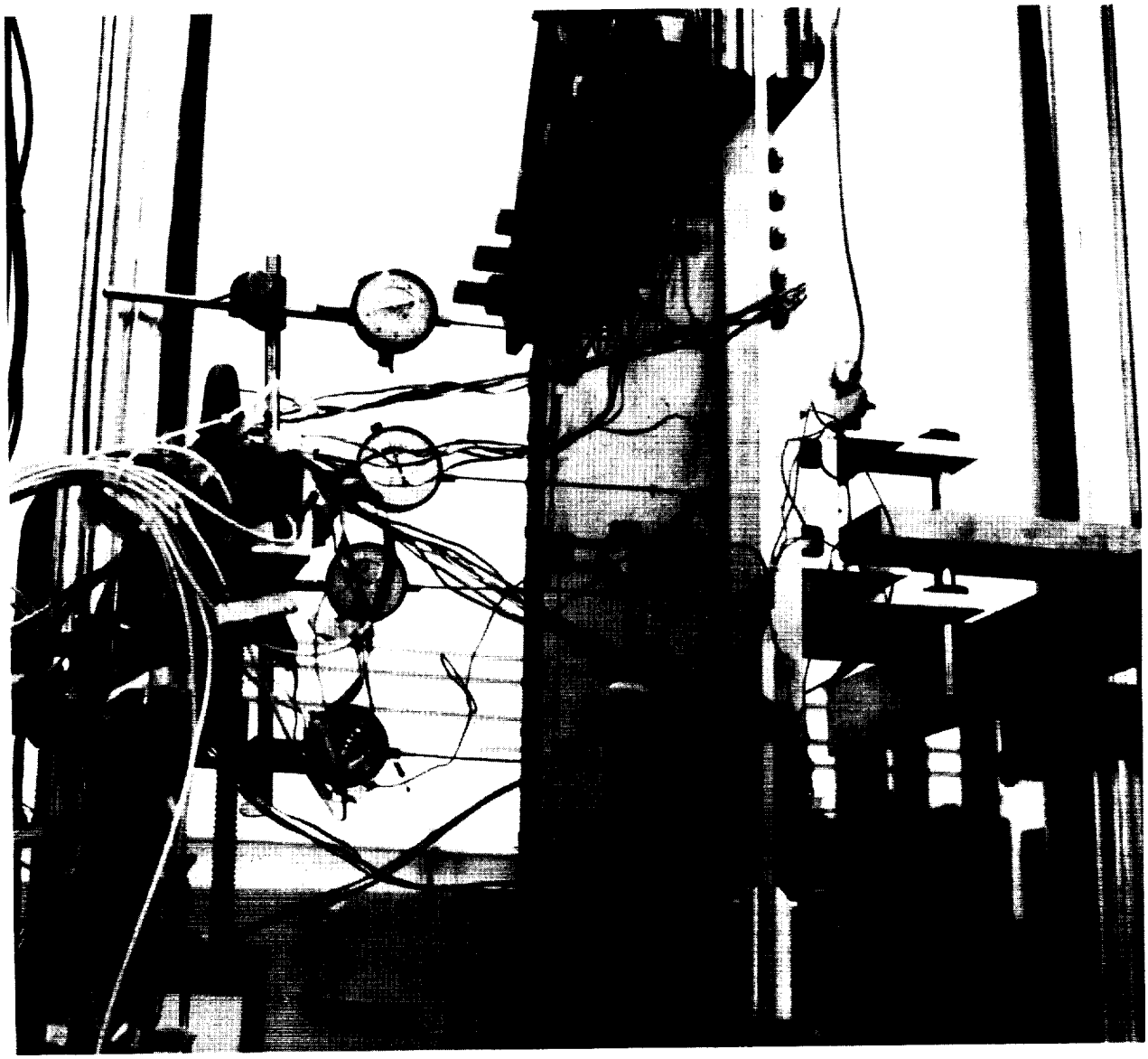

FIGURE 136. VIEW OF DIAL GAGES AND RIB SUPPORTS WITH ONE ATTACHMENT TO THE VERTICAL COLUMN

ORIGINAL PAGE
BLACK AND WHITE PHOTOGRAPH

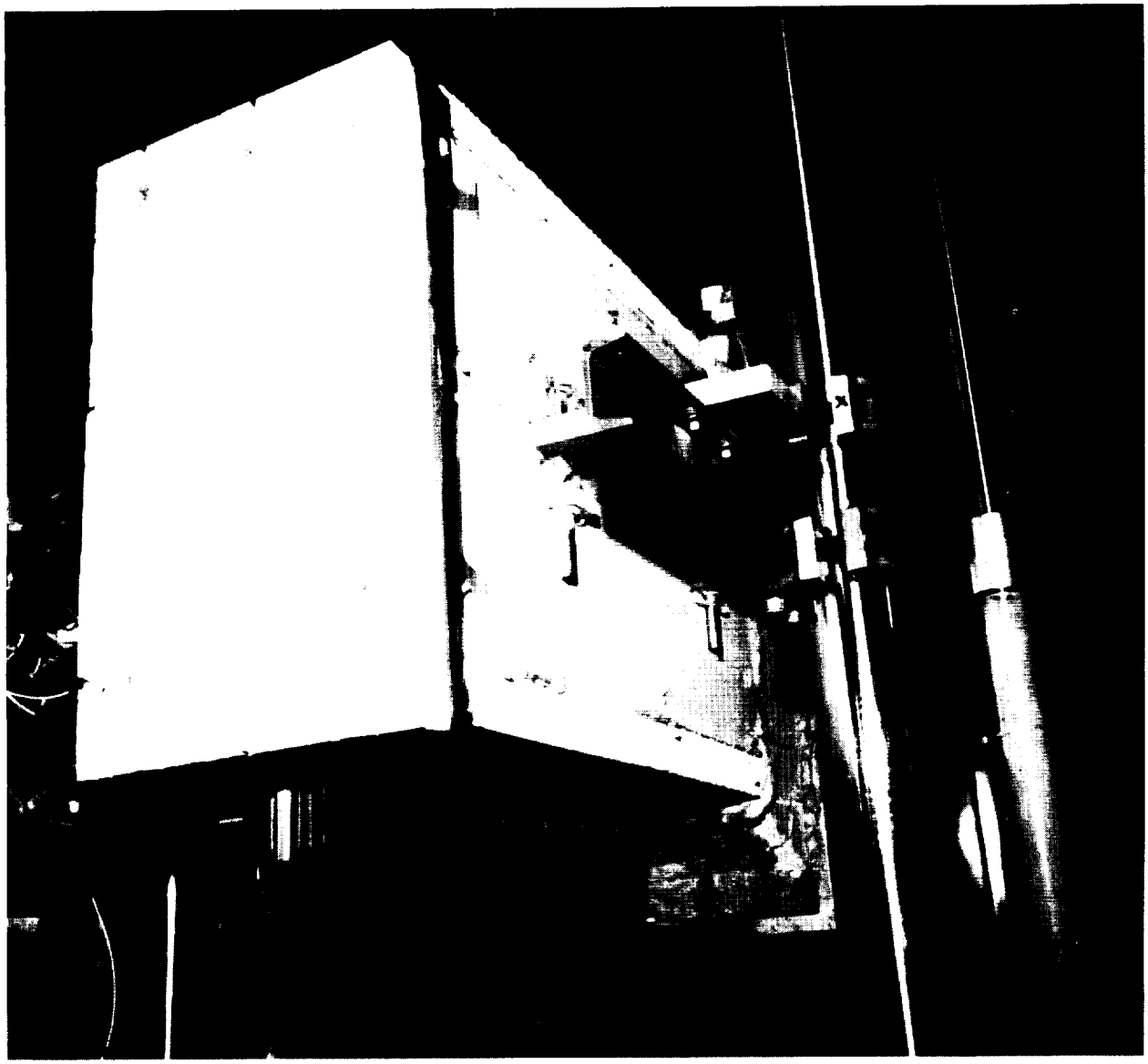

FIGURE 137. ENVIRONMENTAL BOX WITH SPECIMENS ENCLOSED

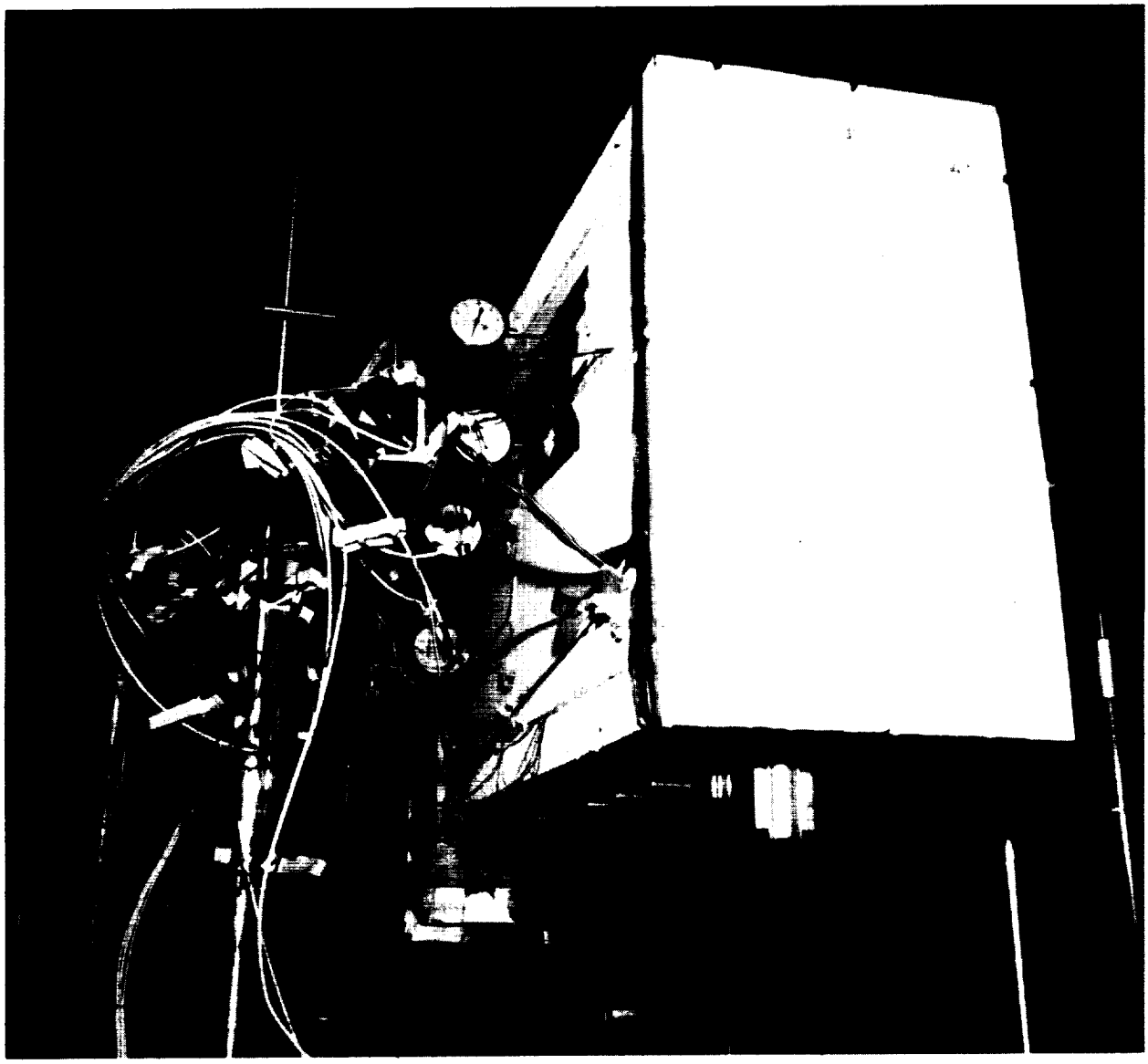

FIGURE 138. VIEW SHOWING DIAL GAGES PENETRATING THROUGH THE ENVIRONMENTAL BOX TO MEASURE THE PANEL DEFLECTIONS

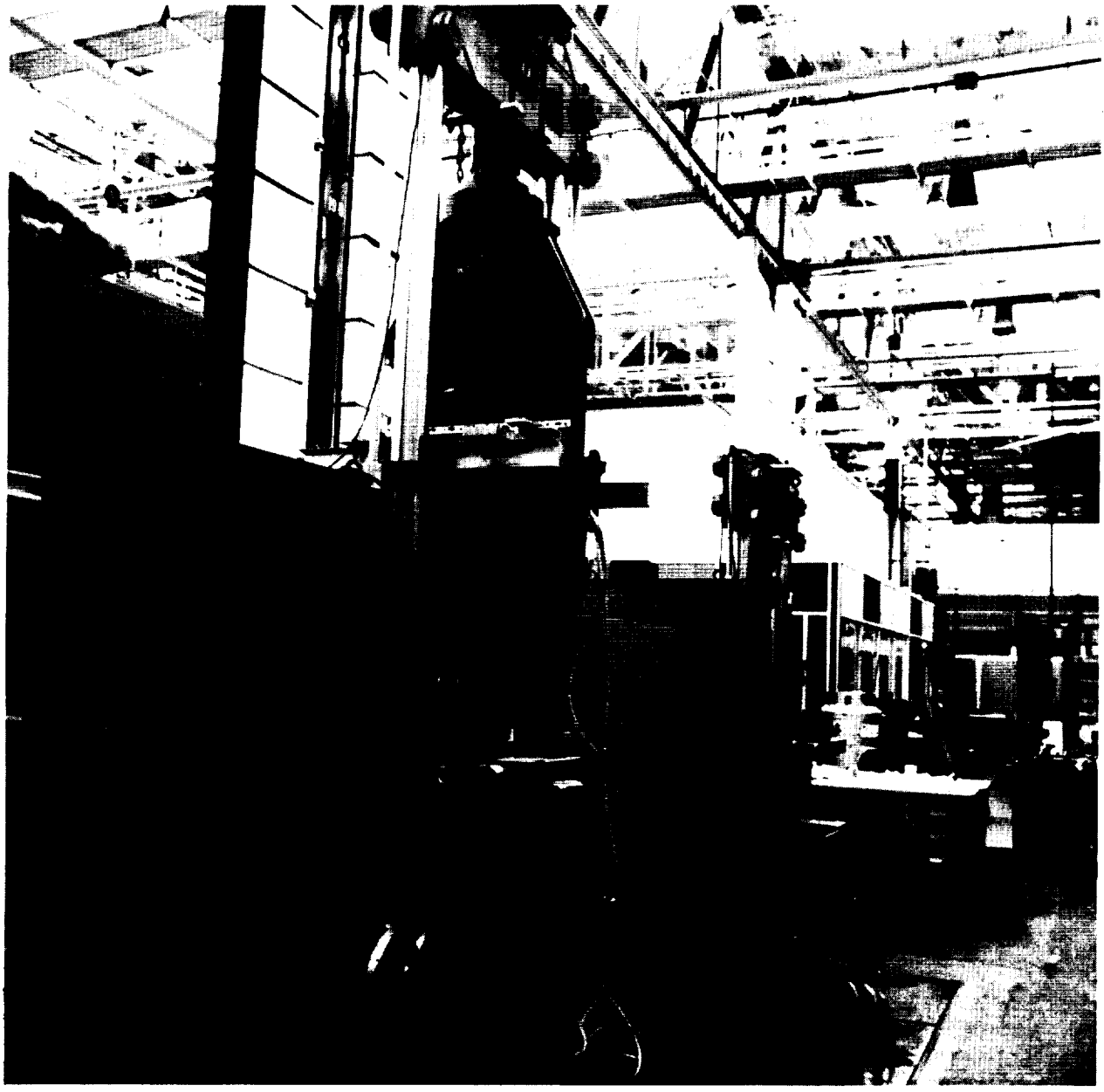

FIGURE 139. TENSION TEST SPECIMEN OF SLIDING-JOINT PANEL IN JIG FOR TEMPERATURE TEST

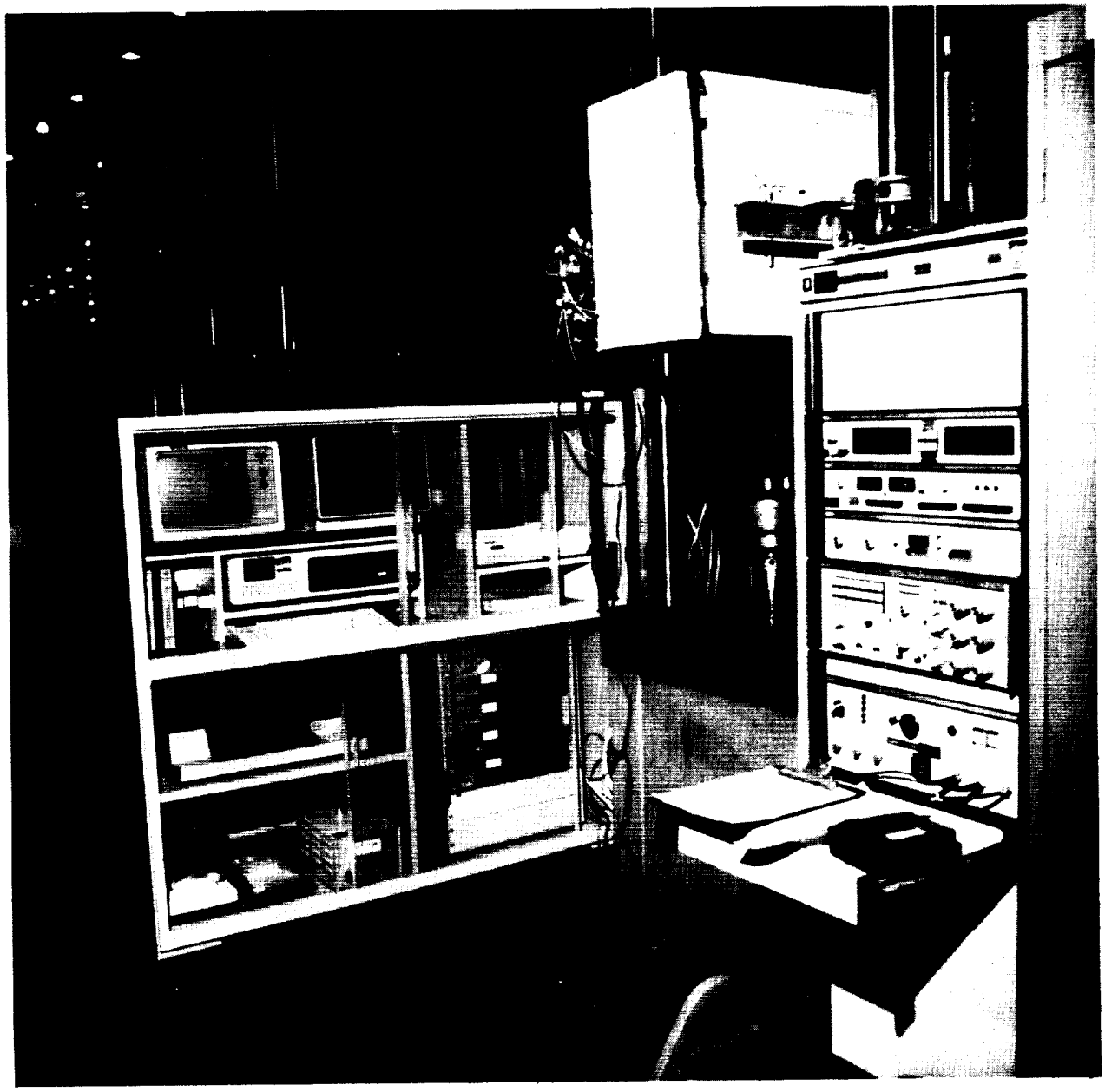

FIGURE 140. TENSION TEST SPECIMEN IN TEST MACHINE WITH ENVIRONMENTAL BOX INSTALLED FOR ELEVATED- AND COLD-TEMPERATURE TESTS

LOAD (1,000 LB)	UPPER	CTR UPPER	CTR LOWER	LOWER
0	0	0	0	0
4	+0.0015	+0.0032	+0.0012	–0.0020
8	+0.0060	+0.0086	+0.0042	–0.0020
12	+0.0070	+0.0091	+0.0045	–0.0030
16	+0.0080	+0.0134	+0.0047	–0.0050
18	+0.0080	+0.0146	+0.0057	–0.0065
20	+0.0083	+0.0157	+0.0067	–0.0070
22	+0.0090	+0.0168	+0.0069	–0.0082
24	+0.0090	+0.0182	+0.0075	–0.0090
26	+0.0097	+0.0193	+0.0080	–0.0090
28	+0.0099	+0.0205	+0.0086	–0.0090
0	+0.0015	+0.0028	+0.0016	–0.0005

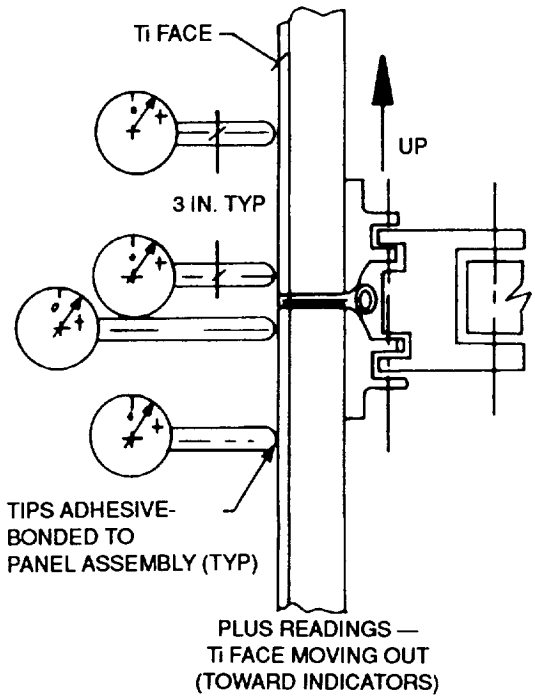

FIGURE 141. TENSION TEST FOR LARGE SLIDING-JOINT PANEL ASSEMBLY (24 BY 30 IN.) ROOM TEMPERATURE RUN NO. 2 (WITH ADDITIONAL RIB CONSTRAINT)

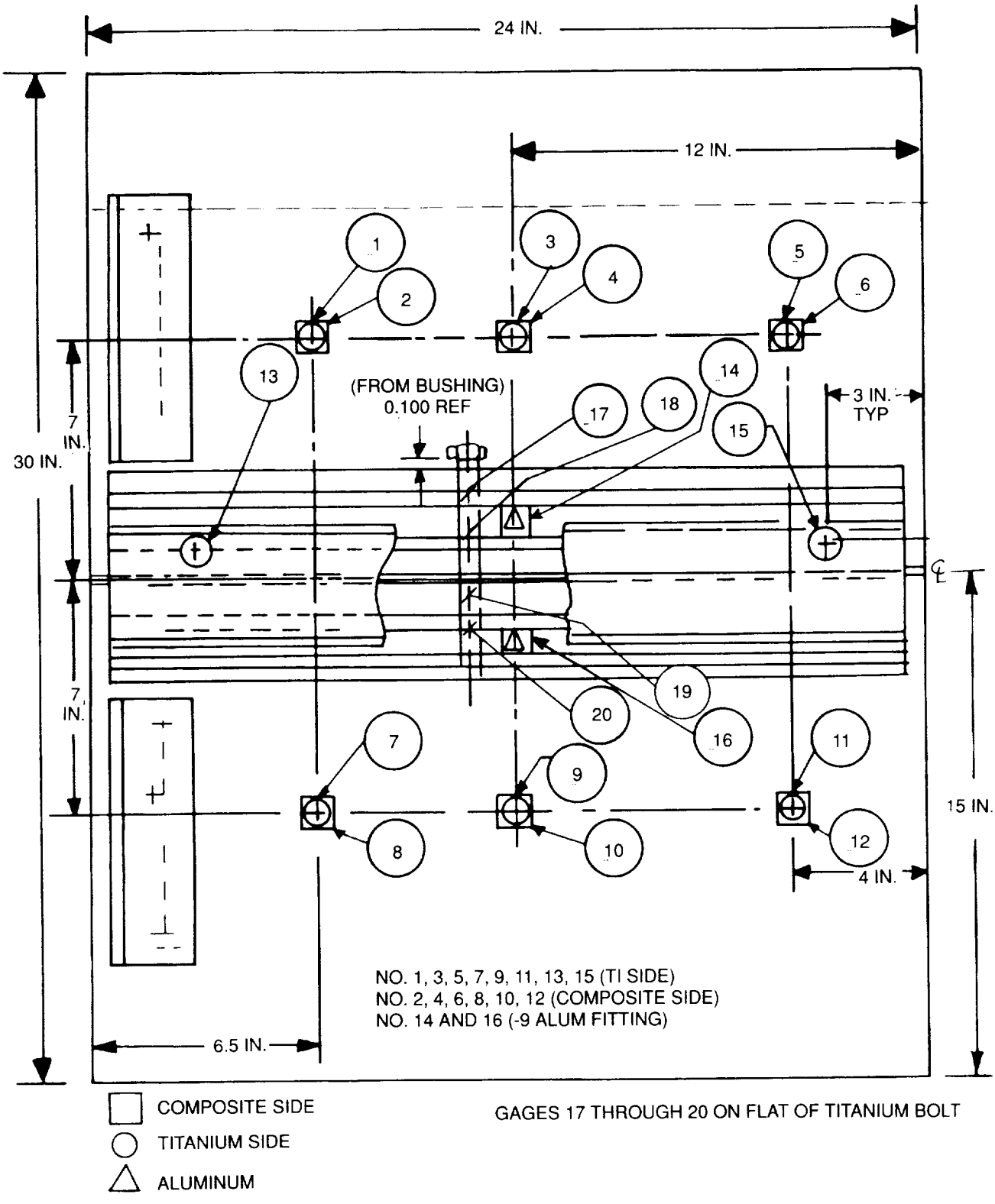

FIGURE 142. STRAIN GAGE PLACEMENT FOR TENSION TEST OF THE LARGE SLIDING-JOINT PANEL

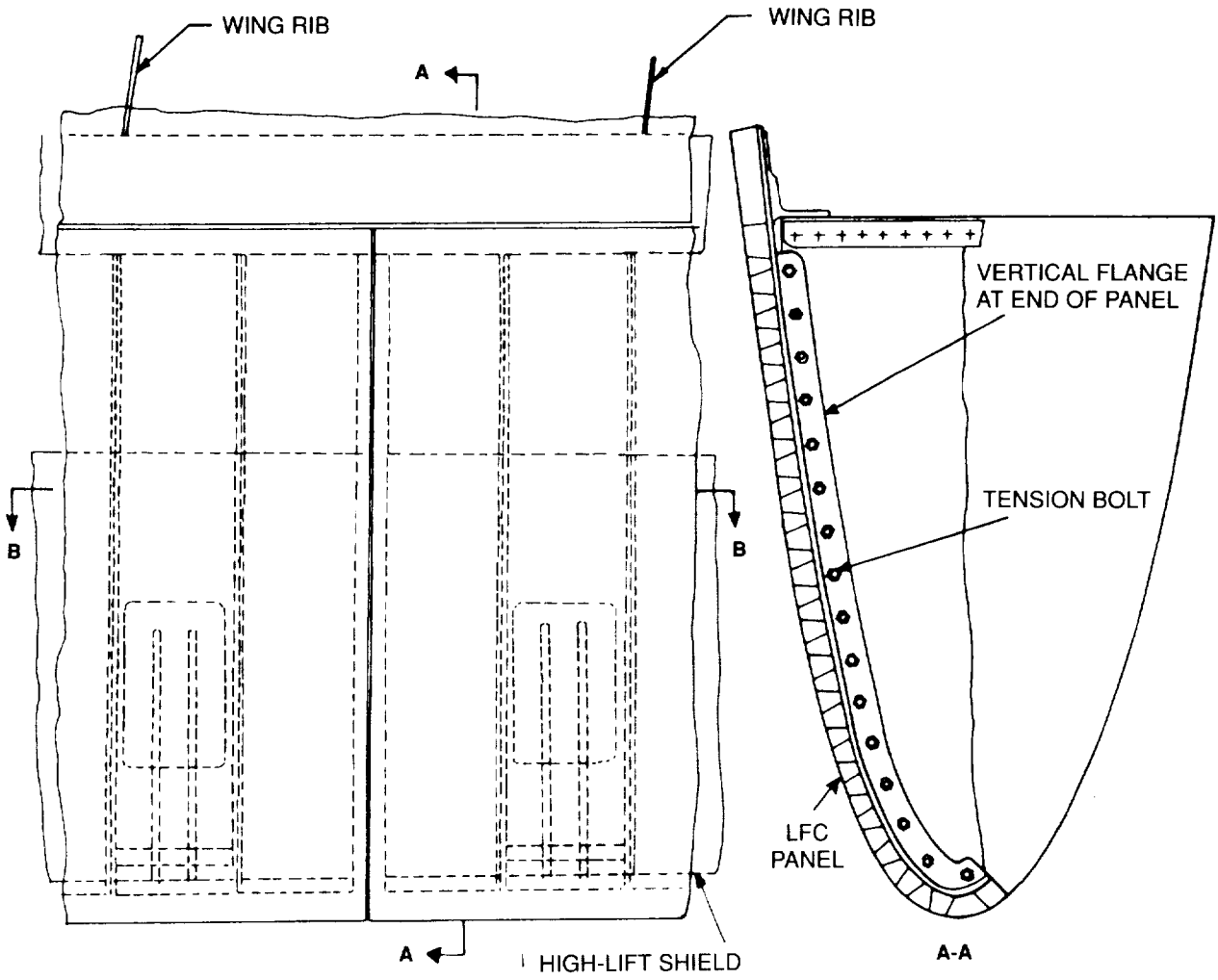

FIGURE 143. WING LEADING EDGE WITH MODIFIED THREE-RIB JOINT

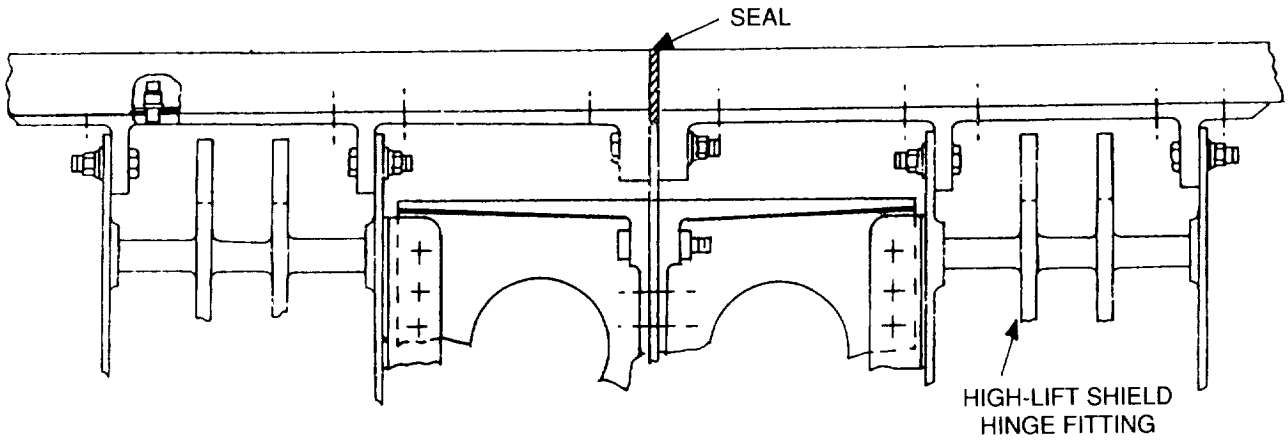

FIGURE 144. MODIFIED THREE-RIB JOINT (SECTION BB FROM FIGURE 110)

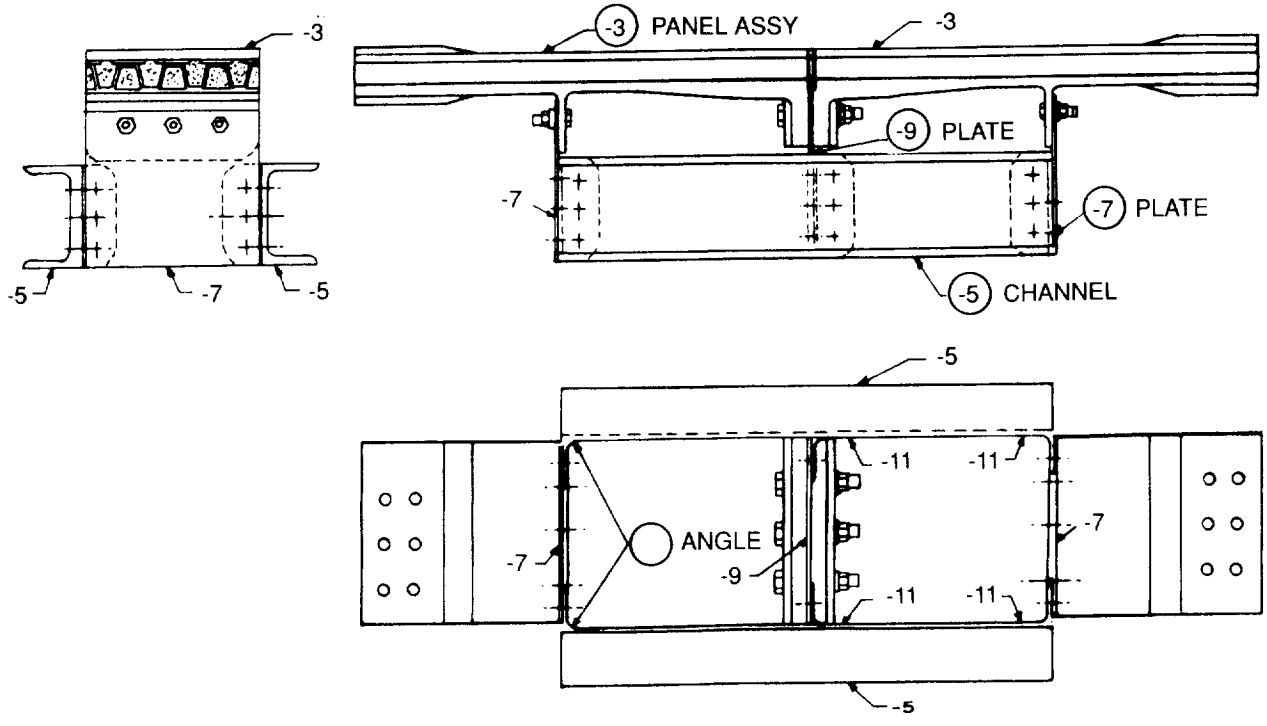

FIGURE 145. MODIFIED THREE-VIEW OF TEST SPECIMEN

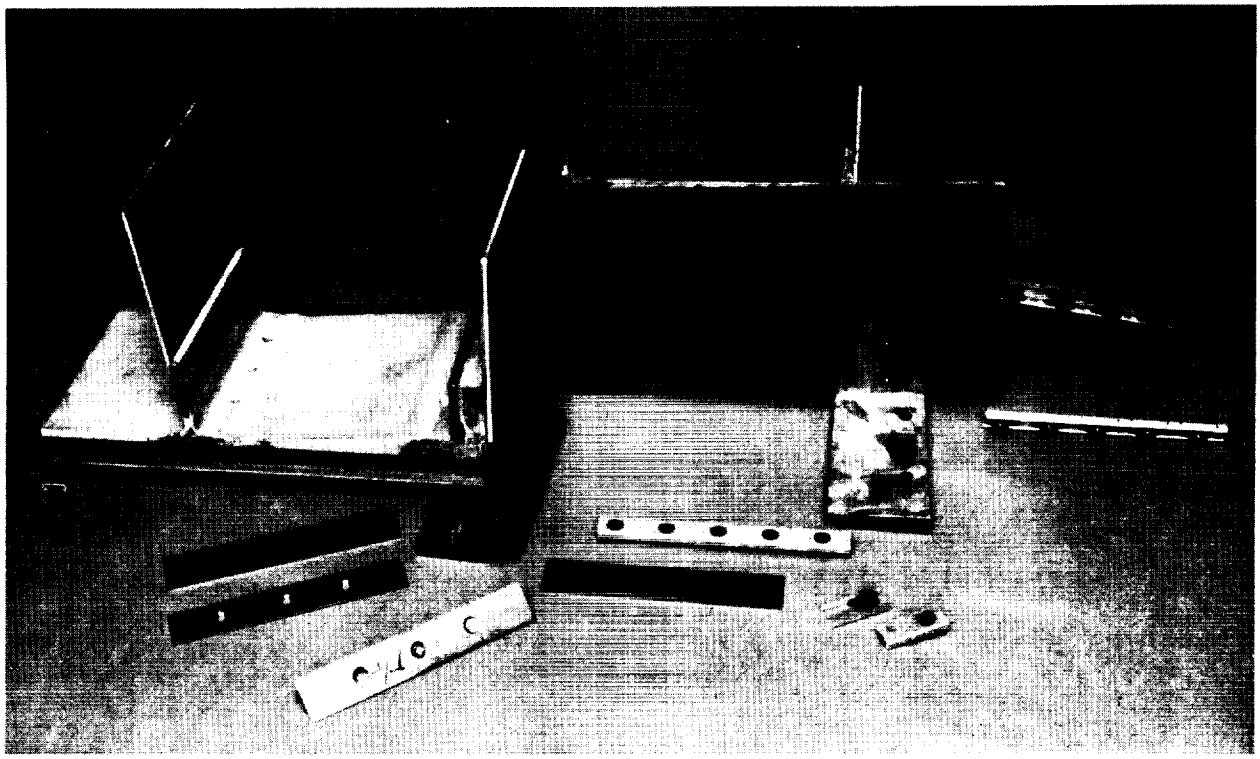

FIGURE 146. MODIFIED JOINT DESIGN SHOWING ASSEMBLY AND DETAILED PARTS

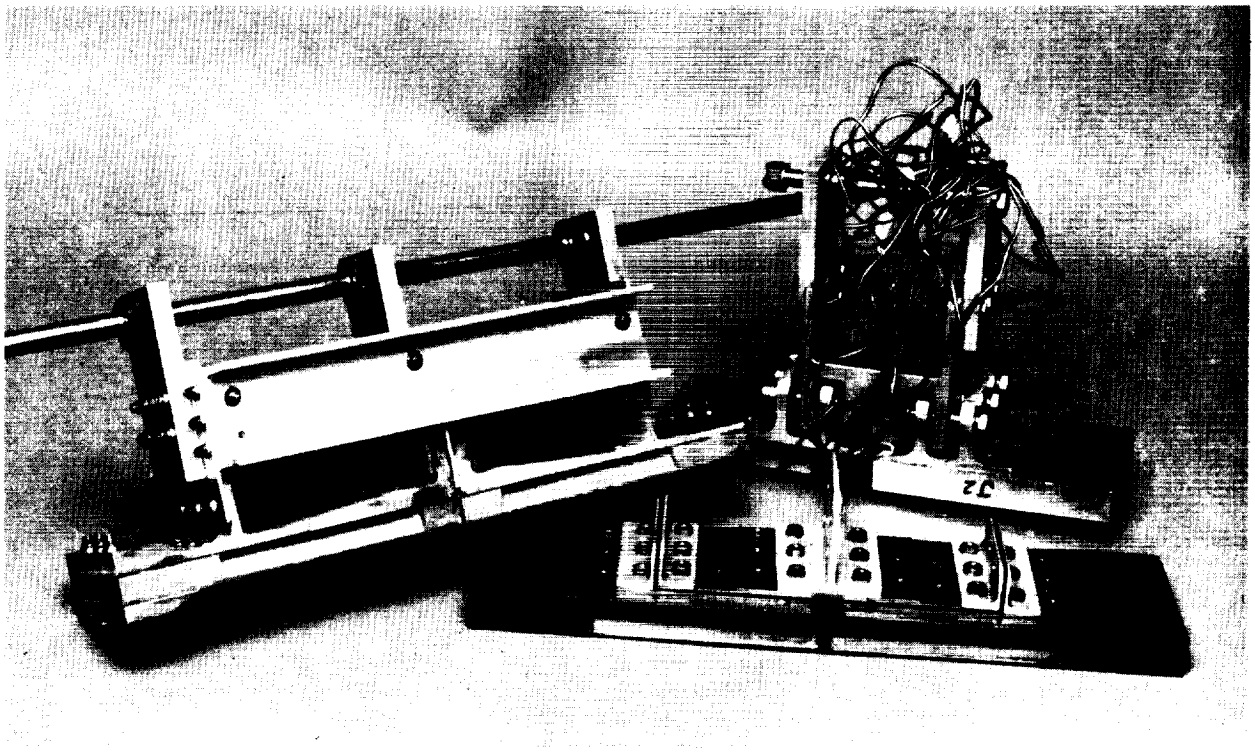

FIGURE 147. MODIFIED JOINT ON THE LEFT, THREE-RIB JOINT IN FOREGROUND, AND SLIDING JOINT IN BACKGROUND

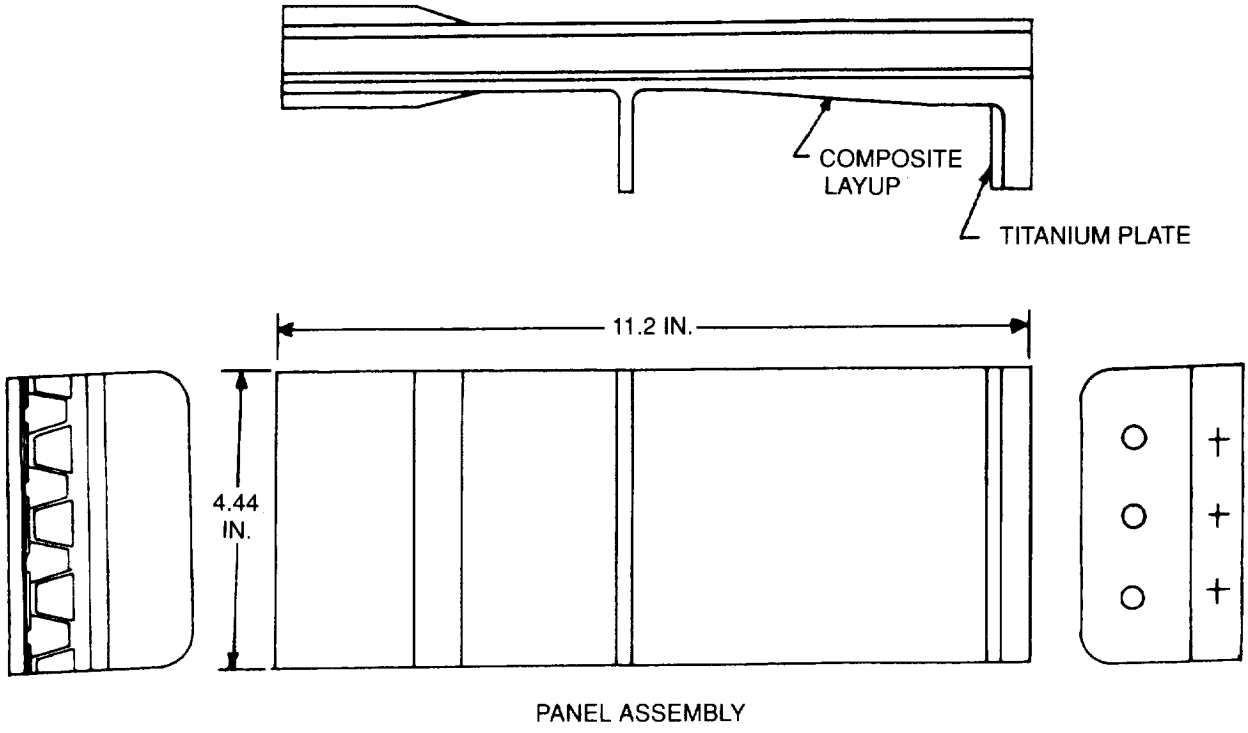

FIGURE 148. MODIFIED THREE-RIB JOINT TEST SPECIMEN

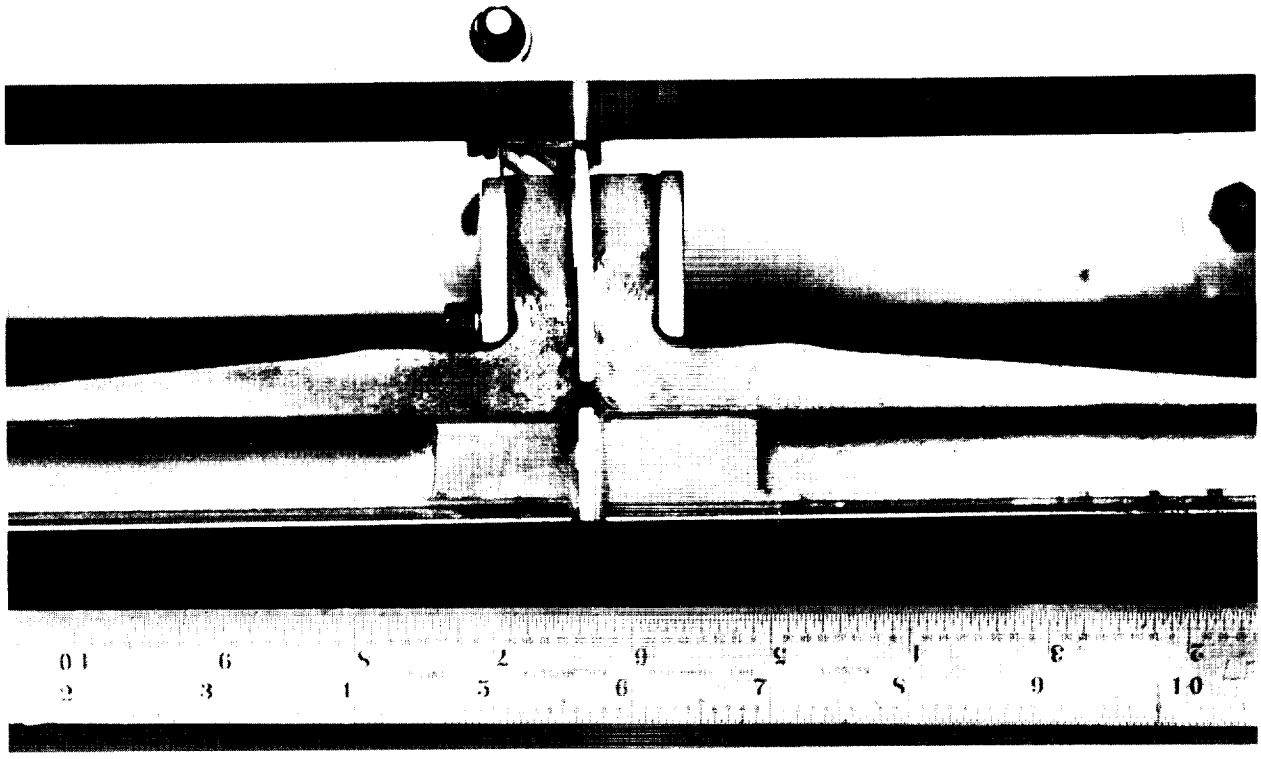

FIGURE 149. CLOSE-UP OF MODIFIED JOINT ASSEMBLY

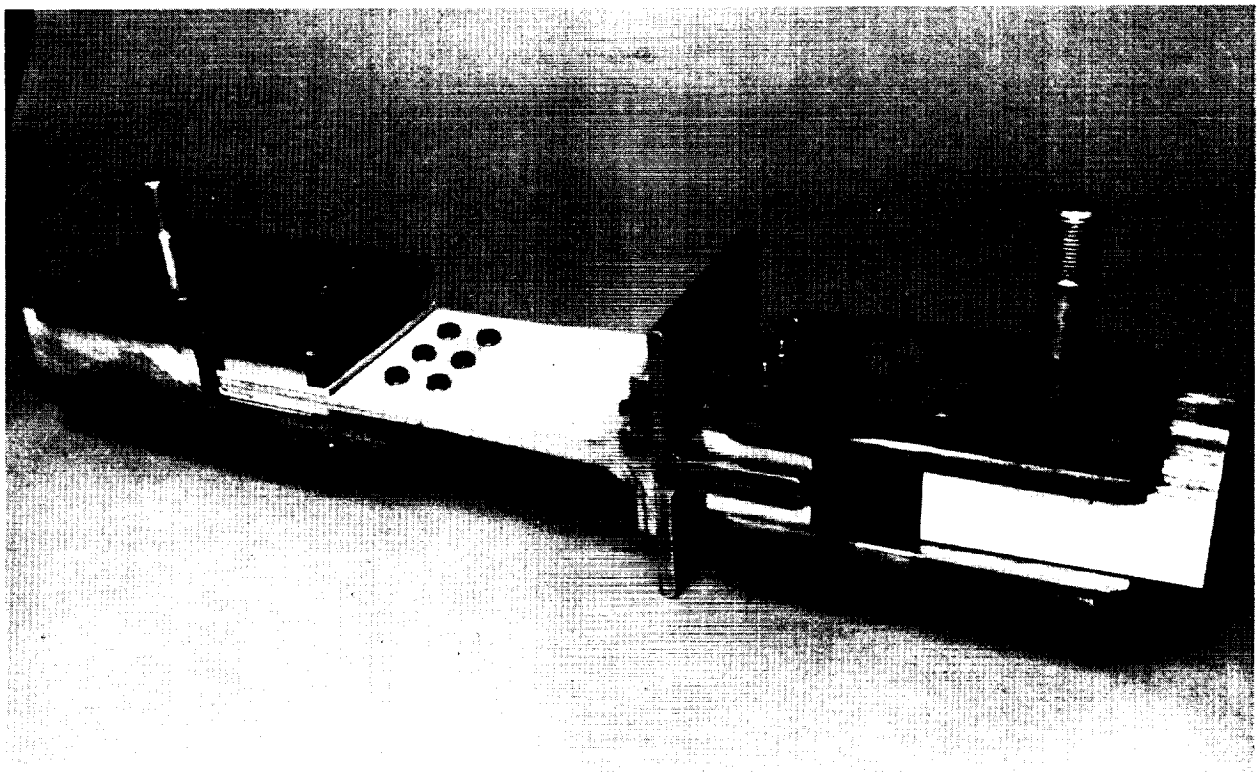

FIGURE 150. SIDE VIEW OF FLANGED COMPOSITE LAY-UP READY FOR TENSION TEST

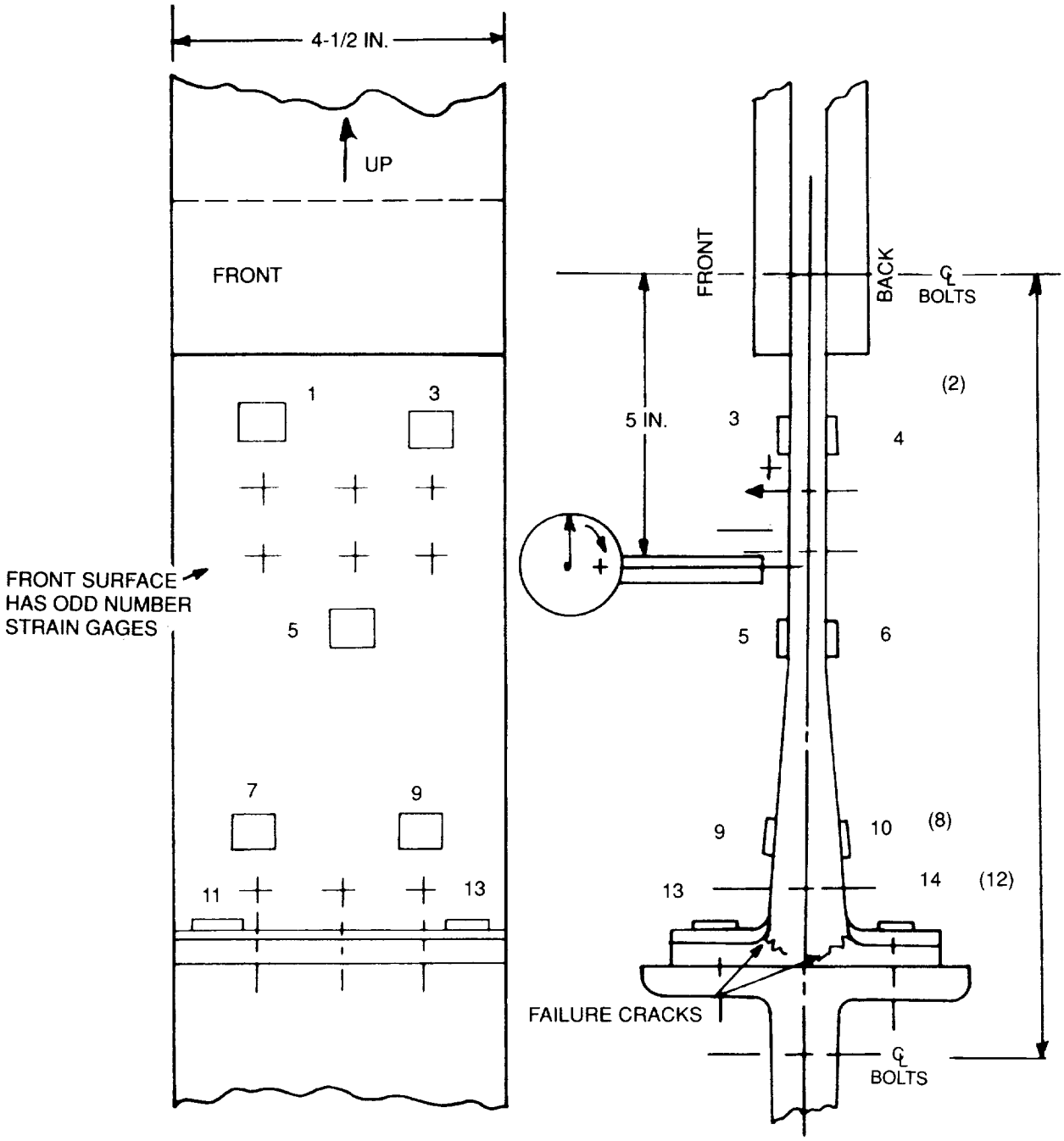

FIGURE 151. COMPOSITE FLANGED JOINT GAGE LOCATIONS

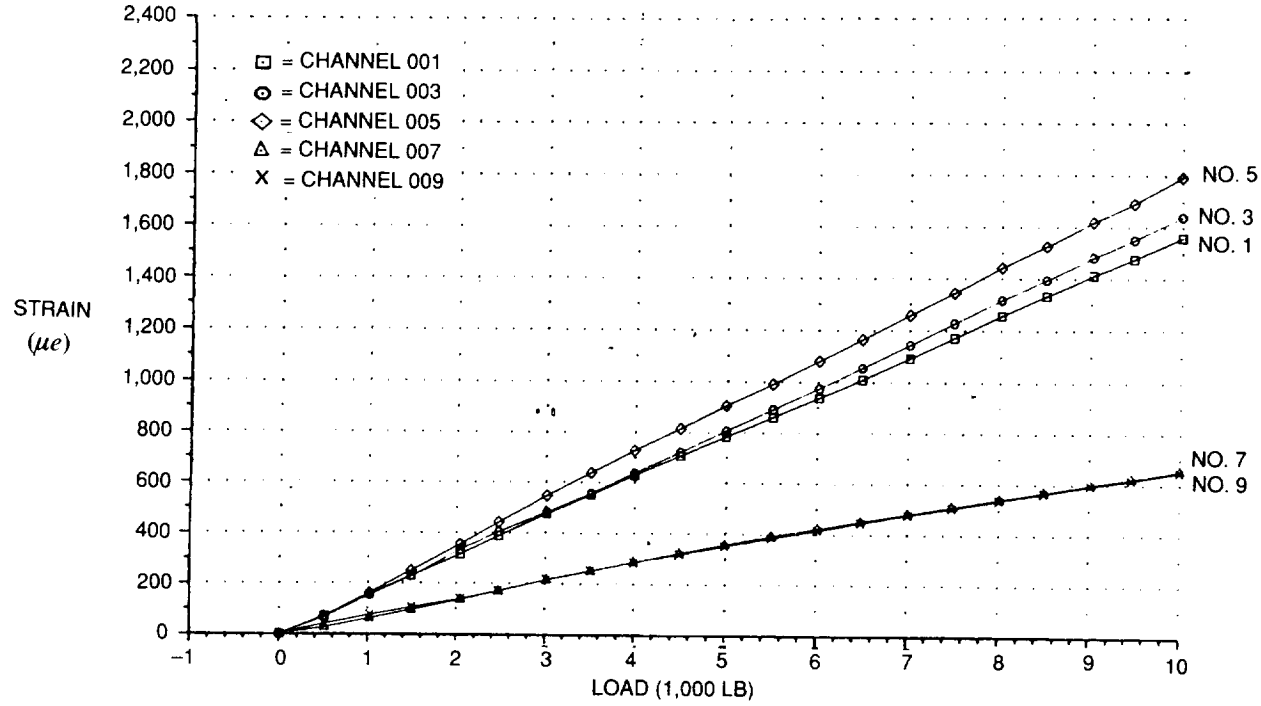

FIGURE 152. COMPOSITE FLANGE TENSION TEST AT ROOM TEMPERATURE — STRAIN GAGE READINGS

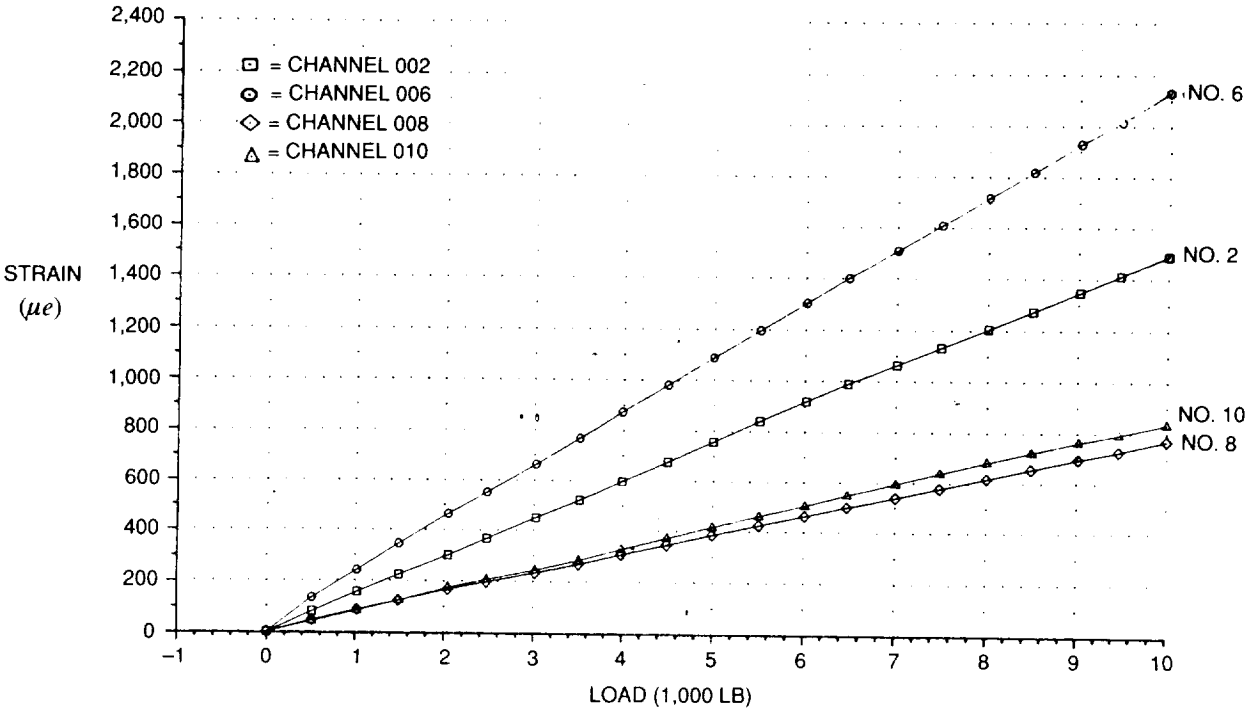

FIGURE 153. COMPOSITE FLANGE TENSION TEST AT ROOM TEMPERATURE — STRAIN GAGE READINGS

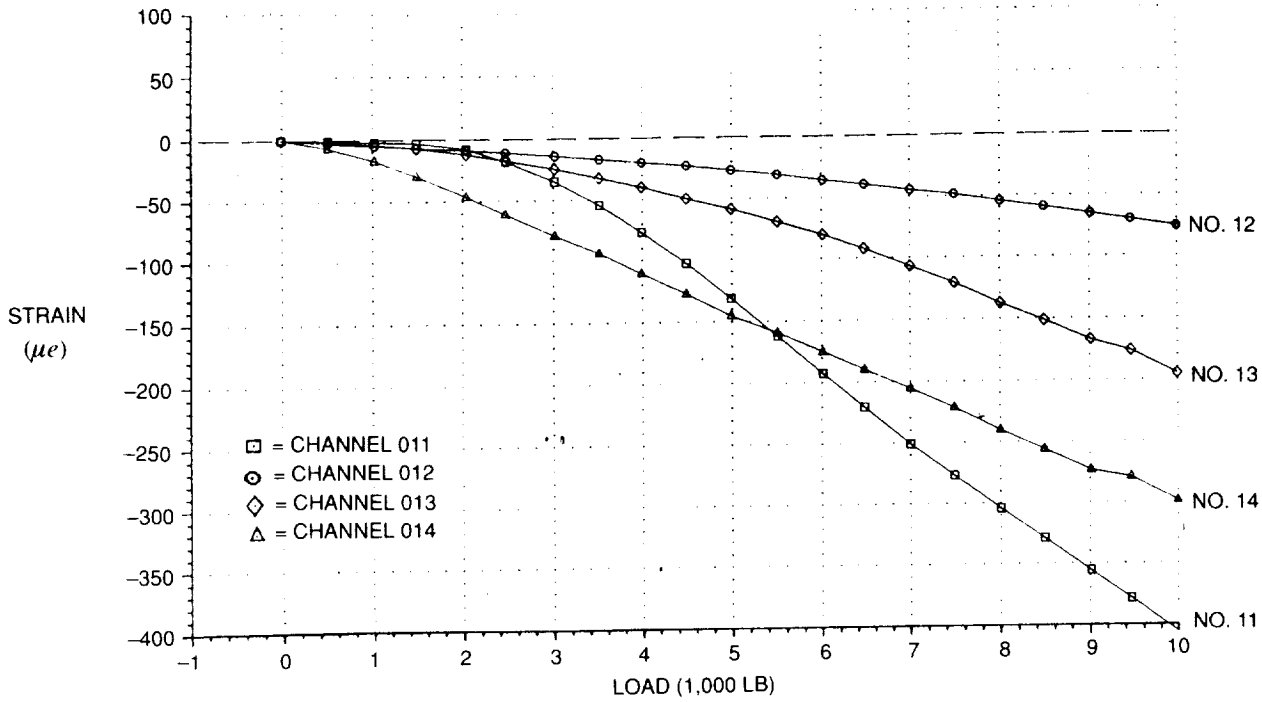

FIGURE 154. COMPOSITE FLANGE TENSION TEST AT ROOM TEMPERATURE — STRAIN GAGE READINGS

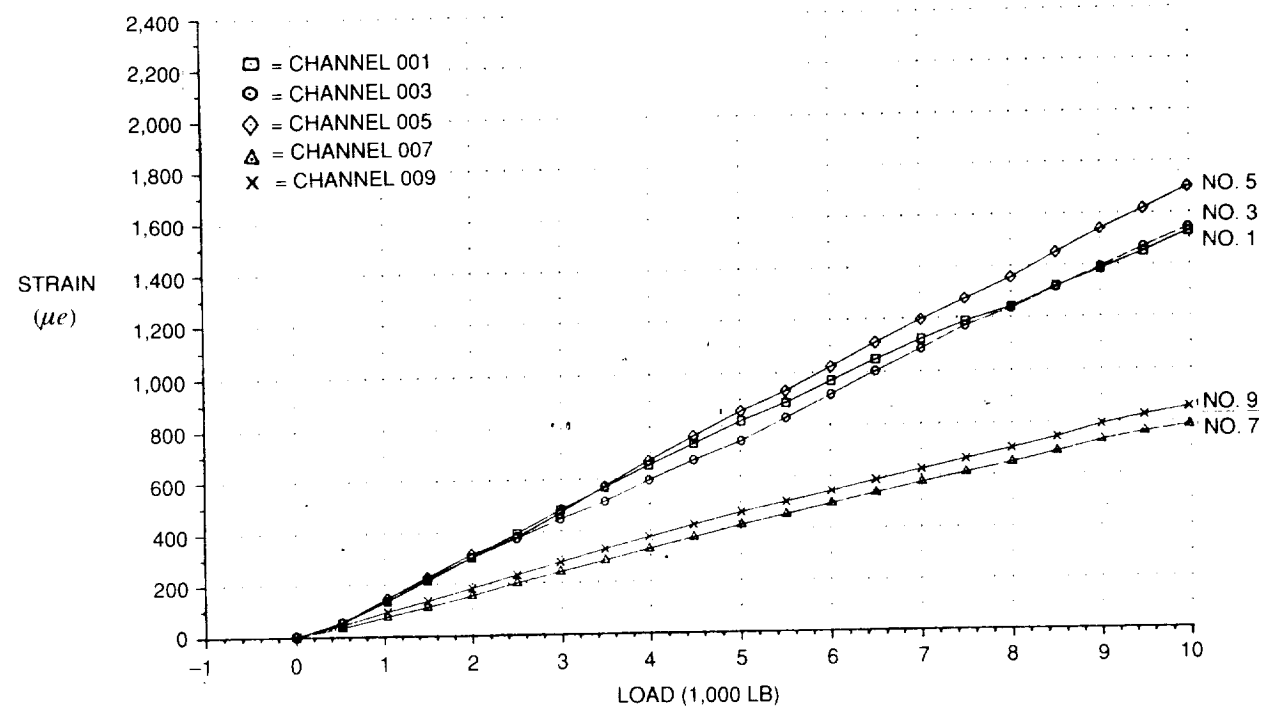

FIGURE 155. COMPOSITE FLANGE TENSION TEST AT –65°F — STRAIN GAGE READINGS

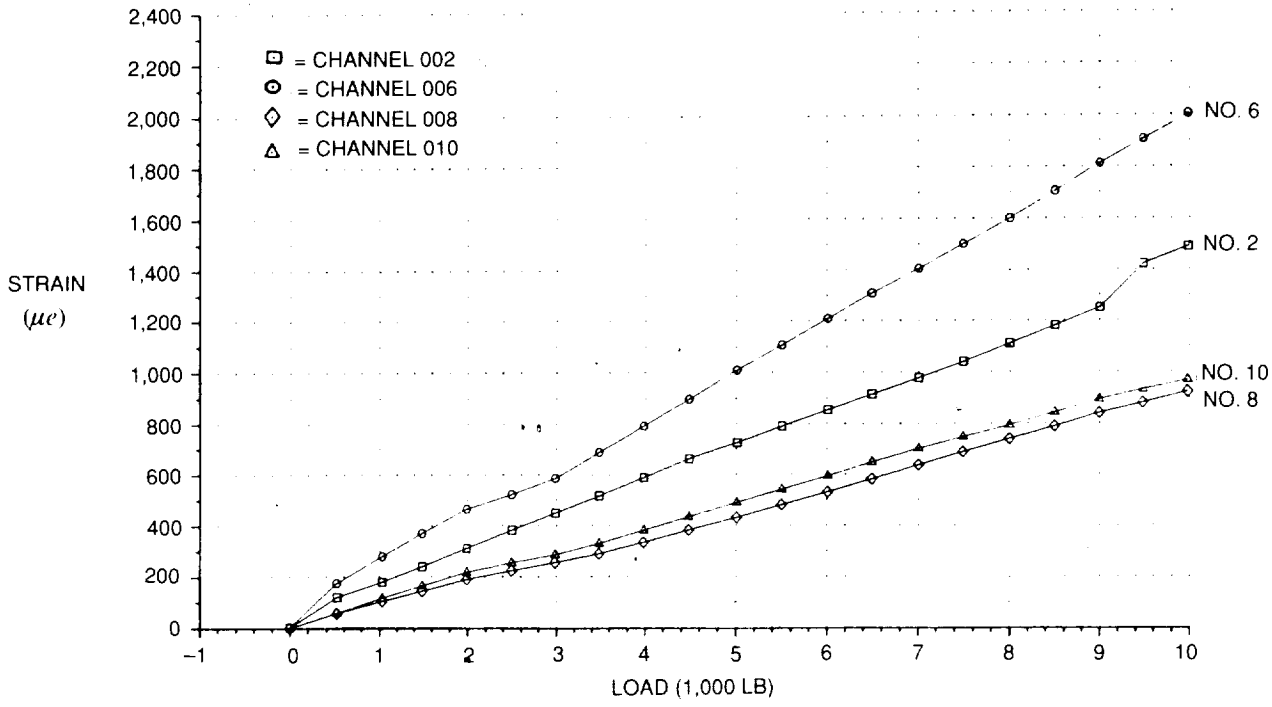

FIGURE 156. COMPOSITE FLANGE TENSION TEST AT –65°F — STRAIN GAGE READINGS

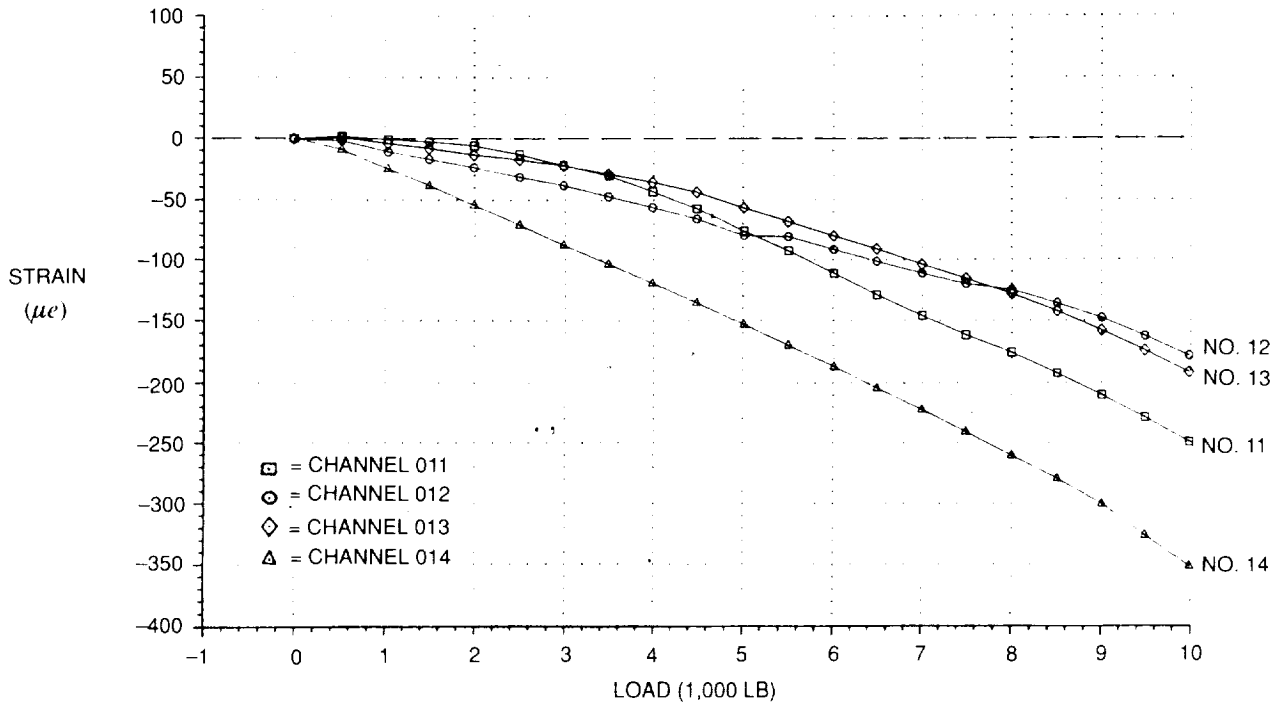

FIGURE 157. COMPOSITE FLANGE TENSION TEST AT –65°F — STRAIN GAGE READINGS

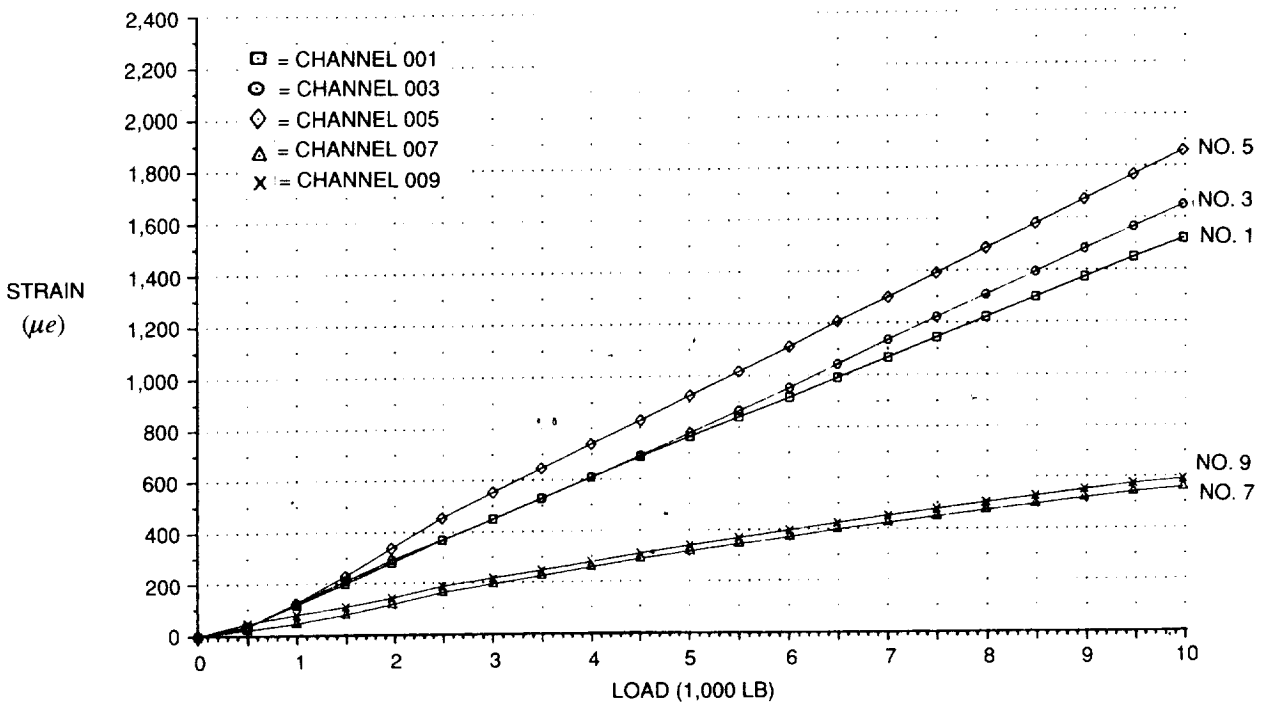

FIGURE 158. COMPOSITE FLANGE TENSION TEST AT 160°F — STRAIN GAGE READINGS

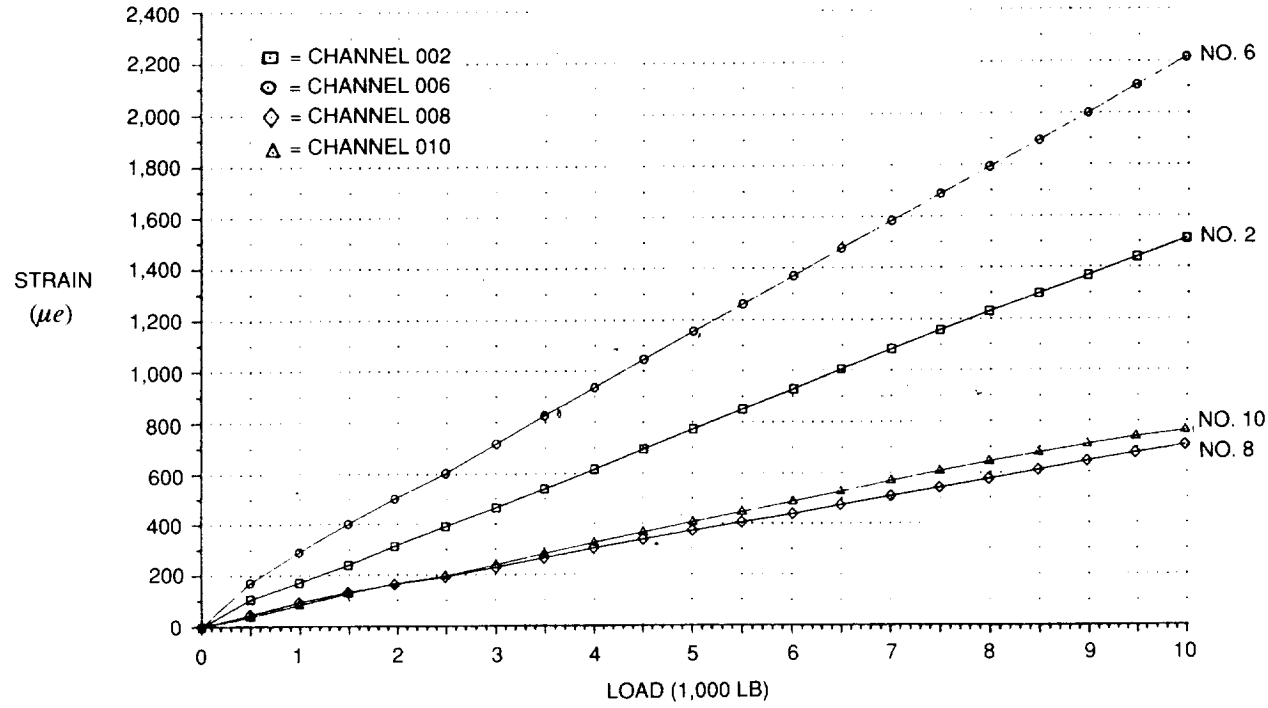

FIGURE 159. COMPOSITE FLANGE TENSION TEST AT 160°F — STRAIN GAGE READINGS

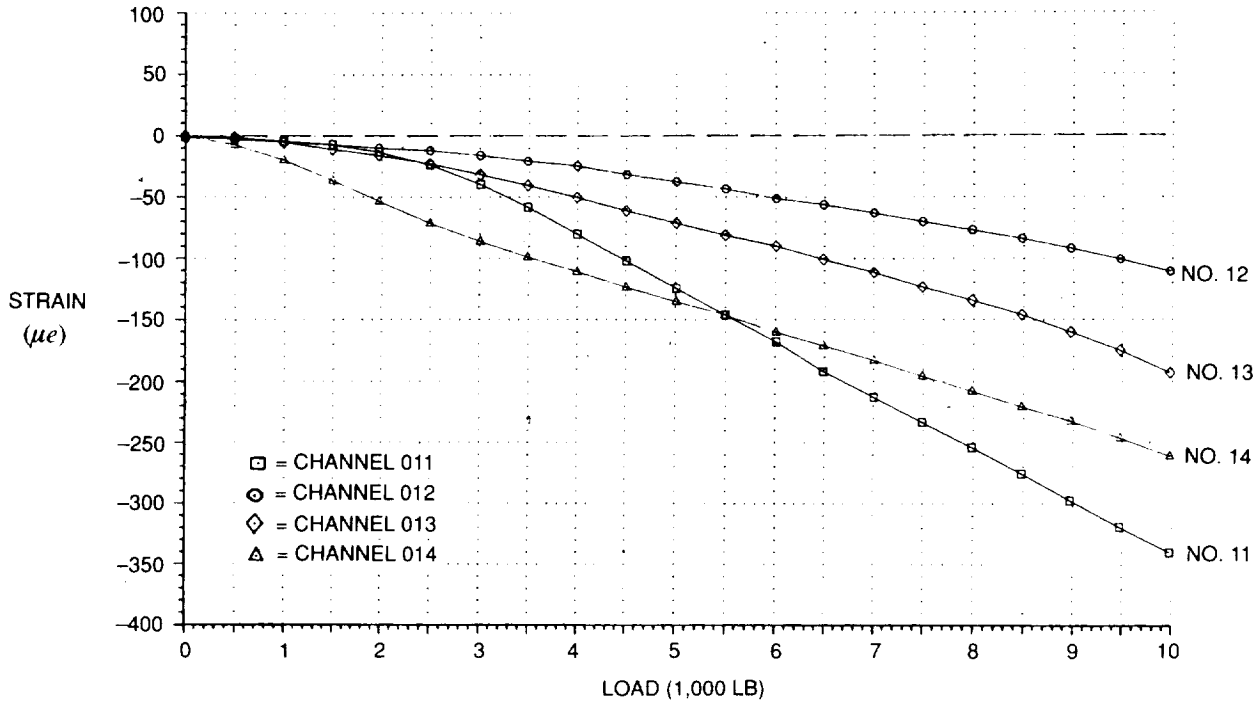

FIGURE 160. COMPOSITE FLANGE TENSION TEST AT 160°F — STRAIN GAGE READINGS

ORIGINAL PAGE
BLACK AND WHITE PHOTOGRAPH

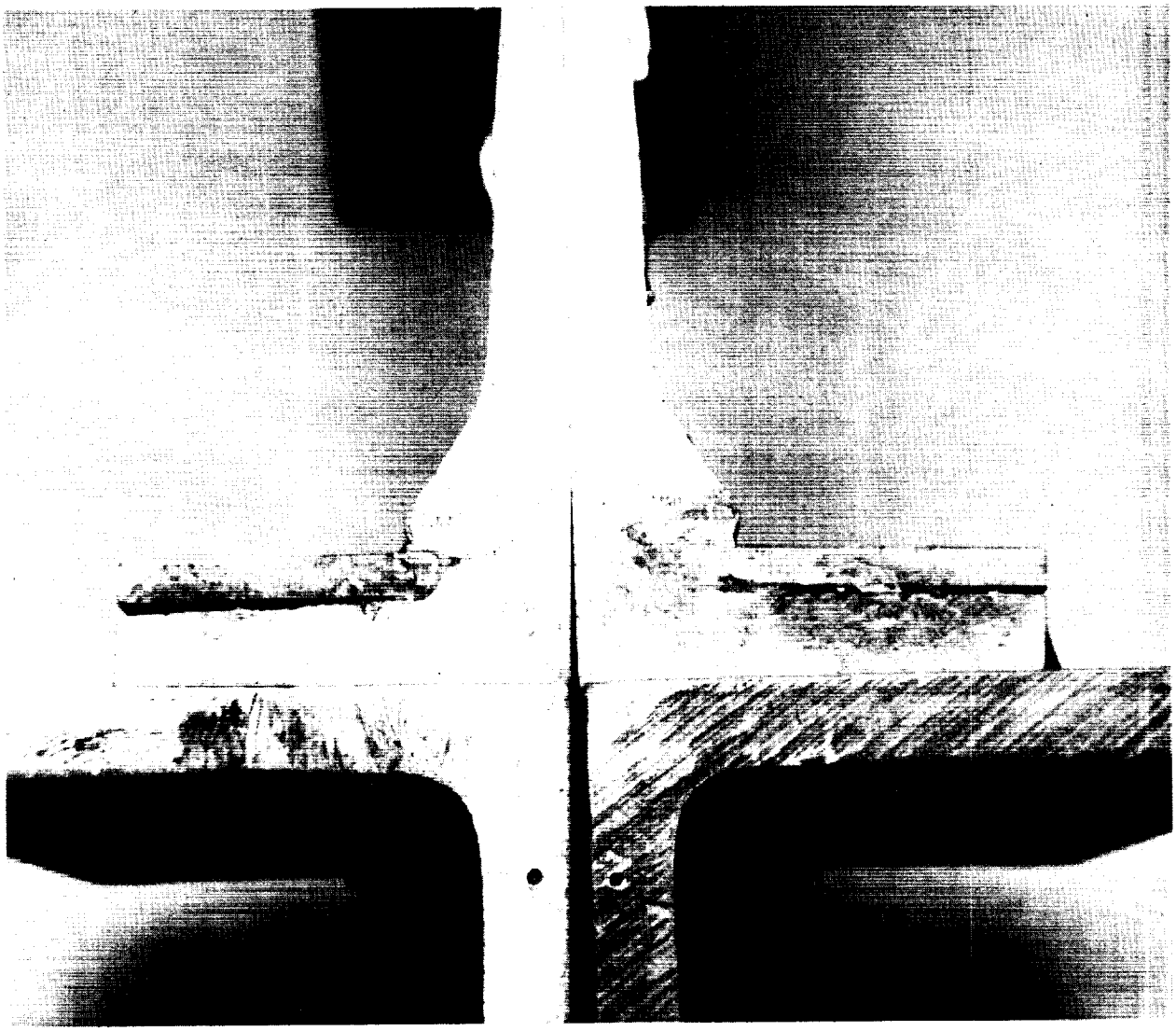

FIGURE 161. CLOSE-UP OF FLANGED JOINT FAILURE

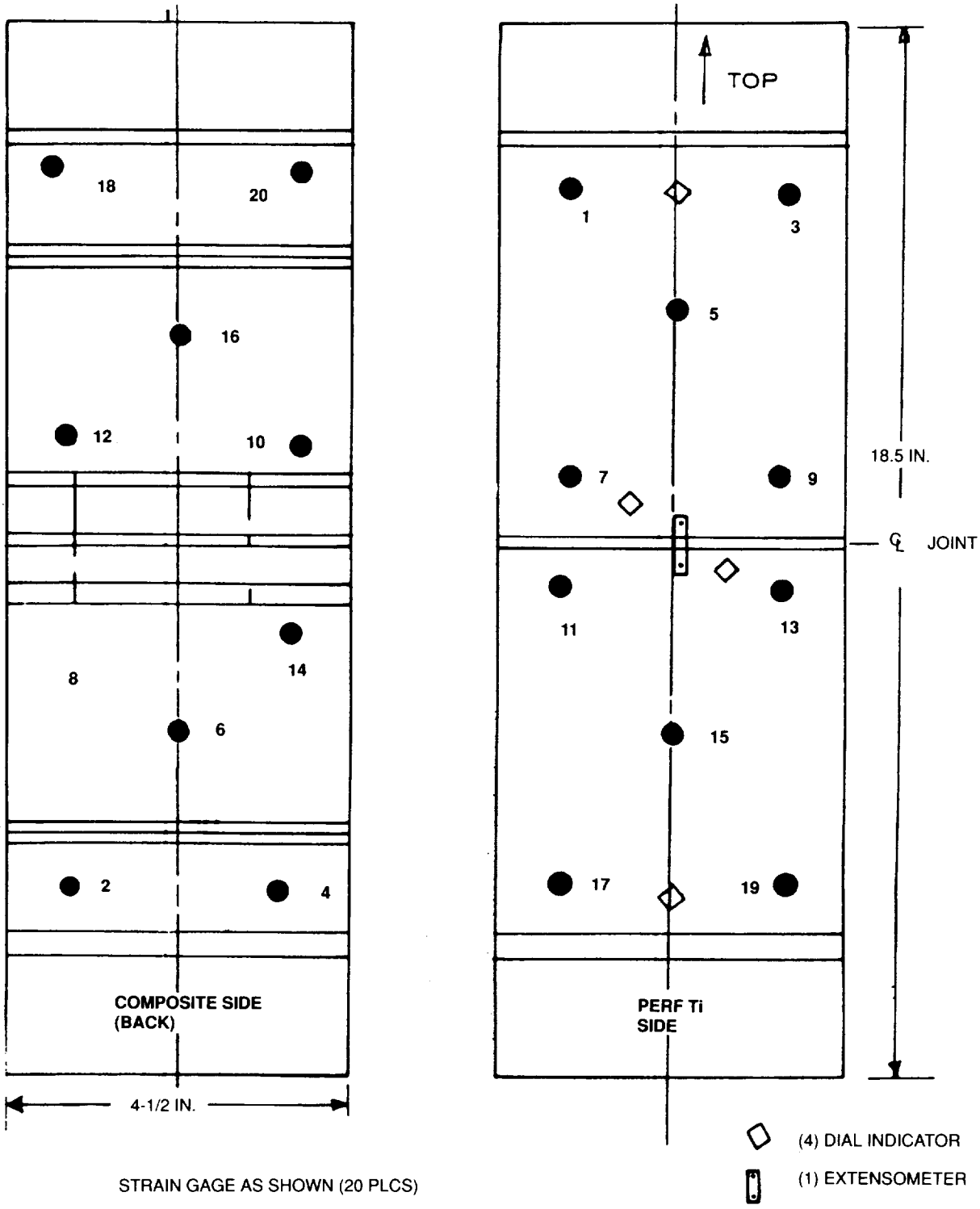

- ODD NUMBERS ON PERFORATED TITANIUM SIDE (FRONT)
- EVEN NUMBERS ON BACK SIDE (EVEN OPPOSITE ODD)

FIGURE 162. STRAIN, DIAL, AND EXTENSOMETER LOCATIONS FOR THE MODIFIED JOINT PANEL

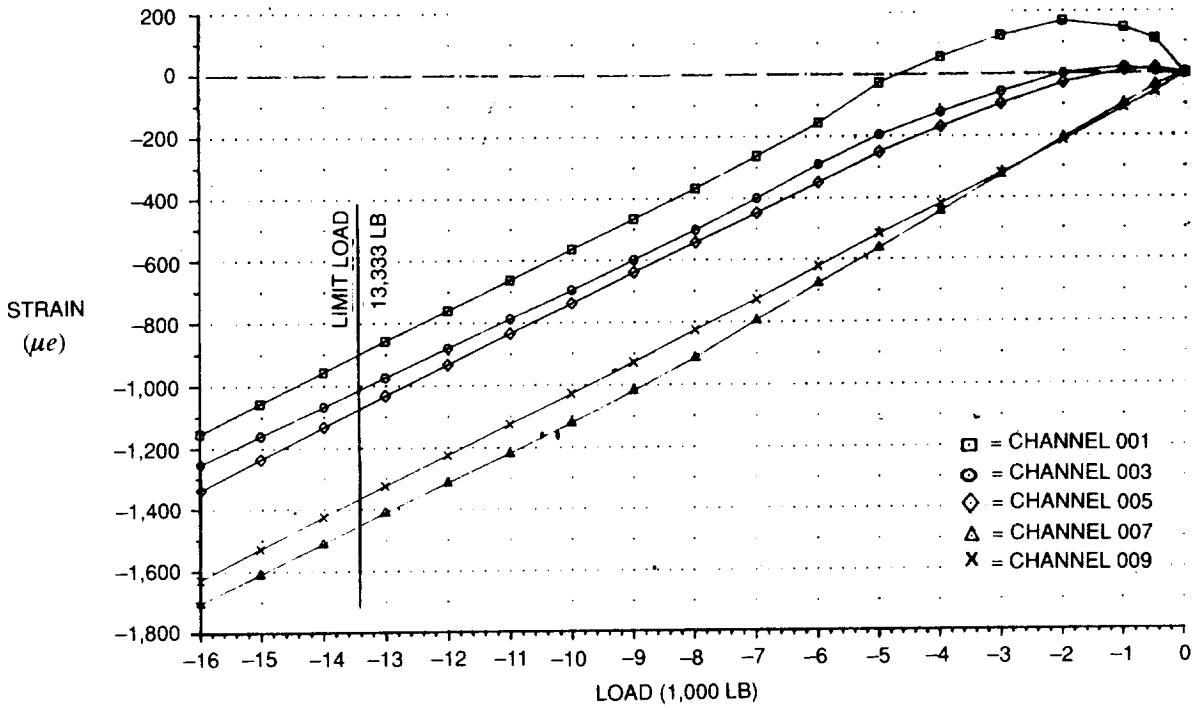

FIGURE 163. MODIFIED JOINT COMPRESSION STRAIN GAGE READINGS

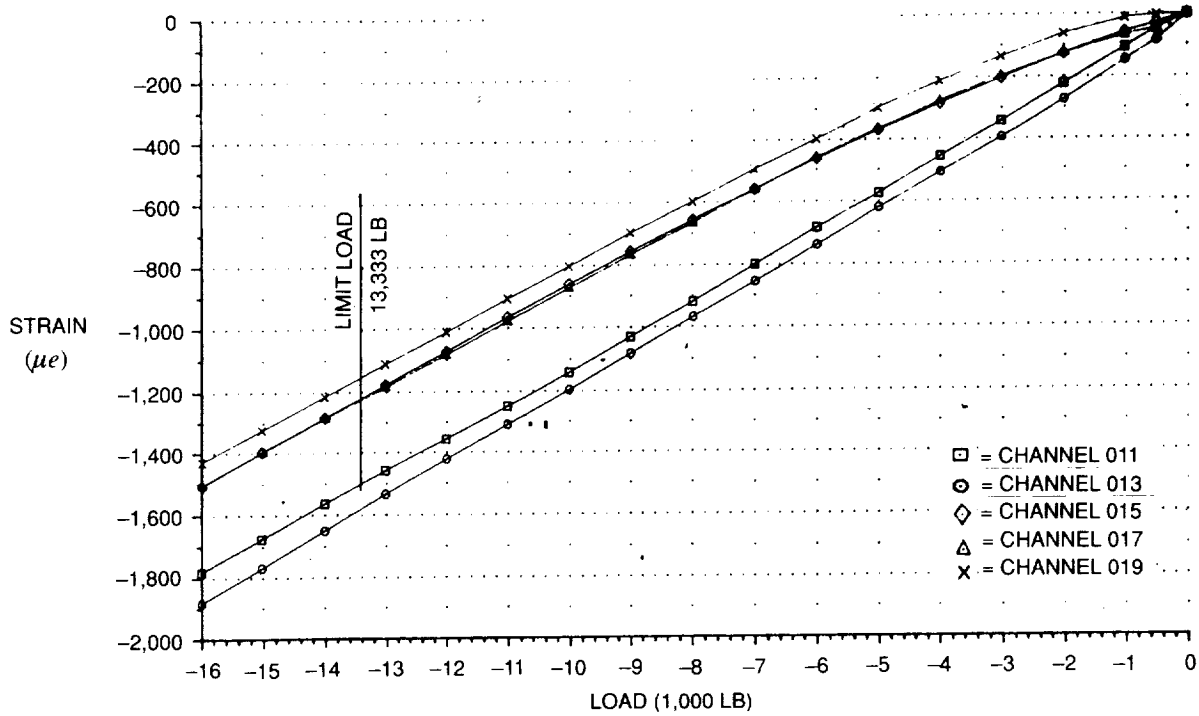

FIGURE 164. MODIFIED JOINT COMPRESSION TEST AT ROOM TEMPERATURE — STRAIN GAGE READINGS

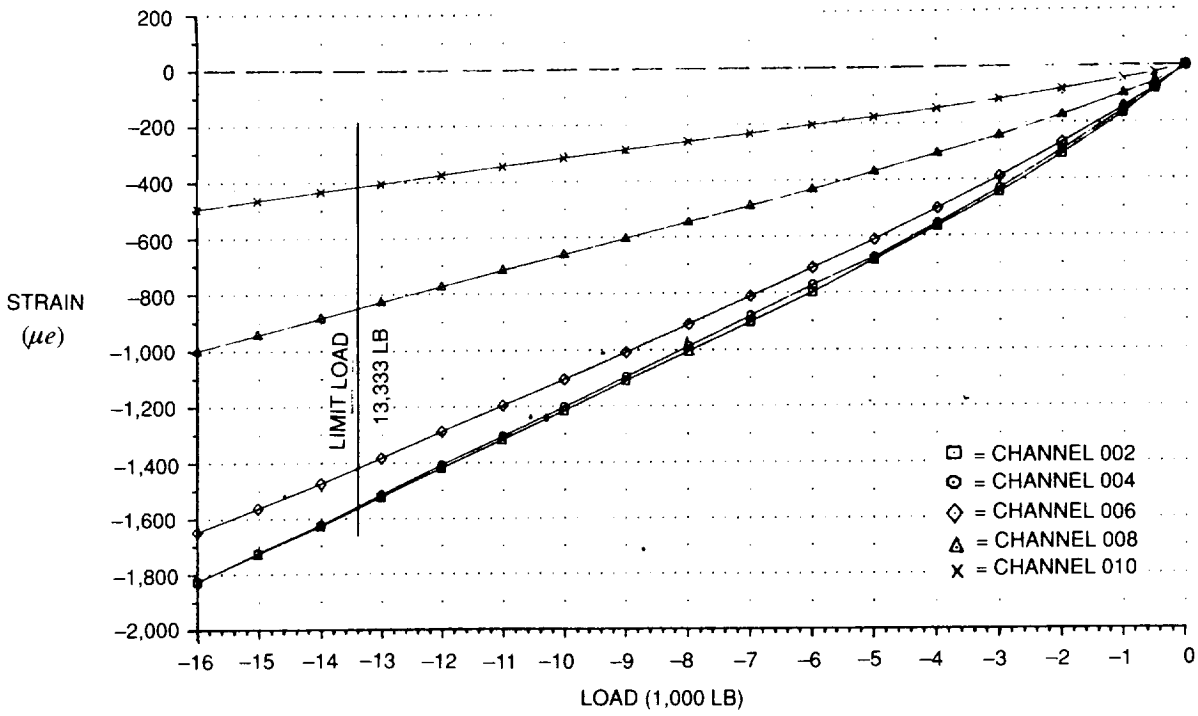

FIGURE 165. MODIFIED JOINT COMPRESSION TEST AT ROOM TEMPERATURE — STRAIN GAGE READINGS

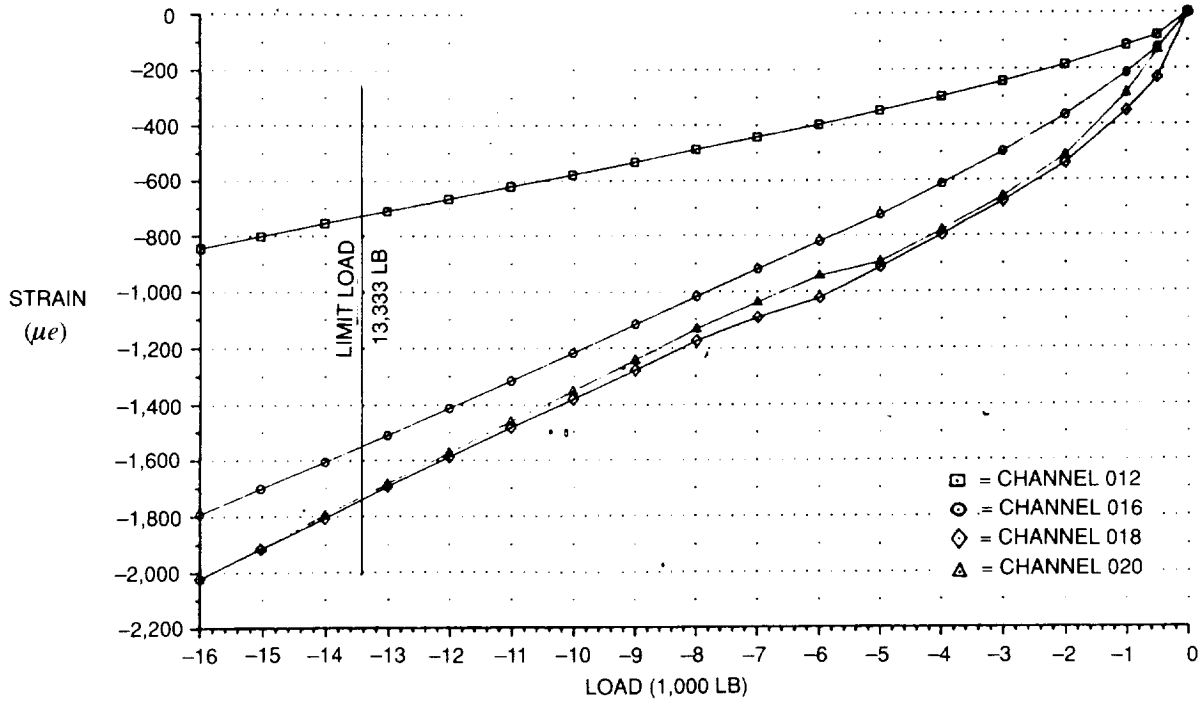

FIGURE 166. MODIFIED JOINT COMPRESSION TEST AT ROOM TEMPERATURE — STRAIN GAGE READINGS

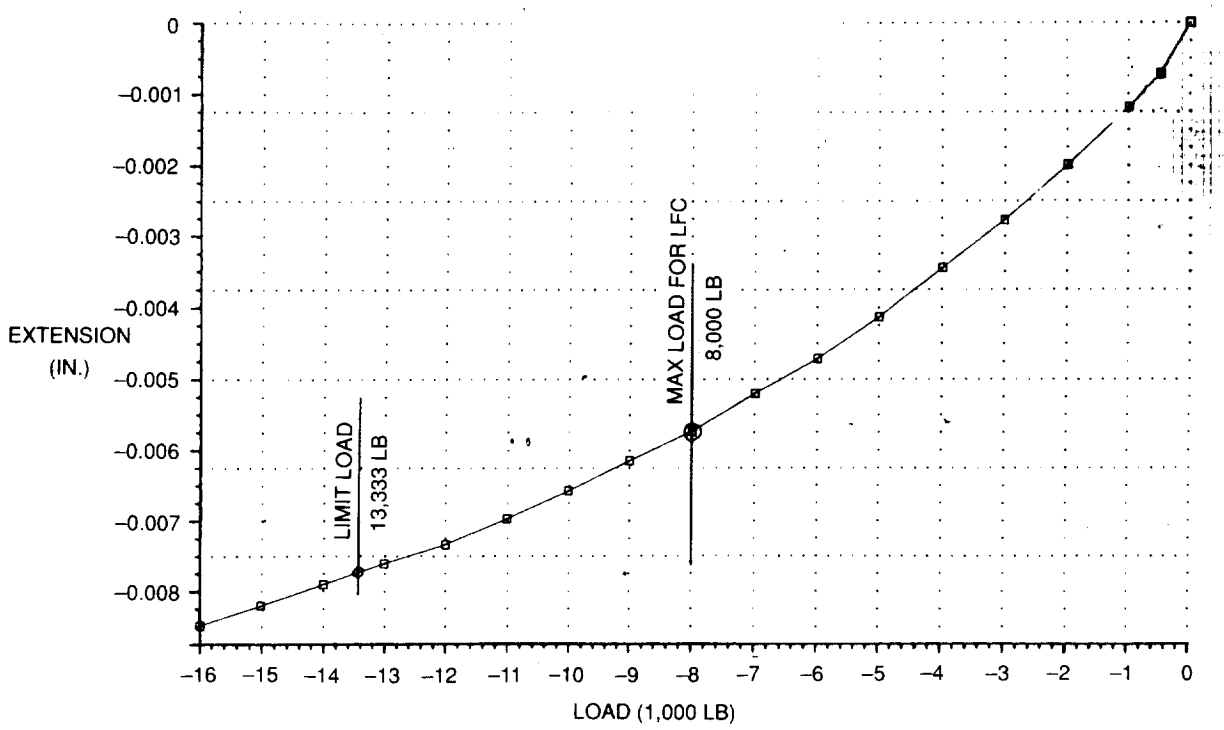

FIGURE 167. MODIFIED JOINT COMPRESSION TEST AT ROOM TEMPERATURE — EXTENSOMETER READINGS

LOAD (1,000 LB)	UPPER	CTR UPPER	CTR LOWER	LOWER
0	0	0	0	0
0.5	−0.0010	−0.00	+0.0001	−0.0010
1	+0.0018	−0.00	+0.0001	−0.0023
2	+0.0038	−0.00	+0.0004	−0.0032
3	+0.0040	+0.0001	+0.0003	−0.0040
4	+0.0048	+0.0001	+0.0003	−0.0035
5	+0.0052	+0.0004	+0.0004	−0.0030
6	+0.0052	+0.0005	+0.0003	−0.0020
7	+0.0050	+0.0005	+0.0003	−0.0020
8	+0.0050	+0.0005	+0.0003	+0.0010
9	+0.0048	+0.0006	+0.0003	+0.0004
10	+0.0042	+0.0006	+0.0003	+0.0002
11	+0.0042	+0.0005	+0.0003	+0.0012
12	+0.0047	+0.0015	+0.0024	+0.0020
13	+0.0035	+0.0015	+0.0023	+0.0030
14	+0.0035	+0.0025	+0.0024	+0.0040
0	−0.0017	−0.0018	−0.0007	−0.0031

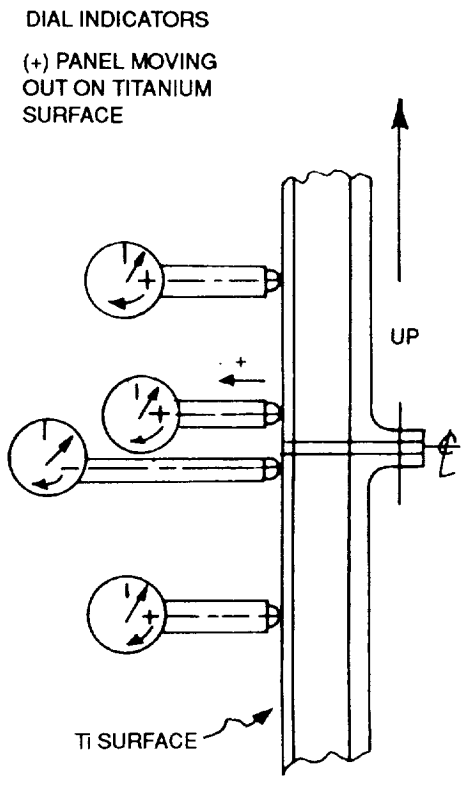

FIGURE 168. DIAL GAGE READINGS FOR MODIFIED JOINT PANEL IN COMPRESSION AT −65°F

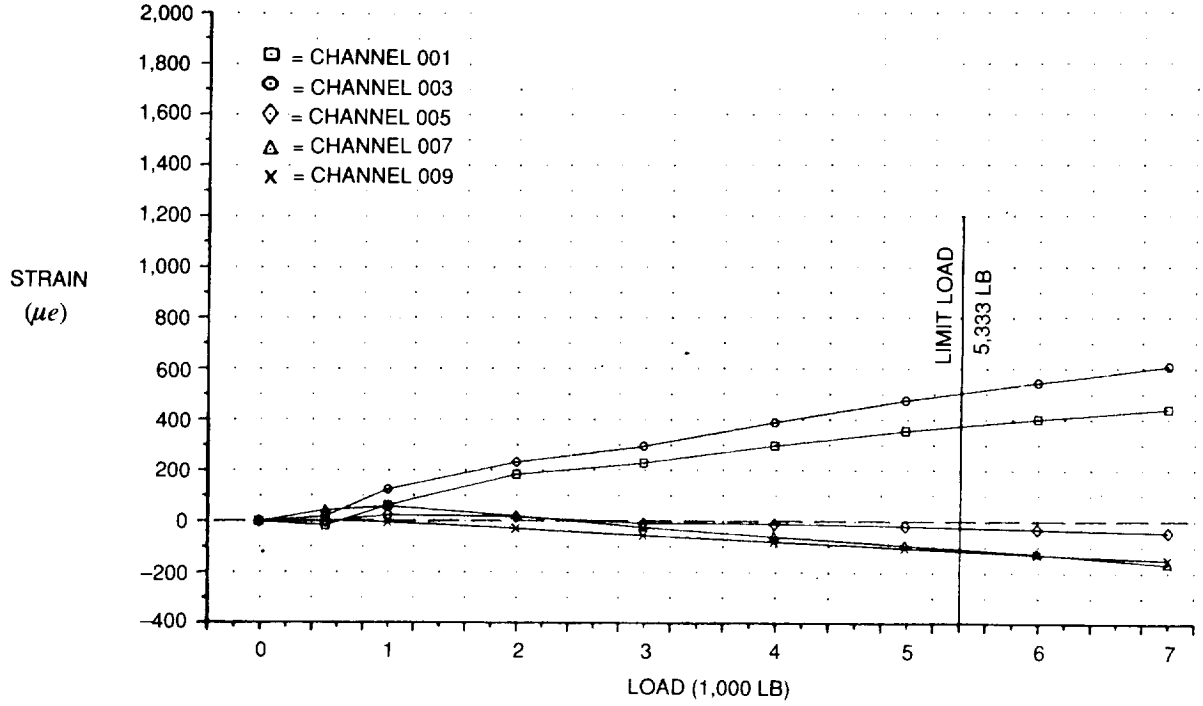

FIGURE 169. MODIFIED JOINT TENSION TEST AT ROOM TEMPERATURE — STRAIN GAGE READINGS

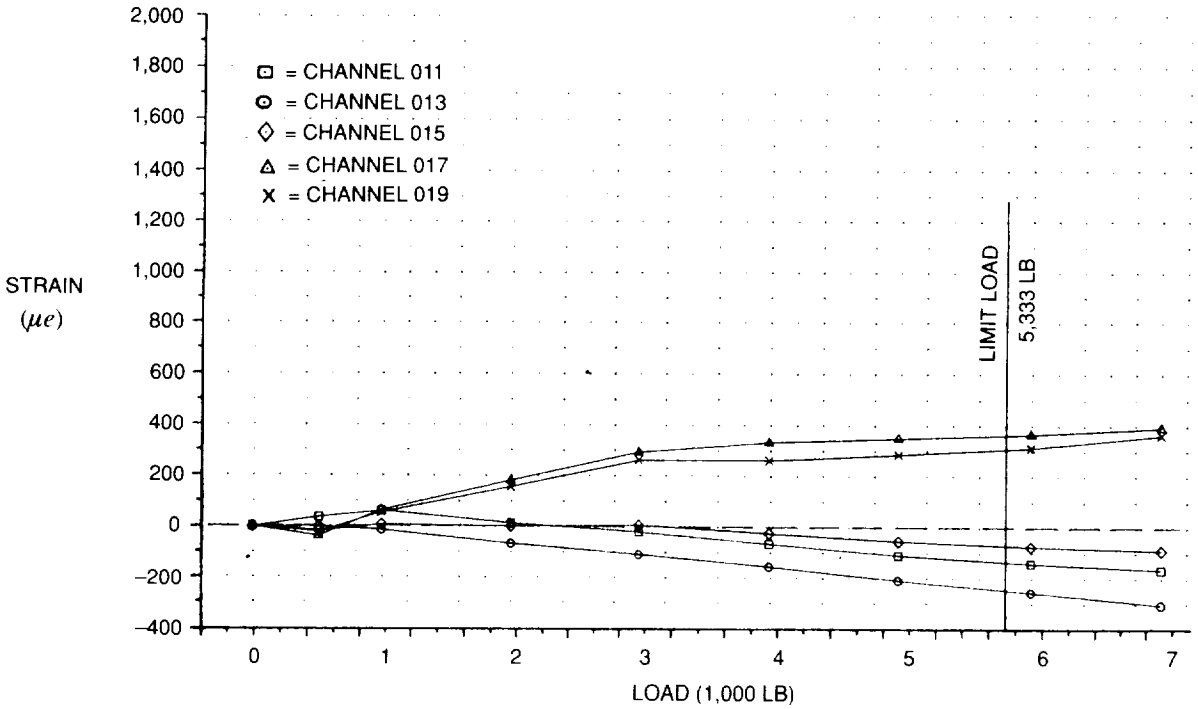

FIGURE 170. MODIFIED JOINT TENSION TEST AT ROOM TEMPERATURE — STRAIN GAGE READINGS

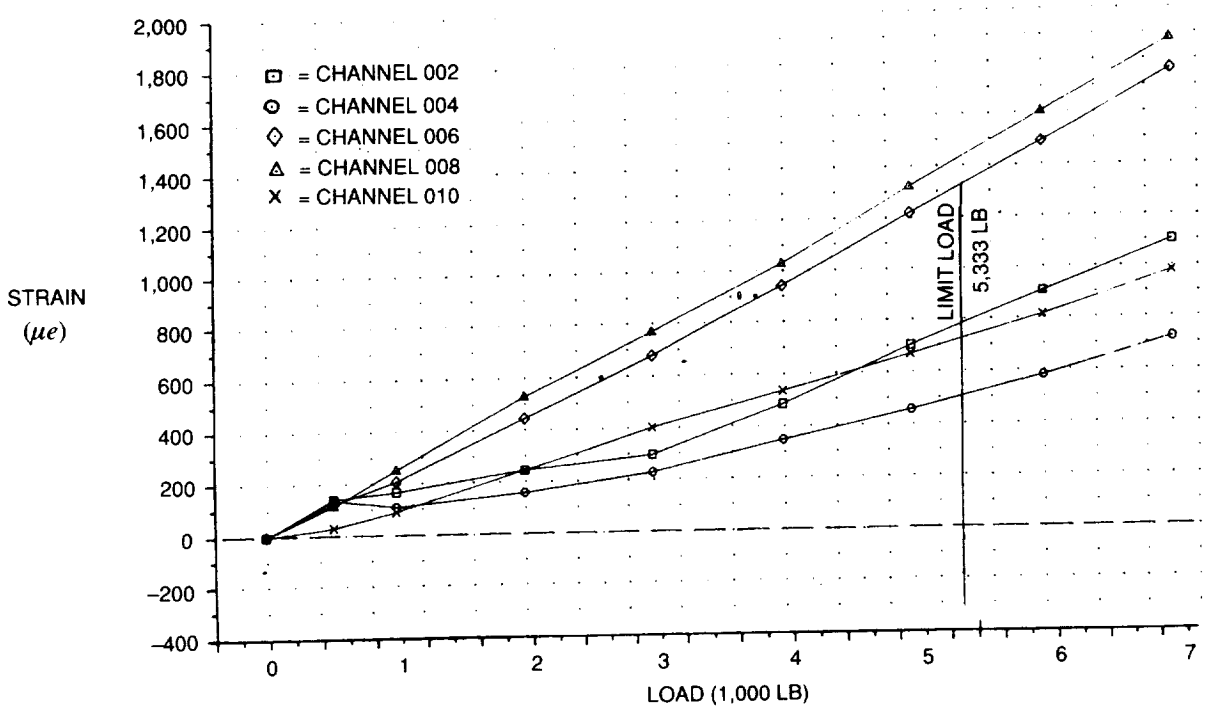

FIGURE 171. MODIFIED JOINT TENSION TEST AT ROOM TEMPERATURE — STRAIN GAGE READINGS

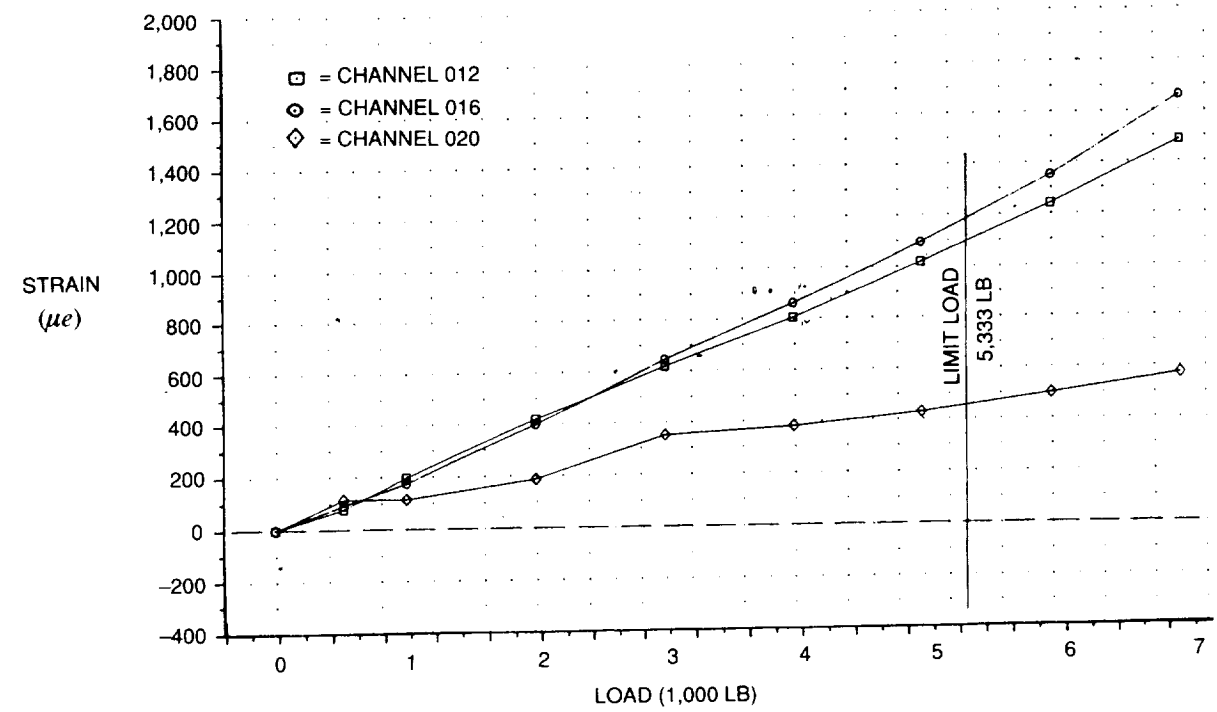

FIGURE 172. MODIFIED JOINT TENSION TEST AT ROOM TEMPERATURE — STRAIN GAGE READINGS

LOAD (1,000 LB)	UPPER	CTR UPPER	CTR LOWER	LOWER
0	0	0	0	0
0.5	+0.0052	+0.0008	–0.0019	–0.0061
1	+0.0052	+0.0010	–0.0024	–0.0082
2	+0.0043	+0.0028	–0.0044	–0.0120
3	+0.0025	+0.0045	–0.0050	–0.011
4	–0.0010	+0.0066	–0.0042	–0.0130
5	–0.0025	+0.0082	–0.0056	–0.0170
6	–0.0048	–0.0004	–0.0042	–0.0200
7	–0.0070	+0.0016	–0.0061	–0.0024
0	+0.0082	+0.0022	–0.0057	+0.0060

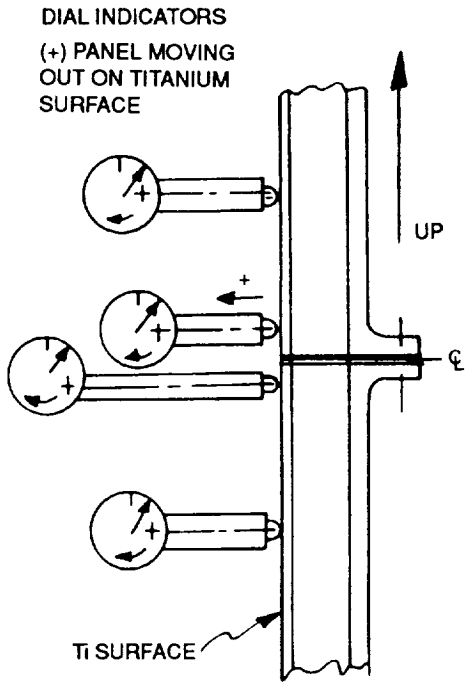

FIGURE 173. DIAL GAGE READINGS FOR MODIFIED JOINT PANEL IN TENSION AT ROOM TEMPERATURE

This page intentionally left blank

TABLE 1
PANELS FABRICATED AND TESTED

PANEL	LENGTH (IN.)	WIDTH (IN.)	THICKNESS (IN.)
SMALL SLIDING JOINT	14.0	4.5	0.88
THREE-RIB WITH TITANIUM DOUBLERS	18.0	4.5	1.1
HYBRID PANEL – BACK-TO-BACK FIBERGLASS WITH FLANGES	10.5	4.5	0.5
THREE-RIB WITH FIBERGLASS TAPERED DOUBLER – MODIFIED JOINT PANEL	18.0	4.5	1.0
LARGE SLIDING JOINT	30.0	23.0	0.88

TABLE 2
JOINT CONCEPTS

ADVANTAGES	DISADVANTAGES
Joint Concept 1 — Sliding 1. Ease of assembly — Joining and aligning of joint is accomplished by inserting pin 2. Ease of attachment to ribs — Rivet on assembly 3. Aluminum fittings are easy to machine 4. Fitting balances out the eccentric movement	1. Panels slide axially from tension and compression loads. Panel edge loads shear into front spar cap. Analyses must be done to ensure spar caps, ribs, and attachments are adequate. 2. The sliding fittings are heavy. 3. Test panels must be long enough to represent the load transfer from a typical leading edge section to the front spar. 4. Pin bending might occur from foreign object damage, making it difficult to remove and replace. 5. End of panels require a plate and additional filler in flutes to avoid crushing the composite walls from high-compression end loads. 6. If damage occurs, the fittings might not always slide. Any misalignment would increase friction.
Joint Concept 2 — Three-Rib Concept 1. Simple plates, ribs and attachments 2. Eccentric axial moments sustained by ribs	1. Panels are aligned by bonding plates to panel inner surface to maintain standard panel thickness at ends of panel. 2. Joining requires many attachments, which must be installed through the inner face of the panel and secured by gang channels. 3. Difficult to put in gang channels and line up attachments. 4. Difficult to replace damaged nut plates and gang channels in the field. 5. Difficult to replace damaged panels because wing loading condition is different from original assembly condition. Must duplicate original assembly condition to remove any replacement panels and align attachment holes. 6. Eccentric moment causes additional bending stresses in the bonded and splice plates and attachments.
Joint Concept 3 — Two-Rib Concept 1. Simple plates, ribs, and a machined fitting 2. Eccentric axial moments sustained by ribs and splice beam	1-6. Same as Concept 2. 7. Required moment of inertia to maintain sufficiently small deflections might result in an excessively large splice beam.
Joint Concept 4 — Expansion Concept 1. Contact plate and attach angles are easy to assemble to the metal plate bonded to the panel 2. Fasteners through inner face of panel and gang channels are eliminated	1. Same as Concept 2. 2. Tension loadings at the two attach tees must transfer to the ribs through attach tee stems. The thin stems might have high stresses in bending at the attachment, and delamination at corners might occur.
Joint Concept 5 — Blade Concept 1. Simple plates and extrusions used 2. Alignment of panels is accomplished by precision drilling and reaming of holes rather than by maintaining constant panel thickness 3. Eccentric axial moments sustained by ribs and splice beam	1. Assembly procedure is complicated. 5-6. Same as Concept 2. 7. Same as Concept 3.
Joint Concept 6 — Beam Concept 1. Splice plate beam can be machined easily and can be made stiff enough to sustain the panel bowing 2. Rib splicing can be larger than in Concept 2	1-6. From Concept 2. 7. Bowing of panel due to lack of end continuity stiffening may exceed desired deflection criteria. 8. Lack of middle rib may cause induced attachment bending more severe than Concept 2. 9. Tee attachment to ribs may be deficient.

The final product is an improved three-rib design that combines the best features of joint Concepts 1 and 2 without their disadvantages. In addition, the long bolts of Joint Concept 1 were improved by making back-to-back composite angles joined by much shorter bolts. This composite design was tested to ultimate load before being used as part of the improved three-rib design.

TABLE 3
READINGS OF FOUR REGULAR DIAL GAGES AT ROOM TEMPERATURE
LABORATORY TEST DATA COMPRESSION TEST — J3 LARGE SLIDING-JOINT PANELS

LOAD (1,000 LB)	UPPER	CENTER		LOWER
0	0	UPPER 0 LOWER		0
4	–0.001	0	–0.001	+0.0010
8				
12	–0.001	0	–0.0025	+0.0005
16				
20	0	0	–0.0030	+0.0007
24				
28	+0.0007	0	–0.0030	+0.0010
32				
36	+0.0010	0	–0.0030	+0.0020
40				
44	+0.0005	0	–0.0035	+0.0020
48	+0.0010	0	–0.0030	+0.0025
52	+0.0011	0	–0.0030	+0.0030
56	+0.0015	0	–0.0030	+0.0035
60	+0.0007	0	–0.0030	+0.0037
64	+0.0010	0	–0.0030	+0.0042
68	+0.0016	0	–0.0030	+0.0040
72	+0.0020	0	–0.0027	+0.0051
28.8	–0.0018	0	–0.0040	+0.0020
0	–0.005	0	–0.0015	+0

TABLE 4
THREE-RIB CONCEPT
STRAINS IN COMPRESSION AT ROOM TEMPERATURE

LOAD	STRAIN (μ IN./IN.)									
	SG 1	SG 2	SG 3	SG 4	SG 5	SG 6	SG 7	SG 8	SG 9	SG 10
0	0	0	0	0	0	0	0	0	0	0
3,000	–356	–126	–314	–86	–372	–11	–314	–10	–377	+32
5,000	–513	–265	–467	–201	–531	–22	–469	–23	–560	+25
0	RECALIBRATED AT 5,000 LB					*		*		
8,000	–737	–407	–680	–366	–755	+2	–708	–2	–823	+17
10,000	–888	–522	–830	–476	–917	+7	–872	–3	–1,003	+13
12,500	–1,086	–682	–1,027	–633	–1,137	+13	–1,072	–5	–1,211	+11
15,000	–1,262	–816	–1,212	–782	–1,363	+19	–1,299	–2	–1,464	+8
17,500	1,533	–912	–1,484	–877	–1,663	+31	–1,596	0	–1,771	+30
20,000	–1,797	–970	–1,755	–913	–2,011	+52	–1,952	0	–2,149	+68
0	–12	0	–11	+4	–2	–69	–19	–15	–6	+5
LOAD	**SG 11**	**SG 12**	**SG 13**	**SG 14**	**SG 15**	**SG 16**	**SG 17**	**SG 18**	**SG 19**	**SG 20**
0	0	0	0	0	0	0	0	0	0	0
3,000	+295	–9	+41	–82	+299	–92	+386	+393	+272	+255
5,000	–476	+3	+602	–87	+499	–100	+573	+600	+500	+437
0		*		RECALIBRATED AT 5,000 LB						
8,000	–733	0	+870	–96	–2,218	–100	+801	+860	+783	+689
10,000	–909	+3	+1,056	–98	–2,043	–101	+952	+1,039	+968	+855
12,500	–1,122	+3	+1,288	–101	–1,817	–103	+1,135	+1,265	+1,212	+1,072
15,000	–1,368	+6	+1,536	–111	–1,567	–111	+1,334	+1,506	+1,475	+1,312
17,500	–1,672	+6	+1,844	–142	–1,265	–138	+1,570	+1,798	+1,786	+1,594
20,000	–2,050	+13	+2,218	–190	–866	–184	+1,858	+2,166	+2,204	+1,966
0	+2	–25	+1	–72	+3,031**	+93	–40	+5	–9	–16

* SG 6 (TOP RIB), SG 8 (MIDDLE RIB), SG 12 (BOTTOM RIB) – RIB LOCATION STRAINS ADDED AFTER 5,000 LB, AFTER DISCONNECTING SGs 5, 7, AND 11

**PROBLEM SG 15 – CANCEL VALUES

TABLE 5
THREE-RIB CONCEPT (WITH SEAL)
STRAIN IN COMPRESSION AT –65°F AND +160°F

	STRAIN (μ IN./IN.)									
LOAD	**SG 1**	**SG 2**	**SG 3**	**SG 4**	**SG 5**	**SG 6**	**SG 7**	**SG 8**	**SG 9**	**SG 10**
–65°F										
0	0	0	0	0	0	0	0	0	0	0
3,000	–112	–758	–105	0	–177	–33	–170	–34	–282	20
5,000	–347	–837	–360	0	–454	–22	–461	–21	–577	53
8,000	–633	–1,000	–676	0	–780	–16	–813	–15	–928	84
10,000	–818	–1,102	–870	0	–995	–14	–1,039	–14	–1,154	98
12,500	–1,077	–1,242	–1,149	0	–1,282	–14	–1,338	–4	–1,448	118
15,000	–1,341	–1,333	–1,436	0	–1,593	–12	–1,656	11	–1,763	145
17,500	–1,628	–1,450	–1,736	0	–1,921	–6	–1,999	29	–2,099	175
20,000	–1,922	–1,543	–2,051	0	–2,256	4	–2,344	54	–2,436	208
+160°F										
0	0	0	0	0	0	0	0	0	0	0
3,000	–242	–151	–242	0	–298	–20	–290	10	–338	60
5,000	–422	–230	–444	0	–525	–25	–535	14	–593	108
8,000	–641	–351	–691	0	–830	–36	–866	19	–933	158
10,000	–758	–433	–833	0	–1,035	–47	–1,085	29	–1,155	194
12,500	–863	–555	–966	0	–1,283	–51	–1,351	54	–1,457	250
15,000	–962	–688	–1,087	0	–1,537	–51	–1,625	92	–1,766	323
17,500	–1,099	–771	–1,225	0	–1,808	–42	–1,910	141	–2,086	409
20,000	–1,248	–846	–1,373	0	–2,070	–27	–2,175	206	–2,418	529
LOAD	**SG 11**	**SG 12**	**SG 13**	**SG 14**	**SG 16**	**SG 17**	**SG 18**	**SG 19**	**SG 20**	
–65°F										
0	0	0	0	0	0	0	0	0	0	
3,000	–235	–9	361	–91	–88	525	410	310	386	
5,000	–531	18	660	–129	–120	846	723	640	717	
8,000	–907	42	1,033	–166	–151	1,191	1,102	1,042	1,088	
10,000	–1,147	54	1,276	–188	–170	1,403	1,348	1,299	1,325	
12,500	–1,449	73	1,582	–218	–191	1,655	1,659	1,633	1,607	
15,000	–1,777	99	1,901	–248	–218	1,910	1,975	1,960	1,897	
17,500	–2,117	128	2,242	–280	–244	2,166	2,310	2,316	2,192	
20,000	–2,463	161	2,593	–315	–275	2,435	2,655	2,679	2,507	
+160°F										
0	0	0	0	0	0	0	0	0	0	
3,000	–321	60	363	–178	–160	165	325	330	244	
5,000	–588	100	621	–273	–246	785	560	595	406	
8,000	–953	144	971	–404	–358	433	880	956	623	
10,000	–1,186	176	1,204	–496	–437	523	1,096	1,203	756	
12,500	–1,505	231	1,507	–625	–555	633	1,381	1,527	923	
15,000	–1,831	296	1,821	–765	–676	743	1,669	1,855	1,092	
17,500	–2,161	377	2,137	–926	–824	870	1,987	2,159	1,130	
20,000	–2,474	495	2,160	–1,116	–1,030	999	2,285	2,423	1,200	

TABLE 6
THREE-RIB CONCEPT (WITHOUT SEAL)
STRAINS IN COMPRESSION AT –65°F AND +160°F

	STRAIN (μ IN./IN.)								
LOAD	**SG 1**	**SG 2**	**SG 3**	**SG 5**	**SG 6**	**SG 7**	**SG 8**	**SG 9**	**SG 10**
–65°F									
0	0	0	0	0	0	0	0	0	0
3,000	–79	–158	–65	–170	–88	–174	–60	–208	138
5,000	–71	–284	–63	–214	–143	–224	–84	–271	204
8,000	–71	–505	–62	–284	–212	–300	–115	–363	278
10,000	–72	–635	–58	–352	–252	–365	–138	–459	348
12,500	–80	–794	–56	–443	–296	–457	–158	–601	464
15,000	–70	–848	–57	–560	–374	–606	–135	–860	715
0*	170	–190	203	185	–16	241	–87	86	–209
17,500	–509	–685	–620	–1,483	–380	–1,660	–74	–1,799	554
20,000	–659	–740	–788	–1,793	–380	–1,962	–30	–2,254	592
+160°F									
0	0	0	0	0	0	0	0	0	0
3,000	–50	0	–70	–245	–30	–254	30	–296	149
5,000	–118	0	–163	–465	–43	–490	80	–529	250
8,000	–285	0	–360	–841	–64	–892	206	–868	360
10,000	–526	0	–665	–1,258	–46	–1,386	330	–1,270	466
12,500	–872	0	–1,088	–1,829	–5	–2,026	428	–1,952	512
15,000	–1,303	0	–1,628	–2,526	52	–2,831	535	–2,764	550
17,500	16,850 POUNDS – BENT AT JOINT								
LOAD	**SG 11**	**SG 12**	**SG 13**	**SG 14**	**SG 16**	**SG 17**	**SG 18**	**SG 19**	**SG 20**
–65°F									
0	0	0	0	0	0	0	0	0	0
3,000	–205	121	183	–472	–431	–5	129	–149	5
5,000	–268	169	237	–660	–615	–17	164	–187	0
8,000	–362	229	319	–849	–840	–43	222	–242	–1
10,000	–452	290	401	–982	–991	–61	282	–302	–5
12,500	–597	398	540	–1,165	–1,167	–78	376	–400	–11
15,000	–864	646	791	–1,430	–1,413	–105	573	–578	–15
0*	126	–103	–125	–290	–360	–94	–54	–13	–56
17,500	–1,910	727	1,607	–1,323	–1,389	392	1,290	–1,551	824
20,000	–2,390	770	2,168	–1,352	–1,410	1,150	1,921	–2,158	1,484
+160°F									
0	0	0	0	0	0	0	0	0	0
3,000	–279	161	236	–370	–450	–56	160	–168	–23
5,000	–496	277	410	–626	–698	–123	274	–304	–42
8,000	–812	457	647	–966	–1,027	–209	425	–486	–79
10,000	–1,310	603	975	–1,165	–1,213	–195	698	–1,020	–125
12,500	–2,093	662	1,823	–2,024	–1,276	702	1,664	–2,110	1,125
15,000	–2,976	710	2,760	–1,253	–1,313	1,752	2,672	–3,176	2,087
17,500	16,850 POUNDS – BENT AT JOINT								

*AT ABOUT 16,500 POUNDS, SPECIMEN SLIPPED IN LOADING. DISCONTINUED TEST TO INSPECT SPECIMEN. CONTINUED TEST AT 17,500 AND 20,000 POUNDS.

TABLE 7
TENSION TEST AT ROOM TEMPERATURE
THREE-RIB JOINT

STRAIN GAGE NO.	LOAD (LB)											
	500	1,000	1,500	2,000	2,500	3,000	3,500	4,000	5,000	6,000	7,000	8,000
	STRAIN (μ IN./IN.)											
1	–17	–25	–6	–25	–52	–80	–107	–135	–188	–223	–255	–284
2	52	118	159	215	289	346	409	472	600	716	840	969
19	–2	–1	12	15	17	19	25	26	35	46	56	62
4	50	107	168	231	328	407	500	578	730	874	1,019	1,159
5	–11	–16	8	–10	–33	–52	–75	–91	–127	–154	–176	–200
6	19	35	48	64	89	113	137	158	207	258	312	362
7	–10	–16	9	–9	–26	–42	–60	–74	–104	–126	–149	–174
8	11	24	39	63	90	116	139	162	210	249	286	308
9	–6	–2	22	17	10	5	0	–4	–10	–7	–1	2
10	1	–6	–25	–36	–43	–51	–60	–68	–84	–100	–114	–123
11	–2	0	24	22	19	14	11	10	8	13	18	23
12	2	–3	–21	–27	–32	–37	–40	–48	–64	–80	–93	–98
13	0	–6	24	–24	–22	–21	–21	–23	–30	–40	–52	–61
16	43	111	213	269	321	367	413	460	535	609	680	750
17	–4	–3	0	–2	0	0	0	0	1	3	4	5
18	–6	–8	–15	–14	–12	–11	–12	–13	–17	–22	–28	–30

TABLE 8
TENSION TEST AT +160°F
LFC CHORDWISE JOINT (WITHOUT SEAL)

STRAIN GAGE NO.	LOAD (LB)									
	500	1,000	1,500	2,000	3,000	4,000	5,000	6,000	7,000	8,000
	STRAIN (μ IN./IN.)									
1	–5	–24	–60	–95	–165	–218	–258	–291	–333	–372
2	42	95	150	204	318	437	572	705	844	983
4	51	135	226	314	506	682	850	1,018	1,188	1,347
5	–9	–20	–45	–72	–133	–172	–207	–236	–269	–302
6	13	22	31	43	76	116	159	200	248	292
7	–5	–9	–18	–30	–69	–104	–146	–181	–216	–251
8	2	16	35	59	117	167	209	250	290	330
9	7	11	11	3	–20	–35	–48	–58	–69	–81
10	–8	–21	–36	–47	–65	–76	–87	–102	–112	–122
11	4	11	16	15	3	–9	–22	–35	–46	–60
12	–9	–22	–30	–34	–42	–50	–57	–70	–80	–91
13	–10	–20	–27	–26	–19	–14	–14	–13	–14	–13
20	–4	–3	–5	–5	–5	–6	–7	–8	–8	–10
16	56	126	177	218	293	360	426	497	568	633
17	0	0	0	0	–3	–5	–6	–6	–5	–5
18	–4	–11	–15	–16	–14	–11	–11	–13	–15	–17

TABLE 9
TENSION TEST AT –65°F LFC
CHORDWISE JOINT (WITHOUT SEAL)

STRAIN GAGE NO.	LOAD (LB)									
	500	1,000	1,500	2,000	3,000	4,000	5,000	6,000	7,000	8,000
	STRAIN (μIN./IN.)									
1	–15	–45	–72	–96	–148	–196	–237	–274	–316	–366
4	28	104	202	284	445	602	750	900	1049	1203
5	113	90	74	63	20	–21	–54	–86	–120	–158
6	10	22	37	51	88	135	186	235	285	337
7	–2	–4	3	9	–10	–49	–84	–118	–149	–187
8	4	25	47	71	133	182	228	274	315	353
9	3	9	20	26	10	–9	–20	–30	–40	–50
10	–12	–34	–56	–74	–94	–106	–119	–130	–137	–142
11	7	18	38	48	48	35	24	15	6	–4
12	–15	–28	–46	–54	–58	–66	–72	–76	–80	–82
13	–5	–13	–23	–29	–24	–18	–16	–15	–13	–12
20	0	2	2	3	7	9	12	13	15	15
16	49	105	172	216	288	354	427	494	555	613
17	–1	–3	–6	–9	–13	–13	–12	–12	–12	–12
18	–25	–28	–28	–29	–29	–22	–20	–19	–16	–15

TABLE 10
COMPRESSION TEST AT ROOM TEMPERATURE
LFC SHORT SLIDING-JOINT PANEL

STRAIN GAGE NO.	LOAD (LB)							
	3,000	5,000	8,000	10,000	12,500	15,000	17,500	20,000
	STRAIN (μIN./IN.)							
1	–543	–765	–1,092	–1,312	–1,580	–1,853	–2,118	–2,390
2	–305	–623	–1,106	–1,433	–1,845	–2,265	–2,695	–3,137
3	–482	–766	–1,205	–1,503	–1,880	–2,260	–2,648	–3,014
4	42	60	92	113	143	172	203	235
5	–412	–680	–1,099	–1,371	–1,725	–2,100	–2,457	–2,857
6	–31	–45	–62	–67	–69	–68	–63	–38
7	–310	–534	–890	–1,126	–1,412	–1,717	–1,211	–2,322
8	24	35	47	58	78	105	132	166
9	–358	–615	–1,033	–1,322	–1,674	–2,048	–2,419	–2,798
10	–19	–26	–16	2	20	44	67	90
11	–94	–23	–475	–654	–876	–1,112	–1,332	–1,562
12	–551	–899	–1,402	–1,766	–2,220	–2,694	–3,175	–3,675
13	–32	–69	–155	–246	–377	–529	–674	–837
14	–65	–80	–108	–141	–180	–230	–300	–380
15	–24	–42	–70	–83	–100	–116	–140	–179
16	–124	–213	–339	–420	–525	–640	–742	–849
17	244	448	760	980	1,264	1,540	1,823	2,128
18	440	684	1,025	1,257	1,545	1,825	2,098	2,378
19	15	12	14	14	14	14	15	15
20	5	6	2	0	0	–3	–7	–13

TABLE 11
COMPRESSION TEST AT −65°F
LFC SHORT SLIDING-JOINT PANEL

STRAIN GAGE NO.	LOAD (LB)							
	3,000	5,000	8,000	10,000	12,500	15,000	17,500	20,000
	STRAIN (μIN./IN.)							
1	−683	−977	−1,324	−1,552	−1,829	−2,102	−2,369	−2,633
2	−97	−331	−741	−1,026	−1,378	−1,738	−2,083	−2,448
3	−499	−812	−1,255	−1,556	−1,927	−2,308	−2,670	−3,049
4	56	77	106	128	158	191	215	245
5	−404	−722	−1,228	−1,522	−1,926	−2,323	−2,700	−3,092
6	25	33	31	29	23	20	10	8
7	−338	−586	−970	−1,227	−1,563	−1,898	−2,222	−2,550
8	51	109	149	175	200	222	228	236
9	−339	−606	−1,008	−1,287	−1,633	−1,991	−2,336	−2,688
10	−19	−21	−18	−5	9	28	40	57
11	−99	−217	−429	−593	−803	−1,022	−1,236	−1,463
12	−555	−866	−1,329	−1,644	−2,043	−2,455	−2,857	−3,291
13	0	3	0	0	0	1	1	2
14	−63	−83	−116	−137	−168	−206	−244	−283
15	−22	−18	−23	−26	−35	−46	−55	−67
16	−181	−243	−327	−383	−455	−529	−605	−683
17	266	450	748	955	1,219	1,489	1,764	2,036
18	450	700	1,039	1,255	1,526	1,797	2,064	2,327

TABLE 12
COMPRESSION TEST AT +160°F
LFC SHORT SLIDING-JOINT PANEL

STRAIN GAGE NO.	LOAD (LB)							
	3,000	5,000	8,000	10,000	12,500	15,000	17,500	20,000
	STRAIN (μIN./IN.)							
1	−715	−1,096	−1,506	−1,773	−2,099	−2,420	−2,736	−3,027
2	−224	−484	−1,003	−1,400	−1,910	−2,396	−2,845	−3,470
3	−526	−874	−1,335	−1,644	−2,025	−2,409	−2,795	−3,129
4	−39	73	115	149	190	232	281	336
5	−415	−719	−1,120	−1,366	−1,669	−1,952	−2,209	−2,393
6	14	55	82	102	139	162	200	320
7	−268	−476	−781	−981	−1,220	−1,460	−1,650	−1,763
8	−14	−11	70	125	214	287	395	544
9	−350	−632	−1,062	−1,355	−1,732	−2,107	−2,479	−2,841
10	−36	81	106	139	189	235	284	345
11	−63	−181	−427	−608	−841	−1,077	−1,295	−1,484
12	−785	−1,275	−1,999	−2,483	−3,107	−3,744	−4,454	−5,206
13	22	22	20	14	9	6	7	5
14	−96	−136	−217	−282	−382	−480	−607	−784
15	−71	−147	−205	−243	−285	−311	−332	−359
16	−260	−394	−514	−596	−696	−797	−904	−1,033
17	232	459	813	1,074	1,402	1,739	2,108	2,511
18	449	722	1,100	1,344	1,634	1,927	2,220	2,529

TABLE 13
STRAIN GAGE READINGS FOR SMALL SLIDING JOINT (J2) AT ROOM TEMPERATURE
LABORATORY TEST DATA
TENSION TEST

STRAIN GAGE NO.	LOAD (LB)													
	0	500	1,000	1,500	2,000	2,500	3,000	3,500	4,000	5,000	6,000	7,000	8,000	0
	STRAIN (μIN./IN.)													
1	0	–15	–45	–109	–181	–265	–344	–440	–525	–642	–681	–418	–404	80
2	0	160	340	554	780	1,019	1,250	1,495	1,754	2,112	2,460	2,642	2,950	–41
3	0	40	79	111	140	170	194	215	235	265	273	310	213	–14
4	0	–89	–184	–286	–394	–508	–622	–720	–824	–1,030	–1,280	–1,568	–1,783	–113
5	0	0	–2	–2	–6	–9	–13	–17	–21	–36	–51	–73	–89	4
6	0	24	53	80	106	132	157	186	215	280	335	435	427	4
7	0	2	2	0	1	0	–1	–3	–6	–12	–24	–33	–40	15
8	0	15	47	78	104	130	154	174	190	213	222	248	252	0
9	0	38	79	119	154	186	208	223	232	234	194	162	122	30
10	0	–67	–180	305	–437	–565	–660	–744	–837	–1,051	–1,326	–1,608	–1,870	–154
11	0	–3	–32	–84	–150	–228	–320	–412	–499	–605	–653	–665	–715	96
12	0	154	327	523	740	970	1,226	1,468	1,740	2,214	2,620	2,916	3,439	19
13	0	–491	–794	1,030	–1,255	–1,466	–1,794	–2,021	–2,275	–2,809	–3,408	–4,152	–4,760	–120
14	0	–239	–429	–572	–693	–851	–997	–1,164	–1,355	–1,779	–2,233	–2,778	–3,244	–169
15	0	193	295	396	492	629	678	710	717	721	771	852	912	–106
16	0	–368	–656	–882	–1,074	–1,315	–1,592	–1,890	–2,170	–2,742	–3,393	–4,125	–4,940	–149
17	0	66	129	191	255	338	410	484	562	761	1,024	1,310	1,505	62
18	0	–45	–94	142	–193	–260	–335	–399	–478	–686	–920	–1,002	–1,048	–27

TABLE 14
STRAIN GAGE READINGS FOR SMALL SLIDING JOINT (J2) AT –65°F
LABORATORY TEST DATA
TENSION TEST

STRAIN GAGE NO.	LOAD (LB)								
	500	1,000	1,500	2,000	2,500	3,000	3,500	4,000	0
	STRAIN (μIN./IN.)								
1	–20	–13	–15	–92	–125	–152	–177	–168	+37
2	+148	+288	+473	+652	+829	+1,010	+1,185	+1,305	–36
3	–6	+10	+14	+12	+13	+13	+21	+14	+11
4	+21	+24	+5	–18	–46	–80	–129	–189	–30
5	+2	+6	+4	+5	+9	+9	+12	+7	+25
6	–22	–18	–12	–14	–10	–9	+3	+16	+6
7	0	+5	+7	+8	+10	+11	+12	+13	+43
8	+10	+20	+33	+46	+58	+68	+82	+95	+31
9	+21	+39	+58	+70	+84	+90	+100	+109	+84
10	–57	–131	–216	–300	–387	–482	–578	–679	–80
11	–43	+103	–150	–200	–254	–313	–368	–414	+78
12	+163	+372	+575	+782	+989	+1,207	+1,418	+622	+26
13	–367	–663	–916	–1,169	–1,402	–1,640	–1,875	–2,101	–32
14	–220	–460	–705	–930	–1,140	–1,357	–1,556	–1,740	+2
15	+109	+104	+98	+98	+95	+100	+130	+175	–49
16	–324	–699	–1,032	–1,344	–1,618	–1,870	–2,100	–2,313	–70
17	+60	+119	+186	+259	+330	+406	+486	+567	+30
18	+44	+106	+176	+246	+312	+376	+440	+497	+52
19	–37	+71	–108	–150	–146	–249	–299	–350	–11
VOLTS	1.33	2.34	3.26	4.12	4.89	5.63	6.35	7.00	0.59
EXT (IN.)	0.0266	0.0468	0.0652	0.0824	0.0978	0.1126	0.1270	0.140	0.0118

TABLE 15
STRAIN GAGE READINGS FOR SMALL SLIDING JOINT (J2) AT +160°F
LABORATORY TEST DATA
TENSION TEST

STRAIN GAGE NO.	LOAD (LB)						
	500	1,000	1,500	2,000	2,500	3,000	0
	STRAIN (μIN./IN.)						
1	−10	−50	−80	−100	−122	−137	+104
2	+166	+370	+574	+784	+997	+1,215	+15
3	−6	−7	−7	−7	−5	−1	+24
4	+33	+11	−28	−80	−143	−235	−18
5	−7	−11	−16	−24	−30	−38	−5
6	−2	+4	+15	+27	+44	+68	+38
7	−5	−9	−14	−19	−23	−29	+2
8	+27	+37	+60	+86	+110	+140	+50
9	+24	+23	+27	+29	+28	+27	+29
10	−84	−174	−293	−426	−560	−703	−72
11	−17	−75	−125	−172	−220	−262	+75
12	+170	+399	+620	+820	+1,057	+1,290	−35
13	−390	−713	−1,020	−1,302	−1,573	−1,860	−78
14	−438	−737	−1,030	−1,301	−1,570	−1,813	−140
15	+62	+49	+29	+12	0	+25	−80
16	−485	−865	−1,205	−1,512	−1,795	−2,054	−134
17	+69	+130	+198	+272	+350	+433	0
18	+25	+87	+150	+217	+282	+350	+1
19	−949	−900	−843	−814	−771	−722	−1,003
VOLTS	2.36	3.51	4.50	5.38	6.22	7.01	1.62
EXT (IN.)	0.0422	0.0702	0.0900	0.1076	0.1244	0.1402	0.0324

TABLE 16
DIAL INDICATOR READINGS
ROOM TEMPERATURE TEST — J1 THREE-RIB JOINT SPECIMEN

LOAD (LB)	TOP	MIDDLE	BOTTOM
PRELOAD 150	0	0	0
3,000	+0.005	−0.009	−0.003
5,000	+0.004	−0.009	−0.005
8,000	+0.004	−0.011	−0.006
10,000	+0.004	−0.0125	−0.0075
12,500	+0.004	−0.014	−0.012
15,000	+0.005	−0.0165	−0.0095
17,500	+0.004	−0.022	−0.012
20,000	+0.004	−0.028	−0.0135
0 LOAD	—	+0.005	+0.002

NOTE: 12-IN. SPAN BETWEEN TOP AND BOTTOM INDICATORS

NOTE: POSITIVE READINGS ARE INCREASING MEASUREMENTS ON PERFORATED TITANIUM SURFACE (SURFACE MOVING OUT AT INDICATOR TIP). NEGATIVE READINGS ARE DECREASING (SURFACE MOVING IN AT INDICATOR TIP)

TABLE 17
DIAL INDICATOR READINGS FOR THREE–RIB JOINT IN TENSION AT ROOM TEMPERATURE

LOAD (LB)	TOP	MIDDLE	BOTTOM
PRELOAD 100	0	0	0
500	+0.001	+0.002	+0.002
1,000	+0.005	+0.009	+0.007
1,500	+0.015	+0.025	+0.019
2,000	+0.020	+0.032	+0.024
2,500	+0.024	+0.039	+0.026
3,000	+0.026	+0.043	+0.030
3,500	+0.028	+0.048	+0.033
4,000	+0.030	+0.053	+0.037
5,000	+0.035	+0.062	+0.043
6,000	+0.040	+0.071	+0.050
7,000	+0.045	+0.080	+0.056
8,000	+0.049	+0.090	+0.063
0	+0.008	+0.014	+0.009

(+) IS DEFLECTING OUT FROM Ti FACE
(–) IS DEFLECTING IN FROM Ti FACE

TABLE 18
DIAL INDICATOR READINGS AT ROOM TEMPERATURE

LOAD (LB)	TOP	MIDDLE	BOTTOM
3,000	–0.012	–0.017	–0.020
5,000	–0.014	–0.019	–0.018
8,000	–0.016	–0.021	–0.017
10,000	–0.018	–0.023	–0.016
12,500	–0.019	–0.025	–0.014
15,000	–0.021	–0.028	–0.013
17,500	–0.023	–0.031	–0.012
20,000	–0.026	–0.032	–0.011
0	–0.010	–0.012	–0.012

TABLE 19
TENSION TEST OF SMALL SLIDING JOINT AT ROOM TEMPERATURE

LOAD (LB)	DIAL GAGES (IN.)			VOLTS	GAP BETWEEN PANEL (IN.)
	UPPER	CENTER	LOWER		
0	0	0	0	0	0
500	+0.050	+0.055	+0.045	0.052	0.026
1,000	+0.065	+0.105	+0.078	0.91	0.046
1,500	+0.115	+0.140	+0.110	1.24	0.062
2,000	+0.145	+0.178	+0.137	1.59	0.080
2,500	+0.172	+0.211	+0.162	1.84	0.092
3,000	+0.195	+0.240	+0.186	2.19	0.110
3,500	+0.215	+0.270	+0.209	2.49	0.125
4,000	+0.234	+0.296	+0.228	2.79	0.140
5,000	+0.267	+0.343	+0.261	3.39	0.170
6,000	+0.298	+0.380	+0.294	4.04	0.202
7,000	+0.326	+0.438	+0.329	4.81	0.240
8,000	+0.354	+0.482	+0.360	5.70	0.285
0	+0.030	+0.128	+0.020	0.94	0.047

TABLE 20
READINGS OF CENTER TWO DIAL GAGES SENSITIVE TO 0.0001 INCH COMPRESSION TEST — J3 LARGE SLIDING JOINT

LOAD (1,000 LB)	CENTER UPPER	CENTER LOWER
0	0	0
4	+0.00070	+0.00090
8	+0.00100	+0.00110
12	+0.00138	+0.00140
16	+0.00175	+0.00170
20	+0.00242	+0.00208
24	+0.00250	+0.00226
28	+0.00264	+0.00288
32	+0.00316	+0.00288
36	+0.00362	+0.00320
40	+0.00398	+0.00360
44	+0.00438	+0.0394
48	+0.00472	+0.00430
52	+0.00510	+0.00470
56	+0.00518	+0.00562
60	+0.00598	+0.00554
64	+0.00656	+0.00604
68	+0.00700	+0.00648
72	+0.00760	+0.00692
28.8	+0.00340	+0.00278
0	+0.00022	−0.000050

TABLE 21
GAGE READINGS FOR TENSION TESTS OF LARGE SLIDING-JOINT PANEL

TEST MACHINE MTS NO. 6
50,000-LB LOAD RANGE 100-PERCENT STRAIN RANGE 20-PERCENT STROKE RANGE
CHANNEL DESCRIPTIONS
CH 41 = TEMP (F) OF TITANIUM CH 42 = TEMP (F) OF COMPOSITE CH 43 = TEMP (F) OF ALUMINUM FITTING CH 44 = TEMP (F) OF TITANIUM BOLT CH 60 = LOAD = 5,000 LB/VOLT CH 61 = DISPLACEMENT = 0.020 INCH/VOLT CH 62 = STROKE DISPLACEMENT = 0.100 INCH/VOLT EXTENSOMETER: S/N 260

TABLE 22
STRAINS AT ZERO LOAD VALUE

ALL CHANNELS

CHANNEL 1 — STRAIN GAGE	0 με	CHANNEL 15 — STRAIN GAGE	0 με
CHANNEL 2 — STRAIN GAGE	0 με	CHANNEL 16 — STRAIN GAGE	0 με
CHANNEL 3 — STRAIN GAGE	0 με	CHANNEL 17 — STRAIN GAGE	1 με
CHANNEL 4 — STRAIN GAGE	0 με	CHANNEL 18 — STRAIN GAGE	0 με
CHANNEL 5 — STRAIN GAGE	0 με	CHANNEL 19 — STRAIN GAGE	0 με
CHANNEL 6 — STRAIN GAGE	0 με	CHANNEL 20 — STRAIN GAGE	0 με
CHANNEL 7 — STRAIN GAGE	0 με	CHANNEL 40 — THERMOCOUPLE	78°F
CHANNEL 8 — STRAIN GAGE	1 με	CHANNEL 41 — THERMOCOUPLE	75°F
CHANNEL 9 — STRAIN GAGE	0 με	CHANNEL 42 — THERMOCOUPLE	76°F
CHANNEL 10 — STRAIN GAGE	0 με	CHANNEL 43 — THERMOCOUPLE	75°F
CHANNEL 11 — STRAIN GAGE	0 με	CHANNEL 44 — THERMOCOUPLE	75°F
CHANNEL 12 — STRAIN GAGE	0 με	CHANNEL 60 — VOLTS OR mV	0.0000 V
CHANNEL 13 — STRAIN GAGE	−1 με	CHANNEL 61 — VOLTS OR mV	0.0000 V
CHANNEL 14 — STRAIN GAGE	1 με	CHANNEL 62 — VOLTS OR mV	0.0006 V

0.0 DISPLACEMENT

TABLE 23
STRAINS AT 3,995 POUNDS TENSION

ALL CHANNELS

CHANNEL 1 — STRAIN GAGE	19 με	CHANNEL 15 — STRAIN GAGE	15 με
CHANNEL 2 — STRAIN GAGE	75 με	CHANNEL 16 — STRAIN GAGE	4 με
CHANNEL 3 — STRAIN GAGE	16 με	CHANNEL 17 — STRAIN GAGE	0 με
CHANNEL 4 — STRAIN GAGE	11 με	CHANNEL 18 — STRAIN GAGE	0 με
CHANNEL 5 — STRAIN GAGE	48 με	CHANNEL 19 — STRAIN GAGE	−4 με
CHANNEL 6 — STRAIN GAGE	0.95 με	CHANNEL 20 — STRAIN GAGE	−2 με
CHANNEL 7 — STRAIN GAGE	−1 με	CHANNEL 40 — THERMOCOUPLE	78°F
CHANNEL 8 — STRAIN GAGE	64 με	CHANNEL 41 — THERMOCOUPLE	75°F
CHANNEL 9 — STRAIN GAGE	−14 με	CHANNEL 42 — THERMOCOUPLE	76°F
CHANNEL 10 — STRAIN GAGE	82 με	CHANNEL 43 — THERMOCOUPLE	75°F
CHANNEL 11 — STRAIN GAGE	39 με	CHANNEL 44 — THERMOCOUPLE	75°F
CHANNEL 12 — STRAIN GAGE	146 με	CHANNEL 60 — VOLTS OR mV	0.7990 V
CHANNEL 13 — STRAIN GAGE	−2 με	CHANNEL 61 — VOLTS OR mV	0.2936 V
CHANNEL 14 — STRAIN GAGE	8 με	CHANNEL 62 — VOLTS OR mV	0.0000 V

0.0059-INCH DISPLACEMENT

TABLE 24
STRAIN VALUES AT 8,029 POUNDS

ALL CHANNELS

CHANNEL 1 — STRAIN GAGE	49 με
CHANNEL 2 — STRAIN GAGE	91 με
CHANNEL 3 — STRAIN GAGE	51 με
CHANNEL 4 — STRAIN GAGE	157 με
CHANNEL 5 — STRAIN GAGE	120 με
CHANNEL 6 — STRAIN GAGE	178 με
CHANNEL 7 — STRAIN GAGE	5 με
CHANNEL 8 — STRAIN GAGE	103 με
CHANNEL 9 — STRAIN GAGE	−14 με
CHANNEL 10 — STRAIN GAGE	151 με
CHANNEL 11 — STRAIN GAGE	96 με
CHANNEL 12 — STRAIN GAGE	290 με
CHANNEL 13 — STRAIN GAGE	−2 με
CHANNEL 14 — STRAIN GAGE	16 με
CHANNEL 15 — STRAIN GAGE	32 με
CHANNEL 16 — STRAIN GAGE	12 με
CHANNEL 17 — STRAIN GAGE	0 με
CHANNEL 18 — STRAIN GAGE	2 με
CHANNEL 19 — STRAIN GAGE	4 με
CHANNEL 20 — STRAIN GAGE	8 με
CHANNEL 40 — THERMOCOUPLE	78°F
CHANNEL 41 — THERMOCOUPLE	75°F
CHANNEL 42 — THERMOCOUPLE	76°F
CHANNEL 43 — THERMOCOUPLE	75°F
CHANNEL 44 — THERMOCOUPLE	75°F
CHANNEL 60 — VOLTS OR mV	1.6058 V
CHANNEL 61 — VOLTS OR mV	0.6537 V
CHANNEL 62 — VOLTS OR mV	0.1538 V

0.0131-INCH DISPLACEMENT

TABLE 25
STRAIN VALUES AT 11,991 POUNDS

ALL CHANNELS

CHANNEL 1 — STRAIN GAGE	60 με
CHANNEL 2 — STRAIN GAGE	128 με
CHANNEL 3 — STRAIN GAGE	60 με
CHANNEL 4 — STRAIN GAGE	230 με
CHANNEL 5 — STRAIN GAGE	176 με
CHANNEL 6 — STRAIN GAGE	297 με
CHANNEL 7 — STRAIN GAGE	17 με
CHANNEL 8 — STRAIN GAGE	132 με
CHANNEL 9 — STRAIN GAGE	−4 με
CHANNEL 10 — STRAIN GAGE	221 με
CHANNEL 11 — STRAIN GAGE	159 με
CHANNEL 12 — STRAIN GAGE	425 με
CHANNEL 13 — STRAIN GAGE	−2 με
CHANNEL 14 — STRAIN GAGE	23 με
CHANNEL 15 — STRAIN GAGE	51 με
CHANNEL 16 — STRAIN GAGE	21 με
CHANNEL 17 — STRAIN GAGE	0 με
CHANNEL 18 — STRAIN GAGE	2 με
CHANNEL 19 — STRAIN GAGE	−6 με
CHANNEL 20 — STRAIN GAGE	3 με
CHANNEL 40 — THERMOCOUPLE	78°F
CHANNEL 41 — THERMOCOUPLE	75°F
CHANNEL 42 — THERMOCOUPLE	76°F
CHANNEL 43 — THERMOCOUPLE	75°F
CHANNEL 44 — THERMOCOUPLE	75°F
CHANNEL 60 — VOLTS OR mV	2.3981 V
CHANNEL 61 — VOLTS OR mV	0.9918 V
CHANNEL 62 — VOLTS OR mV	0.2728 V

0.0198-INCH DISPLACEMENT

TABLE 26
STRAIN VALUES AT 16,037 POUNDS

ALL CHANNELS

CHANNEL 1 — STRAIN GAGE	65 με	CHANNEL 15 — STRAIN GAGE	71 με
CHANNEL 2 — STRAIN GAGE	170 με	CHANNEL 16 — STRAIN GAGE	25 με
CHANNEL 3 — STRAIN GAGE	69 με	CHANNEL 17 — STRAIN GAGE	−1 με
CHANNEL 4 — STRAIN GAGE	328 με	CHANNEL 18 — STRAIN GAGE	−4 με
CHANNEL 5 — STRAIN GAGE	239 με	CHANNEL 19 — STRAIN GAGE	−29 με
CHANNEL 6 — STRAIN GAGE	430 με	CHANNEL 20 — STRAIN GAGE	−15 με
CHANNEL 7 — STRAIN GAGE	27 με	CHANNEL 40 — THERMOCOUPLE	79°F
CHANNEL 8 — STRAIN GAGE	164 με	CHANNEL 41 — THERMOCOUPLE	75°F
CHANNEL 9 — STRAIN GAGE	8 με	CHANNEL 42 — THERMOCOUPLE	76°F
CHANNEL 10 — STRAIN GAGE	309 με	CHANNEL 43 — THERMOCOUPLE	75°F
CHANNEL 11 — STRAIN GAGE	214 με	CHANNEL 44 — THERMOCOUPLE	75°F
CHANNEL 12 — STRAIN GAGE	562 με	CHANNEL 60 — VOLTS OR mV	3.2074 V
CHANNEL 13 — STRAIN GAGE	−3 με	CHANNEL 61 — VOLTS OR mV	1.4081 V
CHANNEL 14 — STRAIN GAGE	29 με	CHANNEL 62 — VOLTS OR mV	0.4095 V

0.0282-INCH DISPLACEMENT

TABLE 27
STRAIN VALUES AT 20,035 POUNDS

ALL CHANNELS

CHANNEL 1 — STRAIN GAGE	73 με	CHANNEL 15 — STRAIN GAGE	85 με
CHANNEL 2 — STRAIN GAGE	208 με	CHANNEL 16 — STRAIN GAGE	30 με
CHANNEL 3 — STRAIN GAGE	84 με	CHANNEL 17 — STRAIN GAGE	−2 με
CHANNEL 4 — STRAIN GAGE	429 με	CHANNEL 18 — STRAIN GAGE	−14 με
CHANNEL 5 — STRAIN GAGE	304 με	CHANNEL 19 — STRAIN GAGE	−65 με
CHANNEL 6 — STRAIN GAGE	554 με	CHANNEL 20 — STRAIN GAGE	−44 με
CHANNEL 7 — STRAIN GAGE	41 με	CHANNEL 40 — THERMOCOUPLE	79°F
CHANNEL 8 — STRAIN GAGE	208 με	CHANNEL 41 — THERMOCOUPLE	76°F
CHANNEL 9 — STRAIN GAGE	25 με	CHANNEL 42 — THERMOCOUPLE	76°F
CHANNEL 10 — STRAIN GAGE	408 με	CHANNEL 43 — THERMOCOUPLE	75°F
CHANNEL 11 — STRAIN GAGE	269 με	CHANNEL 44 — THERMOCOUPLE	75°F
CHANNEL 12 — STRAIN GAGE	690 με	CHANNEL 60 — VOLTS OR mV	4.0070 V
CHANNEL 13 — STRAIN GAGE	−4 με	CHANNEL 61 — VOLTS OR mV	1.8506 V
CHANNEL 14 — STRAIN GAGE	40 με	CHANNEL 62 — VOLTS OR mV	0.5573 V

0.0370-INCH DISPLACEMENT

TABLE 28
STRAIN VALUES AT 23,981 POUNDS

ALL CHANNELS

CHANNEL 1 — STRAIN GAGE	86 με
CHANNEL 2 — STRAIN GAGE	234 με
CHANNEL 3 — STRAIN GAGE	99 με
CHANNEL 4 — STRAIN GAGE	516 με
CHANNEL 5 — STRAIN GAGE	366 με
CHANNEL 6 — STRAIN GAGE	675 με
CHANNEL 7 — STRAIN GAGE	49 με
CHANNEL 8 — STRAIN GAGE	246 με
CHANNEL 9 — STRAIN GAGE	43 με
CHANNEL 10 — STRAIN GAGE	509 με
CHANNEL 11 — STRAIN GAGE	426 με
CHANNEL 12 — STRAIN GAGE	813 με
CHANNEL 13 — STRAIN GAGE	−4 με
CHANNEL 14 — STRAIN GAGE	46 με
CHANNEL 15 — STRAIN GAGE	103 με
CHANNEL 16 — STRAIN GAGE	32 με
CHANNEL 17 — STRAIN GAGE	−6 με
CHANNEL 18 — STRAIN GAGE	−27 με
CHANNEL 19 — STRAIN GAGE	−101 με
CHANNEL 20 — STRAIN GAGE	−73 με
CHANNEL 40 — THERMOCOUPLE	78°F
CHANNEL 41 — THERMOCOUPLE	76°F
CHANNEL 42 — THERMOCOUPLE	76°F
CHANNEL 43 — THERMOCOUPLE	75°F
CHANNEL 44 — THERMOCOUPLE	75°F
CHANNEL 60 — VOLTS OR mV	4.7961 V
CHANNEL 61 — VOLTS OR mV	2.2351 V
CHANNEL 62 — VOLTS OR mV	0.6897 V

0.0447-INCH DISPLACEMENT

TABLE 29
STRAIN VALUES AT 27,490 POUNDS

ALL CHANNELS

CHANNEL 1 — STRAIN GAGE	104 με
CHANNEL 2 — STRAIN GAGE	275 με
CHANNEL 3 — STRAIN GAGE	103 με
CHANNEL 4 — STRAIN GAGE	539 με
CHANNEL 5 — STRAIN GAGE	456 με
CHANNEL 6 — STRAIN GAGE	789 με
CHANNEL 7 — STRAIN GAGE	58 με
CHANNEL 8 — STRAIN GAGE	285 με
CHANNEL 9 — STRAIN GAGE	62 με
CHANNEL 10 — STRAIN GAGE	609 με
CHANNEL 11 — STRAIN GAGE	467 με
CHANNEL 12 — STRAIN GAGE	936 με
CHANNEL 13 — STRAIN GAGE	1 με
CHANNEL 14 — STRAIN GAGE	55 με
CHANNEL 15 — STRAIN GAGE	132 με
CHANNEL 16 — STRAIN GAGE	30 με
CHANNEL 17 — STRAIN GAGE	−9 με
CHANNEL 18 — STRAIN GAGE	−40 με
CHANNEL 19 — STRAIN GAGE	−139 με
CHANNEL 20 — STRAIN GAGE	−104 με
CHANNEL 40 — THERMOCOUPLE	78°F
CHANNEL 41 — THERMOCOUPLE	76°F
CHANNEL 42 — THERMOCOUPLE	76°F
CHANNEL 43 — THERMOCOUPLE	75°F
CHANNEL 44 — THERMOCOUPLE	75°F
CHANNEL 60 — VOLTS OR mV	5.4980 V
CHANNEL 61 — VOLTS OR mV	2.6526 V
CHANNEL 62 — VOLTS OR mV	0.8270 V

0.0531-INCH DISPLACEMENT

TABLE 30
STRAIN VALUES AT 27,829 POUNDS

ALL CHANNELS

CHANNEL 1 — STRAIN GAGE	106 με	CHANNEL 15 — STRAIN GAGE	133 με
CHANNEL 2 — STRAIN GAGE	267 με	CHANNEL 16 — STRAIN GAGE	33 με
CHANNEL 3 — STRAIN GAGE	104 με	CHANNEL 17 — STRAIN GAGE	−9 με
CHANNEL 4 — STRAIN GAGE	542 με	CHANNEL 18 — STRAIN GAGE	−41 με
CHANNEL 5 — STRAIN GAGE	461 με	CHANNEL 19 — STRAIN GAGE	−141 με
CHANNEL 6 — STRAIN GAGE	794 με	CHANNEL 20 — STRAIN GAGE	−107 με
CHANNEL 7 — STRAIN GAGE	61 με	CHANNEL 40 — THERMOCOUPLE	78°F
CHANNEL 8 — STRAIN GAGE	282 με	CHANNEL 41 — THERMOCOUPLE	76°F
CHANNEL 9 — STRAIN GAGE	64 με	CHANNEL 42 — THERMOCOUPLE	76°F
CHANNEL 10 — STRAIN GAGE	609 με	CHANNEL 43 — THERMOCOUPLE	75°F
CHANNEL 11 — STRAIN GAGE	473 με	CHANNEL 44 — THERMOCOUPLE	75°F
CHANNEL 12 — STRAIN GAGE	935 με	CHANNEL 60 — VOLTS OR mV	5.5658 V
CHANNEL 13 — STRAIN GAGE	−1 με	CHANNEL 61 — VOLTS OR mV	2.6471 V
CHANNEL 14 — STRAIN GAGE	55 με	CHANNEL 62 — VOLTS OR mV	0.8270 V

0.0529-INCH DISPLACEMENT

TABLE 31
COMPOSITE FLANGED JOINT STRAIN GAGE READINGS AT ROOM TEMPERATURE TENSION LOADING – FRONT SURFACE

C001 ($\mu\epsilon$)	C003 ($\mu\epsilon$)	C005 ($\mu\epsilon$)	C007 ($\mu\epsilon$)	C009 ($\mu\epsilon$)	C0011 ($\mu\epsilon$)	C0013 ($\mu\epsilon$)	C041 (°F)	LOAD (LB)
0	-1	-1	0	+1	0	0	+01	0
+72	+65	+70	+26	+41	-1	-1	+82	510
+156	+151	+161	+61	+75	-2	-4	+81	1,020
+230	+227	+251	+95	+105	-3	-7	+81	1,500
+316	+333	+355	+135	+138	-8	-12	+82	2,040
+388	+403	+442	+170	+171	-18	-17	+81	2,470
+477	+483	+548	+216	+216	-35	-24	+81	3,020
+553	+556	+638	+252	+253	-54	-32	+81	3,510
+629	+637	+727	+288	+286	-77	-40	+81	3,990
+707	+720	+815	+322	+318	-103	-49	+81	4,500
+784	+806	+905	+357	+351	-131	-58	+81	4,990
+861	+890	+992	+391	+383	-162	-69	+81	5,510
+938	+975	+1,082	+423	+415	-193	-00	+81	6,010
+1,010	+1,054	+1,161	+452	+446	-220	-92	+81	6,480
+1,093	+1,144	+1,258	+482	+477	-251	-107	+81	7,000
+1,172	+1,226	+1,344	+511	+506	-277	-120	+01	7,490
+1,256	+1,315	+1,443	+542	+538	-304	-137	+81	8,000
+1,332	+1,394	+1,526	+570	+565	-329	-151	+81	8,490
+1,413	+1,481	+1,620	+600	+595	-356	-176	+81	9,010
+1,477	+1,550	+1,691	+624	+617	-378	-176	+81	9,470
+1,560	+1,639	+1,793	+656	+649	-405	-195	+81	10,000
-6	+3	+10	-3	+1	0	-2	+81	0

TABLE 32
COMPOSITE FLANGED JOINT STRAIN GAGE READINGS AT ROOM TEMPERATURE TENSION LOADING – BACK SURFACE

C002 ($\mu\epsilon$)	C006 ($\mu\epsilon$)	C008 ($\mu\epsilon$)	C010 ($\mu\epsilon$)	C012 ($\mu\epsilon$)	C014 ($\mu\epsilon$)	THERMO-COUPLE C042 ($\mu\epsilon$)	EXTEN-SOMETER C060 (°F)	LOAD (LB)
0	+1	0	+1	0	0	+80	0.00	0
+81	+133	+47	+42	-3	-7	+80	+0.51	510
+157	+242	+88	+84	-5	-17	+80	+1.02	1,020
+367	+345	+125	+124	-7	-30	+80	+1.50	1,500
+302	+462	+168	+176	-9	-46	+80	+2.04	2,040
+367	+551	+198	+207	-11	-61	+80	+2.47	2,470
+450	+664	+234	+246	-14	-79	+80	+3.02	3,020
+523	+768	+270	+285	-17	-94	+80	+3.51	3,510
+598	+873	+307	+328	-20	-111	+80	+3.99	3,990
+677	+980	+346	+372	-23	-127	+80	+4.50	4,500
+757	+1,088	+385	+417	-27	-145	+80	+4.99	4,990
+841	+1,196	+424	+461	-31	-159	+80	+5.51	5,510
+920	+1,302	+462	+505	-36	-175	+80	+6.01	6,010
+990	+1,400	+500	+549	-39	-190	+80	+6.48	6,480
+1,064	+1,508	+540	+595	-44	-206	+80	+7.00	700
+1,133	+1,608	+577	+639	-48	-221	+80	+7.49	7,490
+1,205	+1,719	+618	+682	-54	-240	+80	+8.00	8,000
+1,273	+1,818	+656	+722	-59	-256	+80	+8.49	8,490
+1,347	+1,929	+696	+763	-65	-273	+80	+9.01	9,010
+1,413	+2,015	+726	+794	-70	-279	+80	+9.47	9,470
+1,490	+2,131	+770	+835	-76	-298	+80	10.00	10,000
+14	+12	-3	-2	-2	0	+80	0.00	0

TABLE 33
COMPOSITE FLANGED JOINT STRAIN GAGE READINGS AT -65°F
TENSION LOADING – FRONT SURFACE

C002 (με)	C006 (με)	C008 (με)	C010 (με)	C012 (με)	C014 (με)	C042 (°F)	C060 (V)	LOAD (LB)
+1	+2	0	0	+1	0	+67	0.00	0
+118	+174	+56	+58	-2	-9	+64	+0.52	520
+179	+278	+103	+115	-11	-25	-68	+1.04	1,040
+239	+369	+143	+165	-17	-39	-67	+1.50	1,500
+311	+464	+190	+217	-24	-54	-66	+2.00	2,000
+382	+522	+224	+255	-32	-71	-66	+2.50	2,500
+449	+585	+256	+286	-38	-88	+65	+2.99	2,990
+516	+687	+290	+330	-47	-104	-64	+3.49	3,490
+588	+793	+334	+380	-56	-120	-64	+3.99	3,990
+622	+896	+381	+433	-66	-135	-64	+4.49	4,490
+726	+1,008	+431	+490	-80	-153	-72	+5.01	5,010
+791	+1,106	+481	+541	-81	-170	-67	+5.50	5,500
+854	+1,207	+531	+594	-92	-187	-67	+6.01	6,010
+915	+1,308	+582	+648	-102	-205	-66	+6.49	6,490
+977	+1,405	+637	+701	-112	-222	-66	+7.01	7,010
+1,039	+1,500	+688	+747	-120	-241	-65	+7.50	7,500
+1,111	+1,599	+740	+794	-125	-261	-64	+8.00	8,000
+1,180	+1,705	+790	+843	-136	-280	-63	+8.50	8,500
+1,250	+1,811	+841	+894	-148	-300	-69	+9.00	9,000
+1,421	+1,905	+881	+932	-163	-326	-71	+9.49	9,490
+1,489	+2,004	+924	+967	-179	-352	-68	+9.99	9,990
+1,566	+2,120	+957	+989	-192	-388	-65	+5.27	10,540
+1,627	+2,211	+997	+1,025	-206	-408	-65	+5.48	10,960
+1,703	+2,324	+1,023	+1,041	-229	-64	+5.74		11,480
+1,781	+2,444	+1,046	+1,068	-249	-486	-64	+6.01	12,020
+1,850	+2,558	+1,064	+1,087	-273	-526	-69	+6,26	12,520
+1,910	+2,650	+1,078	+1,082	-297	-567	-71	+6.47	12,940
+17	-21	-39	-69	-9	-38	-67	+0.00	0

TABLE 34
COMPOSITE FLANGED JOINT STRAIN GAGE READINGS AT -65°F
TENSION LOADING – BACK SURFACE

C001 (με)	C003 (με)	C005 (με)	C007 (με)	C009 (με)	C011 (με)	C013 (με)	C041 (°F)	LOAD (LB)
-3	+1	-2	+1	+1	-1	0	+159	0
+35	+34	+32	+22	+45	-2	-1	+162	500
+116	+121	+123	+44	+76	-4	-5	+162	990
+199	+208	+228	+76	+107	-7	-11	+162	1,490
+280	+291	+337	+116	+140	-13	-16	-162	1,970
+368	+370	+456	+162	+187	-24	-23	+162	2,490
+450	+451	+553	+195	+218	-40	-32	+162	3,000
+529	+530	+646	+226	+248	-58	-40	+162	3,490
+609	+610	+740	+259	+280	-80	-50	+162	4,000
+689	+693	+831	+290	+310	-102	-61	+161	4,510
+766	+780	+927	+318	+340	-176	-56	-69	5,010
+841	+866	+1,017	+345	+369	-146	-81	+161	5,500
+918	+954	+1,111	+371	+397	-168	-90	+160	6,010
+993	+1,042	+1,206	+399	+425	-192	-101	+160	6,490
+1,069	+1,134	+1,298	+425	+453	-212	-112	+160	7,000
+1,144	+1,220	+1,391	+449	+477	-233	-123	+160	7,490
+1,221	+1,306	+1,486	+473	+503	-254	-134	+160	7,990
+1,298	+1,393	+1,578	+496	+528	-276	-146	+160	8,480
+1,374	+1,481	+1,672	+520	+552	-297	-160	+159	8,980
+1,449	+1,564	+1,766	+541	+573	-319	-175	+159	9,480
+1,520	+1,648	+1,860	+558	+590	-340	-193	+160	9,980
+1,596	+1,737	+1,959	+577	+607	-360	-215	+161	10,500
+1,666	+1,817	+2,046	+604	+630	-382	-237	+162	10,960
-18	-8	-13	-36	-28	+3	-10	+162	0
+1,728	+1,923	+2,148	+643	+644	-402	-276	+160	11,480
+1,787	+1,975	+2,246	+667	+682	-429	-306	+160	11,980
+1,849	+2,062	+2,329	+691	+709	-453	-332	+160	12,420
+1,920	+2,155	+2,430	+718	+739	-489	-374	+169	12,940
+1,997	+2,245	+2,530	+756	+839	-543	-479	+159	13,420
+2,111	+2,346	+2,701	+835	+937	-634	-678	+159	13,900

TABLE 35
COMPOSITE FLANGED JOINT STRAIN GAGE READINGS AT +160°F
TENSION LOADING – FRONT SURFACE

C001 (με)	C003 (με)	C005 (με)	C007 (με)	C009 (με)	C011 (με)	C013 (με)	C041 (°F)	LOAD (LB)
0	-1	+1	0	0	0	0	-67	0
+51	+53	+49	+32	+42	+2	+1	-64	520
+133	+145	+144	+73	+92	-1	-4	-67	1,040
+213	+220	+228	+110	+133	-3	-8	-66	1,500
+302	+300	+315	+152	+181	-6	-13	-66	2,000
+393	+373	+378	+202	+233	-13	-17	-66	2,500
+482	+447	+470	+243	+280	-22	-22	-65	2,990
+567	+512	+573	+285	+328	-31	-29	-64	3,490
+652	+592	+670	+326	+373	-43	-36	-64	3,990
+734	+669	+764	+370	+418	-57	-43	-64	4,490
+819	+741	+858	+416	+464	-76	-56	-69	5,010
+888	+828	+933	+454	+502	-93	-68	-67	5,550
+969	+917	+1,023	+494	+542	-112	-80	-66	6,010
+1,048	+1,002	+1,112	+534	+583	-129	-91	-66	6,490
+1,122	+1,086	+1,197	+573	+624	-146	-104	-66	7,010
+1,187	+1,169	+1,277	+610	+663	-162	-116	-65	7,500
+1,242	+1,234	+1,356	+647	+704	-176	-128	-65	8,000
+1,320	+1,316	+1,451	+689	+744	-193	-142	-64	8,500
+1,385	+1,393	+1,593	+731	+791	-210	-158	-66	9,000
+1,450	+1,466	+1,617	+761	+825	-229	-174	-68	9,490
+1,526	+1,540	+1,700	+785	+855	-250	-192	-67	9,990
+1,603	+1,622	+1,790	+802	+872	-285	-212	-65	10,540
+1,676	+1,698	+1,872	+827	+899	-306	-228	-65	10,960
+1,676	+1,698	+1,872	+827	+899	-306	-228	-65	10,960
+1,753	+1,780	+1,964	+828	+913	-341	-252	-65	11,480
+1,830	+1,864	+2,061	+840	+904	-379	-276	-64	12,020
+1,901	+1,960	+2,157	+853	+916	-419	-303	-67	12,520
+1,968	+2,032	+2,231	+847	+905	-456	-328	-69	12,940
-48	-81	+1	-34	+14	-23	-4	-67	0

TABLE 36.
COMPOSITE FLANGED JOINT STRAIN GAGE READINGS AT +160° F
TENSION LOADING – BACK SURFACE

C002 (με)	C006 (με)	C008 (με)	C010 (με)	C012 (με)	C014 (με)	C042 (°F)	C060 (V)	LOAD (LB)
-2	-1	0	0	0	0	+160	+0.00	0
+107	+171	+45	+38	-3	-7	+160	+0.50	500
+172	+291	+94	+83	-5	-20	+160	+0.99	990
+240	+400	+132	+127	-7	-37	+160	+1.49	1,490
+313	+501	+163	+166	-10	-53	+161	-1.97	1,970
+466	+717	+230	+241	-16	-86	+161	+3.00	3,000
+541	+826	+266	+283	-21	-99	+161	+3.49	3,490
+617	+936	+302	+324	-25	-111	+160	+4.00	4,000
+696	+1,045	+336	+364	-32	-124	+160	+4.51	4,510
+774	+1,156	+372	+407	-38	-135	+160	+5.01	5,010
+851	+1,261	+405	+447	-43	-146	+160	+5.50	5,500
+929	+1,370	+439	+489	-51	-160	+160	+6.01	6,010
+1,006	+1,476	+474	+529	-56	-171	+160	+6.49	6,490
+1,085	+1,583	+510	+572	-63	-183	-160	+7.00	7,000
+1,159	+1,688	+543	+608	-70	-196	+160	+7.49	7,490
+1,231	+1,792	+578	+646	-77	-208	+160	+7.99	7,990
+1,299	+1,894	+612	+679	-84	-220	+160	+8.48	8,480
+1,369	+2,000	+646	+712	-92	-232	+160	+8.98	8,980
+1,440	+2,107	+678	+740	-101	-246	+160	+9.48	9,480
+1,512	+2,215	+708	+765	-111	-261	+160	+9.98	9,980
+1,591	+2,330	+740	+792	-120	-276	+160	+5.25	10,500
+1,662	+2,424	+799	+892	-131	-293	+160	+5.48	10,960
+1,596	+1,737	+1,959	+577	+607	-360	-215	+161	10,500
+1,666	+1,817	+2,046	+604	+630	-382	-237	+162	10,960
+11	+15	-45	-13	-17	-17	+161	+0.00	0
+1,725	+2,511	+862	+966	-151	-315	+160	+5.74	11,480
+1,796	+2,619	+917	+1,022	-166	-336	+160	-5.99	11,980
+1,858	+2,708	+968	+1,067	-176	-352	+160	+6.21	12,420
+1,931	+2,816	+1,040	+1,127	-192	-374	+160	+6.47	12,940
+1,997	+2,882	+1,125	+1,322	-212	-351	+160	+6.71	13,420
+2,050	+2,874	+1,172	+1,380	-240	-327	+160	+6.95	13,900

This page intentionally left blank

End Date Feb 20, 1991

NASA National Aeronautics and Space Administration

Report Documentation Page

1. Report No.	2. Government Accession No.	3. Recipient's Catalog No.
NASA CR-181888		

4. Title and Subtitle
Structural Development of Laminar Flow Control Aircraft Chordwise Wing Joint Designs

5. Report Date
April 1989

6. Performing Organization Code

7. Author(s)
J.E. Fischler, N.M. Jerstad, F.H. Gallimore, Jr., and T.J. Pollard

8. Performing Organization Report No.

10. Work Unit No.
505-60-41-01

9. Performing Organization Name and Address
Douglas Aircraft Company
McDonnell Douglas Corporation
Long Beach, California 90846

11. Contract or Grant No.
NAS1-18037

13. Type of Report and Period Covered
Contractor Report

12. Sponsoring Agency Name and Address
National Aeronautics and Space Administration
Washington, DC 20546

14. Sponsoring Agency Code

15. Supplementary Notes
LANGLEY TECHNICAL MONITOR - MR. D.V. MADDALON

16. Abstract

The results of the investigation of many candidate chordwise joint concepts for laminar flow control have been reported. Three leading concepts have been fabricated and tested to determine their strength and deformation characteristics at room temperature, -65°. and at 160°F. The wave tolerance limits for turbulence were measured and were not exceeded for these three leading concepts. After the analysis of six candidates and the fabrication and testing of two candidates, the advantages and disadvantages of the two were compared. Finally, an improved design was created that combined the most favorable characteristics of the leading candidates. This improved design was fabricated, tested, and analyzed. The tests and analyses indicated that an economical chordwise joint is possible that meets all the strength and wave tolerance limits for turbulence and can be easily replaced in the field.

The results of this task indicated that sufficient verification has been obtained to fabricate a hybrid laminar flow control leading edge panel of at least 130 inches in length for a demonstration vehicle. This panel should have one or two of the improved design chordwise joints.

17. Key Words (Suggested by Author(s))	18. Distribution Statement
LAMINAR FLOW CONTROL, PERFORATED SURFACES, SURFACE WAVINESS, GAP AND STEP AT THE JOINT, WIDTH OF NONPOROUS STEP AT THE JOINT FOR ADEQUATE STRENGTH AND STIFFNESS, SLIDING JOINT, THREE-RIB SUPPORT JOINT, SEAL	Unclassified-Unlimited Subject Category 05

19. Security Classif. (of this report)	20. Security Classif. (of this page)	21. No. of pages	22. Price
Unclassified	Unclassified	203	A10

NASA FORM 1626 OCT 86